Investigations on the structure, biosynthesis and biology of antibacterial cyclic lipopeptides

Dissertation

zur

Erlangung des Doktorgrades (Dr. rer. nat.)

der

Mathematisch-Naturwissenschaftlichen Fakultät

der

Rheinischen Friedrich-Wilhelms-Universität Bonn

vorgelegt von

Yvonne Schmidt

aus

Mannheim

Bonn, 2012

Angefertigt mit Genehmigung der Mathematisch-
Naturwissenschaftlichen Fakultät der Rheinischen Friedrich-
Wilhelms Universität Bonn

1. Gutachter: Prof. Dr. G. M. König
2. Gutachter: Prof. Dr. H. Groß
Tag der Promotion: 28.02.2013
Erscheinungsjahr: 2013

Vorveröffentlichungen der Dissertation/

In Advance Publications of the Dissertation

Teilergebnisse dieser Arbeit wurden mit Genehmigung der Mathematisch- Naturwissenschaftlichen Fakultät, vertreten durch Herrn Prof. Dr. H. Gross und Frau Prof. Dr. G. M. König, in folgenden Beiträgen vorab veröffentlicht:

Parts of this study have been published in advance by permission of the faculty of Mathematics and Natural Sciences, represented by the supervisors of this study:

Publikationen/ Research Papers

Müller, A., Münch, D., Schmidt, Y., Reder-Christ, K., Schiffer, G., Bendas, G., Gross, H., Sahl, H.-G., Schneider, T., Brötz-Oesterhelt, H.; Lipodepsipeptide empedopeptin inhibits cell wall biosynthesis through Ca^{2+}-dependent complex formation with peptidoglycan precursors, J. Biol. Chem. (2012), 287 (24): 20270-20280

Reder-Christ, K., Schmidt, Y., Dörr, M., Sahl, H.-G., Josten, M., Raaijmakers, J. M., Gross, H., Bendas, G.; Model membrane studies for characterisation of different antibiotic activities of lipopeptides from *Pseudomonas*, Biochim. Biophys. Acta (2012), 1818 (2): 566-573

Tagungsbeiträge/ Research Presentations

Schmidt, Y., Heimer, P., Schäfers, F., Höver, T., König, G., Raaijmakers, J. M., Gulder, T. A. M., Gross, H.; The antimicrobial cyclocarbamate brabantamide A: Small molecule, intriguing biosynthesis; poster presented at the "International VAAM Workshop 2011", Bonn, Germany, September 5th – 8th, 2011, Abstract book P82

Schmidt, Y., Höver, T., Gulder, T. A. M., König, G., Raaijmakers, J. M., Gross, H.; Update on the biosynthesis of the antimicrobial cyclocarbamate SB-253514; poster presented at the "Nat Pharma: Nature Aided Drug Discovery (NADD)", Naples, Italy, June 5th – 8th, 2011, book of *congress abstracts* P 22

Reder- Christ, K., Schmidt, Y., Dörr, M., Sahl, H.-G., Josten, M., Raaijmakers, J. M., Bendas, G., Gross, H.; Model membrane approaches to simulate and explain the antibiotic activity of structural diverse cyclic lipopeptides from Pseudomonads, "International symposium of the DFG Research Unit FOR 845", Königswinter, Germany, 10^{th} – 12^{th} October 2010

Schmidt, Y., Raaijmakers, J. M., Gross, H.; Biosynthetic studies of SB-253514 – an antimicrobial lipodipeptide in disguise; "International symposium of the DFG Research Unit FOR 845", Königswinter, Germany, 10^{th} – 12^{th} October 2010

Müller, A., Schmidt, Y., Christ, K., Schiffer, G., Bendas, G., Gross, H., Sahl H.-G., Schneider, T., Brötz-Oesterhelt, H.; The lipodepsipeptide empedopeptin inhibits cell wall biosynthesis through Ca^{2+}-dependent lipid II complexation; "International symposium of the DFG Research Unit FOR 845", Königswinter, Germany, 10^{th} – 12^{th} October 2010

Schmidt, Y., Raaijmakers, J. M., Gross, H.; Biosynthetic studies of the cyclocarbamate SB-253514; poster presented at the "58^{th} International Congress and Annual Meeting of the Society for Medicinal Plant and Natural Product Research (GA)", Berlin, Germany, 29^{th} August–2^{nd} September 2010, *Planta Med.* 76 (P-185) and at the John Innes/Rudjer Bošković "Summer School on Microbial Metabolites: Signals to Drugs", IUC Dubrovnik, Croatia, August 21^{th}- 29^{th}, 2010

Acknowledgements

I wish to express my cordial gratitude to *Prof. Dr. G. M. König* and *Prof. Dr. H. Gross*, my supervisors, for the expert guidance, the opportunity to do a doctorate in the field of Pharmaceutical Biology and their support during the course of this project. The latter mentioned I also want to thank for proofreading my manuscript.

My appreciation also goes to *Prof. Dr. G. Bendas* and *Prof. Dr. Bierbaum* for participating in my examination committee.

Furthermore, I want to thank the German Research Foundation for financial funding of this study.

This study involved many specific tasks, e.g. execution of diverse biological assays which were in part performed in cooperation with other research groups. For this work, thanks go to:

Ms. E. Eguereva for the measurement of any number of LC-MS samples during the whole study and for excellent technical assistance

Ms. E. Neu for her overall technical assistance, her general support and her unforgettable ´cornucopia of charity´ with which I was overwhelmed again and yet again

Dr. Stefan Kehraus for essential help with the NMR data, his friendly support and his serenity

Associate Prof. Dr. J. M. Raaijmakers, Laboratory of Phytopathology, University of Wageningen, the Netherlands, for providing exclusive access for the strain *Pseudomonas* sp. SH-C52 which granted investigations without competition

Dr. M. van der Voort, Laboratory of Phytopathology, University of Wageningen, the Netherlands, for the generation of knock-out strains of *P.* sp. SH-C52

Prof. Dr. J. Piel, Kekulé-Institute of Organic Chemistry and Biochemistry, University of Bonn, for enabling me to participate in the summer school in Dubrovnik

Dr. T. A. M. Gulder, Kekulé-Institute of Organic Chemistry and Biochemistry, University of Bonn, for introducing me into the world of molecular biology and for big support regarding bioinformatics tools

Dr. K. Reder-Christ and the *research group of Prof. Dr. G. Bendas*, Pharmaceutical Institute, Pharmaceutical Chemistry II, University of Bonn, for the performance of model-membrane studies

Dr. R. Hartmann, Jülich Research Centre, Jülich, for the NMR-measurements of empedopeptin

Prof. Dr. H. Brötz-Oesterhelt, Institute of Pharmaceutical Biology and Biotechnology, University of Düsseldorf, *Prof. Dr. H.-G. Sahl,* Institute for Microbiology und Biotechnology, Pharmaceutical Microbiology, University of Bonn *and their teams* for the work on the elucidation of the mode of action of brabantamide A and empedopeptin, respectively

Ms. M. Josten, IMMIP, Pharmaceutical Microbiology Unit, University of Bonn for determinations of the antibacterial activity and tests regarding the incorporation of radioactive metabolites

Ms. M. Engeser and heir team, Department of Chemistry, University of Bonn, for (HR)ESI-MS measurements

Further, I want to thank *PD. Dr. M. Neugebauer* for supervising the ´Weiterbildung zum Fachapotheker für Toxikologie und Ökologie´.

Special thanks go to:

All colleagues of the Institute of Pharmaceutical Biology for contributing to a relaxed atmosphere and nice times

Prof. Dr. Kostenis and heir working group who adopted me for their social events. Thanks. It was great.

Prof. Dr. Samina Mehnaz, Department of Microbiology and Molecular Genetics, University of Punjab, Pakistan, for very good company in the working group, her great sense of (sometimes grim) humour and for encouraging me all the time

T. Kögler and *E. Issi* for reanimation of my laptop

A. Schmitz for letting me win by default

T. Höver and *T. Schäberle* for a funny time in Naples

Emilia Goralski and *Imke Jenniches* for being my friends and entire support over the last years, Thank you so much.

Tina Runde, Birgit Pötzsch and *Christiane Enkeler* for being my friends, smarten up my time in Cologne, catering for dissipation and enduring every phase of the study.

Barbara Cassuccio, for being my friend of many years

Björn and *Alex Vallen*, my coaches, for shooing me

And last but surely not least I wish to thank *my family* for support not only for this study but concerning my whole lifetime. For being as they are, knowing me and encouraging me.

And especially I want to thank *my sister* for indispensable help facing everyday struggles.

And I want to thank the little lady **ANTONIA**, who sent me a friend-postcard and can only read her name in capitals.

Table of contents

Abbreviations and units

$[\alpha]_D^T$	specific optical rotation, sodium D line (589 nm); T: temperature
δ	NMR chemical shift [ppm]
λ	wavelength [nm]
µ	micro (10^{-6})
µ	specific growth rate (in connection with growth determination of bacteria)
°C	degrees Celsius
Å	Ångström
A (-domain)	adenylation (-domain)
AA/aa	amino acid
ACP	acyl carrier protein
ADP	adenosine diphosphate
AMP	adenosine monophosphate
ATCC	American Type Culture Collection
ATP	adenosine triphosphate
ATR	attenuated total reflection
BALB/3T3	mouse embryonic fibroblast cell line
bp	base pair(s)
Bq	Becquerel, 1 Bq equals 1 cpm
BV (MO)	Baeyer – Villiger (monooxygenase)
c	concentration [g/100ml] (in connection with optical rotation)
C (-domain)	condensation (-domain)
calc.	calculated
CAT	regular NRPS module composed of a C- an A- and a T-domain
CAZy	Carbohydrate-Active Enzymes database
CD	circular dichroism
CDA	calcium-dependent antibiotic
$CDCl_3$	deuterated chloroform
$(CD_3)_2CO$	deuterated acetone
CD_3OD	deuterated methanol
CFU	colony forming unit
Ci	Curie, 1 Ci = 3.7 x 10^{10} Bq
Cl (-domain)	halogenase (-domain)
CLDP	cyclic lipodepsipeptide
CLP	cyclic lipopeptide
CoA/HS-CoA	coenzyme A
conc.	concentrated

COSY	correlated spectroscopy
cpm	counts per minute
cSSSI	complicated skin and skin structure infection
CV	cyclic voltammetry
Cy (-domain)	cyclisation (-domain)
d	doublet (in connection with NMR data)
DA	Dalton
DAD	diode array detector
DCM	dichloromethane
DEPT	distortionless enhancement by polarisation transfer
DFG	´Deutsche Forschungsgemeinschaft´; German Research Foundation
DH	dehydratase
DMB/DMBgly	Davis minimal broth without dextrose / Davis minimal broth without dextrose, supplemented with glycerol
DMEM	Dulbecco's modified eagle medium
DMSO	dimethyl sulfoxide
DMSO-d_6	deuterated dimethyl sulfoxide
DNA	deoxyribonucleic acid
E (-domain)	epimerisation (-domain)
EC	endcapped
e.g.	Latin ´exempli gratia´; for example
ER	enoyl reductase
ERY^R	erythromycin-resistant
ES	efflux system
ESI	electro spray ionisation
EtOAc	ethyl acetate
FA	fatty acid
FAD	flavin adenine dinucleotide
FAS	fatty acid synthase
FOR	´Forschergruppe´; research unit
FP	flavoprotein
FPMO	flavoprotein monooxygenases
FT-IR	Fourier transformation infrared
g	gram
GT	glycosyltransferase
h	hour
3-HAD	3-hydroxydecanoic acid
HMBC	heteronuclear multiple-bond correlation spectroscopy
H_2O	water
3-HOA	3-hydroxyoctanoic acid
hPhg	4-OH-phenylglycine
HPLC	high performance liquid chromatography

HR	high resolution
HSQC	heteronuclear single quantum correlation
HSV-1	herpes simplex virus type 1
Hz	hertz
IC_{50}	half maximal inhibitory concentration
i.e.	Latin ´id est´; that is
IMMIP	Institute of Medical Microbiology, Immunology and Parasitology
IR	infrared
J	spin-spin coupling constant [Hz]
KB	King's broth
KR	ketoreductase
KS	ketosynthase
L/l	litre
LB	lysogeny broth
LC	liquid chromatography
LDL	low-density lipoprotein
$LpPLA_2$	lipoprotein associated phospholipase A_2
LTA	lipoteichoic acid
m	multiplet (in connection with NMR data)
M	molar [mol/l]
MALDI-TOF	matrix-assisted laser desorption/ionisation-time of flight
MAT	malonyl-acetyl transferase
Mb	mega base pairs = 1,000,000 bp
MDR	multidrug resistance (transporter)
MeOH	methanol
MFP	membrane fusion protein
MH	Mueller-Hinton
MHz	Megahertz
MIC	minimal inhibitory concentration
925 MM	925 minimal medium broth
MO	monooxygenase
MoA	mode of action
MR	methicillin-resistant
MRSA	methicillin-resistant *Staphylococcus aureus*
MS	methicillin-susceptible (in context with bioassays)
MS	mass spectrometry (in context with analytics)
MT	methyltransferase
MWCO	molecular weight cut off
m/z	mass-to-charge ratio
NADH	nicotinamide adenine dinucleotide
NADPH	nicotinamide adenine dinucleotide phosphate

N-AHL	*N*-acylhomoserine lactone
nanoDESI	nanospray desorption electro spray ionisation technique
NB	Nutrient broth
NCBI	National Center of Biotechnology Information
n.d.	not determined
NH_4OAc	ammonium acetate
nm	nanometer
NMR	nuclear magnetic resonance
no.	number
NOE	nuclear Overhauser effect
NOESY	nuclear Overhauser effect spectroscopy
nov.	latin ´novum´; new
NRPS	nonribosomal peptide synthetase
n.t.	not tested
OAA	oxaloacetate
$OD/OD_0/OD_{600}$	optical density / at t_0 / at λ= 600 nm
OMF	outer membrane factor
ORF	open reading frame
OSMAC	one strain many compounds
PCP	peptidyl carrier protein
pH	potential hydrogenii
PKS	polyketides synthase
4´-PP	4´-phosphopantetheinyl
ppm	part per million
pv.	pathovar
QCM	quartz crystal microbalance
R (-domain)	reductase (-domain)
R	residue (in combination with chemical structures)
R^2	coefficient of determination
RFU	relative fluorescence unit
RNA	ribonucleic acid
RND	resistance nodulation division
RP	reversed phase
rpm	rounds per minute
RPMI	Roswell Park Memorial Institute medium
RT	room temperature
s	singlet (in connection with NMR data)
SFV	Semliki Forest virus (togaviridae, a model virus for the hepatitis G virus)
SHV-1	suid herpes virus type 1 (herpesviridae, a model virus for human herpes viruses)
sp.	species

SPE	solid phase extraction
spp.	species (plural)
SRM HG	syringomycin minimal medium modified according to Prof. Dr. H. Gross
t	triplet (in connection with NMR data)
T (-domain)	thiolation (-domain)
TCA	trichloroacetic acid
t_d	doubling time
TDP	thymidine diphosphate
TE (-domain)/ TE-I/TE-II	thioesterase (-domain) / type I TE / type II TE
TFA	trifluoroacetic acid
THP1	human acute monocytic leukemia cell line
TOCSY	total correlation spectroscopy
t_R	retention time
TSB	tryptic soy broth
U	unit
UV	ultraviolet
VIS	visible
VLC	vacuum - liquid chromatography
VSV (= VSIV)	vesicular stomatitis Indiana virus (often abbreviated with VSV), rhabdoviridae
v/v	volume/volume
WHO	World Health Organisation

Abbreviations for amino acids

amino acid	one letter code	three letter code
alanine	A	Ala
arginine	R	Arg
asparagine	N	Asn
aspartic acid	D	Asp
cysteine	C	Cys
glutamic acid	E	Glu
glutamine	Q	Gln
glycine	G	Gly
histidine	H	His
isoleucine	I	Ile
leucine	L	Leu
lysine	K	Lys
methionine	M	Met
phenylalanine	F	Phe
proline	P	Pro
serine	S	Ser
threonine	T	Thr
tryptophan	W	Trp
tyrosine	Y	Tyr
valine	V	Val

Abbreviations for unusual amino acids

Dab	2,4-diaminobutyric acid
Dhb	2,3-dihydro-2-aminobutyric acid
hAsn	3-OH asparagine
hAsp	3-OH aspartic acid
Hse	homoserine
Kyn	kynurenine
3mGlu	3-methyl glutamic acid
mOAsp	methoxyaspartic acid
Sar	sarcosine
Thr[4-Cl]	4-chlorothreonine
ΔTRP	*Z*-2,3-dehydrotryptophan

1 Introduction

Antibiotics are one of the most powerful therapeutic tools in medicine. They inhibit the growth of bacteria, thereby helping the body to fight serious bacterial infections. Antibacterial drugs have been successfully applied for the treatment of various bacterial infections in human beings since the 1940s. However, already in the early 60s the first resistant bacterial strains occurred and the era of the ´golden age´ of antibiotics between the 1940s and the 1970s (see figure 1.1) has drawn to a close (Fernebro, 2011). The upraising resistance was additionally triggered by misapplication of antimicrobial agents, often combined with an over-usage in many parts of the world or the misuse due to lack of access to appropriate treatment (WHO, 2001). Furthermore, resistance spread out by the increasing availability of generic drugs related to the advancing global travel, global healthcare and medical tourism (Grundmann *et al.*, 2011). The awareness about the importance of resistance took time to get established. Instead of the necessary intensified search for new antibiotics, industry stopped their research programs.

As a consequence of this development, the pipeline of new drugs by now is running dry (WHO, 2001), while the development of antibiotic resistance of almost all clinically important pathogens increased (Fernebro, 2011). These facts give rise to an urgent need of alternatives to conventional antibiotics (Fernebro, 2011).

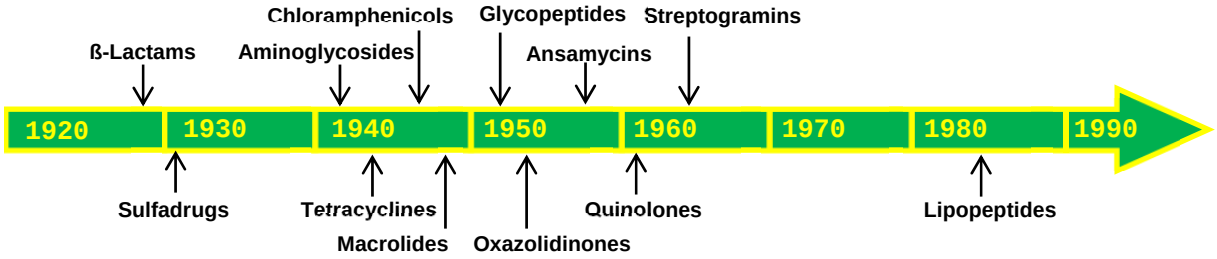

Figure 1.1: antibiotic discovery timeline (adopted from Lewis, 2012)

Looking into the recent developments, it becomes apparent that most of the few approved antibiotics – most likely due to the reduced industrial drug discovery programs - simply represent

derivatives of known compound classes. Only occasionally a new compound class, acting at new targets came to the market, e.g. the gyrase inhibitors or the cyclic lipopeptide daptomycin.

A recent comparative analysis of systemic antibacterial agents revealed that only fifteen candidates out of 90 agents actually act by new modes of action or act on new targets (Freire-Moran *et al.*, 2011). Among these 15 innovative candidates, seven active substances belong to the group with new modes of action and two thereof – WAP 8294A2 and friulimicin B – belong to the group of cyclic lipodepsipeptides (Freire-Moran *et al.*, 2011).

Based on these facts, cyclic lipopeptides (CLPs) of bacterial origin apparently represent a promising class of antibiotics with presumably new mode of actions.

1.1 Cyclic lipopeptides

Cyclic lipopeptides are a structurally diverse class of compounds which are composed of a fatty acid chain in the length of 5-20 carbon atoms and an oligopeptide ranging from 7-25 amino acids, whereby 4-14 residues thereof form a ring system (Gross & Loper, 2009; Hashizume & Nishimura, 2008). This general structure causes the amphiphilic properties of cyclic lipopeptides which account for most of the functions CLPs possess in nature.

The peptide antibiotics often contain non-proteinogenic amino acids, such as *D*-configurated, *O*-methylated, *N*-methylated, halogenated and *β*-amino acids (see figure 1.1.1). The incorporation of these unusual amino acids is attributable to the fact that CLPs are biosynthesised by non-ribosomal peptide synthetases (NRPSs, see chapter 1.1.1). It has been hypothesised that these features protect the compound class towards regular ubiquitary peptidases (Hashizume & Nishimura, 2008). Variations of the amino acid residues including their sequence as well as variations of the side chain regarding length, branching and oxidation status and different cyclization schemes generate an enormous structural diversity, occupying a huge three-dimensional chemical space.

Since most of the CLPs lose their activity upon cleavage of the cyclic structure, the biological activity is dependent on the three-dimensional structure (Hashizume & Nishimura, 2008). Further factors that influence the potency of CLPs are the applied pH value and the presence of bivalent cations.

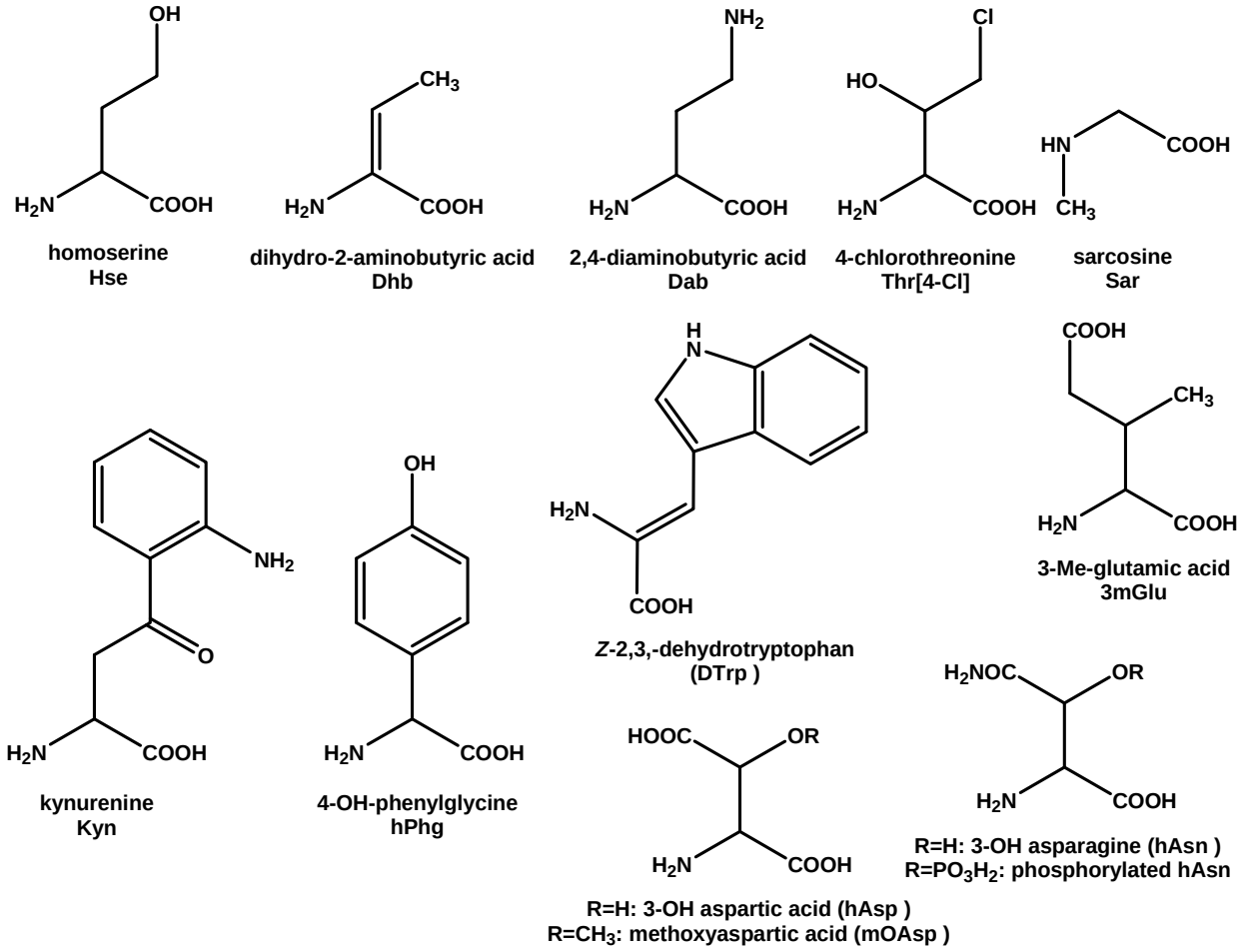

Figure 1.1.1: non-proteinogenic amino acids occurring in lipopeptides

Cyclic lipopeptides are produced by a variety of species e.g. Pseudomonads (see chapter 1.2.1), *Bacillus* spp., *Actinomyces* spp. (e.g. friulimicin), *Streptomyces* spp., *Actinoplanes* spp. (ramoplanin), Burkholderiae and by some members of Xantomonadaceae and Flavobacteriaceae (e.g. empedopeptin). Furthermore, structurally divers CLPs have been isolated from marine organisms e.g. from cyanobacteria of the genus *Microcystis* or *Nostoc* or from marine sponges (Hashizume & Nishimura, 2008).

CLPs display activity against a variety of species, including multi-resistant human-pathogenic bacteria like MRSA and viruses (Vollenbroich *et al.*, 1997a). Furthermore, they possess antitumor (Wang *et al.*, 2007), cytotoxic (de Lucca *et al.*,

1999), immunosuppressant (Cameotra & Makkar, 2004) and surfactant properties. The latter property seems to be accountable for the potential of CLPs to increase the bioavailability of water-insoluble substrates, to lower surface tension and to interact with cellular membranes (Raaijmakers *et al*., 2006).

Beside these properties and functions, cyclic lipopeptides play an essential role in the protection of their producer for instance against predators as toxic compounds or by reduction of the susceptibility to antibiotic treatment by development and formation of biofilms (Raaijmakers *et al*., 2010; Mazzola *et al*., 2009).

In addition, CLPs are important for the infection process in plant pathogenic *Pseudomonas* species, while in non-pathogenic strains of the genera *Pseudomonas* and *Bacillus* CLPs were observed to stimulate the plant immune system (Raaijmakers *et al*., 2010).

Other natural functions of cyclic lipopeptides are their ability to chelate and degrade xenobiotic compounds (reviewed by Raaijmakers *et al*., 2010), their role in motility and attachment to surfaces (Raaijmakers *et al*., 2006) and their function as signalling molecules for coordinated growth and differentiation (Mahariel *et al*., 1997).

1.1.1 Biosynthesis of cyclic lipopeptides

Cyclic lipopeptides are produced on multi – enzyme complexes called nonribosomal peptide synthetases (NRPS) that are organised in a modular fashion. In contrast to the ribosomal synthesis of peptides which are restricted to a very confined substrate pool consisting of the 21 proteinogenic amino acids, NRPSs are capable to incorporate also non-proteinogenic amino acids, like for example hydroxy and N-methylated amino acid residues (see figure 1.1.1; Mahariel *et al*., 1997; Mootz *et al*., 2002; Schwarzer *et al*., 2003).

Nonribosomal peptide synthetases typically contain the same number and order of modules as the resulting number and sequence

of amino acids in the corresponding peptide product. This so-called ´colinearity rule´ results from the construction of the multi-enzyme complex. Each module contains at least three core domains for one complete elongation cycle of the peptide moiety: the adenylation domain (A-domain), the peptidyl-carrier protein (PCP-domain, syn. = thiolation domain / T-domain) and the condensation domain (C-domain). The A-domain selects a specific amino acid monomer from the available substrate pool, activates it by formation of an amino acyl adenylate under consumption of ATP.

Subsequently, the activated amino acid is transferred to the PCP-domain forming an aminoacyl thioester, which is covalently linked to the cysteamine group of an enzyme-bound 4´-phosphopantetheinyl (4´-PP) cofactor. This covalent tether allows the transport to the adjacent catalytic centres of the multienzyme. In the next step, the C-domain located between every successive pair of A- and PCP-domains catalyses the formation of a peptide bond which finalises one elongation cycle (Fischbach & Walsh, 2006; Challis & Naismith, 2004; Challis *et al.*, 2000).

Aside the three mentioned core domains, additional domains can be integrated affording modifications of incorporated residues: epimerisation (E) domains enable the conversion of L-configured amino acids into the corresponding D-form, methyltransferase (MT) domains are responsible for N-methylation, while cyclisation (Cy) domains catalyse the formation of heterocyclic ring systems and reductase (R) domains change the oxidation status of atoms.

When the specific length of the peptide chain is reached, a terminal thioesterase (TE) domain finalises the assembly line. The TE-domain catalyses the release of the product by hydrolysis and optionally performs a cyclisation. TE-domains can be subdivided into two types: type I TE-domains (TE-I), usually representing the last domain in the multienzyme responsible for cleavage of the assembled product and type II TE-domains (TE-II).

TE-II are associated with NRPSs and involved in the regeneration of misprimed PCPs by removing short acyl chains from the 4´-PP cofactors. Otherwise, e.g. tethered acetyl-CoA would inactivate

the NRPS, because substrates without an amino-group cannot be elongated (Linne *et al.*, 2004; Schwarzer *et al.*, 2002). Moreover, Walsh and co-workers could demonstrate that the TE-II domains possess the ability to cleave amino acids from NRPS modules at moderate rates and to discriminate ´correct´ from ´incorrect´ amino acids based on the half-life of unprocessed intermediates displaced from the normal binding sites (Yeh *et al.*, 2004). Furthermore, TE-domains of type II also interact with TE-I-domains and possess a strong impact on the efficacy of the biosynthetic machinery. This fact derives from the observation that the knockout of TE-II in arthrofactin biosynthesis lead to a decrease of arthrofactin production by 95% (Roongsawang *et al.*, 2007).

Nonribosomal peptide synthetases can be subdivided into three types (A-C), differing in the organisation of their modules (Mootz *et al.*, 2002):

Type A: linear NRPSs

In type A NRPSs the core domains are arranged in the order CAT, adding one amino acid per elongation cycle. In the first module, the C-domain is missing and the terminal module usually contains a TE-domain (in fungi often replaced by special C-domains). Type A NRPSs usually act in accordance with the ´colinearity rule´ (see above).

Type B: iterative NRPSs

In iterative NRPSs the modules are used more than once in the biosynthesis and correspond to only one set of a repeated sequence of the multimeric product. The final PCP or TE domain is responsible for the number of iterative cycles and the chemical nature of the bonds between the monomers (Mootz *et al.*, 2002). An iterative use of modules was described in the coelichelin biosynthesis in *Streptomyces coelicolor* (Lautru *et al.*, 2005) and in the biosynthesis of congocidine, produced by *Streptomyces ambofaciens* (Juguet *et al.*, 2009).

Type C: nonlinear NRPSs

Nonlinear NRPSs deviate in at least one module from the usual arrangement of the core domains (e.g. NRPS of syringomycin; Guenzi *et al.*, 1998).

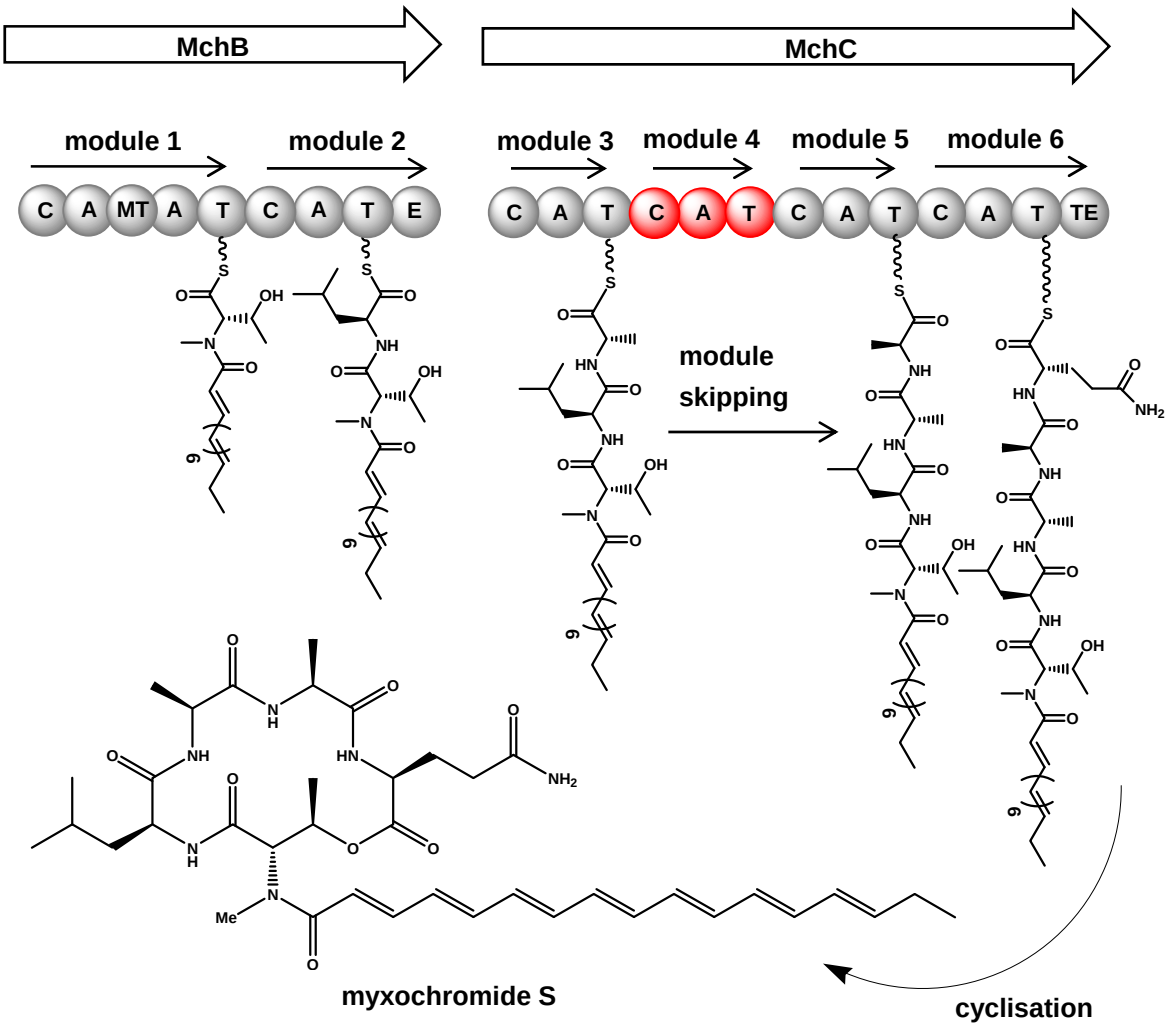

Figure 1.1.2: module skipping in the biosynthesis of myxochromide S with transfer of the peptide chain from the T-domain of module 3 to the T-domain of module 5. Figure modified according to (Wenzel *et al.*, 2005)

This deviation is often accompanied by unusual internal cyclisations (e.g. bleomycin) or branch-point synthesis (e.g. vibriobactin) and results in nonlinear peptide products. In contrast to linear NRPSs, type C NRPSs are able to incorporate small soluble molecules lacking a carboxyl-group such as amines.

An extension to the described deviations of the usual NRPS machinery can be observed in the ´module skipping´ (e.g. in the myxochromide S biosynthesis) in modular NRPSs (see figure 1.1.2). In this case not the skipping of modules as an aberrant process resulting in truncated minor metabolites is meant, but skipping as programmed event (Wenzel & Müller, 2005).

1.1.2 Cyclic lipopeptide antibiotics

Corresponding to the structural diversity, cyclic lipopeptides exhibit bioactivity against a broad spectrum of other microorganisms.

In this study the antibacterial aspects of CLPs were highlighted, this is why in the following an in-depth overview about this part of the antibiotic spectrum of CLPs will be given.

In general, cyclic lipopeptides are rather active against Gram-positive than Gram-negative bacteria. This might be caused by the Gram-negative outer membrane or peptidoglycan-layer, which probably hinders CLPs to access the plasma membrane (Nybroe & Sørensen, 2004). An exception represents the polymyxins, which are selectively toxic for Gram-negative bacteria.

The medicinal significance of this compound class shall be illustrated by examples of the following cyclic lipopeptides that are already in clinical use or that are currently investigated in clinical trials.

Daptomycin (see figure 1.1.3), which was introduced in the market as Cubicin® in 2003, impressively demonstrates the potential of this substance class featuring activity against a variety of Gram-positive bacteria including multi-resistant human pathogenic species causing serious infections.
The approved indications of Cubicin® are complicated skin and skin structure infections (cSSSI) for example caused by MRSA and bacteraemia including those with right-sided infective endocarditis (Steenbergen *et al.*, 2005). Daptomycin is produced by *Streptomyces roseosporus* and exhibits bactericidal activity *in vitro* thereby showing MICs of ≤ 1µg/ml for most of the tested strains (Baltz *et al.*, 2005).
Daptomycin belongs to the group of acidic lipopeptide antibiotics which are predominately produced by *Actinomycetales* and share a straight or branched-chain fatty acid moiety with 6-16 carbons, differing in the degree of saturation and the oxidation state (Strieker & Mahariel, 2009), which is invariably attached to the macrocyclic peptide core.

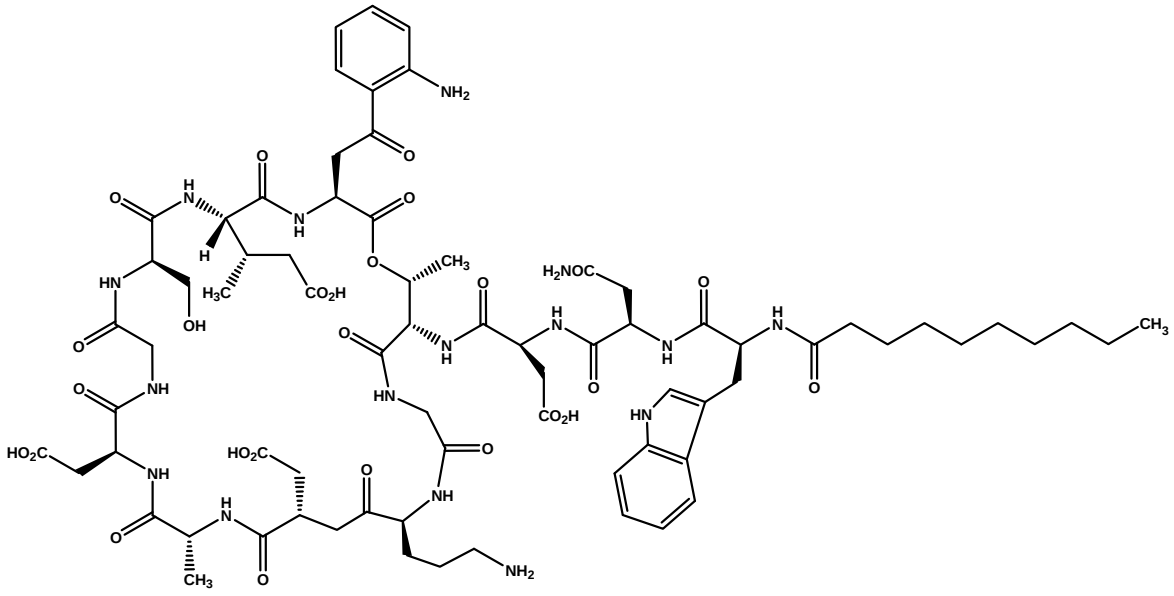

Figure 1.1.3: daptomycin (Cubicin®)

Together with CDA (calcium-dependent antibiotic), isolated from *Streptomyces coelicolor* A3 (2) (Lakey *et al.*, 1983), CDA-derived CLPs and CLPs of the A21978C-complex, daptomycin belongs to the subgroup of acidic cyclic lipodepsipeptides (CLDPs), i.e. that at least one amide bond of the macrocycle is exchanged by an ester bond. The acidity is attributable to the presence of two aspartic acid residues in the conserved motif Asp-X-Asp-Gly of the ring structure and further acidic amino acids in the peptide moiety like 3-methoxy-aspartic acid or additional Asp-residues (Strieker & Mahariel, 2009).

Other important representatives of this group are WAP-8294A2 and friulimicin B (see figure 1.1.4), which both are in Phase I of clinical development (Freire-Moran *et al.*, 2011).

WAP-8294A2 is produced by *Lysobacter* sp. and exhibits activity against MRSA as well as against various strains of *Propionibacterium acnes* including clinical isolates and multi-drug resistant strains. Therefore, it is under investigation for systemic use against MRSA and formulated as a cream against acne (Pirri *et al.*, 2009).

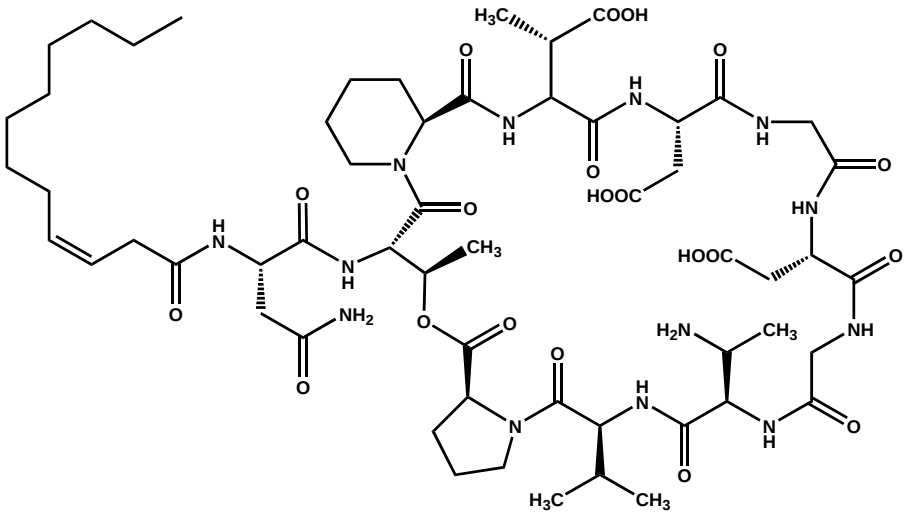

Figure 1.1.4: friulimicin B

Friulimicin B, produced by *Actinoplanes friuliensis* DSM 7358 (Aretz *et al.*, 2000), shows an antagonistic spectrum similar to that of daptomycin, both featuring higher antibiotic potency than teicoplanin (Bemer *et al.*, 2003). Friulimicin B possesses a unique mode of action and affects the cell envelope of Gram-positive bacteria by interruption of the cell wall precursor cycle through the formation of a Ca^{2+}-dependent complex with the bactoprenol phosphate carrier C_{55}-P (Schneider *et al.*, 2009).

However, despite the structural similarity and potency, daptomycin does not interact with this target. Its mode of action is still lacking complete elucidation and is the subject of intense debate since a long time. Aside the obvious dependency of the activity on the presence of calcium, earliest assumptions pointed towards the energised cytoplasmic membrane as target leading to an interference of the peptidoglycan biosynthesis (Alborn *et al.*, 1991).

Later, other authors proposed, that an enzyme of the lipoteichoic acid (LTA) biosynthesis represents the decisive target (Canepari *et al.*, 1990). However, Laganas and co-workers refuted this hypothesis by pointing out the lack of the essential kinetic specifity (Laganas *et al.*, 2003), which would be required for this theory. Meanwhile, it is resolved, that the mode of action of daptomycin involves the calcium-dependent insertion of the compound into the bacterial cytoplasmic membrane (Jung *et al.*, 2004), while the mechanism of bacterial killing still remains even more controversial and may involve multiple activities. Among these, effects on membrane integrity,

rapid inhibition of protein, DNA and RNA synthesis and inhibition of lipoteichoic acid synthesis are currently being discussed (Hancock, 2005).

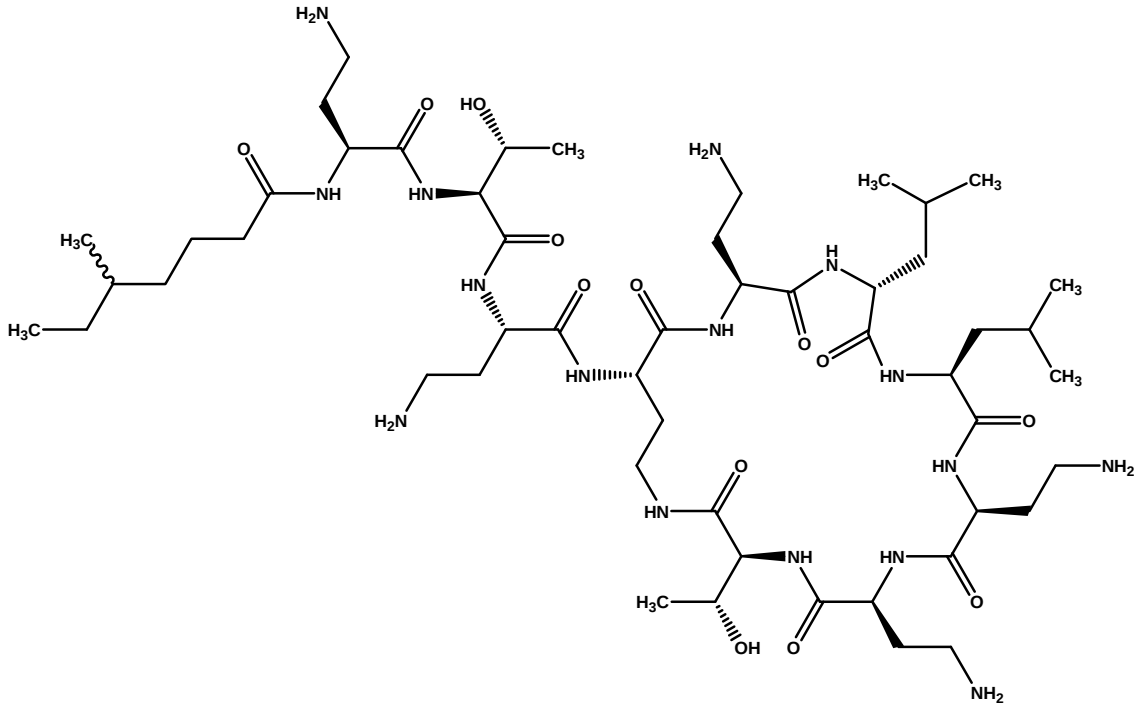

Figure 1.1.5: colistin (polymyxin E)

Another group of CLPs which already reached the market are the polymyxins which were primarily isolated in the late 1940s from *Bacillus polymyxa* and consist of five chemically different compounds (polymyxins A-E; Storm *et al.*, 1977). The polymyxins are active against selected Gram-negative bacteria, including *P. aeruginosa, Klebsiella, Actinobacter* and *Enterobacter* species. The two candidates being in clinical use since the 1950s (polymyxins B and E (= colistin, see figure 1.1.5)) were restricted to local use except for treatment of cystic fibrosis in the 1980s due to their high nephro- and neurotoxicity. Meanwhile, a revival has taken place and the intravenous treatment of serious *P. aeruginosa* and *A. baumannii* infections with polymyxins is reconsidered as a valuable option due to the increase of resistances and a lack of alternatives (Falagas & Kasiakou, 2005). Colistin targets the bacterial cell membrane through electrostatic interaction between the cationic polypeptide and the anionic lipopolysaccharide molecules in the outer membrane of the Gram-negative bacteria. Subsequently, it displaces magnesium and calcium ions from the membrane, leading to an increase of the permeability of the cell envelope, leakage

of cell contents and finally cell death (Falagas & Kasiakou, 2005).

Ramoplanins, first isolated in 1984 from *Actinoplanes* sp. ATCC 33076 (Cavalleri *et al.*, 1984), are a family of the macrocyclic lipopeptides which represent also promising clinical candidates for the treatment of infectious diseases caused by Gram-positive bacteria. Ramoplanin inhibits the bacterial translocase during a late step of peptidoglycan biosynthesis by binding as a dimer to lipid II, the substrate for these enzymes (Hashizume & Nishimura, 2008).

Another significant example for the activity of CLPs is empedopeptin, which was isolated from the Gram-negative soil bacterium *Empedobacter* sp. (Konishi *et al.*, 1984). The antibacterial spectrum resembles that of amphomycin and vancomycin, inhibiting predominately Gram-positive and anaerobic bacteria. Empedopeptin belongs to the group of guanidine-containing CLPs, which are characterised by the presence of arginine and two hydroxy aspartic acids. Furthermore, they share proline, hydroxy-proline and serine as common amino acids in their peptide nucleus. The activity includes resistant strains and shows therapeutic effects in models of staphylococcal septicaemia in mice (Hashizume & Nishimura, 2008).

1.2 Pseudomonads as an underexplored source for new cyclic lipopeptide antibiotics

Pseudomonas is a genus of Gram-negative Gammaproteobacteria which is spread ubiquitous in nature colonising a wide variety of niches like soil, water, plant surfaces or animals due to their ability to use diverse organic compounds as energy sources (Gross & Loper, 2009). *Pseudomonas* are prominent for their plant- and human-pathogenic species like *Pseudomonas syringae* and *Pseudomonas aeruginosa,* respectively, but the genus includes also species that degrade xenobiotic compounds, promote plant growth, antagonise plant pathogenic fungi and induce resistance in plants (Raaijmakers *et al.*, 2006).

The facility to culture *Pseudomonas* strains *in vitro* and the growing availability of genome sequences makes the genus an excellent focus for scientific research. Starting with the publication of the whole genome sequence of *Pseudomonas aeruginosa* PAO1 in 2000 (Stover *et al.*, 2000), up to date more than thirty complete genome sequences are available (NCBI search, May 2012) and a strong increase in numbers can be predicted due to modern sequencing technologies (Gross & Loper, 2009). The genome size ranges between 4.5 Mb and 7.2 Mb having a GC content of 57.5-66.6 %. Up to 7 % of the genomic information can be devoted to secondary metabolism which demonstrates the huge biosynthetic capacity of this genus.

Pseudomonads are hereby capable to produce an enormous spectrum of bioactive and structural diverse secondary metabolites ranging from polyketides, alkaloids to quinones and many small sophisticated highly bioactive compounds (Gross & Loper, 2009).

Pseudomonads are also an excellent source for cyclic lipopeptide antibiotics as nearly every *Pseudomonas* species produces a CLP for physiological or defence purposes.

Pseudomonas lipopeptides were so far mostly investigated only in their agricultural, phytochemical and biofilm-controlling context, but rarely systematically as antibiotics. Thus, this genus represents a huge reservoir for new promising antibiotic active CLPs, which are currently underexplored. In the following, an overview about the current classification system of *Pseudomonas* lipopeptides will be given.

1.2.1 Cyclic lipopeptides produced by *Pseudomonas* spp.

Cyclic lipopeptides produced by *Pseudomonas* spp. cyclise between two amino acids in the peptide moiety to form a lactone ring and can be subdivided into several classes according to the number, type and configuration of the incorporated amino acids and the length and composition of the fatty acid tail (Raaijmakers *et al.*, 2006). Based on an initial classification by Nybroe and Sørensen in 2004, who distributed *Pseudomonas*-derived CLPs into four major groups, the viscosin-, amphisin-, tolaasin- and

syringomycin-group (Nybroe & Sørensen, 2004), several increments of the classification have been published including further isolated CLPs (e.g. Raaijmakers *et al.*, 2006; Gross & Loper, 2009). Hence, a division in at least nine groups (see table 1.2.1) can be conducted as described in the following.

Cyclic lipopeptides of the plusbacin group belong to the guanidine-containing cyclic lipopeptides and share arginine, proline, serine, hydroxyroline and two hydroxyaspartic acid residues as the common amino acids in their peptide nucleus (Hashizume & Nishimura, 2008). The plusbacin group contains plusbacins A_1-A_4 and B_1-B_4 (Shoji *et al.*, 1992a), differing in the second hydroxyproline residue between A and B and in the fatty acid residue between A_1 to A_4. Plusbacins as well as arthrofactin (see below) cyclise via lactone ring formation between the fatty acid chain and the terminal amino acid (Shoji *et al.*, 1992b). Thus, these two *Pseudomonas* CLPs represent the only members of this compound class that deviate from the usual ring formation pattern in which the lactonisation takes place between two amino acids of the peptide portion.

CLPs of the viscosin and amphisin group are composed of nine respectively 11 amino acids building the peptide moiety. For both groups the fatty acid chain is in most cases 3-hydroxydecanoic acid (3-HDA). The lactone is formed between the C-terminal amino acid and the Thr-residue found at amino acid position three (Nybroe & Sørensen, 2004). The only exception is the aforementioned arthrofactin, belonging to the amphisin group, which is described to cyclise into the fatty acid chain (Morikawa *et al.*, 1993).

Along with the isolation of orfamide from *P. fluorescens* Pf-5 in 2007 an additional class of CLPs was founded, the orfamide group (Gross *et al.*, 2007). The orfamide group is characterised by a 3-hydroxy dodecanoic or tetradecanoic (myristic) acid connected to the N-terminus of a ten amino acid containing cyclic peptide.

The syringomycin group is regarding the number of amino acids structurally related to the viscosin group, both containing nine AA in the peptide chain. However, in contrast to the viscosin group, the syringomycin group contains unusual amino acids such as 2,4-diaminobutyric acid (Dab), 2,3-dihydro-2-aminobutyric acid (Dhb) and a C-terminal chlorinated threonine residue (4-Cl-

L-Thr) which is responsible for the antifungal activity of syringomycin (Grgurina *et al.*, 1994).

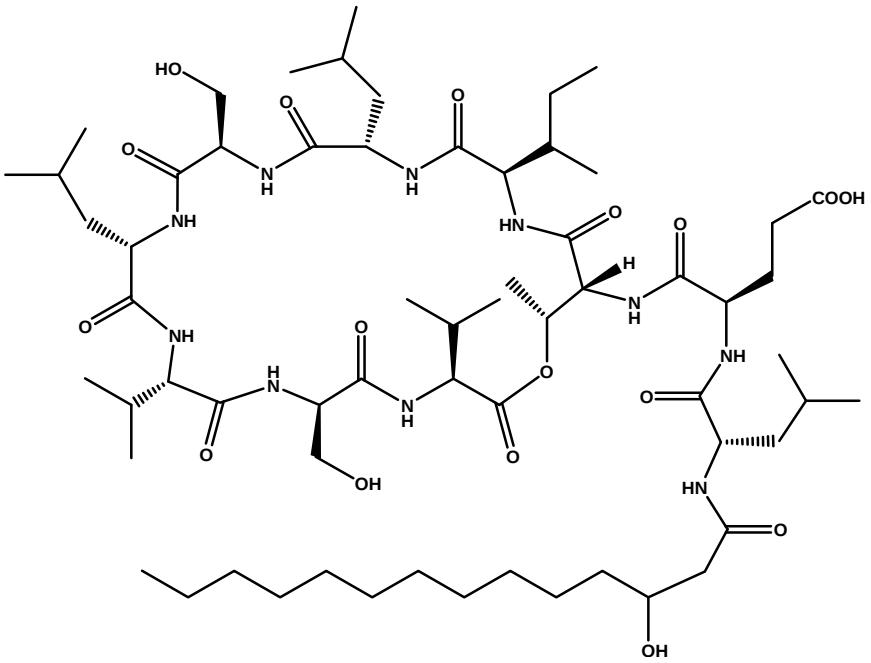

Figure 1.2.1: orfamide A, a cyclic lipopeptide isolated from *P. fluorescens* Pf-5

The cyclisation takes place between the N-terminal serine and the C-terminal 4-Cl-L-Thr. Furthermore, the fatty acid chains can consist of a 3-hydroxy or a 3,4-dihydroxy fatty acid chain in the length of 10-14 carbon atoms (Raaijmakers *et al.*, 2006).

Cyclic lipopeptides of the tolaasin group are distinguished by the so far mentioned CLP groups by shorter side chains and larger peptide moieties. Their lipid tail is either 3-hydroxy-pentanoic acid, 3-HDA or 3-hydroxyoctanoic acid (3-HOA) and the peptide moiety can be composed of 19-25 amino acids, containing unusual amino acids like homoserine (Hse), Dab and Dhb. The lactone ring is formed between the *allo*-Thr residue and the C-terminal amino acid and contains 5-8 amino acids (Bassarello *et al.*, 2004; Nutkins *et al.*, 1991). CLPs belonging to this group are often produced by plant-pathogenic Pseudomonads and constitute important virulence factors (Raaijmakers *et al.*, 2006).

The isolation of entolysins A and B from *P. entomophila* L 48 in 2010 led to a new group of CLPs, harbouring a peptide moiety which contains 14 amino acids as a specific feature. The formation of the lactone ring takes place between the C-terminal

carboxyl-group (Ile) and the 10th amino acid (Ser) (Vallet-Gely *et al.*, 2010; Bode *et al.*, 2012).

Table 1.2.1: primary structures of representatives of the eight classes of CLPs produced by *Pseudomonas* spp.

Name [Ref.]	FA	1	2	3	4	5	6	7	8	9	10	11	12	13	14	15	16	17	18	19	20	21	22	23	24	25
Plusbacin group																										
Plusbacin A_1	C_{14}OH	D-*a*-Thr	D-Ala	L-Pro (3-OH)	L-Arg	L-Asp (3-OH)	D-Ser	L-Pro (3-OH)	L-Asp (3-OH)																	
Plusbacin A_2	C_{15}OH	D-*a*-Thr	D-Ala	L-Pro (3-OH)	L-Arg	L-Asp (3-OH)	D-Ser	L-Pro (3-OH)	L-Asp (3-OH)																	
Plusbacin A_3	$^{i}C_{16}$OH	D-*a*-Thr	D-Ala	L-Pro (3-OH)	L-Arg	L-Asp (3-OH)	D-Ser	L-Pro (3-OH)	L-Asp (3-OH)																	
Plusbacin B_1	C_{14}OH	D-*a*-Thr	D-Ala	L-Pro	L-Arg	L-Asp (3-OH)	D-Ser	L-Pro (3-OH)	L-Asp (3-OH)																	
Plusbacin B_2	C_{15}OH	D-*a*-Thr	D-Ala	L-Pro	L-Arg	L-Asp (3-OH)	D-Ser	L-Pro (3-OH)	L-Asp (3-OH)																	
Plusbacin B_3	$^{i}C_{16}$OH	D-*a*-Thr	D-Ala	L-Pro	L-Arg	L-Asp (3-OH)	D-Ser	L-Pro (3-OH)	L-Asp (3-OH)																	
Viscosin group																										
Viscosin	C_{10}OH	L-Leu	D-Glu	D-*a*-Thr	D-Val	L-Leu	D-Ser	L-Leu	D-Ser	L-Ile																
Viscosinamide	C_{10}OH	L-Leu	D-Gln	D-*a*-Thr	D-Val	L-Leu	D-Ser	L-Leu	D-Ser	L-Ile																
WLIP	C_{10}OH	L-Leu	D-Glu	D-*a*-Thr	D-Val	D-Leu	D-Ser	L-Leu	D-Ser	L-Ile																
Massetolide A	C_{10}OH	L-Leu	D-Glu	D-*a*-Thr	D-*a*-Ile	L-Leu	D-Ser	L-Leu	D-Ser	L-Ile																
Massetolide D	C_{10}OH	L-Leu	D-Glu	D-*a*-Thr	D-*a*-Ile	L-Leu	D-Ser	L-Leu	D-Ser	L-Leu																
Pseudophomin A	C_{10}OH	L-Leu	D-Glu	D-*a*-Thr	D-Ile	D-Leu	D-Ser	L-Leu	D-Ser	L-Ile																
Pseudophomin B	C_{12}OH	L-Leu	D-Glu	D-*a*-Thr	D-Ile	D-Leu	D-Ser	L-Leu	D-Ser	L-Ile																
Pseudodesmin A	C_{10}OH	L-Leu	D-Gln	D-*a*-Thr	D-Val	D-Leu	D-Ser	L-Leu	D-Ser	L-Ile																
Pseudodesmin B	C_{10}OH	L-Leu	D-Gln	D-*a*-Thr	D-Val	D-Leu	D-Ser	L-Leu	D-Ser	L-Val																
Syringomycin group																										
Syringomycin SRA1	C_{10}OH	L-Ser	D-Ser	D-Dab	L-Dab	L-Arg	L-Phe	Z-Dhb	L-Asp (3-OH)	4-Cl-L-Thr																
Syringomycin SRE	C_{12}OH	L-Ser	D-Ser	D-Dab	L-Dab	L-Arg	L-Phe	Z-Dhb	L-Asp (3-OH)	4-Cl-L-Thr																
Syringostatin A	C_{14}OH	L-Ser	D-Dab	L-Dab	D-Hse	L-Orn	L-*a*-Thr	Z-Dhb	L-Asp (3-OH)	4-Cl-L-Thr																
Syringotoxin B	C_{14}OH	L-Ser	D-Dab	Gly	D-Hse	L-Orn	L-*a*-Thr	Z-Dhb	L-Asp (3-OH)	4-Cl-L-Thr																
Pseudomycin A	C_{14}diOH	L-Ser	D-Dab	L-Asp	L-Lys	L-Dab	L-*a*-Thr	Z-Dhb	L-Asp (3-OH)	4-Cl-L-Thr																
Cormycin A	C_{16}diOH	L-Ser	D-Orn	L-Asn	D-Hse	L-His	L-*a*-Thr	Z-Dhb	L-Asp (3-OH)	4-Cl-L-Thr																
Orfamide group																										
orfamide A	C_{14}OH	L-Leu	D-Glu	D-α-Thr	D-α-Ile	L-Leu	D-Ser	L-Leu	L-Leu	D-Ser	L-Val															
orfamide B	C_{14}OH	Leu	Glu	Thr	Val	Leu	Ser	Leu	Leu	Ser	Val															
orfamide C	C_{12}OH	Leu	Glu	Thr	Ile	Leu	Ser	Leu	Leu	Ser	Val															
Amphisin group																										
Amphisin	C_{10}OH	D-Leu	D-Asp	D-*a*-Thr	D-Leu	D-Leu	D-Ser	L-Leu	D-Gln	L-Leu	L-Ile	L-Asp														
Tensin	C_{10}OH	D-Leu	D-Asp	D-*a*-Thr	D-Leu	D-Leu	D-Ser	L-Leu	D-Gln	L-Leu	L-Ile	L-Glu														
Pholipeptin	C_{10}OH	D-Leu	L-Asp	L-Thr	D-Leu	D-Leu	D-Ser	D-Leu	D-Ser	D-Leu	L-Ile	D-Asp														
Lokisin	C_{10}OH	Leu	Asp	D-*a*-Thr	Leu	Leu	D-Ser	Leu	D-Ser	Leu	L-Ile	Asp														
Arthrofactin	C_{10}OH	D-Leu	D-Asp	D-Thr	D-Leu	D-Leu	D-Ser	L-Leu	D-Ser	L-Ile	L-Ile	L-Asp														
Putisolvin group																										
Putisolvin I	C_6	Leu	Glu	Leu	Ile	Gln	Ser	Val	Ile	Ser	Leu	Val	Ser													
Putisolvin II	C_6	Leu	Glu	Leu	Ile	Gln	Ser	Val	Ile	Ser	Leu	Leu/Ile	Ser													
Entolysin group																										
entolysin A	C_{10}OH	D-Leu	D-Glu	D-Glu	D-Val	D-Leu	D-Gln	D-Val	D-Leu	D-Gln	D-Ser	L-Val	L-Leu	D-Ser	Ile											
Tolaasin group																										
Tolaasin I	C_8OH	Dhb	Pro	Ser	Leu	Val	Ser	Leu	Val	Val	Gln	Leu	-	-	-	-	Val	Dhb	*a*-Thr	Ile	Hse	Dab	Lys			
Tolaasin II	C_8OH	Dhb	Pro	Ser	Leu	Val	Ser	Leu	Val	Val	Gln	Leu	-	-	-	-	Val	Dhb	*a*-Thr	Ile	Gly	Dab	Lys			
Tolaasin A	C_8OH	Dhb	Pro	Ser	Leu	Val	Ser	Leu	Val	Val	Gln	Leu	-	-	-	-	Val	Dhb	*a*-Thr	Ile	Hse	Dab	Lys			
Tolaasin B	C_8OH	Dhb	Pro	Ser	Leu	Val	Ser	Leu	Val	Val	Gln	Leu	-	-	-	-	Val	Dhb	*a*-Thr	Val	Hse	Dab	Lys			
FP-B	C_8OH	Dhb	Pro	Leu	Ala	Ala	Ala	Ala	Val	Gly	Ala	Val	Ala	-	-	-	Val	Dhb	*a*-Thr	Ala	Dab	Dab	Phe			
Corpeptin A	C_{10}OH	Dhb	Pro	Ala	Ala	Ala	Val	Val	Dhb	Hse	Val	*a*lle	Dhb	Ala	Ala	Ala	Val	Dhb	*a*-Thr	Ala	Dab	Ser	Ile			
Syringopeptin group																										
SP22	C_{10}OH	Dhb	Pro	Val	Val	Ala	Ala	Val	-	-	-	Val	Dhb	Ala	Val	Ala	Ala	*Dhb*	*a*-Thr	Ser	Ala	Dhb	Ala	Dab	Dab	Tyr
SP25A	C_{10}OH	Dhb	Pro	Val	Ala	Ala	Val	Leu	Ala	Ala	Dhb	Val	Dhb	Ala	Val	Ala	Ala	Dhb	*a*-Thr	Ser	Ala	Val	Ala	Dab	Dab	Tyr
Phe25-SP25A	C_{10}OH	Dhb	Pro	Val	Ala	Ala	Val	Leu	Ala	Ala	Dhb	Val	Dhb	Ala	Val	Ala	Ala	Dhb	*a*-Thr	Ser	Ala	Val	Ala	Dab	Dab	Phe

Deviations of a considered CLP from the name-giving CLP of a class are denoted in light grey, consensus amino acids are denoted in dark grey. Abbreviations: Dab: 2,4-diaminobutyric acid, Dhb: 2,3-dehydroaminobutyric acid, Hse: homoserine α-Thr: *allo*-threonine, D-α-Ile: D-*allo*-isoleucine. All other amino acids are identified by standard three-letter biochemical notation. (Table adopted from Gross *et al.*, 2009); ^{i} = iso - fatty acid

The putisolvin group includes putisolvin A and B, isolated from *P. putida* PCL1445, both characterised by a hexanoic lipid tail, a peptide moiety of 12 AA and a cyclisation which occurs between the C-terminal carboxyl group and the ninth amino acid residue (Kuiper *et al.*, 2004).

Finally, the syringopeptin group contains CLPs composed of 22-25 amino acids, connected to 3-hydroxy-decanoic acid, forming a lactone ring including the terminal 8 AAs.

1.2.2 Antibacterial *Pseudomonas* CLPs

Antibiotically active highlights of *Pseudomonas* CLPs represent the massetolides (massetolide A see figure 1.2.2) and syringomycin E, both exhibiting strong activity e.g. against *Mycobacterium species* (see table 1.2.2; Gerard *et al.*, 1997).

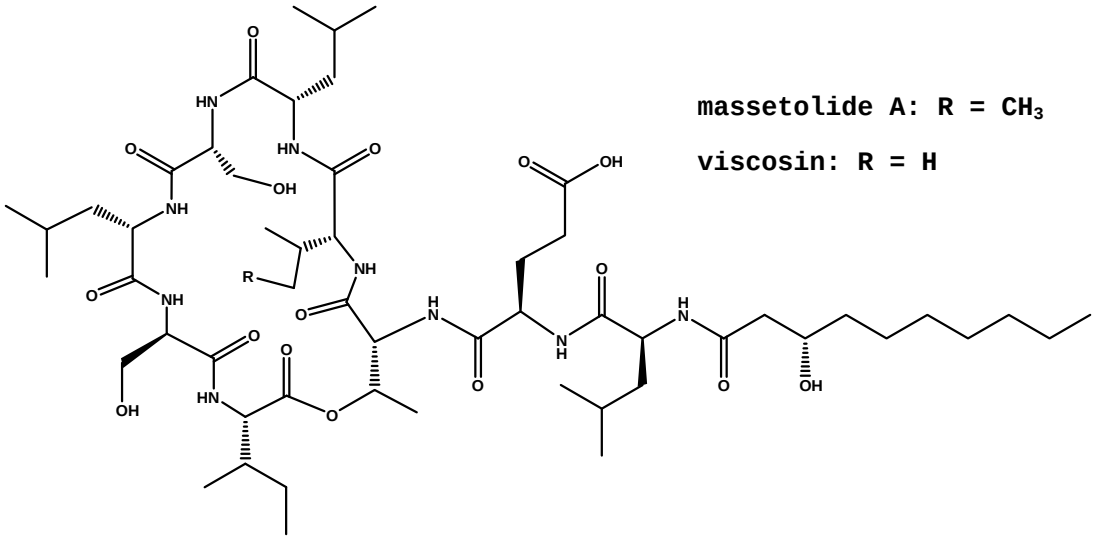

Figure 1.2.2: massetolide A and viscosin, two antimycobacterial cyclic lipopeptides

Mycobacteria constitute a group within the Gram-positives who are eminently sensitive to *Pseudomonas* CLPs which could be traceable to the hydrophobic, waxy cell surface of mycobacteria whereby the passage of hydrophobic CLPs through the plasma membrane might be facilitated (Nybroe & Sørensen, 2004).

Further CLPs isolated from *Pseudomonas* spp. display activities towards *Bacillus megaterium* and *B. cereus* such as the corpeptins, the syringopeptins and tolaasin (Lavermicocca *et al.*, 1997; Emanuele *et al.*, 1998). Low micro molar minimal inhibitory concentrations against *B. megaterium* like 3.75 µM and 4.20 µM for corpeptin A and B, respectively demonstrate again the potency of this substance class.

Table 1.2.2: antimycobacterial activities of selected *Pseudomonas* CLPs

Mycobacterium	**CLP**	**producer**	**MIC [µg/ ml]**
M. avium-intracellulare[a]	massetolide A	*P. fluorescens* SS101	2.5-5
	viscosin	*P.* sp. MF-30	5-10
M. tuberculosis[a]	massetolide A	*P. fluorescens* SS101	5-10
	viscosin	*P.* sp. MF-30	10-20
M. smegmatis[b]	syringopeptin 22A	*P. syringae* pv. syringae B359	2-3
	syringomycin E		1.5

[a] Sayed *et al.*, 2000; Gerard *et al.*, 1997
[b] Buber *et al.*, 2002

Another example for the antibiotic activity of *Pseudomonas* CLPs are the plusbacins (see figure 1.2.3), which belong to guanidine-containing CLPs like empedopeptin (see chapter 1.1.2), exhibiting a similar antibiotic spectrum including MRSA. The mode of action of plusbacin A_3 involves blocking of the transglycosylation process and its forgoing steps of cell wall peptidoglycan synthesis, which is distinct from that of vancomycin (Hashizume & Nishimura, 2008).

	R_1	R_2
A_1	$(CH_2)_{10}$-CH_3	OH
A_2	$(CH_2)_9$-$CH(CH_3)$-CH_3	OH
A_3	$(CH_2)_{10}$-$CH(CH_3)$-CH_3	OH
A_4	$(CH_2)_{12}$-CH_3	OH
B_1	$(CH_2)_{10}$-CH_3	H
B_2	$(CH_2)_9$-$CH(CH_3)$-CH_3	H
B_3	$(CH_2)_{10}$-$CH(CH_3)$-CH_3	H
B_4	$(CH_2)_{12}$-CH_3	H

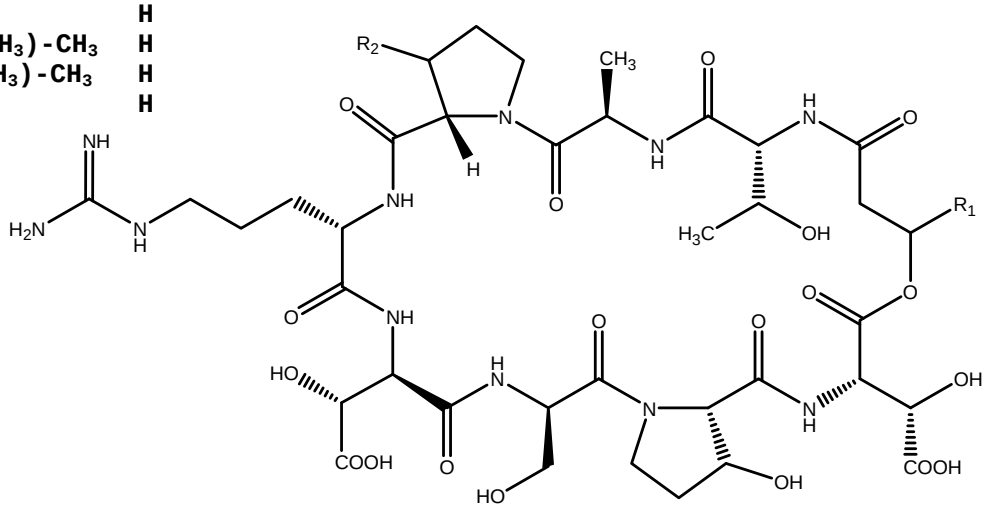

Figure 1.2.3: plusbacins

1.3 Genome mining for CLPs

In recent years the availability of genomes and the affordability of the corresponding analytics strongly increased (Gross & Loper, 2009) and revised the view of the metabolic capabilities of microorganisms (Gross, 2007). As a result of more than 500 microbial genome sequences that are currently available in publicly-accessible databases, it could be observed that the majority of biosynthesis pathways encoding secondary metabolites are hidden in the genome. Empirically, this phenomenon is true for microorganisms possessing a genome size of 4 Mb or higher. This offers a huge potential to find a plethora of new bioactive molecules. Furthermore, in this context a deeper understanding of the biosynthesis of e.g. cyclic lipopeptides and the appearance of the involved genes in the genomes could be gained (Corre & Challis, 2009).

Traditional culture-based, bioassay-guided concepts to discover natural products only lead to a small section of the biosynthetic capacity encoded in the genomes (Gross, 2009). Therefore, new concepts were required to find the new bioactive structures, hidden in the genomes. These perceptions lead to new technologies to screen for specific substance classes with genome mining tools (Zerikly & Challis, 2009; Challis, 2008; Gross *et al.*, 2007).

Several of these tools have been already proposed in this research field (Gross, 2007). To date, four methodologies have been successfully applied (see figure 1.3.1). The ´prediction and screening´ approach predicts at first the substrate specificity of the discovered orphan biosynthetic system as accurately as possible. This bioinformatics analysis allows to propose the resulting secondary metabolite and in addition its corresponding physico-chemical or even bioactive properties. Subsequently, the compound can be discovered by the deduced characteristics, e.g. mass-range or UV-profile.

For orphan gene clusters where only few predictions about the substrate specificity of the encoded enzymes can be made, other approaches such as the ´gene knockout and comparative profiling´ method are more suitable. Hereby, disruption of the gene cluster

of interest by insertion mutagenesis and subsequent comparison of the secondary metabolite spectrum of the resulting mutant with its wild type identifies the corresponding natural product. The metabolite profiling is preferably performed with LC/MS or DAD-HPLC instrumentation.

Another tool applicable to this research field is heterologous expression, i.e. the transfer of the orphan natural product pathway from the original producer into a different optimised bacterial host system.

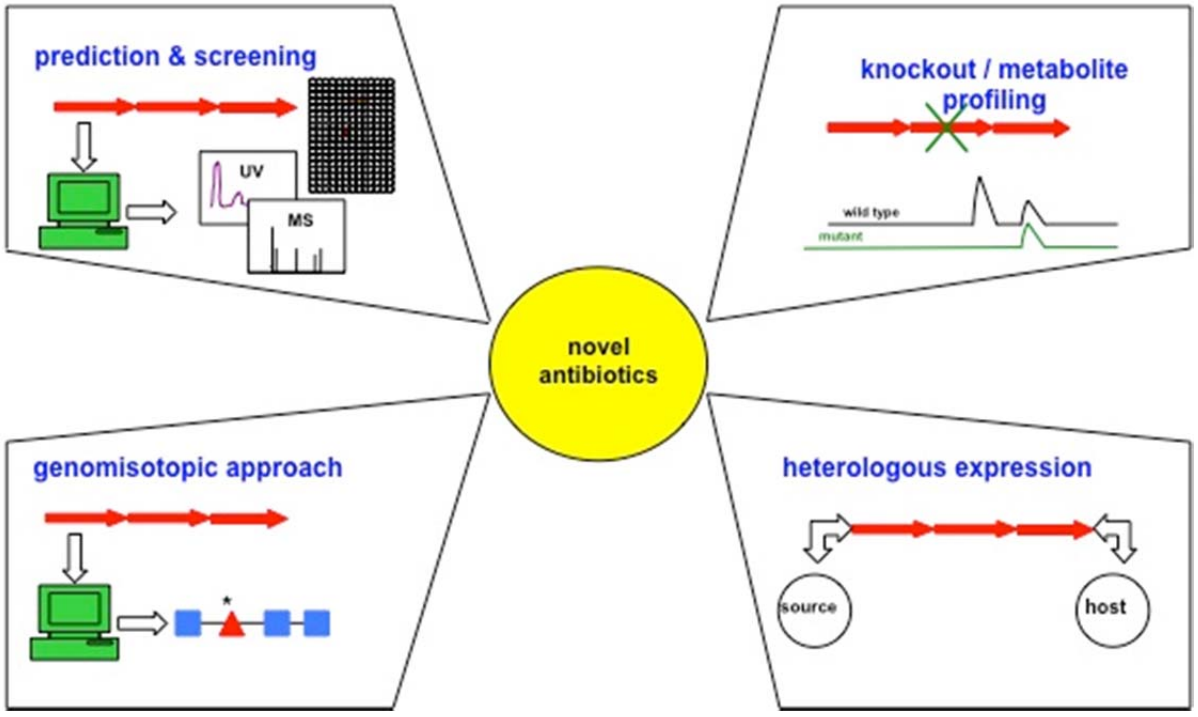

Figure 1.3.1 established genome mining strategies to unveil the products of orphan gene clusters

In 2005, a fourth approach to the genome mining toolbox was added. Hereby, a bioinformatics analysis of the concerned orphan gene cluster allows proposing the resultant secondary metabolite or at least a partial structure. After confirmation of expression, a precursor that will be specifically incorporated into the final product is selected and fed to the microorganism in an isotopically labelled form (e.g. ^{15}N, ^{13}C-amino acids). Natural products utilizing this precursor can then be tracked through the isolation process by ^{1}H-^{15}N, or ^{15}N-^{13}C selective NMR experiments.

Genome mining for new natural product discovery is a method exploiting the evolved availability of DNA sequence data to

locate genes which encode enzymes likely to be involved in natural product synthesis. Hereby, the enzymes can easily be located in sequenced genomes by use of computational sequence comparison tools (Zerikly & Challis, 2009).

In this way, genomes can be ´mined´ for e.g. typical patterns of NRPS, indicating the presence of putative CLP biosynthesis genes. Specific features of NRPS genes involved in CLP synthesis can be the condensation domain of the first NRPS module or the appearance of two TE-domains in the last module of the cluster (de Bruijn *et al*., 2007).

In comparison to traditional isolation strategies, the genome mining approaches offers the following advantages: from the bioinformatics prediction of the resulting compound, the novelty of a compound can be already deduced with a high probability. Thus, isolation efforts will be only undertaken in worthwhile cases. Knowledge about the expected chemical structure including its polarity and stability allows the optimisation of the extraction and isolation strategies to actually obtain the compound. Moreover, genome mining overcomes the difficulty of bioassay-guided technologies to unveil the products of silent pathways by directly screening the genome (Gross, 2009).

Considering the potential of CLPs, their frequent occurrence and structural diversity in the genus Pseudomonas, the application of genome mining tools for the search of NRPS-derived CLPs in Pseudomonads represents a promising approach to find new antimicrobial agents, which might cover the urgent need of new antibiotics.

2 Scope of the present study

The study was performed within the frame of the DFG research group (FOR 854) “Post-genomic strategies for new antibiotic drugs and targets”. Motivated by the globally spreading antibacterial resistance, which represents a serious health threat, the objective of this consortium is to investigate promising new antibiotic compounds, mechanisms and targets, using genomic and reverse genomic approaches. Partial project 8 “Genomic mining for antimicrobial lipopeptides” wanted to contribute to this overall goal by the isolation and testing of antibacterial natural products of the cyclic lipopeptide class. However, instead of employing classical bioassay-guided strategies, a genome driven-approach was applied.

Putative candidate structures should be identified by an *in silico* screening for cyclic lipopeptides in genomes of the promising and underexplored genus *Pseudomonas*. Subsequently, the targeted CLPs will be isolated using chromatographic methods and their structures elucidated by spectroscopic methods e.g. NMR and MS. Upon structure elucidation, the bioactivity of the cyclic lipopeptides should be investigated and first insights into the mode of action shall be gained.

In case of discovery of intriguing biosynthetic backgrounds, the study can be extended by corresponding feeding- and knock-out studies.

In a side-project of this study, the antimicrobial cyclic lipodepsipeptide empedopeptin should be isolated from the strain *Empedobacter haloabium* nov. sp. for the purpose of structural confirmation and collaborative mode of action studies.

3 Material and methods

3.1 Microbiological methods

3.1.1 Media composition

Media	Ingredient	amount [g/l]	reference
DMBgly	Difco™ Minimal Broth Davis without Dextrose	10.6	
	glycerol	1.84	
King´s broth (KB) pH 7.2	Proteose Peptone No.3 (Becton Dickinson)	20	King *et al.*, 1954
	Bacto agar	15	
	glycerol	10	
	K_2HPO_4 (anhydrous)	1.5	
	$MgSO_4$ x 7 H_2O	1.5	
For liquid cultivation the media was composed without Bacto agar.			
Linseed medium pH 7.0	sucrose (= D(+)saccharose)	30	Konishi *et al.*, 1984
	linseed meal	20	
	$(NH_4)_2SO_4$	3	
	$CaCO_3$	5	
Lysogeny broth (LB) pH 7.0	Bacto Tryptone	10	Bertani, 1951
	yeast extract	5	
	NaCl	10	
	glucose	1	
925 Minimal medium broth (925 MM)	K_2HPO_4	3	
	NaH_2PO_4	1	
	NH_4Cl	1	
	$MgSO_4$ x 7 H_2O	0.39	
	saccharose	100	
Saccharose was dissolved in 100 ml water and filtered sterile into the autoclaved media.			

Nutrient broth (NB) pH 7.0	Bacto Peptone	5	
	meat extract	3	
	glycerol	10 ml	
Potato medium	potatoes	300	
	Bacto Peptone	5	
	glucose monohydrate	5	
	NaH_2PO_4 x 12 H_2O	3	
	KH_2PO_4 x 6 H_2O	0.5	
	NaCl	3	

Potatoes were sliced and cooked for 30 min in 500 ml of water. The water was filtered using a round filter, supplemented with the above-mentioned ingredients and refilled with distilled water to one litre.

Seed medium pH 7.0	soluble starch	20	Konishi *et al.*, 1984
	glucose	10	
	meat extract	2	
	yeast extract	2	
	NZ Case	5	
	$CaCO_3$	2	

After suspension of the media ingredients in one litre of water, the medium was left alone till sedimentation took place. Subsequently, the resultant supernatant was decanted and sterilised.

SRM HG*	histidine	4	Mo & Gross, 1991
	$MgSO_4$ x 7 H_2O	0.1971	
	K_2HPO_4	0.8	
	KH_2PO_4	0.8	
	$FeCl_3$	0.0016	
	glucose	10	
	fructose	1	
	arbutin	0.027	

$FeCl_3$, glucose, fructose and arbutin where dissolved in water, proceeded as described in chapter 3.1.4 (heat labile solutions) and added to the autoclaved media.

*syringomycin minimal medium modified according to Prof. Dr. H. Gross

Cultivations containing Amberlite

In case of a subsequent absorber resin-based extraction, the media was supplemented with 2% of Amberlite XAD-16. In order to avoid impurities and to obtain a neutral pH value, the resin was washed in a fritted funnel with 10 litre of water before use.

3.1.2 Bacterial strains

Table 3.1.1: bacterial strains used during this study

bacterial strain	relevant characteristics or purpose	reference(s) or source
E. haloabium nov. sp.	wild-type strain, contains the full functional empedopeptin gene cluster	ATCC 31962
P. syringae pv. syringae B728a	Rifampin-resistant mutant of a wild-type strain originally collected from bean leaves; strain for *in silico* screening	Loper & Lindow, 1987
P. syringae pv. tomato DC3000	Rifampin derivative of DC52 (wild-type *P. syringae* pv. tomato race 0 strain), pathogen of tomato and *Arabidopsis* spp., strain for *in silico* screening	Cuppels, 1986
P. entomophila	strain for *in silico* screening, containing three putative lipopeptide gene clusters	Vodovar *et al.*, 2006
P. sp. SH-C52	wild-type, isolated in the province of Noord-Brabant, The Netherlands, within the frame of a project investigating disease suppressive soils	J. M. Raaijmakers*
C52Δ26[a] (*P.* sp. SH-C52)	knockout mutant, lacking the glycosyltransferase and containing a gentamycin resistance cassette	M. van der Voort, Raaijmakers group
C52Δ26IF[a] (*P.* sp. SH-C52)	in frame knockout mutant missing the glycosyltransferase	M. van der Voort, Raaijmakers group
C52Δ27[a] (*P.* sp. SH-C52)	knockout of the structural NRPS gene	M. van der Voort, Raaijmakers group
C52Δ28[a] (*P.* sp. SH-C52)	knockout of the corresponding monooxygenase comprising a gentamycin resistance cassette	M. van der Voort, Raaijmakers group
C52Δ33[b] (*P.* sp. SH-C52)	knockout of the structural NRPS gene	M. van der Voort, Raaijmakers group

* Associate Professor, Laboratory of Phytopathology, University of Wageningen, the Netherlands

[a] knockout mutants with mutations in the gene cluster predicted to be responsible for the production of a lipodipeptide

[b] knockout mutants with mutations in the genes hypothetically belonging to a chlorinated syringomycin-like lipopeptide

3.1.3 Cultivation of bacteria

Precultures of *Pseudomonas* strains

Precultures were grown 24-48 h at room temperature on a Gerhardt LS30 horizontal shaker at 100 rpm in 50 ml Falcon tubes containing 12 ml DMBgly, inoculated with 80-100 µl cryo culture.

Cultivations for screening of *Pseudomonas* strains using an OSMAC approach

Liquid cultures were inoculated with 250 µl of the corresponding preculture and grown on a small scale (each 250 ml) in KB, LB, NB, DMBgly, 925 MM, SRM HG and potato medium (see chapter 3.1.2) over a period of three days, incubated at different temperatures (RT, 18°C and 28°C) and 140 rpm using an INFORS HT Multitron incubator shaker. For each experiment, the corresponding medium without inoculum served as a control.

Cultivation of main cultures

Main cultures were cultivated in DMBgly in 5 l Erlenmeyer flasks, containing 1.5 l medium, inoculated with 1.5 ml of the preculture and incubated for 3 d at RT and 140 rpm using an INFORS HT Multitron incubator shaker.

Cultivations were done either on a 4.5 l (labelling experiments) or 9 l scale.

Solid cultures

Agar plates were inoculated with a sufficient amount of preculture by streaking and incubated at RT over a period of three days.

Cultivation of *Empedobacter haloabium* nov. sp. (ATCC 31962)

The cultivation of *Empedobacter haloabium* nov. sp. (ATCC31962) was handled using Biosafety Level 2 practices and containment, and performed as described previously (Konishi *et al.*, 1984).

Precultures were cultivated in 10 ml seed media inoculated with 100 µl cryo culture in 50 ml Falcon tubes for 48 h at RT on a Gerhardt LS30 horizontal shaker at 100 rpm. 3 l of the main culture were grown in linseed medium (see fig. no. 3.1.1) in 5 l Erlenmeyer flasks, each containing 1 l of the culture broth and inoculated with 5 ml of preculture. Cultures were fermented for four days at 27°C on an INFORS HT Multitron incubator shaker shaking at 140 rpm.

Figure 3.1.1: linseed medium, cultivation of *E. haloabium* nov. sp.

3.1.4 Sterilisation

Heat-stable media, buffers and solutions and glassware were sterilised in a steam autoclave (Varioklav) at 121°C and 1.2 bar for 20 min. In case culture media contained, or autoclavable equipment had contact with bacteria belonging to biosafety class two, the exhaust filter system was additionally activated. Filters with cellulose acetate membranes (Millipore, Renner, Darmstadt, Germany) with a pore diameter of 0.22 µm were used to filter sterilise heat sensitive solutions.

3.1.5 Bacterial growth curve determination and quantitative analysis of brabantamide A production over a 72 h period

For the determination of doubling time and growth rate nine cultures were prepared. These were grown in 5 l Erlenmeyer flasks filled with 1.5 l DMBgly medium. To prevent cultivation differences and achieve a uniform growth it was decided to work with nine 1.5 l cultures instead of growing many small cultures.

All flasks were inoculated with 1.5 ml preculture. The time of inoculation was set as the starting point.

Samples were taken every 1.5 hours over a period of four days and processed to the following experimental steps:

Three of nine cultures were rotationately harvested at all defined harvesting times to assure similar culture volumes and growth conditions. 100 ml of each of the cultures were withdrawn under sterile conditions after shaking the flasks to guarantee a uniform distribution of cells and secreted substances. 1 ml of every sample was transferred into a cuvette to measure the optical density on a Shimadzu UV mini 1240 UV-VIS spectrophotometer at 600 nm.

After determination of the UV absorption, the remaining culture was acidified with $HCl_{conc.}$ to a pH value of 2 and extracted three times with EtOAC (1:1). The combined organic supernatants were evaporated to dryness and analysed by LC-MS.

For product quantification, five standard solutions were prepared:

Stock solution: 0.5 mg/ml of brabantamide A in MeOH

Solution 1: 250 µl stock solution + 750 µl MeOH = standard 5 [0.125 mg/ml]

Solution 2: 50 µl stock solution + 4950 µl MeOH = standard 4 [0.005 mg/ml]

Solution 3: 250 µl of solution 2 + 250 µl MeOH = standard 3 [0.0025 mg/ml]

Solution 4: 100 µl of solution 2 + 900 µl MeOH = standard 2 [0.0005 mg/ml]

Solution 5: 400 µl of solution 4 + 400 µl MeOH = standard 1 [0.00025 mg/ml]

Calculation of the specific growth rate and the doubling time

OD = optical density
OD_0 = optical density at t_0
t = time [h]
µ = specific growth rate
t_d = doubling time [h]

$$OD = OD_0 \times e^{\mu t}$$

$$\mu = \frac{\ln 2}{t_d}$$

3.1.6 Investigation of suitable carbon sources for *Pseudomonas* sp. SH-C52

In order to optimise the cultivation medium for maximum secondary metabolite production, it was investigated, which carbon sources can be utilised by the strain *Pseudomonas* sp. SH-C52. For this purpose an API®50CH standardised test (Biomerieux, Marcy l'Etoile France) system was employed. The system associates 50 biochemical tests for the study of the carbohydrate metabolism of microorganisms. API®50 CH was used in conjunction with API®50CHB/E Medium.

Inoculum cultures with a turbidity equivalent to 2 McFarland (0.451 at 600 nm) were prepared according to the manufacturer´s protocol and control strips applied. Test strips were read after 24 and 48 hours of incubation at room temperature.

With the exception of the esculin test, a positive test result is indicated by a change in colour of the medium from red to yellow. This reaction is based on acidification of the media by a growing culture, i.e. utilisation of the carbon source, which is visualized by the pH dependent indicator phenol red. In case, the bacterium can hydrolyse the compound esculin as carbon source, a change in colour from red to black is observed.

3.1.7 Detection of antibacterial activity

Determinations of the antibacterial activity were performed by Michaele Josten (Member of the research group of Prof. Dr. H. - G. Sahl, Institute of Medical Microbiology, Immunology and Parasitology (IMMIP), Pharmaceutical Microbiology Unit, University of Bonn, Bonn, Germany).

Determination of the MIC

MIC determinations were performed in microtiter plates. Strains were grown in half-concentrated Mueller-Hinton (MH) broth (Oxoid). The only exception was *Arthrobacter crystallopoietes* DSM 20117 which was grown in tryptic soy broth (Oxoid).

MICs with serial twofold dilution steps were performed (1:2). Bacteria were added to give an inoculum of 10 CFU/ml in a volume of 0.2 ml. Bacteria were incubated for 24 h at 37°C. Afterwards the MIC was read as the lowest compound concentration causing inhibition of visible growth. Results are mean values of three independent determinations. Since some lipopeptides were previously reported to possess a calcium dependency for optimum activity (Baltz ***et al.***, 2005), the effect of calcium substituted medium on the MICs was evaluated. Two organisms, ***S. aureus*** SG511 and ***Bacillus subtilis*** 168 were used in the test which consisted of a broth dilution MIC determination in supplemented (0.2 mg/ml $CaCl_2$) and unsupplemented in half-concentrated MH broth.

Agar diffusion assays

The antibacterial activity was determined by agar diffusion assays. Culture plates (5% sheep blood Columbia agar, BD) were overlaid with 3 ml tryptic soy soft agar, inoculated with 3 TSB (tryptic soy broth, Oxoid) growth suspension of the bacteria to be tested. Compounds were diluted with DMSO to a concentration of 1 mg/ml and 3 µl of this dilution were placed on the surface of the agar. After 24 h incubation at 37°C the diameter of the inhibition zone was measured. The indicator strains represent clinical isolates from distinct patients as well as standard laboratory strains and are listed below. The strains were maintained on MH agar or on blood agar.

Gram-positive bacteria:

Arthrobacter crystallopoietes DSM 20017, ***Bacillus megaterium, B. subtilis*** 168, ***Corynebacterium diphteriae, C. pseudodiphteriticum, C. xerosis*** Va 167198, ***Enterococcus faecium*** I-11305b, ***E. faecium*** I-11054, ***Listeria welchimeri*** DSM 20650, ***Micrococcus luteus*** ATCC 1856, ***Mycobacterium smegmatis*** ATCC 70084, ***Staphylococcus aureus*** SG511, ***S. aureus*** 5185 (MS*), ***S. aureus*** LT-1334 (MR*), ***S. epidermidis*** LT-1324 (MR*), ***S. epidermidis*** ATCC 12228, ***S. simulans*** 22,

Gram-negative bacteria:

Eschericha coli DH5 alpha, ***Escherichia coli*** O-19592, ***Klebsiella pneumonia*** subsp. ***ozeanae*** I-10910, ***Citrobacter freundii*** I-11090, ***Pseudomonas aeruginosa*** I-10968, ***Serratia marcescens, Stenotrophomonas maltophila O-16451 and S. maltophila I-10717***

Fungi:

Candida albicans

*MS = methicillin – susceptible, MR = methicillin - resistant

3.1.8 Determination of cytotoxicity

Cytotoxicity tests were performed by the research group of Prof. Dr. H. Brötz-Österhelt (Institute of Pharmaceutical Biology and Biotechnology, University of Düsseldorf, Germany).

Toxicity towards THP1 human leukemic monocyte cells and BALB/3T3 mouse embryonic fibroblast cells were measured using a fluorometric Alamar Blue assay.

THP1 cells were grown in DMEM medium (PAN Biotech GmbH), containing 4.5 g/l glucose and 3.7 g/l $NaHCO_3$, supplemented with 10% foetal calf serum (v/v), 1% sodium pyruvate and 1% L-glutamine. BALB/3T3 cells were cultured in RPMI-1640 medium (PAN Biotech GmbH) containing 2.0 g/l $NaHCO_3$, supplemented with 10% foetal calf serum (v/v), 1% L-glutamine and 1 % penicillin-streptomycin (10000 U/ml penicillin and 10 mg/ml streptomycin; PAN Biotech GmbH).

Cells were seeded in 96-well plates at 10 000 cells/well in 190 µl. Pure compounds were dissolved in 20 µl DMSO. For serial dilutions, a suspension of 2 mg/ml was generated, using medium as diluent, and 11-fold serial dilutions thereof were made; 10 µl sample of a dilution was added per well, resulting in a final assay concentration of 0.031 – 64 µg test compound per ml. The plates were incubated for 72 h in a humidified atmosphere of 5% CO_2 and at 37 °C. Negative controls consisted of the indicated medium, while cycloheximide served as a positive control.

After 48 h, 10 µl Alamar Blue/well were added and the incubation continued for another 24 h. After 72 h of total incubation time, the fluorescence was read using a 96-well fluorometer (Tecan) with excitation at 560 nm and emission at 600 nm. Results are expressed in relative fluorescence units (RFU), i.e. the ratio of fluorescence emitted by treated cells vs. fluorescence emitted by the control (medium only). RFU were plotted against sample concentrations and the corresponding IC_{50} values computed.

3.1.9 Luciferase reporter gene assay

Luciferase reporter gene assays were performed by the research group of Prof. Dr. H. Brötz-Österhelt (Institute of Pharmaceutical Biology and Biotechnology, University of Düsseldorf, Germany).

Table 3.1.2: applied *Bacillus subtilis* reporter strains

reporter strains	constructs of the promoters
***B. subtilis* 1S34pS63MH124**	**yvgS* promoter fused to firefly luciferase gene, transcription reporter gene assay, Ery^R
***B. subtilis* 1S34pS72**	**yheI* promoter fused to firefly luciferase gene, translation reporter gene assay, Ery^R
***B. subtilis* 1S34pS77**	**yorB* promoter fused to firefly luciferase gene, replication reporter gene assay, Ery^R
***B. subtilis* 1S34pS107**	**ypuA* promoter fused to firefly luciferase gene, cell wall synthesis and cell envelope stress reporter gene assay, Ery^R
***B. subtilis* 1S34pS130**	*yvqI* promoter fused to firefly luciferase gene, cell wall synthesis and cell envelope reporter gene assay, Ery^R

* Urban *et al.*, 2007; Ery^R = erythromycin-resistant

Reporter strains were grown on LB agar and then cultured overnight in 10 ml LB medium, both supplemented with 5 µg/ml erythromycin at 37°C and 200 rpm. Cultures were diluted to an OD_{600} of 0.05 in 20 ml LB medium or Belitzky minimal medium (Stülke *et al.*, 1993) with 5 µg/ml erythromycin, grown to an OD_{600} of 0.9 or 0.4 (*yheI* strain) under the conditions described above and diluted to an OD_{600} of 0.02.

A serial twofold dilution of each test compound (0.031 µg/ml to 64 µg/ml) in 60 µl LB broth in a white 96-well flat bottom polystyrol microtiter plate (Greiner) was inoculated with 60 µl of the adjusted bacterial suspension. Each microtiter plate contained negative controls (full assay mixture without compound addition) and positive controls (reference antibiotics known to cause maximal signal induction).

Table 3.1.3: antibiotics used as reference compounds

antibiotic	**source**	**concentration**	**strain**
chloramphenicol	Sigma-Aldrich	0.049- 100 µg/ml	*yheI*
ciprofloxacin	Fluka	0.003- 6.25 µg/ml	*yorB*
rifampicin	AppliChem	3x 10^{-5} – 0.0625 µg/ml	*yvgS*
vancomycin	AppliChem	0.049- 100 µg/ml	*yvgI* and *ypuA*

Microtiter plates were incubated at 37°C for a period depending on the induction kinetics of the reporter strain: 1 h for the *yvqI* and *ypuA* strains, 1.5 h for the *yvgS* strain, 3.5 h for the *yorB* strain and 4 h for the *yheI* strain. After this incubation step 60 µl citrate buffer (0.1 M, pH 5) containing 2 mM luciferin (Serva) was added and flash luminescence was measured using a microtiter plate reader (Mithras, Berthold or Infinite 200, Tecan).

3.1.10 Incorporation of radioactive metabolites

Tests regarding the incorporation of radioactive metabolites were performed by Michaele Josten (IMMIP, Pharmaceutical Microbiology Unit, University of Bonn, Bonn, Germany).

A culture of *Pseudomonas* sp. SH-C52 was grown in half-concentrated MH broth (Oxoid). The culture was incubated overnight at 37°C and subsequently diluted to an optical density (OD) of ~ 0.04. The culture was divided into two 10 ml aliquots in Erlenmeyer flasks. The first aliquot was grown up to an OD of 0.5 and the second sample up to an OD of 0.95. After 10 min each culture was supplemented with 25 µl ^{14}C-proline (0.5 nmol/ml). Samples were drawn on schedule. 500 µl of the culture were pipetted into 2 ml ice cold trichloroacetic acid (10% TCA + 1 M

NaCl + 1 ml cool metabolite). Precipitations rested at least 30 min on ice before filtering with Whatman glass fibre filters and washing with 5 ml of a solution containing 2.5% TCA, 1 M NaCl and 50 mM cold metabolite. Filters were dried and transferred to counting vials filled with scintillation fluid (Quickszint 100; Zinsser, Frankfurt, Germany). The radioactivity was measured in a beta-counter (1900CA; Packard, Downers Grove, IL, USA).

3.2 Biosynthetic investigations of brabantamides

Biosynthetic studies were carried out by provision of putative isotopically labelled precursors of brabantamide to the bacterium *P.* sp. SH-C52. The cultivation of the bacterium for the labelling experiments was performed according to established procedures (chapter 3.1.1) and done on a 4.5 litres scale. The addition of precursors occurred 4 h after inoculation.

Precursors were dissolved in a small amount of purest water to avoid a significant increase of the culture volume. The solution was sterile filtered, divided into equal parts and pipetted into three 5 l Erlenmeyer flasks, each containing the 1.5 l of bacterial broth.

Thus were added:

1.0 g 1-^{13}C – sodium acetate (222.2 mg/l)

1.0 g 1,2-^{13}C - sodium acetate (222.2 mg/l)

1.0 g 1-^{13}C - L-glycine (222.2 mg/l)

250 mg 1-^{13}C – L-proline (55.6 mg/l)

1.0 g 1-^{13}C - hydrogen carbonate (222.2 mg/l)

500 mg 1-^{13}C – L-serine (111.1 mg/l)

250 mg U-^{13}C – L-serine (55.6 mg/l)

The isotopically labelled compounds were obtained from Cambridge Isotope Laboratories or from Aldrich, respectively.

After addition of the dissolved stable isotope precursors, the cultivation was continued as described above.

3.3 Chemical methods

3.3.1 Extraction of bacteria

Extraction of *Pseudomonas* cultures

Liquid cultivation:

The culture broth was adjusted with $HCl_{conc.}$ to a pH value of 2. The acidified cultures were extracted three times with ethyl acetate (1:1) and the resulting organic supernatant was evaporated to dryness with a vacuum rotary evaporator at 30°C. The water phase was discarded.

Liquid cultivation containing Amberlite XAD-16:

Cells and XAD absorber resin was harvested from the culture broth employing a fritted funnel. Subsequently, the residue was washed with water to remove adherent cells from the harvested resin. The washed adsorber resin was extracted by rinsing 3 x 1 l of EtOAc through the fritted funnel. The crude extract was dried by evaporation in vacuum at 30 degree.

Solid cultivation:

The complete agar material was chopped into pieces and transferred into Erlenmeyer flasks (see figure 3.3.1). Extraction was performed by addition of an equal amount of acidified ethyl acetate (250 ml per plate) and stirring over a period of 30 min. This procedure was repeated twice and the resulting organic supernatant was evaporated to dryness using a vacuum evaporator at 30°C.

Figure 3.3.1: extraction of solid cultivations

Extraction of ***Empedobacter haloabium*** nov. spec.

The culture broth was acidified with $HCl_{conc.}$ to a pH-value of 3. After addition of an equal volume of n-butanol, the two-phase system was stirred under the laminar air flow over a period of one day. The organic supernatant was decanted and evaporated to dryness with a vacuum rotary evaporator at 40°C. The aqueous layer was discarded.

3.3.2 Vacuum liquid chromatography

VLC was carried out using column with a diameter of 65 mm filled with Polygoprep 60 C18 material (0.05 mm, Macherey-Nagel 711500.1000; reversed phase). For this purpose the columns were wet-packed with an adequate amount of Polygoprep dissolved in methanol and condensed with vacuum. Afterwards, the columns were equilibrated with the starting composition of the eluents (methanol - water – mixtures).

The crude extract was dissolved in a small amount of the first eluent and applied to the top of the column with a spoon to avoid destruction of the column bed. Elution was started by pouring mobile phase on the top of the column and if necessary vacuum was applied.

In general, the following stepwise gradient was applied:

Fraction 1: MeOH/H_2O 50:50

Fraction 2: MeOH/H_2O 70:30

Fraction 3: MeOH/H_2O 90:10

Fraction 4: MeOH/H_2O 100:0

Fraction 5: DCM 100%

The volume of solvents was adjusted to the column size. Typically 400 ml of the first eluent was used for equilibration and 400 ml of the mixtures for fractions 1-3 were applied. Fractions 4 and 5 were performed employing 600 ml solvent to achieve complete recovery of the extracts. Fractions were

collected in round-bottom flasks and evaporated to dryness at 30°C under reduced pressure using a rotary evaporator.

3.3.3 High performance liquid chromatography

HPLC was carried out using one of the following HPLC systems:

System 1: a Merck-Hitachi system consisting of a D-6000A interface with D-7000 HSM software version 4.0, a L-6200A pump, a Rheodyne 7725i injector and a L-4500 diode array detector.

System 2: an Agilent system (1100 series) containing a G1379A degasser, a G1312A binary pump, a G1312A auto sampler and a G1315C diode array detector; software: ChemStation.

System 3: a Waters system equipped with a 600 controller pump, a 717 plus auto sampler with inline degasser Waters AF and a 996 photodiode array detector; software: Millenium[32].

System 4: a Merck-Hitachi system consisting of a Knauer interface box, a L-6200A pump, a Rheodyne 7125 injector and an UV-VIS L-7420 detector; software: Knauer EuroChrom® 2000 version 1.65.

Applied columns:

Column 1: Macherey-Nagel Nucleosil 120-5 C_{18} (5 µm, 250 x 4 mm)

Column 2: Nucleodur C_{18} Isis (5 µm, 250 x 4.6 mm, EC)

Column 3: Nuleodur 100-5 HILIC (250 x 4.6 mm, EC)

Column 4: XTerra™ RP_{18} (5 µm, 250 x 4.6 mm)

Column 5: Waters Symmetry Shield RP 18 (5 µm, 250 x 4.6 mm)

Column 6: Knauer Eurospher-100 C18 (5 µm, 250 x 8 mm)

Column 7: Macherey-Nagel Nucleodur 100-5 C_{18} (5 µm, 250 x 8 mm)

Typical flow rates were 0.8 ml/min and 1.5-1.8 ml/min for 4.6 mm columns and 8 mm HPLC columns, respectively. All solvents except H_2O were either distilled prior to use or of HPLC-grade quality. Buffer solutions like ammonium acetate buffer were sterile

filtered to avoid injection of insoluble parts which otherwise would cause an elevated backpressure.

3.3.4 NMR spectrometry

NMR spectra of the isolated compounds were recorded on a Bruker Avance 300 DPX operating at 300 MHz (^{1}H) and 75 MHz (^{13}C), a Bruker Avance 500 DPX spectrometer operating at 500 MHz (^{1}H) and 125 MHz (^{13}C), a Varian INOVA 600 spectrometer operating at 600 MHz (^{1}H) and 150 MHz (^{13}C) or a Varian INOVA 900 spectrometer, operating at 900 MHz (^{1}H) and 225 MHz (^{13}C). NMR spectra were processed using Bruker XWIN-NMR Version 2.6, 3.1 and 3.5 software or MNova. Spectra were referenced to residual solvent signals with resonances at $\delta_{H/C}$ 2.04/29.8 ($(CD_3)_2CO$), $\delta_{H/C}$ 3.35/49.0 (CD_3OD) and $\delta_{H/C}$ 2.50/39.5 (DMSO). To deduce the multiplicity of carbons, DEPT experiments were performed. In order to elucidate the complete structures the following NMR experiments were carried out:

^{1}H, ^{13}C, DEPT135, ^{1}H-^{1}H COSY, HSQC (^{1}H-^{13}C direct correlation) and HMBC (^{1}H-^{13}C long-range correlation), NOESY (Nuclear Overhauser Effect Spectroscopy) employing different mixing times (300 ms, 400 ms, 500 ms and 1500 ms)

Calculation of the incorporation ratio of ^{13}C labelled compounds

Experiments with single labelled substances:

To evaluate the enrichment of the labelled carbon atoms, the integral of carbon 6´ of brabantamide A was set to 1.000 in every spectrum and the integrals of the other carbons were compared in the spectra of the labelled and the non-labelled compound.

Enrichment = enhancement of the signal x 1.1% - 1.1%

Enhancement of the signal = quotient of the integrals (enriched value / natural abundance)

1.1% = natural abundance of ^{13}C atoms

Labelling experiment with 1,2-^{13}C-acetate:

To evaluate the relative enrichments first the total integral of the ^{13}C-NMR signal for each resonance of brabantamide A was measured. The integration value of the ^{13}C signal appearing in the centre of each cluster, representing those ^{13}C atoms not coupled to adjacent ^{13}C atoms for each resonance of brabantamide A was quantified and the quotient was determined (Chang ***et al.***, 2004).

$$\text{Relative enrichment [\%]} = \frac{\textit{total integral of enriched carbon atom}}{\textit{integral of uncoupled signal}} \times 100$$

3.3.5 Mass spectrometry

HPLC-ESI-MS measurements were conducted by E. Eguereva (Institute for Pharmaceutical Biology, University of Bonn) using an Agilent 1100 series HPLC including diode array detector, coupled with an API 2000 Triple Quadrupole LC/MS/MS. Prior to the measurement, the samples were dissolved in LC/MS-grade methanol, setting up to a final concentration of 5 mg/ml and transferred to IVA TPX vials 32 x 11.6 mm with an integrated glass micro insert (0.2 ml). HPLC was carried out employing a Macherey-Nagel Nucleodur 100 C-18 column (5 µm, 125 mm x 2 mm) and a buffered (2 mmol NH_4OAc) gradient system ($MeOH/H_2O$). At a flow of 0.25 ml/min the percentage of MeOH was increased from 10 % to 100% over 20 min followed by 10 min isocratic elution at 100 % MeOH. Experiments were recorded in positive (+Q1) as well as negative (-Q1) mode using a declustering potential of either 30 V or 70 V. Spectra were processed via Applied Biosystems/MDS Sciex Analyst Software.

HR-ESI-MS measurements were performed by Ms. Peters-Pflaumbaum, Department of Chemistry, University of Bonn using a Bruker Daltonics micrOTOF-Q instrument.

3.3.6 Optical rotation

The optical rotation was measured on a Jasco model DIP-140 polarimeter. The standard measurement was carried out in methanol at λ = 589 nm corresponding to the sodium D line. The temperature was monitored by an external thermometer. The sample cell length was 1 dm.

$$[\alpha]_D^T = \frac{\alpha}{c \times d} \times 10^4$$

$[\alpha]_D^T$ = specific optical rotation [°]

D = sodium D line (λ = 589 nm)

T = Temperature [°C]

α = rotation angle [°]

c = concentration [g/100 ml]

d = cell length [mm]

The values for the rotation angle α were determined by an average value based on at least 12 measurements.

3.3.7 IR spectroscopy

IR spectra were obtained employing a Perkin-Elmer FT-IR Spectrum BX spectrometer interfaced with a Specac Golden Gate Diamond ATR system. Data processing was conducted with Spectrum v3.01 software.

3.3.8 UV spectroscopy

UV spectra were recorded on a Perkin-Elmer Lambda 40 with UV WinLab Version 2.80.03 software, using 1.0 cm quartz cells. The molar absorption coefficient ε was determined in accordance with the Lambert-Beer-Law. Spectra were measured in methanol.

$$A = \varepsilon \times c \times d$$

A = Absorption

ε = molar absorption coefficient $[\frac{l}{mol \times cm}]$

c = concentration $[\frac{mol}{l}]$

d = cell length [cm]

3.3.9 CD spectroscopy

CD spectra were recorded using a J-810 spectropolarimeter at the Kekulé Institute of Organic and Biochemistry, University of Bonn. The sample was dissolved in methanol to a concentration of 0.5 mg/ml and measured at a wavelength range of 190 to 400 nm. The average value of 5 measurements was taken with a sensitivity of 100 mdeg and a scanning speed of 50 nm/min at 20 degree. The obtained raw-spectrum was further processed with the smoothing function integrated in the measurement software.

3.3.10 Solid phase extraction (SPE)

Solid phase extraction was carried out using Bakerbond prepacked columns RP with 2000 mg capacity. The column was equilibrated with the initial mobile phase (methanol-water – mixture).

The crude extract was dissolved in a small amount of the first eluent mixture and applied to the top of the column with a pipette. Elution was started by pouring mobile phase on the top

of the column and vacuum was applied using a JT Baker SPE-24G glass vacuum chamber 7423-00.

30 ml of the following eluents were used:

Fraction 1: MeOH/H_2O 50:50

Fraction 2: MeOH/H_2O 70:30

Fraction 3: MeOH/H_2O 90:10

Fraction 4: MeOH/H_2O 100:0

Fraction 5: DCM 100%

Fractions were collected in round-bottom flasks and evaporated to dryness at 30°C under reduced pressure using a rotary evaporator.

3.4 Bioinformatics tools

Genes and operons for ***in silico*** analysis were found by BLAST homology and by searching the corresponding genomes in GenBank (NCBI database).

Open reading frames (ORFs) were identified using ORF Finder from the NCBI database, translated with the ExPASy translate tool (http://web.expasy.org/translate/) and analysed with Blastp in the NCBI database.

The NRPS/PKS predictor software (Bachmann & Ravel, 2009) was used to predict the backbone of cyclic lipopeptides, to identify different domains and to extract the corresponding sequences. For further investigations on the composition of gene clusters, antiSMASH: rapid identification, annotation and analysis of secondary metabolite biosynthesis gene clusters (Medema ***et al.***, 2011) was used. For phylogenetic analyses of different domains, alignments were performed with ClustalW2 (Larkin ***et al.***, 2007). Phylogenetic trees were generated using Genious v5.5, created by Biomatters, available from http://www.geneious.com.

For classifications of C-domains, the web-based software NaPDos (Natural Product Domain Seeker; Ziemert ***et al.***, 2012) was applied.

4 Results and discussion

4.1 *In silico* screening for cyclic lipopeptides

At the beginning of the study and continually during the study genome sequences of the genus *Pseudomonas* or of related genera, which were either publicly available or available in collaboration with other research labs, were subjected to an *in silico* screening for cyclic lipopeptides.

Initially, eight gene clusters were found and analysed. A bioinformatical analysis of the corresponding genes led to first insights into the expected size and structure of the products of the orphan gene clusters.

P. entomophila L48

Already in the publication about the genome sequence of *P. entomophila* L48 three putative NRPS-based biosynthetic gene clusters were reported (Vodovar *et al.*, 2006).

The first of the three lipopeptide biosynthesis gene clusters in *P. entomophila* L48, located on the genes *pseen2716-pseen2718* is predicted to encode a hexa-lipopeptide (see figure 4.1.1).

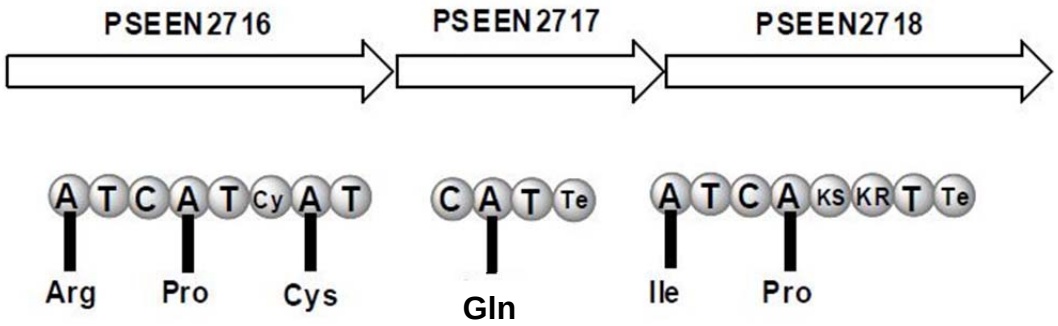

Figure 4.1.1: putative hexa-lipopeptide in *P. entomophila* L48 (also present in *P. syringae* pv. syringae B728a and phaseolica 1448A)

Analysis of the deduced amino acid sequences revealed that the proteins PSEEN2716, PSEEN2717 and PSEEN2718 comprise in total six NRPS-modules. With the exception of the first and third module, each module is composed of a condensation domain, an adenylation domain and a thiolation domain, whereby PSEEN2718 is furthermore

extended by polyketidic domains and represents therefore a hybrid NRPS-PKS.

In case of PSEEN2716 and PSEEN2718, the first module is lacking the condensation domain and PSEEN2716 comprises a cyclisation domain instead of the C-domain in module three. TE-domains were located terminally in PSEEN2717 and PSEEN2718. Using NRPS/PKS web based software (see chapter 3.4) the primary structures of the six A-domains were analysed, leading to the following proposed composition of the peptide moiety: Arg-Pro-Cys-Gln-Ile-Pro.

The second lipopeptide biosynthesis gene cluster in the genome of *P. entomophila* L48, located on *pseen0132*, *pseen3044-pseen3045* and *pseen3332* is suggested to encode, depending on the role of *pseen0132* and *pseen3332* either a dodeca-, tetradeca- or a pentadeca-lipopeptide (see figure 4.1.2). In case of a 14-AA or 15-AA containing peptide, the cluster appears to be split and with the exception of the tandem thioesterase and the missing C domain in PSEEN0132 canonical.

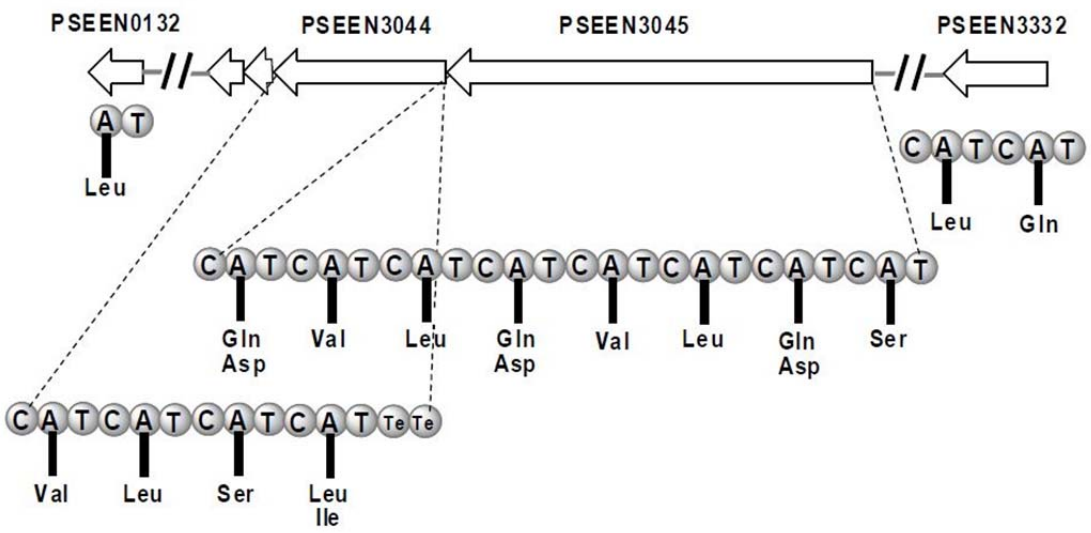

Figure 4.1.2: putative dodeca-, tetradeca- or pentadeca-lipopeptide (possibly putisolvin-like) present in *P. entomophila* L48 (entolysin)

During the course of this study the tetradeca-lipopeptide entolysin could be isolated and correlated to the aforementioned gene cluster by Lemaitre and co-workers (Vallet-Gely *et al.*, 2010). The corresponding genes *pseen3332* and *pseen3044-pseen3045* were renamed as *etlA*, *etlC* and *etlB*, respectively, whereas it was shown, that *pseen0132* was not essential for the production of the resulting entolysins.

The third lipopeptide predicted to be produced by *P. entomophila* L48 (*pseen2139-pseen2156*) was a putative penta-lipopeptide (see figure 4.1.3). Analysis of the corresponding amino acid sequences showed one typical module (CAT) each one encoded by *pseen2149* and *pseen2150* and three by *pseen2155*, respectively. Furthermore, a TE-domain in PSEEN2139, a ketosynthase and a T-domain in PSEEN2153 could be assigned to the biosynthesis gene cluster.

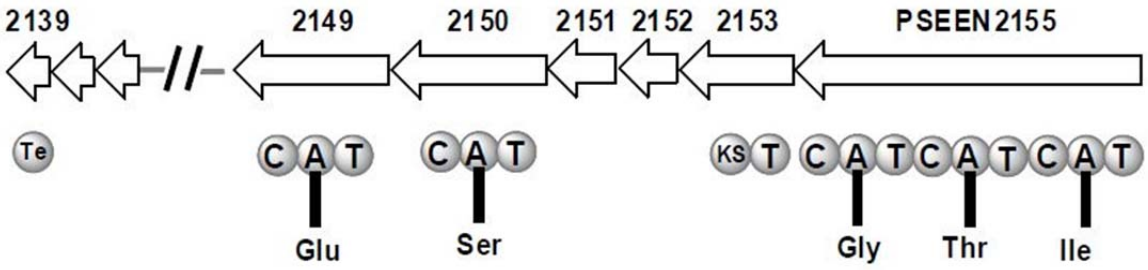

Figure 4.1.3: putative pentalipopeptide (also present in *P. syringae* pv. syringae, *psyr_1792-1794*)

Using NRPS/PKS web based software (see chapter 3.4) the primary structures of the five A-domains were analysed, leading to the following proposed composition of the peptide moiety: Ile-Thr-Gly-Ser-Glu.

Pseudomonas syringae pv. syringae B728a and pv. tomato DC3000

By homology blast further NRPS-clusters coding for lipopeptides could be observed in both *Pseudomonas syringae* strains (Feil *et al.*, 2005; Buell *et al.*, 2003).

In the genome sequence of *P. syringae* pv. syringae B728a (Feil *et al.*, 2005) three orphan lipopeptides were identified. The first one, *psyr_*2576-*psyr_*2577, was predicted to produce an unusual octa-lipopeptide (figure 4.1.4). A homolog of this cluster was also found in the strain of the pathovar tomato DC3000 (Buell *et al.*, 2003). For *P. syringae* pv. tomato DC3000 the corresponding lipopeptide (named syringafactin) was isolated and the structure was determined (Berti *et al.*, 2007).

Syringafactins were suggested to be linear lipopeptides, making this class of CLPs a solitary exception to the usual cyclic lipopeptides generated by Pseudomonads.

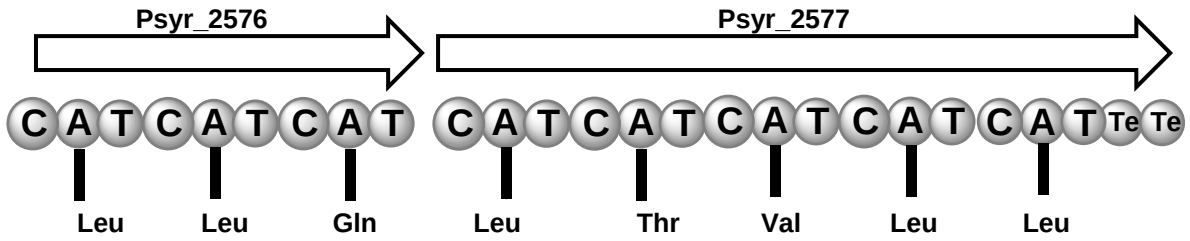

Figure 4.1.4: putative octa-lipopeptide (also present in *P. syringae* pv. tomato DC3000, *pspto_2829* and *pspto_2830*)

Regarding the second gene cluster, encoding a putative hexa-lipopeptide (see figure 4.1.5), located on *psyr_3722*, it was indicated, that the ortholog appearing in *P. syringae* pv. tomato DC3000 is truncated and therefore likely to be non-functional or to produce a different peptide (Feil *et al.*, 2005).

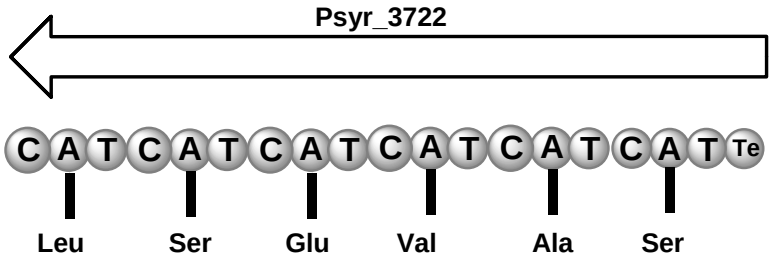

Figure 4.1.5: putative hexa-lipopeptide present in *P. syringae* pv. syringae B728a

Analysis of the biosynthesis gene cluster *psyr_3722* revealed six regular NRPS-modules (CAT), with the last one additionally comprising a TE-domain. The prediction of the specificity of the corresponding A-domains using standard bioinformatics tools delivered only low identity scores for known amino acids (resulting aa´s depicted in figure 4.1.5). Hence, the analysis was complemented with a phylogenetic analysis (see figure 4.1.7). This approach revealed that all six A-domains surprisingly cluster together and form a new yet uncharacterized clade.

The third CLP cluster represents a homolog of a CLP cluster present in *P. entomophila* L48 (figure 4.1.2) and might be responsible for the production of the abovementioned pentalipopeptide.

A sequence alignment comparing *pseen2716* with *psyr_1792*, *pseen2717* with *psyr_1793* and *pseen2718* with *psyr_1794* showed 72%, 74% and 67% identity, respectively (data not shown).

Pseudomonas sp. SH-C52

In the draft genome of *Pseudomonas* sp. SH-C52, two gene clusters could be identified. The first was predicted to encode a di-lipopeptide and the second to code for a new chlorinated nona-lipopeptide with a syringomycin-like structure (see chapter 4.3.1).

Ralstonia solanacaerum GMI 1000

Since the genus *Ralstonia* was formerly classified as *Pseudomonas* with similarity in most aspects, except that it does not produce the typical *Pseudomonas* fluorescent pigments, also genome sequenced strains of this genus were included in the study. In strain *R. solanacaerum* GMI1000 a biosynthesis pathway encoding a putative pentapeptide could be found by homology blast search against the amino acid sequences of the double TE-domain of the orfamide gene cluster. Analysis of the resulting aa-sequence with the NRPS/PKS-predictor showed a non-ribosomal peptide synthetase comprising five modules with canonical architecture and additional two TE-domains (see figure 4.1.6).

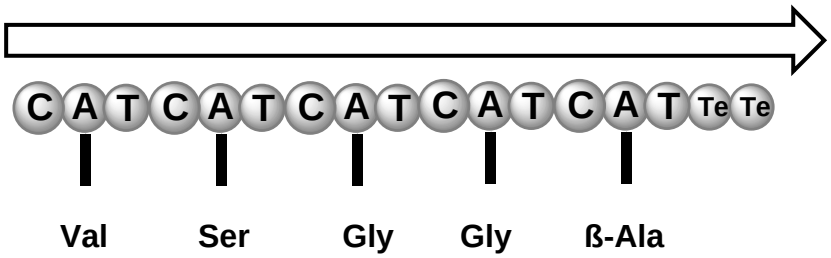

Figure 4.1.6: putative pentapeptide in *Ralstonia solanacaerum* GMI 1000

Regarding the A-domain specificity, only the A-domain of the first module could be unambiguously predicted to be specific for valine. However, similar to gene cluster *psyr_3722*, inspection of the specificity of the remaining A-domains was challenging.

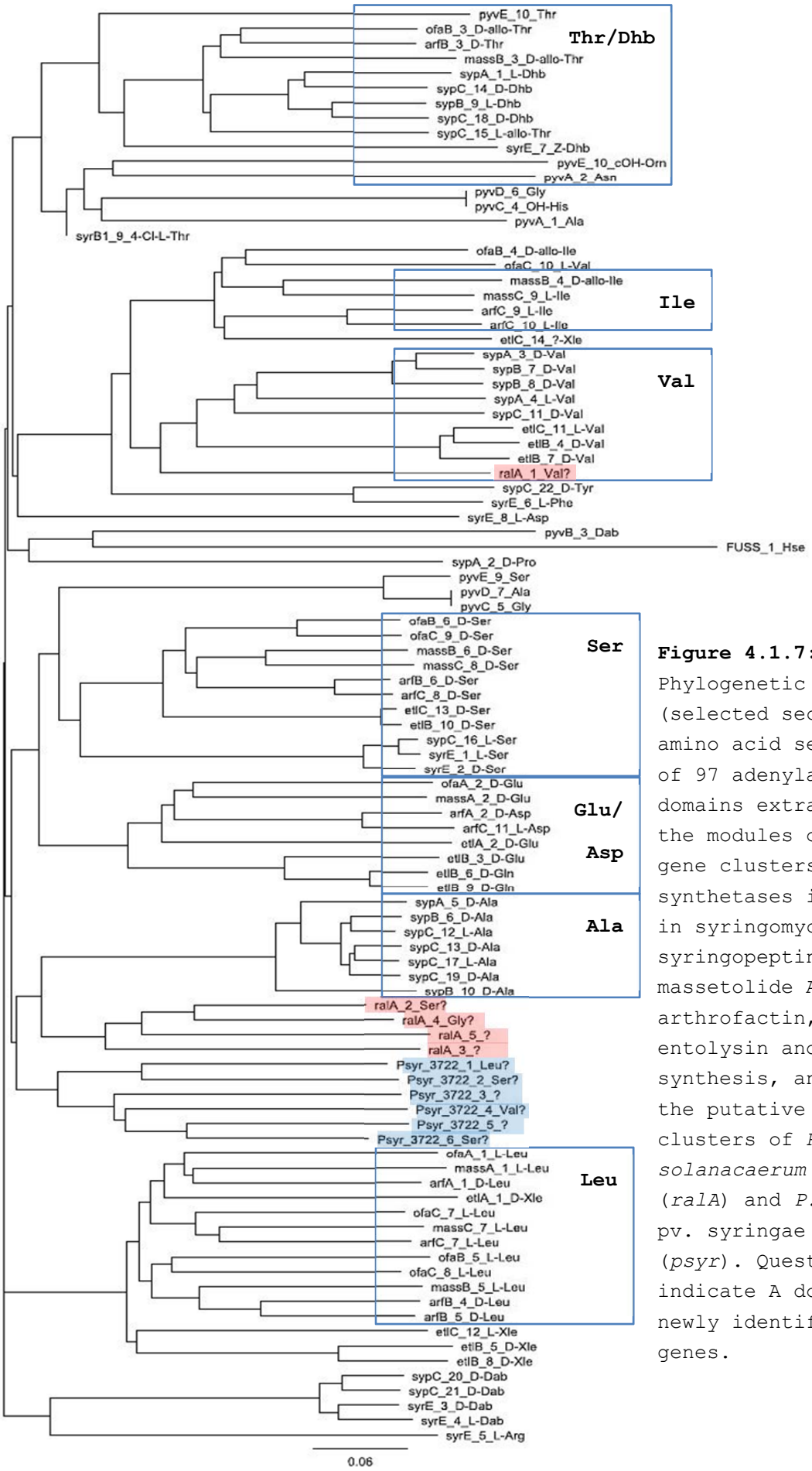

Figure 4.1.7: Phylogenetic analysis (selected section) of amino acid sequences of 97 adenylation domains extracted from the modules of the CLP gene clusters encoding synthetases involved in syringomycin, syringopeptin, massetolide A, arthrofactin, entolysin and orfamide synthesis, and from the putative CLP clusters of *R. solanacaerum* GMI 1000 (*ralA*) and *P. syringae* pv. syringae B728a (*psyr*). Questionmarks indicate A domains in newly identified CLP genes.

Application of standard bioinformatics tools resulted in low probability values for known AA´s (see figure 4.1.6) whereas phylogenetic analyses grouped them into one single clade adjacent to A-domain proteins specific for alanine and those for the yet undetermined clade generated by the A-domains of the *psyr_3722* cluster (see figure 4.1.7).

Subsequent chemical and biosynthetic studies were focussed on the orphan gene clusters of the strain *P.* sp. SH-C52. The decision for this focus was based on several aspects:

Strain *Pseudomonas entomophila* L48 was not available at the beginning of the study and already under investigation regarding the predicted lipopeptides by a research group in France, which reported consequently in 2010 entolysins A and B as products of one of the considered CLP gene (Vallet-Gely *et al.*, 2010) as mentioned above.

The strains of *Pseudomonas syringae* pv. syringae B728a and pv. tomato DC3000 were subjected to a broad screening for the described lipopeptides (see chapter 4.2). These lipopeptide gene clusters were targeted despite the products of one thereof, the syringafactins, were already published (Berti *et al.*, 2007), because only a tentative linear structure was proposed by the authors. Furthermore, other lipopeptides were predicted for the strains as well which were not isolated yet.

R. solanacaerum GMI1000 was already under investigation of a research group in Jena, which yielded the known siderophore micacocidin (Kreutzer *et al.*, 2011).

For the strain *Pseudomonas* sp. SH-C52, an exclusive access was given by collaboration with the University of Wageningen which granted investigations without competition.

4.2 Screening for the predicted CLPs using an OSMAC approach

As described in the previous chapter, the strains of *P. syringae* pv. syringae B728a and pv. tomato DC3000 were subjected to a broad screening for secondary metabolites employing the OSMAC

approach (Bode *et al.*, 2002). In brief, the OSMAC (**o**ne **s**train **ma**ny **c**ompounds) method describes the ability of one strain to produce a variety of secondary metabolites depending on the cultivation conditions.

In the context of this study, the application of the OSMAC approach was used to overcome the low expression of the observed gene clusters encoding for putative CLPs. The cultivation and extraction of the cultures were performed according to the established procedures described in chapter 3.1.3 and 3.3.1.

For each crude extract and the corresponding negative control, an LC-MS analysis was performed and a ^{1}H-NMR spectrum was recorded (data not shown). The ^{1}H-NMR spectra and the DAD-chromatograms were reviewed for characteristic resonances and UV-profiles of lipopeptides, respectively. However, none of the predicted structures could be observed and no CLPs were obtained despite the application of several diverse induction trials.

4.3 Investigations on *Pseudomonas* sp. SH-C52

4.3.1 Genome mining for CLPs

In the draft genome sequence of *Pseudomonas* sp. SH-C52 two NRPS gene cluster encoding putative CLPs could be identified. One cluster was predicted to code for a di-lipopeptide, while the second cluster most likely encodes a new chlorinated nona-lipopeptide with a syringomycin-like structure (see figures 4.3.1 and 4.3.3).

Putative di-lipopeptide

The first gene cluster, located on a generated fosmid (I. de Bruijn, research group of J.M. Raaijmakers, University of Wageningen, The Netherlands), is composed of a glycosyltransferase (GT), a nonribosomal peptide synthetase, a FAD-dependent monooxygenase (MO), a LuxR-type transcriptional regulator (R) and a RND-type efflux system (ES) (see figure 4.3.1).

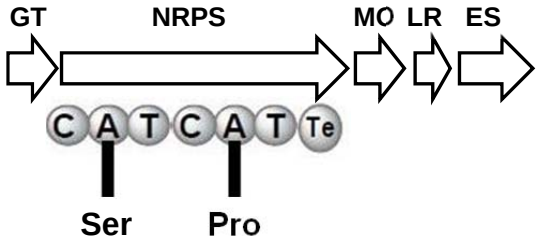

Figure 4.3.1: gene cluster in *P.* sp. SH-C52 encoding a di-lipopeptide

Analysis of the deduced amino acid sequences revealed that the NRPS comprises two modules, each composed of a condensation domain, an adenylation domain and a thiolation domain, and a terminal TE-domain. Using web-based bioinformatics software tools (see chapter 3.4), the specificity of the active centres of the two A-domains were analysed *in silico*, and predicted to activate serine and proline. To verify the specificities of the A-domains, a phylogenetic analysis was performed, including various A-domains of already chemically established CLPs which are correlated with their respective biosynthesis clusters (see figure 4.3.2; Rees *et al.*, 2007; Roongsawang *et al.*, 2003; Scholz-Schroeder *et al.*, 2003; Gross *et al.*, 2007; Miao *et al.*, 2005; Feil *et al.*, 2005; Guenzi *et al.*, 1998; de Bruijn *et al.*, 2008; Vallet-Gely *et al.*, 2010).

In agreement with the initial predicted substrate specificity, the two A-domains of the dilipopeptide, brbA_1_Ser? and brbA_2_Pro? cluster into the clade of serine and proline, respectively, which corroborates the first analysis. In detail, the first A-domain sequence, predicted to incorporate a serine residue is in the same clade of serine-specific A-domains of massetolide, orfamide, arthrofactin, syringomycin, syringopeptin and entolysin.

The second amino acid sequence clusters with proline- and 4-Cl-threonine- specific A-domains of the syringopeptin and syringomycin biosynthesis gene cluster, respectively. Thus, the phylogenetic analysis provides some ambiguity, however taking into consideration, that only one proline-specific A domain is currently available, the phylogenetic analysis suggests also a proline-specificity of the A-domain brbA_2_Pro?.

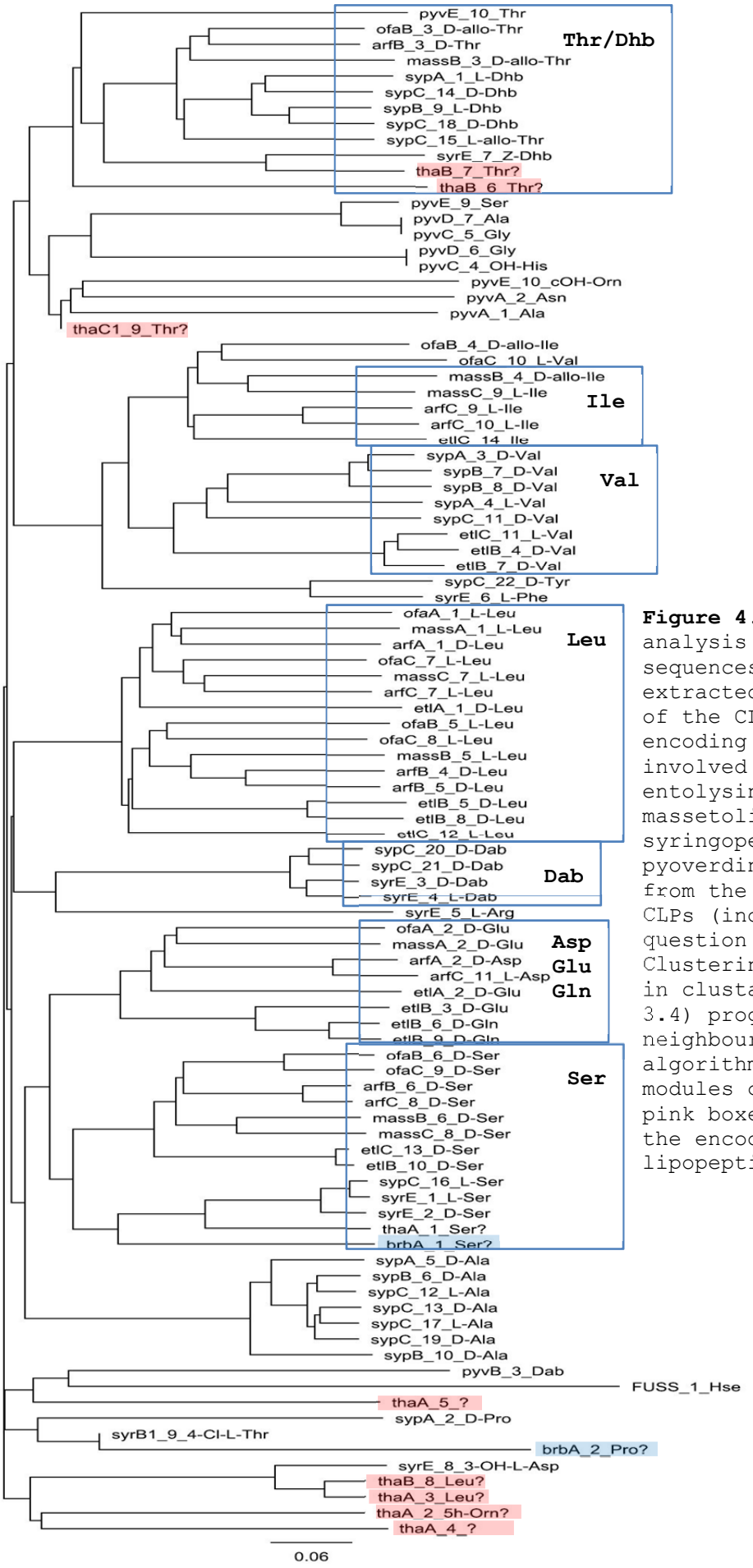

Figure 4.3.2: Phylogenetic analysis of amino acid sequences of 97 A-domains extracted from the modules of the CLP gene clusters encoding synthetases involved in arthrofactin, entolysin, orfamide, massetolide, syringomycin, syringopeptin, fusarin C, pyoverdine synthesis and from the two predicted CLPs (indicated by question marks). Clustering was performed in clustalW2 (see chapter 3.4) program using the neighbour-joining algorithm. Blue boxes mark modules of brabantamide, pink boxes mark modules of the encoded nona-lipopeptide.

In order to gain further insight into the brabantamide gene cluster, also the C-domains were subjected to a phylogenetic analysis (see figure 4.3.4). The analysis revealed that the first condensation domain C1 of the first module represents a typical ´starter C domain´ which acylates the first amino acid with a β-hydroxy fatty acid. The second C-domain of the NRPS cluster was expected to be responsible for the fusion of serine and proline, belonging either to the $^{L}C_{L}$, $^{D}C_{L}$ or the dual E/C (epimerization/ condensation) functional subtype of C-domains (Balibar *et al.*, 2005; von Döhren *et al.*, 1999; Clugston *et al.*, 2003; Rausch *et al.*, 2007).

Table 4.3.1: result of the NapDOS analysis of the C-domains of brabantamide and the predicted nona-lipopeptide

Query ID	Database match ID	% identity	Align length	e-value	Pathway product	Domain class
brbA_C1	syrin1_C1_start	36	366	5e-65	syringomycin	start
brbA_C2	micro1_C1_modAA	32	414	6e-60	microcystin	modAA
thaA_C1	syrin1_C1_start	69	369	4e-153	syringomycin	start
thaA_C2	syrin1_C7_LCL	57	434	5e-125	syringomycin	LCL
thaA_C3	syrin1_C3_dual	61	423	2e-136	syringomycin	dual
thaA_C4	syrin1_C7_LCL	58	434	1e-141	syringomycin	dual
thaA_C5	syrin1_C4_dual	69	416	5e-164	syringomycin	dual
thaB_C1	syrin1_C7_LCL	57	425	9e-125	syringomycin	LCL
thaB_C2	cdaps1_C7_LCL	34	445	3e-46	CDA	LCL
thaB_C3	syrin1_C7_LCL	82	434	0.0	syringomycin	LCL
thaB_C4	syrin1_C8_dual	81	416	0.0	syringomycin	dual
thaB_C5	syrin1_C9_LCL	78	433	0.0	syringomycin	LCL

Within the frame of the phylogenetic investigations, the second C-domain clustered between conventional $^{D}C_{L}/^{L}C_{L}$ domains and dual condensation/ epimerisation domains (see figure 4.3.4). The missing second elongated His-motif (HH(I/L)xxxxGD), described to indicate C-domains with dual functions (Balibar *et al.*, 2005), suggests the assumption, that the second C domain belongs to the conventional C domains. Additional analysis of the C-domains using NapDOS (see table 4.3.1) assigned the first C-domain to the starter C-domains and the second to the modAA domains (modified amino acid domains), whereby a modification of the second amino acid seems to be likely.

In summary, the NRPS gene codes for a lipo-dipeptide, whereby

the peptidic portion consists of Ser and Pro, while the lipid moiety comprises most likely a β-hydroxy fatty acid of unknown chain length. The latter is provided by primary metabolism and its biosynthesis genes are not clustered with the identified di-lipopeptide gene cluster. The alignment of the GT suggests that it utilises rhamnose as substrate. Thus, the resultant glycosyl-residue in the predicted lipopeptide is possibly rhamnose. It showed 51% amini acid identity to a rhamnosyltransferase deriving from *Burkholderia thailandensis* E264.

Further investigations regarding the structural genes of the cluster were made by comparative alignments of the putative glycosyltransferase and the putative MO (for data see tables 8.1.1 and 8.1.2, appendix). The alignment of the GT suggests that that it utilizes rhamnose as substrate. It showed 51% amini acid identity to a rhamnosyltransferase deriving from *Burkholderia thailandensis* E264.

The results of the homology-search for the involved monooxygenase showed a maximum identity of 42% to the aligned sequences. The best hit was a putative FAD-dependent monooxygenase from *Xenorhabdus bovienii* SS-2004. These results suggest that the MO belongs to a new class of enzymes, which is not further investigated up to date.

Putative chlorinated nona-lipopeptide

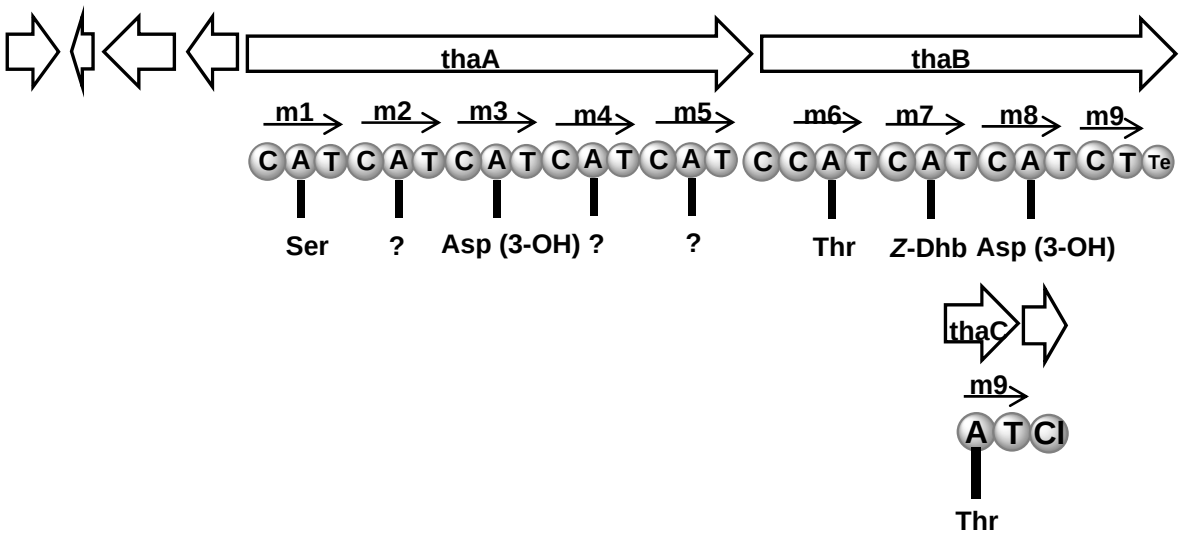

Figure 4.3.3: predicted chlorinated nona-lipopeptide in *P.* sp. SH-C52; m = module

The second lipopeptide gene cluster in *P.* sp. SH-C52 is composed of three NRPS genes (see figure 4.3.3). The first NRPS gene (*thaA*) comprises five modules which show the typical CAT domain pattern. The second NRPS gene (*thaB*) is composed of four modules. Thereby, the typical CAT pattern can only be observed in the first three modules while the fourth module is lacking the A-domain and thus remains incomplete.

Additionally, ThaB codes for a further C-domain upstream of module six and the usual TE-domain which is terminating the NRPS machinery. The third nonribosomal synthetase, ThaC, encodes an A-domain, a T-domain and a halogenase domain (Cl) which is evocative of SyrB and SyrC, comprising an AT-pattern and a Cl-domain, respectively. Thus, it seems likely, that module nine (see figure 4.3.3) is composed of the two incomplete modules belonging to ThaB and ThaC, respectively, thus showing a similar arrangement as SyrE, SyrB and SyrC of the syringomycin biosynthesis gene cluster (Guenzi *et al.*, 1998). Furthermore, it can be hypothesised, that the A-domain of ThaC activates chlorinated threonine in combination with the Cl-domain in the same manner than observed in the syringomycin biosynthesis.

Whether the additional C-domain upstream of module six which is encoded by *thaB* and seems to be a conventional C-domain (see below) is non-functional or skipped or it is used in combination with another A-domain which is not directly adjacent currently remains unclear.

Using multiple NRPS/PKS web-based software (see chapter 3.4) the primary structures of the A-domains were analysed. The predicted specificities of the resulting A-domains led to the assumption, that the majority of the residues in the binding pockets are either rare or even unknown (see table 4.3.2). To get more information about the incorporated amino acids, the sequences were included in the aforementioned phylogenetic analysis (see figure 4.3.2).

The results of the investigation confirmed the predictions for ThaA-1 and ThaB-6 activating Ser and Thr, respectively. ThaB-7 is in the same cluster as ThaB-6, but seems to be closer related to *Z*-Dhb from SyrE-7. The predicted residues of ThaA-3 and ThaB-8 could also be confirmed, clustering directly adjacent to the 3-OH-L-Asp-residue from SyrE-8. The results for the other A-domains

remain inconclusive either by clustering in areas with diverse specificities (ThaA-5 and ThaC-9) or clustering with each other in new yet uncorrelated clades (ThaA-2 and ThaA-4).

Table 4.3.2: prediction of A-domain specificities with different programs

	ThaA-1	**ThaA-2**	**ThaA-3**	**ThaA-4**	**ThaA-5**	**ThaB-6**	**ThaB-7**	**ThaB-8**	**ThaC-9**
Predicted Subst.(1)	Ser	-	Asp	-	-	Thr	Thr	Asp	Thr
NRPSPred. code (1)	Ser	Orn	Asp	Lys	His	Thr	Thr	Asp	Thr
NRPSPred. SVM (1)	Ser	Asp/Asn Glu/Gln Aad	Asp	Asp/Asn Glu/Gln Aad	Val/Leu Ile/Abu Iva	Thr	Thr	Asp	Thr
Minowa HMM (1)	Ser	Arg	Arg	Ala	Ala	Thr	Thr	Gln	Thr-4-Cl
NRPS/ PKS (2)	Ser	5h-Orn	Leu	-	-	Thr	Thr	Leu	Thr
NRPS/ PKS (3)	D-Ser	Asp	Asp (3OH)	Orn	His?	Thr	Thr	Asp (3OH)	Thr-4-Cl

(1) antismash

(2) Bachmann & Ravel, 2009

(3) http://www.nii.res.in/nrps-pks.html

Regarding the C-domains, the cluster shows a starter C-domain in the first module, which is able to attach a fatty acid (figure 4.3.4). Furthermore, it can be observed, that the C-domains of module no. three and four encoded by *thaA* and the C-domain of module no. eight which is encoded by *thaB* seem to display dual activity (condensation and epimerisation). The residual C-domains cluster with conventional C-domains. These results are congruent with the results of the NapDOS-analysis (see table 4.3.1).

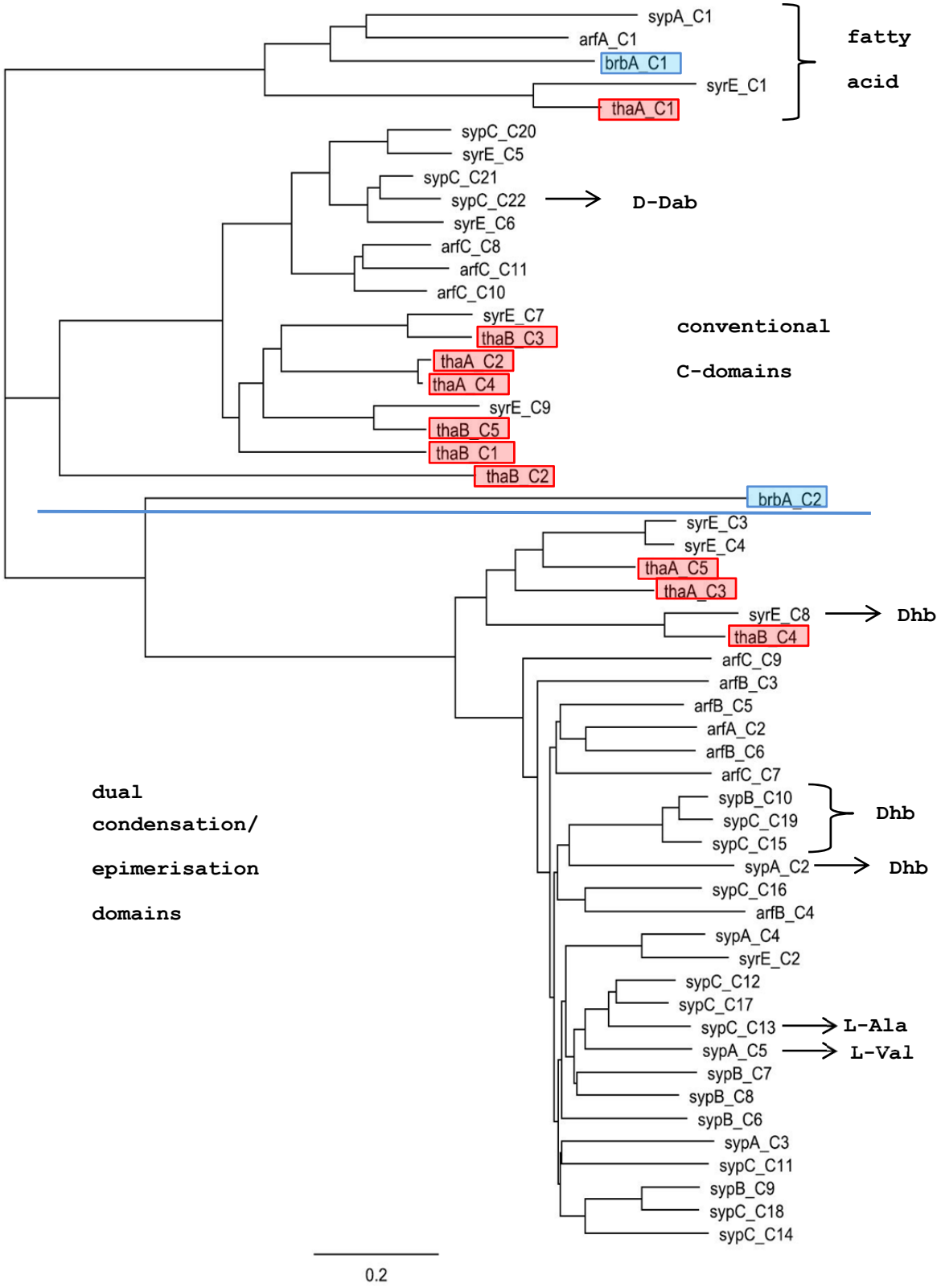

Figure 4.3.4: Phylogenetic analysis of C Domains from arthrofactin, syringomycin, syringopeptin and the two predicted cyclic lipopeptides. C-domains predicted to be conventional are above the blue line, and those predicted to be dual C/E domains are below. Arrows indicate known deviations from the phylogentic predictions. Clustering was performed in clustalW2 (see chapter 3.4) program using the neighbour-joining algorithm. Blue boxes mark C-domains of brabantamide, pink boxes those of the encoded nona-lipopeptide, respectively

4.3.2 Proof of the gene clusters encoding the predicted lipopeptides

For both gene clusters of interest deletion mutants, targeting the structural NRPS genes were generated. Subsequently, the obtained mutant strains C52Δ27 and C52Δ33 and the corresponding wild-type strain of *Pseudomonas* sp. SH-C52 (see chapter 3.1.1) were cultivated and extracted according to established procedures (see chapters 3.1.3 and 3.3.1). The obtained crude extracts were then subjected to LC-MS analysis (see chapter 3.3.5) and a comparison of the secondary metabolite spectrum was performed.

In case of the knockout mutant strain C52Δ27, the LC-MS analysis clearly demonstrated the absence of a peak at t_R = 22.5 min in the chromatogram with a corresponding mass of 555 *m/z* and UV-maxima at 224 nm and 252 nm. To demonstrate unambiguously the affiliation of the expected lipo-dipeptide metabolite to the cluster, the mass traces of the wild-type strain as well as of the knockout strain were extracted for the identified mass and overlaid (see figure 4.3.5).

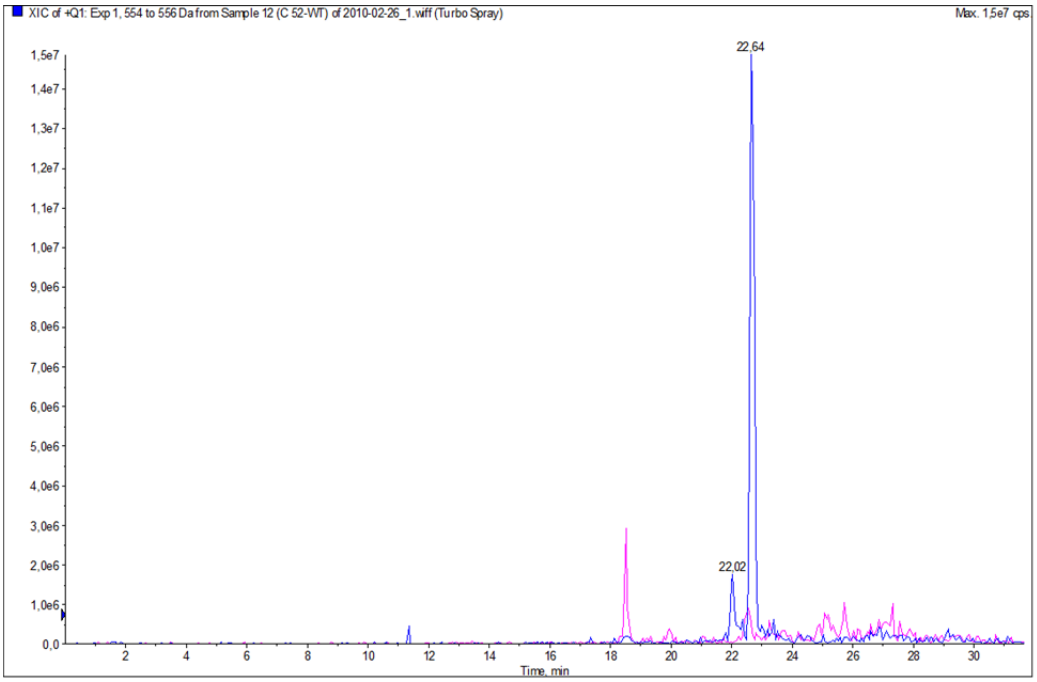

Figure 4.3.5: LC/MS analysis of *P.* sp. SH-C52 knockout (pink) vs. wild-type (blue) strain. The extracted chromatogram (mass range = 554 – 556 *m/z*) is shown.

In the case of knockout-strain C52Δ33 no differences in the metabolite profile to the wild-type strain could be observed. In order to activate the expression of the *thaABC* gene cluster, encoding a lipo-nonapeptide, the OSMAC strategy was applied (see chapter 4.2). However, in none of the tested culture media the comparison of the metabolite profiles showed any differences.

4.3.3 Isolation and structure elucidation of the predicted di-lipopeptide

In order to isolate the identified di-lipopeptide, *Pseudomonas* sp. SH-C52 was cultivated on a nine litre scale (see chapter 3.1.3). Subsequently, the culture was extracted, separated by vacuum liquid chromatography and VLC-fraction 3 was further purified by HPLC (system 4, column 6, UV-monitoring at 224 nm and 252 nm) according to chapters 3.3.1 - 3.3.3. The runs were performed isocratically, using 85% methanol and 15% H_2O supplemented with 0.05% TFA, over a duration of 45 minutes. Three peaks showed the characteristic UV-spectrum (UV-maxima at 224 nm and 252 nm) of the CLP of interest (see chapter 4.3.2) and were isolated for further investigation with yields of 12.6 mg (SH-C52-3B = compound **1**), 3.6 mg (SH-C52-3C = compound **2)** and 2.0 mg (SH-C52-3D = compound **3**).

Structure elucidation

The structure elucidation of the purified compounds was mainly based on NMR experiments (see chapter 3.3.4).

Interpretation of the ^{1}H-^{13}C HSQC spectrum allowed the correlation of all proton resonances to the ^{13}C NMR resonances of directly bonded carbon atoms. The number and resonances of primary, secondary and tertiary carbon atoms was identified via a DEPT135 NMR spectrum (**D**istortionless **E**nhancement by **P**olarisation **T**ransfer, 135° angle) and ^{1}H-^{1}H spin systems were recognized using ^{1}H-^{1}H COSY data. The resulting partial structures were connected using cross correlations of the ^{1}H-^{13}C HMBC spectrum.

Further measurements like UV-spectra, IR, CD and HR ESI-MS were conducted to investigate the physico-chemical properties of the structures (see table 4.3.3).

Table 4.3.3: physico-chemical properties of the isolated compounds

	Compound 1	**Compound 2**	**Compound 3**
Molecular Formula	$C_{28}H_{46}N_2O_9$	$C_{30}H_{48}N_2O_9$	$C_{30}H_{50}N_2O_9$
HR-ESI-MS $[M+Na]^+$	577.3096	603.3253	605.3409
Calc. mass [M]	554.3203	580.3360	582.3516
UV λ_{max} nm (ε MeOH)	224 (945) 252 (1393)	224 (926) 252 (1333)	221 (1025) 252 (1311)
IR ν_{max} cm^{-1}	3396, 2923, 2853, 2359, 2340, 1790, 1732, 1681, 1646, 1505, 1464, 1374	n.d.	n.d.
CD_{max} [nm][a]	288, 255, 215	n.d.	n.d.
$[\alpha]_D^{24}$ [°]	+ 39.7	+ 68.8	+ 11.2

n.d. = not determined

[a] see figure 8.1.1, appendix

Structure elucidation of compound **1**

HR ESI-MS analysis revealed an adduct-ion $[M+Na]^+$ at *m/z* 577.3096, consistent with the molecular formula of $C_{28}H_{46}N_2O_9Na$.

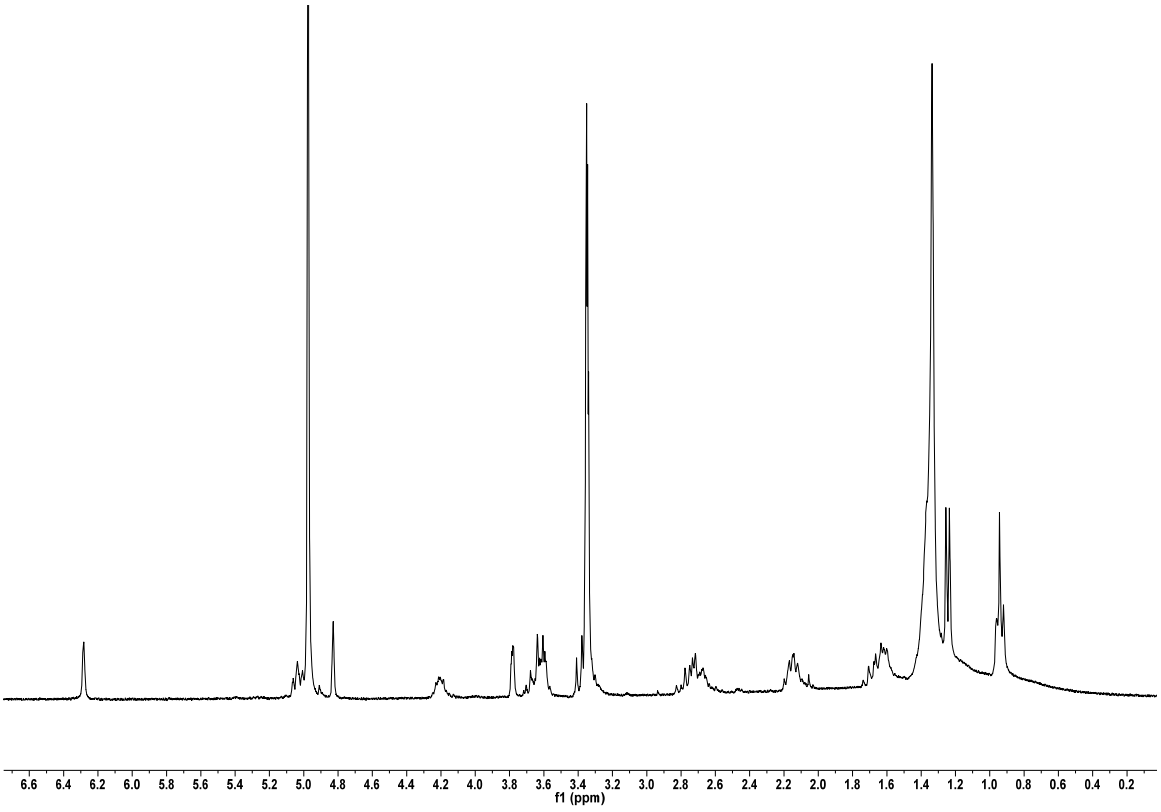

Figure 4.3.6: ^{1}H-NMR spectrum of compound **1** (SB-253514/ brabantamide A) measured in d_4-methanol (300 MHz)

From this molecular formula seven double bond equivalents were deduced. Since the ^{13}C-NMR spectrum of **1** (figure 8.1.2, table 4.3.4) contained three carbonyl groups (δ_C 158.3, 166.4 and 173.7), one double bond (δ_C 166.4 and 98.0), compound **1** had to be tricyclic.
Four isolated spin systems could be distinguished via a ^{1}H-^{1}H COSY spectrum (see figure 8.1.5, appendix).

Spin system A (see figure 4.3.7 – A) comprised the protons of a glycosidic moiety ($H_1$1′- $H_3$6′).

Table 4.3.4: NMR Spectroscopic data (300 MHz, d_4-methanol) for compound **1** (brabantamide A, (δ in ppm))

Atom	δ_C	mult	δ_H [J in Hz]	COSY	HMBC	NOE
2	158.3	qC	-	-	5, 8a	-
4	168.8	qC	-	-	5, 6a, 9	-
5	66.3	CH	5.03, ddd [7.8, 6.6, 9.0]	9*,6a/b	6b,7, 9	6b
6a	31.2	CH_2	1.66, m	5,6b,7	5, 7, 8a, 9#	5*, 6b
6b			2.68, dd, [6.5, 3.8]	5, 6a	5, 7, 8a, 9#	5, 6a, 7
7	27.3	CH_2	2.14, m	6a/b,8a	6b*, 8a/b	5, 6b, 8a/b
8a	47.0	CH_2	3.35, m	7, 8b	6b, 7	7, 8b
8b			3.65, m	7, 8a	6b, 7	7, 8a
9	98.0	CH	6.29, d, [2.3]	5*	5*	-
10	166.4	qC	-	-	-	-
12	173.7	qC	-	-	13, 14	-
13	44.2	CH_2	2.74, m	14	14, 15*	14
14	74.9	CH	4.20, m	13, 15	13	13, 15, 16, 1′
15	34.5	CH_2	1.61, m	14, 16	13	1′, 14
16	25.9	CH_2	1.38, m	15	14*	25
17-22	~30.8	CH_2	1.34, m	-	-	-
23	33.0	CH_2	1.33, m	-	25	-
24	23.8	CH_2	1.34, m	25	23, 25	-
25	14.5	CH_3	0.94, t, [6.6]	24	23	16*
1′	99.9	CH	4.83, s	2′	14	9#, 14, 15, 2′
2′	72.7	CH	3.78, dd, [3.1, 1.6]	1′	-	1′, 3′, 5′
3′	72.4	CH	3.62, m	2′*, (4′)	1′	2′, 9#
4′	73.8	CH	3.39, m	5′/ 3′	2′, 6′	6′, 24
5′	70.5	CH	3.61, m	6′, (4′)	4′, 6′	2′, 6′
6´	18.0	CH_3	1.26, d, [6.2}	5′	4′	4′, 5′, 24

* weak signal, # very weak signal

The presence of a sugar moiety could be verified by ^{13}C-NMR chemical shifts of methine carbons C2′ to C5′, resonating between 70.5 and 73.8 ppm, which is characteristic for carbon atoms attached to oxygen. The ^{13}C-NMR resonance signal of C6′ was shifted highfield to 18.0 ppm, indicating the presence of a

desoxy sugar while C1' showed a downfield shift to 99.9 ppm as estimated for a doubly oxygenated acetale carbon (Pretsch *et al.*, 2001).

The second partial structure (spin systems B-1 and B-2, figure 4.3.7), which could be observed was a fatty acid moiety, demonstrated by the characteristic triplet resonance signal at 0.94 ppm in the ^{1}H-NMR spectrum for the terminal methyl group $H_3$25 and the large number of magnetically equivalent methylene signals at 1.3 – 1.4 ppm ($H_2$16 to $H_2$24). The downfield shift of the α-methylene group of myristic acid ($\delta_{C/H}$ 44.2/ 2.74) and the γ-CH_2 group ($\delta_{C/H}$ 34.5/ 1.61) indicated the expected amide bond of the lipopeptide and an oxygen atom linked to the carbon atom in ß-position, respectively. A ^{1}H-^{13}C HMBC correlation observed between H14 and C1' confirmed the assumption that the rhamnopyranose is linked to the fatty acid chain.

Finally, a third spin system (figure 4.3.7 – C) could be delineated from the COSY spectrum, which defined a proline moiety. The obtained partial structures were subsequently connected with HMBC correlations.

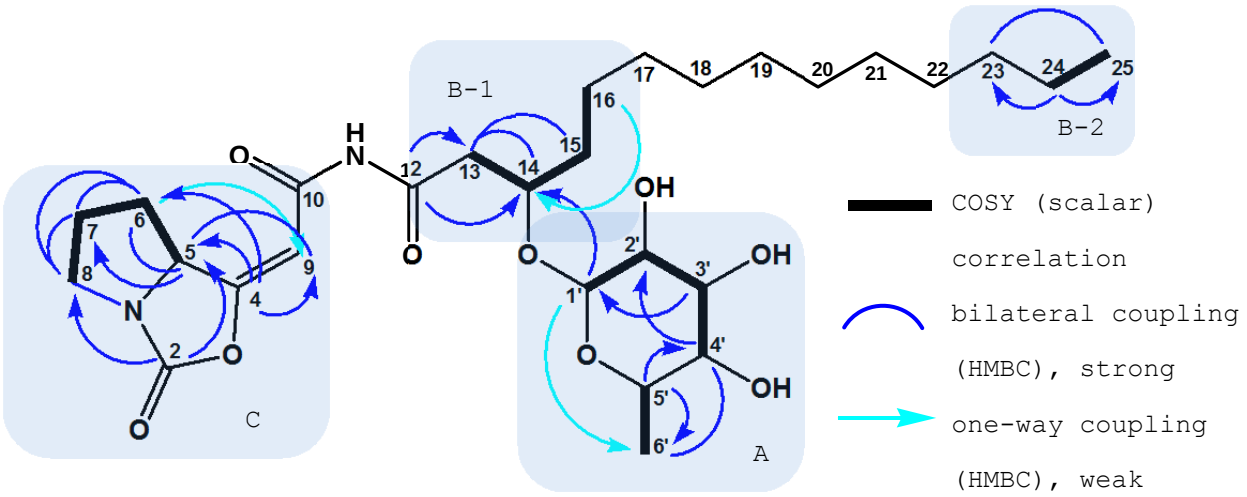

Figure 4.3.7: key correlations of compound **1** (SB-253514/ brabantamide A) with spin systems A, B and C

These efforts resulted in three partial structures, which were used for a de-replication crosscheck with the natural product database ´AntiMarin´. Hereby, compound **1** could be identified as SB-253514, which was first published in 2000 (Thirkettle, 2000a).

Stereochemistry

Due to the small amount of substance, the absolute stereochemistry of the molecule was not determined. Based on the x-ray structure published in 2000 (Busby *et al.*, 2000) the configuration of both stereo centres (C5 and C14) was adopted as *R* and the double bond between C4 and C9 as *trans* configured, respectively (Busby *et al.*, 2000).

Relative configuration of the rhamnose moiety

In order to confirm the stereochemistry of the published α-L-rhamnopyranose, a NOESY spectrum (nuclear Overhauser effect spectroscopy) was measured, which allows analysing through-space interactions of proton atoms (distances smaller than 5 Å).

The obtained ^{1}H-^{1}H-NOESY spectrum confirmed the presence of α-rhamnose revealing correlations between H1’ and H2’ which are both expected to be equatorial protons. Furthermore, the absence of correlations between H1’ and H3’ as well as H1’ and H5’ which should be obtained in case of an axial position of the proton at C1’ support the α-form (see figure 4.3.8).

In contrast to the most naturally occurring sugars which are D-configured, rhamnose occurs in nature usually in its L-form (Dewick, 2001) why the attachment of L-rhamnose seems likely.

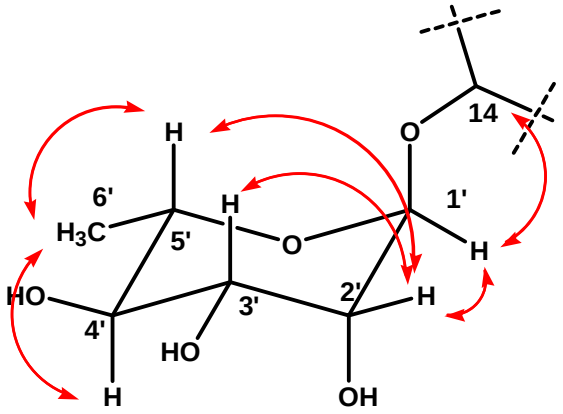

Figure 4.3.8: selected NOESY correlations which support the presence of the α-anomer

Structure elucidation of compound **2**

In an HR MS analysis, compound **2** (brabantamide B) displayed an adduct-ion $[M+Na]^{+}$ at *m/z* 603.3253, consistent with the molecular

formula of $C_{30}H_{48}N_2O_9Na$. Comparison of the ^1H- and ^{13}C-NMR spectra of compound **1** with those of compound **2** proved **2** to be closely related with **1** (see table 4.3.5).

Table 4.3.5: NMR Spectroscopic data (300 MHz, d_4-methanol) for compound **2** (brabantamide B), (δ in ppm))

Atom	δ_C	mult	δ_H, [J in Hz]	COSY	HMBC
2	158.3	qC	-	-	8a/b
4	168.8	qC	-	-	-
5	66.3	CH	5.03	6a/b, 9*	-
6a	31.2	CH_2	1.66	5, 6b, 7	-
6b			2.68	7	5, 9, 8a
7	27.3	CH_2	2.14	6a/b, 8a/b	-
8a	47.0	CH_2	3.35	7	-
8b			3.65	7	-
9	98.0	CH	6.29	5	-
10	166.4	qC	-	-	-
12	173.7	qC	-	-	
13	44.0	CH_2	2.74	14	-
14	74.9	CH	4.21	13	-
15	34.5	CH_2	1.61	16	-
16	25.9	CH_2	1.39	15	-
17/18	~30.8	CH_2	1.35	-	-
19	28.2	CH_2	2.08	20, 21	20, 21
20	130.7	CH_2	5.40, dd, 5.5, 4.0	19	-
21	131.0	CH_2	5.40, dd, 5.5, 4.0	-	19
22	28.2	CH_2	2.08	20, 21	20, 21
23/24	~30.8	CH_2	1.35	-	-
25	33.3	CH_2	1.33	-	27
26	23.8	CH_2	1.34	27	-
27	14.5	CH_3	0.94	26	-
1′	100.1	CH	4.83	2′	-
2′	72.7	CH	3.79	1′, 3′	1′
3′	72.4	CH	3.62	2′	-
4′	73.8	CH	3.39	-	6′
5′	70.5	CH	3.61	6′	1′, 6′
6´	18.0	CH_3	1.26	5′	-

*weak signal

Solely, additional resonances at 2.08 ppm and 5.40 ppm (see figure 4.3.9) could be observed. The latter resonance indicated a double bond, a fact which was corroborated by additional resonances at 130.7 ppm and 131.0 ppm, observed in the ^{13}C-NMR spectrum (figure 4.3.10). Since **2** showed in the NMR spectra only deviations in the lipid moiety, the mass difference of 26 mass

units between compound **1** and compound **2** could be readily ascribed to an elongation of the fatty acid side chain of two carbons (2 x 14 Da = 28 Da) and the occurrence of a double bond in the side chain (-2 Da). A literature and database search revealed that metabolite **2** possibly represents compound SB-253517, which is suggested to possess an unsaturated hexadecenoic acid side chain.

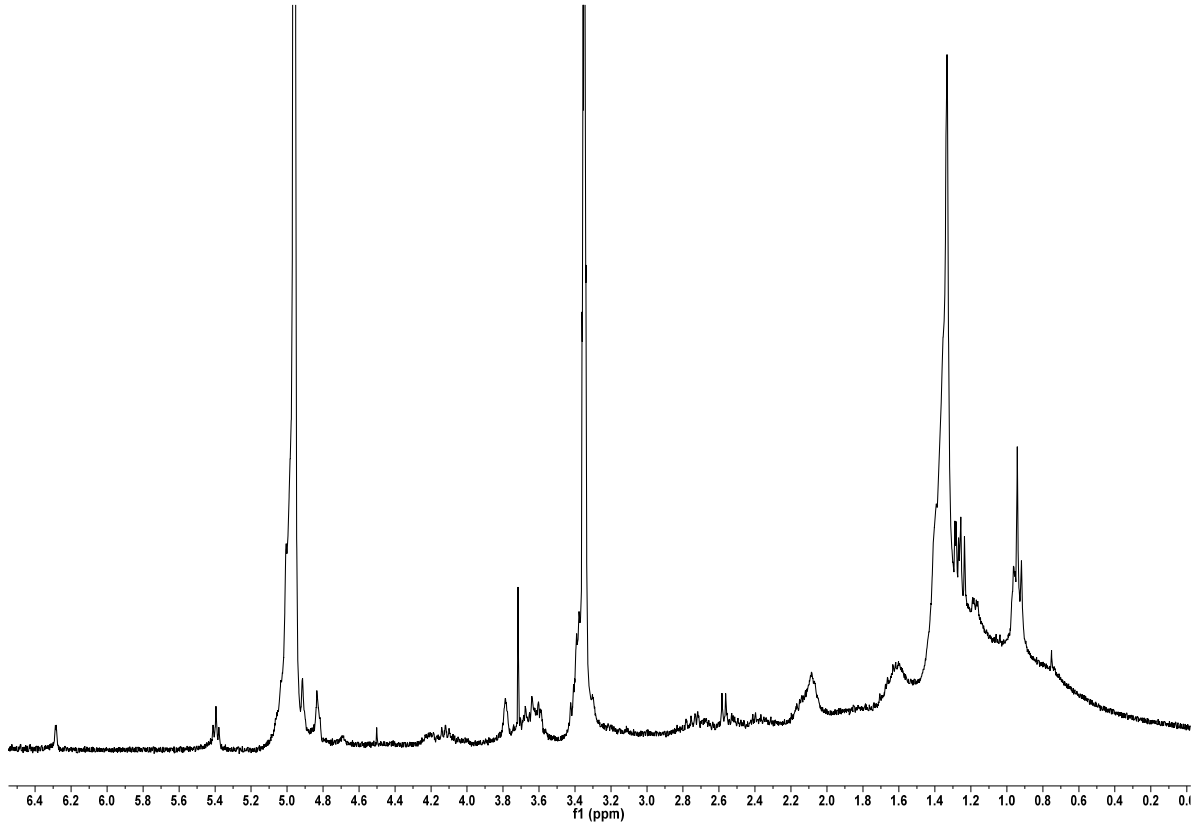

Figure 4.3.9: ^{1}H-NMR spectrum of compound **2** (SB-253517/ brabantamide B) in d_4-methanol (300 MHz)

The *cis*-oid geometry of the double bond was evidenced by a small $^{3}J_{H20,H21}$ coupling constant of 5.5 Hz. This finding was also supported by the chemical shift values of the adjacent carbon atoms C19 and C22 (δ_C 28.2) which were typical for a *cis* configured double bond, since allylic carbon signals of the *Z* and *E* isomers are specifically observed at δ_C 26-28 and δ_C 31-32, respectively (Ishii *et al.*, 2006; Stierle & Faulkner, 1980).

^{1}H-^{1}H COSY couplings (see figure 8.1.7) were suggestive that the double bond is localized between C19 and C20 (numeration confers to compound 1, figure 4.3.7).

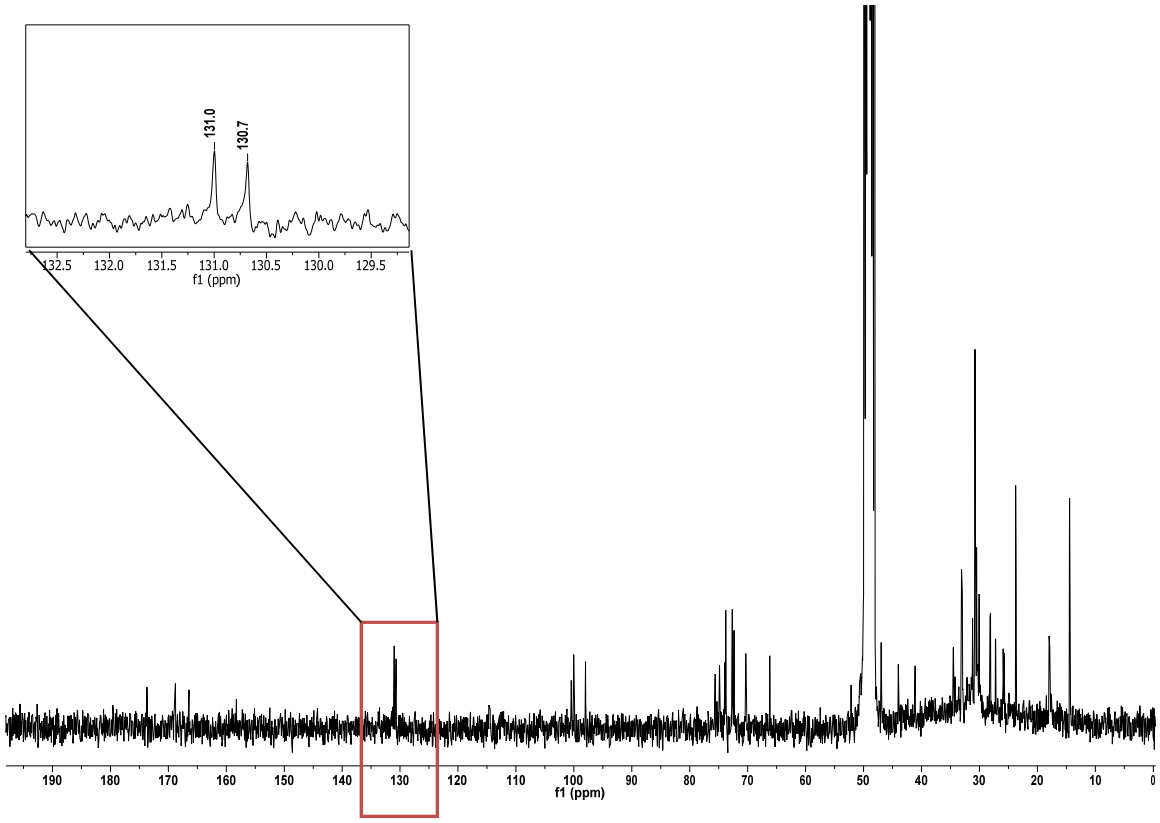

Figure 4.3.10: ^{13}C-NMR spectrum of compound **2** (SB-253517/ brabantamide B) in d_4-methanol (75 MHz)

However, since protons 16-24 span a massive methylene envelope from 1.3 – 1.4 ppm, the proton cannot be unambiguously assigned to one of the CH_2-groups. One indication for the equivalence of compound SB-253517 and compound **2** is the similar peak pattern obtained in the purification by HPLC of the main metabolite with its congeners (data not shown) and the chromatogram shown in the reference publication (Thirkettle, 2000a&b).

As a further attempt for the localisation of the double bond an empirical method was applied. Hereby, the differences of the chemical shifts of the considered olefinic carbon atoms can be employed to determine the configuration and the localisation of a double bond in a fatty acid (Bus *et al.*, 1977; Gunstone, 1993). The values published for different kinds of unsaturated fatty acids and fatty acid methyl esters coincided well with the obtained values from congener **2** (see table 4.3.6).

Application of this method indicated that the double bond belongs to the Δ9 class, which corresponds to a localisation between C20 and C21 of compound **2**. Based on these facts, the substance could be identified as SB-253517 (Thirkettle, 2000a; Thirkettle *et al.*, 2000).

Table 4.3.6: differences in chemical shift (ppm) between the two olefinic carbon atoms in monoene acids and methyl esters in comparison to the measured values of compound **2**

	compound 2	**methyl esters**		**acids**
double bond		*cis*[2]	*cis*[1]	*cis*[2]
Δ6		1.30	1.50	1.60
Δ7		0.73	0.90	0.85
Δ8		0.45	0.50	0.50
Δ9	0.32[3]	0.24	0.35	0.26
Δ10		-	0.20	0.17
Δ11		-	0.10	0.07

[1] values adopted from *Bus et al.*, 1977

[2] values adopted from *Gunstone*, 1993

[3] values for C20 and C21 rounded to two decimal places are 130.68 and 131.00, respectively

Structure elucidation of compound **3**

The molecular formula $C_{30}H_{50}N_2O_9$ of compound **3** was confirmed by HR-ESI-MS measurements (found: 605.3409 g/mol ($C_{30}H_{50}N_2O_9Na$), calculated: 582.3516 g/mol). Thus, the only difference between compound **2** and **3** appeared to be the saturation of the fatty acid side chain in metabolite **3**.

This assumption could be confirmed by NMR measurements which showed all resonances of the core structure of **1** and **2** (see figures 8.1.9 and 8.1.10). In comparison with the ^{1}H-NMR spectrum of compound **2**, compound **3** did not show signals at 5.40 ppm and 2.08 ppm (see table 4.3.7). These protons belong to the carbon atoms of the $\Delta^{20,21}$ double bond in compound **2** (C20 and C21) and the carbon atoms directly related to the double bond (C19 and C22), respectively.

In combination with the NMR data it can be concluded, that compound **3** contains a saturated 3-hydroxy hexadecanoic acid (3-hydroxy palmitic acid) instead of the corresponding unsaturated fatty acid in compound **2**. Thus, the metabolite could be identified as SB-253518, which was also reported in the aforementioned publication (Thirkettle, 2000b).

Table 4.3.7: NMR Spectroscopic data (300 MHz, d_4-methanol) for compound **3** (brabantamide C), (δ in ppm)

Atom	δ_C	mult	δ_H	COSY	HMBC
2	158.3	qC	-	-	8a/b
4	168.8	qC	-	-	-
5	66.3	CH	5.04	6a/b, 9	2, 6a/b, 4*, 9*
6a	31.3	CH_2	1.68	5, 7	5, 8
6b			2.69	7	-
7	27.3	CH_2	2.16	6a/b,8a/b	-
8a	47.0	CH_2	3.35	7	2
8b			3.67	7	-
9	98.2	CH	6.31	5	4, 5
10	166.4	qC	-	-	-
12	173.6	qC	-	-	-
13	44.1	CH_2	2.76	14	14
14	75.1	CH	4.21	13, 15	13, 12*,1′
15	34.6	CH_2	1.63	14	-
16	26.0	CH_2	1.39	-	-
17-24	~30.8	CH_2	1.35	-	-
25	33.1	CH_2	1.34	-	-
26	24.0	CH_2	1.34	-	-
27	14.5	CH_3	0.95	25, 26	2′, 3′
1′	100.2	CH	4.85	2′	2′, 3′
2′	72.8	CH	3.80	1′, 5′	4′
3′	72.4	CH	3.63	6′	-
4′	73.9	CH	3.40	3′	6′
5′	70.4	CH	3.62	2′	-
6´	18.3	CH_3	1.26	2′	4′, 5′

* weak signal

Since metabolites **1**-**3** were isolated from *Pseudomonas* sp. SH-C52, a bacterium obtained from the province of Noord-Brabant of The Netherlands and due to its chemical structure, we suggest the trivial names brabantamides A (**1**), B (**2**) and C (**3**) for these natural products instead of the usage of the industrial acronyms.

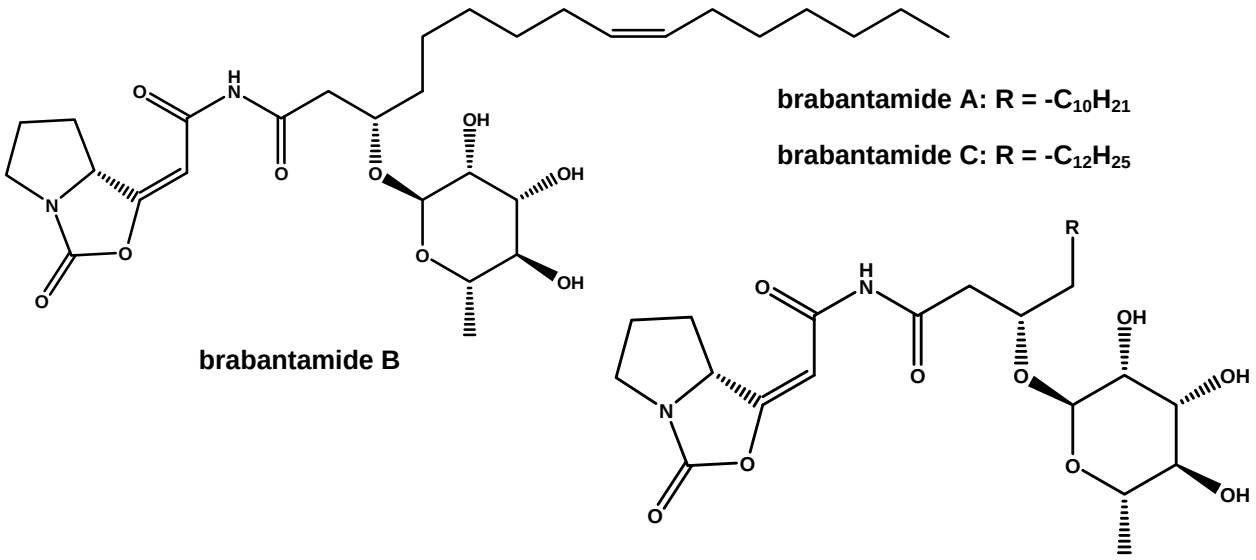

Figure 4.3.11: structures of brabantamides A-C

4.3.4 Hypothetical biosynthesis of brabantamide

The biosynthesis of brabantamide A is suggested to start with the synthesis of the fatty acid in the primary metabolism.

Fatty acid synthases (FASs) generate FAs from C_2 units until the required chain length – in this case 14 for brabantamide A or 16 for brabantamide B and C - is reached (see figure 4.3.12).

The fatty acid synthesis starts with an acetyl starter unit (acetyl-CoA) which is converted into an enzyme-bound thioester of a ketosynthase (KS) and a malonyl-CoA unit bound to an acyl carrier protein (ACP). After Claisen-condensation, the ß-keto-ester is reduced to the corresponding ß-hydroxy-ester by a ketoreductase (KR), dehydrated by a dehydratase (DH) and finally reduced again by an enoyl reductase (ER) (Staunton & Weissman, 2001; Dewick, 2001).

After this first reaction cycle the chain is extended by a further C_2 unit and is repeated until the requested fatty acid chain is achieved. The chain gets passed to a thioesterase (TE) where it is released as a fatty acyl-CoA.

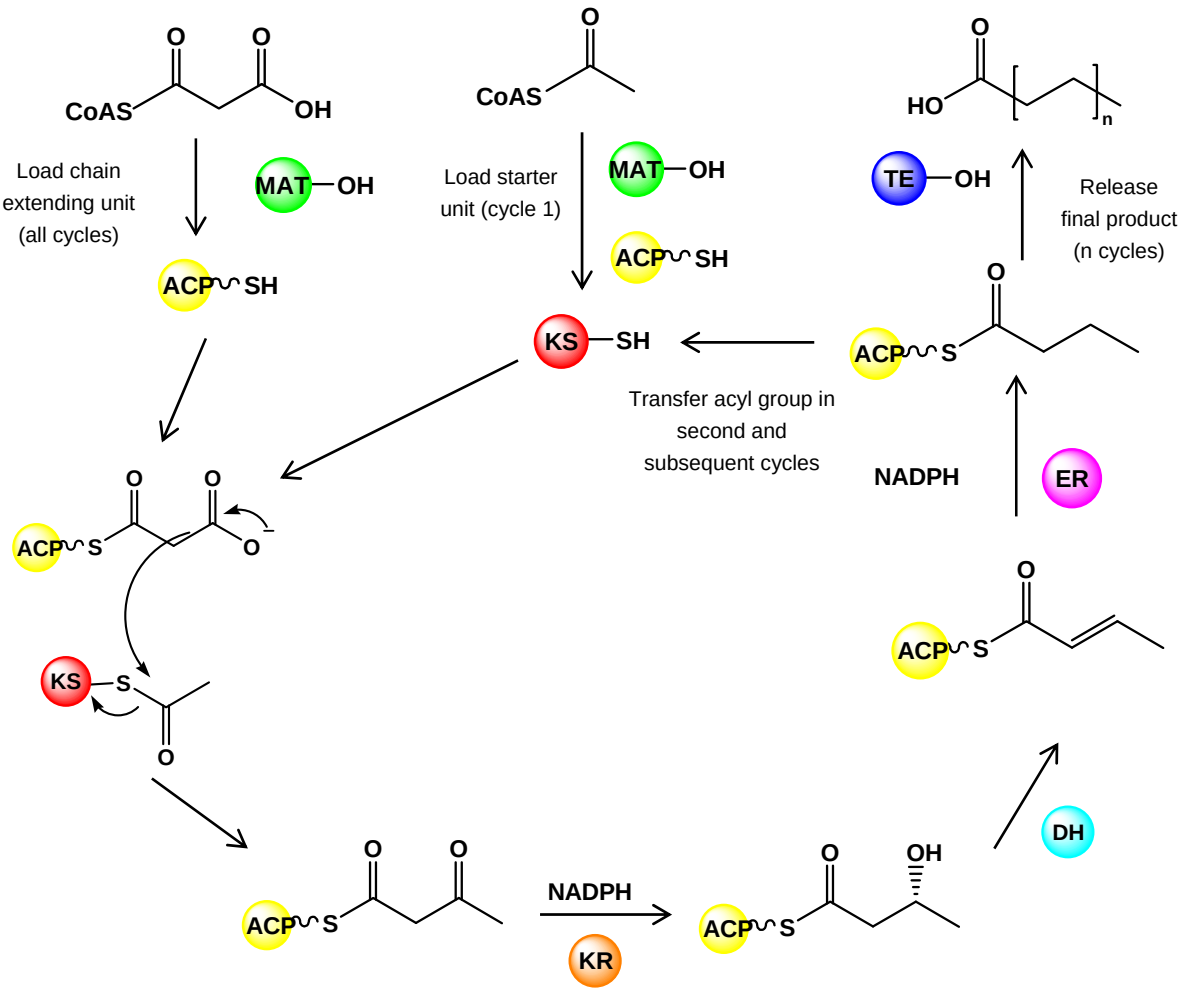

Figure 4.3.12: fatty acid synthesis: MAT: malonyl-acetyl transferase; ACP: acyl carrier protein; KS: ketosynthase; KR: ketoreductase; DH: dehydratase; ER: enoyl reductase; TE: thioesterase (adopted from Staunton & Weissmann, 2001)

After hydroxylation of the generated fatty acid, the synthesised 3-hydroxy myristic acid in its activated form is picked up by the first C-domain from the non-ribosomal peptide synthetase of the brabantamide gene cluster. Subsequently, the fatty acid gets attached to serine, which is bound to the corresponding thiolation domain. The biosynthesis continues with the described mechanism of non-ribosomal synthesis (see chapter 1.1.2), elongating the tethered molecule by the condensation of proline. The resulting lipodipeptide is subsequently passed on to the TE which allegorizes the final enzyme of the NRPS (see figure 4.3.13 (**2**)). The cleavage from the TE-domain is accompanied by an internal cyclisation (**3**) resulting in a 1,3-dioxo-pyrrolizidine (**4**).

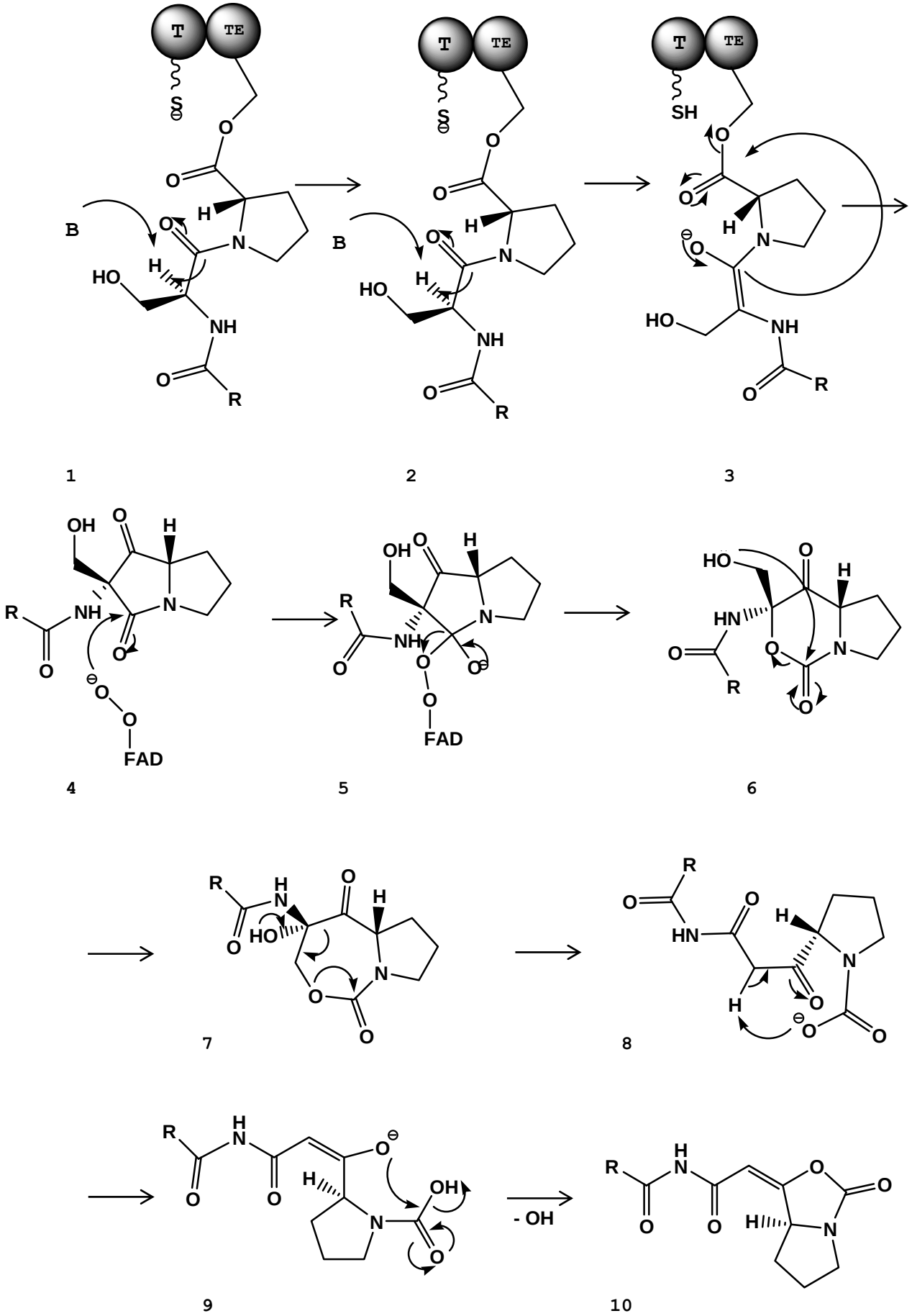

Figure 4.3.13: hypothetical biosynthesis of brabantamide

The presence of a FAD-dependent monooxygenase in the gene cluster leads to the assumption, that the next step in the biosynthesis is a Baeyer-Villiger-like oxidation (Baeyer & Villiger, 1899). In this kind of reactions NADPH, FAD and O_2 are required for the conversion of a ketone to an ester (Dewick, 2001). The FAD cofactor gets reduced by NADPH and subsequently builds a peroxy-enzyme complex (flavinperoxide), a reactive intermediate, by the use of molecular oxygen. The nucleophilic attack at the carbonyl-group of the pyrrolizidine by the peroxide (**4**) generates the typical Criegee-intermediate (**5**).

After rearrangement, the intermediate decomposes under release of 4-hydroxy-flavin and formation of a lactone with an extended ring system (**6**). Subsequently, another intramolecular rearrangement takes place, initiated through a nucleophilic attack of the carbonyl-group of the lactone by the hydroxyl group (**6**) resulting in a further ring extension (**7**). The instable cyclocarbamate decomposes by ring opening to the 2-(2-Tetradecanoylcarbamoyl-acetyl)-pyrrolidine-1-carboxylic acid anion (**8**).
The anion attacks the proton of the α-C-atom of the ketone resulting in an enolat-anion which similarly affects the carboxylic acid (**9**), finally leading to the formation of unglycosylated brabantamide A (**10**). Hypothetically, the final step of the biosynthesis could be the attachment of the rhamnose to the unglycosylated molecule by the glycosyltransferase to give brabantamide A. Another option would be an earlier attachment of the glycosyl-residue while the molecule is still bound to the NRPS at one of the aforementioned steps. The exact time of the attachment cannot be predicted unambiguously.

4.3.5 Investigations on the biosynthesis of brabantamides

The aforementioned hypothetical biosynthesis of brabantamide includes some intriguing steps which so far have been not observed in combination with a common ´NRPS-machinery´ generating lipopeptides. These massive rearrangements postulated in the biosynthesis hypothesis required verification by labelling experiments with stable isotopes.

Initially, a growth curve was performed to identify the point in time of maximum production of brabantamide and to determine the ideal feeding time for the chosen precursors. Subsequently, feeding experiments with L-serine and L-proline, both amino acids predicted to be incorporated by the corresponding specific A-domains of the NRPS, were performed. Following the hypothetical biosynthesis, the labelled carbon atoms of serine should be incorporated at the positions of carbon atoms no. 2, 10 and 9 of brabantamide and the labelled C1-atom of proline at the position of carbon atom no. 4, respectively (see figure 4.3.14). Due to the failed incorporation of proline (see chapter 4.3.5.8), an additional experiment with glycine was performed.

Labelled acetate was used to confirm the biosynthetic origin of the fatty acid moiety which should result in the enhancement of the signals of carbon atoms no. 12, 14, 16, 18, 20, 22 and 24. Universally labelled acetate should additionally approve the intact incorporation of the acetate units (Vederas, 1987).

Furthermore, 1-^{13}C – hydrogen carbonate was used to investigate another possible origin of the carbonyl group of the lactone moiety in case it is not serine-derived.

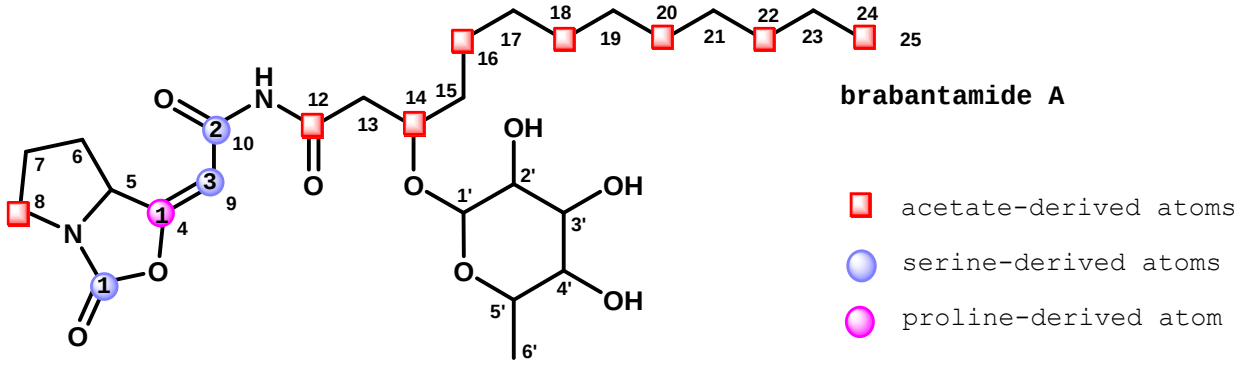

Figure 4.3.14: prediction of the labelling results with different precursors for brabantamide A; the numbers in the labelled atoms mark the associated carbon atom in the original amino acid

4.3.5.1 Carbon sources utilised by *Pseudomonas* sp. SH-C52

The investigations on carbon sources that can be utilised by *Pseudomonas* sp. SH-C52 were performed with the API®50 CH standardised test system (Biomerieux, Marcy l'Etoile France) as

described in chapter 3.1.6. With this test system, the degradation of 49 different carbon sources (see table 4.3.8) can be tested.

Table 4.3.8: carbon sources utilised by *Pseudomonas* sp. SH-C52; + = positive; - = negative; ? = ambigous

carbon source	incubation time		carbon source	incubation time	
	24 h	48 h		24 h	48 h
glycerol	+	+	salicin	-	-
erythritol	?	?	D-cellobiose	-	-
D-arabinose	?	?	D-maltose	-	-
L-arabinose	+	+	D-lactose (bovine origin)	-	-
D-ribose	?	+	D-melibiose	-	-
D-xylose	+	+	D-saccharose (sucrose)	+	+
L-xylose	?	?	D-trehalose	+	+
D-adonitol	-	-	inulin	-	-
methyl- ß-D-xylopyranoside	-	-	D-melezitose	-	-
D-galactose	+	+	D-raffinose	-	-
D-glucose	+	+	amidon (starch)	-	-
D-fructose	+	+	glycogen	-	-
D-mannose	+	+	xylitol	-	-
L-sorbose	-	-	gentiobiose	-	-
L-rhamnose	-	-	D-turanose	-	-
dulcitol	-	-	D-lyxose	-	-
inositol	-	+	D-tagotose	-	-
D-mannitol	?	+	D-fucose	+	+
D-sorbitol	-	?	L-fucose	-	-
methyl- α-D-mannopyranoside	-	-	D-arabitol	-	+
methyl- α-D-glucopyranoside	-	-	L-arabitol	-	-
N-acetylglucosamine	-	-	potassium gluconate	+	+
amygdalin	-	-	potassium 2-ketogluconate	-	-
arbutin	-	-	potassium 5-ketogluconate	-	-
esculin ferric citrate	?	?			

The results show, that *Pseudomonas* sp. SH-C52 mainly utilises monosaccharides as carbon sources, thereby preferring the L-form of arabinose and the D-form of xylose.

The only di-saccharides used by *P.* sp. SH-C52 were sucrose and trehalose whereas no oligo- or polysaccharides were degraded. Furthermore, some alditols (glycerol, mannitol, D-arabitol), a desoxy sugar (D-fucose) and one carboxylic acid (potassium gluconate) could be used as carbon source.

4.3.5.2 Growth curve of *P.* sp. SH-C52 and production rate of brabantamide A

In order to determine the optimal feeding and harvesting time for the labelling experiments, a bacterial growth curve of *Pseudomonas* sp. SH-C52 and a quantitative analysis of brabantamide production were performed (see chapter 3.1.5).

The specific growth rate of *P.* sp. SH-C52 could be determined as 0.3892, with a resulting doubling time of 2.11 hours (see figure 4.3.15).

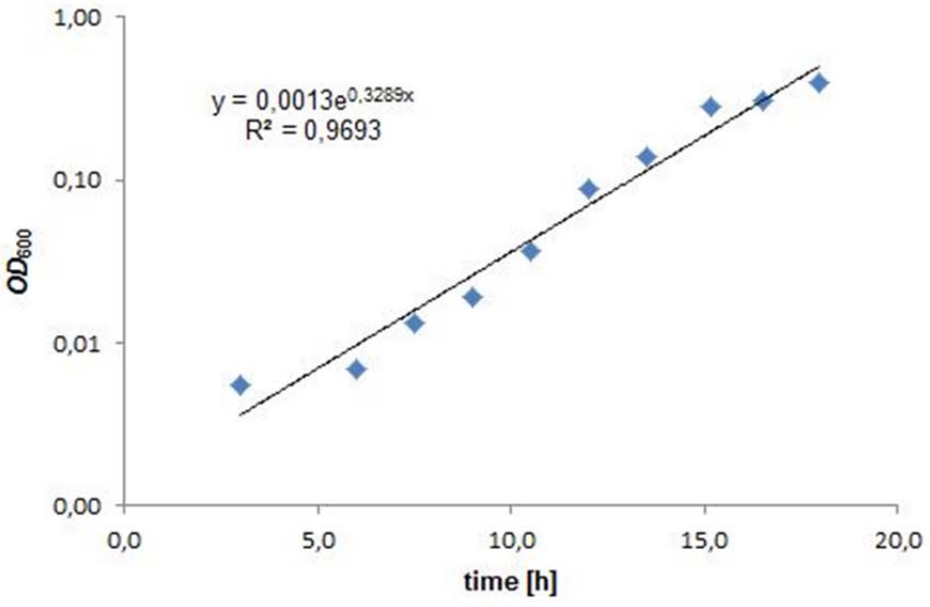

Figure 4.3.15: Determination of the doubling time of *P.* sp. SH-C52

The growth curve (see figure 4.3.16) revealed a lag-phase of ~ 5 h, followed by a starting phase of ~ 3 h and an exponential

phase till 15 h. The slow-down phase lasts till ~ 29 h when the growth of *P.* sp. SH-C52 passes over to stationary phase.

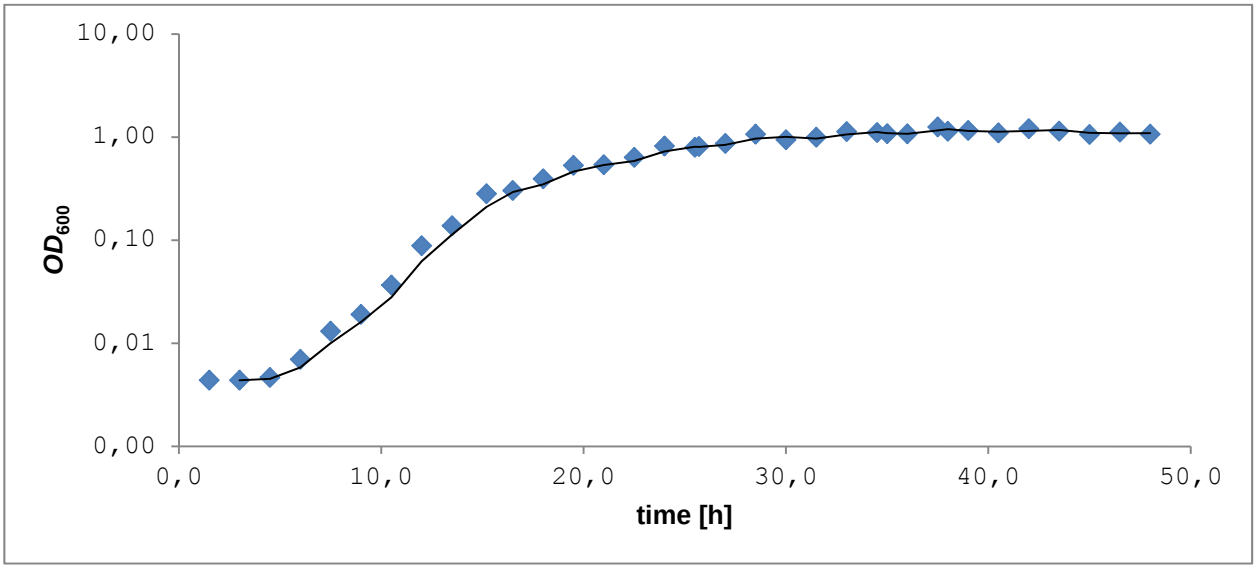

Figure 4.3.16: growth curve of Pseudomonas sp. SH-C52

The calibration line for the determination of the production rate of brabantamide A was determined with standards two till five (see figure 9.1.12). The chromatogram of standard number one exhibited no peak in LC-MS analysis and was therefore not evaluable.

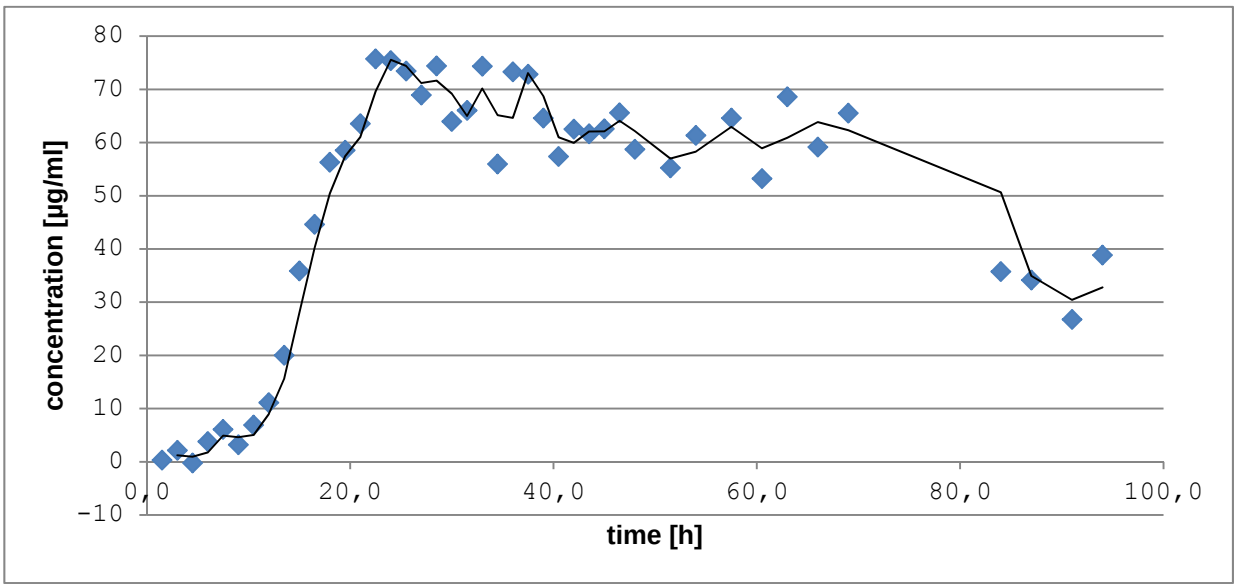

Figure 4.3.17: production of brabantamide A by *Pseudomonas* sp. SH-C52

The optimal feeding time was determined as the end of the starting phase and the following transition to the exponential phase. In accordance with the determined production rate of brabantamide A (see figure 4.3.18), the feeding time was committed to 8 hours. Before this point of time, no significant

production of brabantamide A could be observed. The harvesting time kept at 60-72 hours due to a decreasing production rate after 72 hours.

4.3.5.3 Results of the 1-^{13}C - sodium acetate feeding

The feeding experiment was performed by adding isotopically labelled 1-^{13}C - sodium acetate in a concentration of 222.2 mg/l and subsequent extraction according to the established procedure (see chapters 3.2 and 3.3.1). The crude extract was separated by RP-SPE (see chapter 3.3.10) and the resulting fractions were analysed by ^{1}H-NMR to target the fraction containing the labelled metabolite. In the ^{1}H-NMR spectrum of fraction C, brabantamide could be identified by the typical fatty acid resonances at 0.94 ppm and 1.29 ppm for the terminal methyl group and the methylene groups, respectively, its characteristic methine resonance at 5.03 ppm and the double bond resonance at 6.29 ppm. Hence, this fraction was further purified by HPLC, using system 4 and column 1 (see chapter 3.3.3), employing a linear gradient starting with 70% methanol and 30% water increasing to 100 % methanol in 30 min followed by 10 min isocratic elution with pure methanol.

After purification, fraction C-4 could be identified unambiguously as brabantamide A (see ^{1}H-NMR spectrum appendix figure 8.1.12). The ^{13}C-NMR spectrum of the purified compound showed enhanced signals of the carbon atoms no. 4, 8, 12, 14, 16 and 24 (see table 4.3.9 and figures 4.3.18 and 8.1.13, appendix).

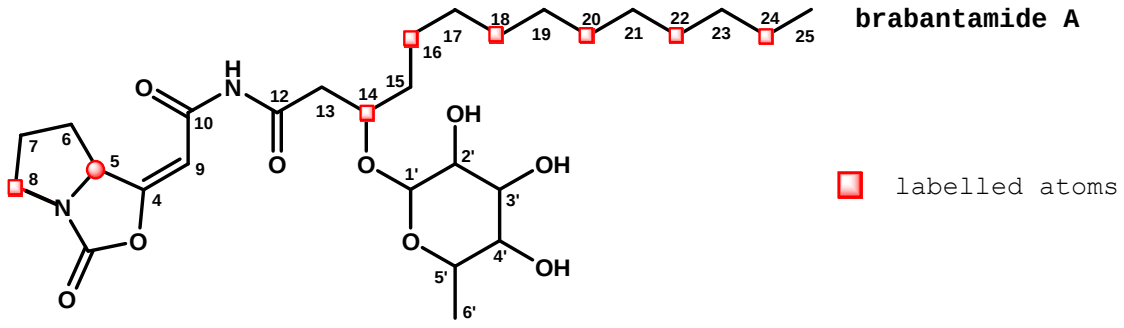

Figure 4.3.18: result of the labelling experiment with 1-^{13}C - sodium acetate

Table 4.3.9: enrichment of carbon atoms in brabantamide A after labelling with 1-^{13}C – sodium acetate

carbon no.	A natural	B labelled	C quotient B/A	D enrichment [%]
2	0.338	0.092	0.24	-
4	0.644	1.900	2.95	2.1
5	1.057	0.994	0.94	-
6	1.160	1.138	0.98	-
7	1.009	0.900	0.89	-
8	0.948	8.638	9.11	8.9
9	1.054	0.672	0.64	-
10	0.434	0.059	0.14	-
12	0.587	2.069	3.52	-
13	1.032	0.551	0.52	-
14	1.054	6.151	5.84	-
15	1.161	0.727	0.63	-
16	0.845	7.294	8.63	8.4
17-22	6.716	34.641	5.16	3.6
23	1.139	0.732	0.64	-
24	1.115	9.221	8.10	7.8
25	1.032	0.688	0.65	-
1′	1.070	0.712	0.91	-
2′	1.095	0.944	0.91	-
3′	1.170	0.881	0.75	-
4′	1.073	0.792	0.74	-
5′	1.046	0.686	0.66	-
6′	1.000	1.000	1.00	-

For calculation purposes carbon atom no. 6´ was set to 1.000; **A**: integrals of the non-labelled compound, **B**: integrals of the labelled compound, **C**: quotient of the integrals (enriched/not enriched), **D**: enrichment of carbon atoms (calculation see chapter 3.3.4)

Furthermore, the signal intensity of the carbons 17-22 increased. The overlapping signals around 30 ppm of these atoms in the ^{13}C-NMR spectrum precluded a detailed discrimination of regular and enhanced carbon atoms. However, considering that carbon 12, 14 and 24 represent secured ^{13}C-enriched carbons, according to biosynthetic rules, the enhancement of the resonances around 30 ppm can be attributed to carbons no. 18, 20 and 22 which have undergone ^{13}C enrichment.

4.3.5.4 Results of the labelling experiment with 1,2-^{13}C – sodium acetate

In order to investigate the incorporation of intact acetate, universally labelled sodium acetate (U-^{13}C sodium acetate) was added to the culture four hours after inoculation at a concentration of 222.2 mg/ml. Subsequently, the established

procedure comprising three days of growth, extraction and purification by VLC and HPLC was applied (see chapters 3.3.1-3.3.3).

The expected peak – pattern of the HPLC-chromatogram could be observed in fraction C and subsequent purification yielded 2.4 mg brabantamide A which was confirmed by ^{1}H-NMR spectroscopy (see figure 8.1.14).

Table 4.3.10: enrichment of carbon atoms in brabantamide A after labelling with 1,2-^{13}C – sodium acetate

carbon no.	A natural	B labelled	C quotient B/A	D enrichment [%]
4	0.644	0.35	0.54	-
6	1.160	-[a]	-[a]	-[a]
9	1.054	0.54	0.51	-
13	1.032	0.97	0.94	-
16	0.845	0.93	1.10	0.1
17-22	6.716	18.31	2.72	1.9
23	1.139	2.17	1.91	1.0
1'	1.070	0.43	0.41	-
2'	1.095	0.73	0.67	-
3'	1.170	0.67	0.57	-
4'	1.073	0.75	0.70	-
5'	1.046	0.76	0.73	-
6'	1.000	1.00	1.00	-

For calculation purposes carbon atom no. 6´ was set to 1.000; **A:** integrals of the non-labelled compound, **B:** total integrals of the labelled compound, **C:** quotient of the integrals (enriched/ not enriched), **D:** enrichment of carbon atoms (calculation see chapter 3.3.4).

[a] signal could not be integrated due to overlap with the carbons of the methylene envelope; carbon atoms C2, C10 and C12 were not apparent in the ^{13}C-NMR spectrum

The evaluation of the relative enrichment was performed using two different calculations. To determine whether a position of the carbon skeleton contains more ^{13}C than that corresponding to natural abundance, the spectra of the unlabelled and labelled metabolites were compared (see table 4.3.10; Séquin & Scott, 1974). In case of appearing doublets, indicating acetate units which were incorporated as a whole unit, the enrichment was determined by comparison of the total integral (integral with satellites) to the integration value of the uncoupled signal and the coupling constants were determined (see table 4.3.11 and figure 4.3.19; Chang *et al.*, 2004).

Incorporation of complete acetate units were observed for carbon atoms C-7 and C-8 (J_{cc} 32.4-32.5 Hz), C-14 and C-15 (J_{cc} 36.3-37.8 Hz) and C-24 and C-25(J_{cc} 34.7-34.8 Hz). Furthermore, C-5 (J_{cc}

42.7 Hz) showed satellites, but the expected corresponding enhancement of C-4 was not observed maybe due to the small amount of brabantamide A or its quaternary character.

Table 4.3.11: calculation of the incorporated acetate units into brabantamide A after labelling with U-^{13}C – sodium acetate

carbon no.	A	B	C	D
	J_{CC} [Hz]	total integral of enriched brabantamide A	integration value for uncoupled signal	% relative enrichment from intact incorporation
5	42.7	2.43	1.21	201
7	32.5	5.90	1.68	351
8	32.4	4.93	1.68	293
14	37.8	1.81	1.11	163
15	36.3	3.61	1.63	221
24	34.8; 69.2	5.14	1.70	302
25	34.7	3.53	0.67	527

Further labelled atoms were obtained at positions C-16, C-17 to C-22 and C-23, together building with the above mentioned carbon atoms no. 14, 15, 24 and 25 the expected enhancement of the fatty acid moiety. Carbon atom no. 6 couldn´t be evaluated due to overlap with carbons 17-22.

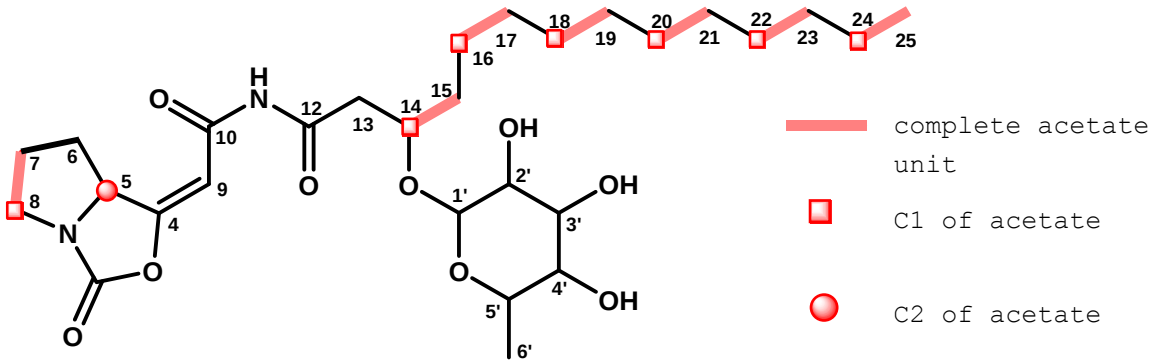

Figure 4.3.19: labelling pattern of brabantamide A after labelling with U-^{13}C - sodium acetate

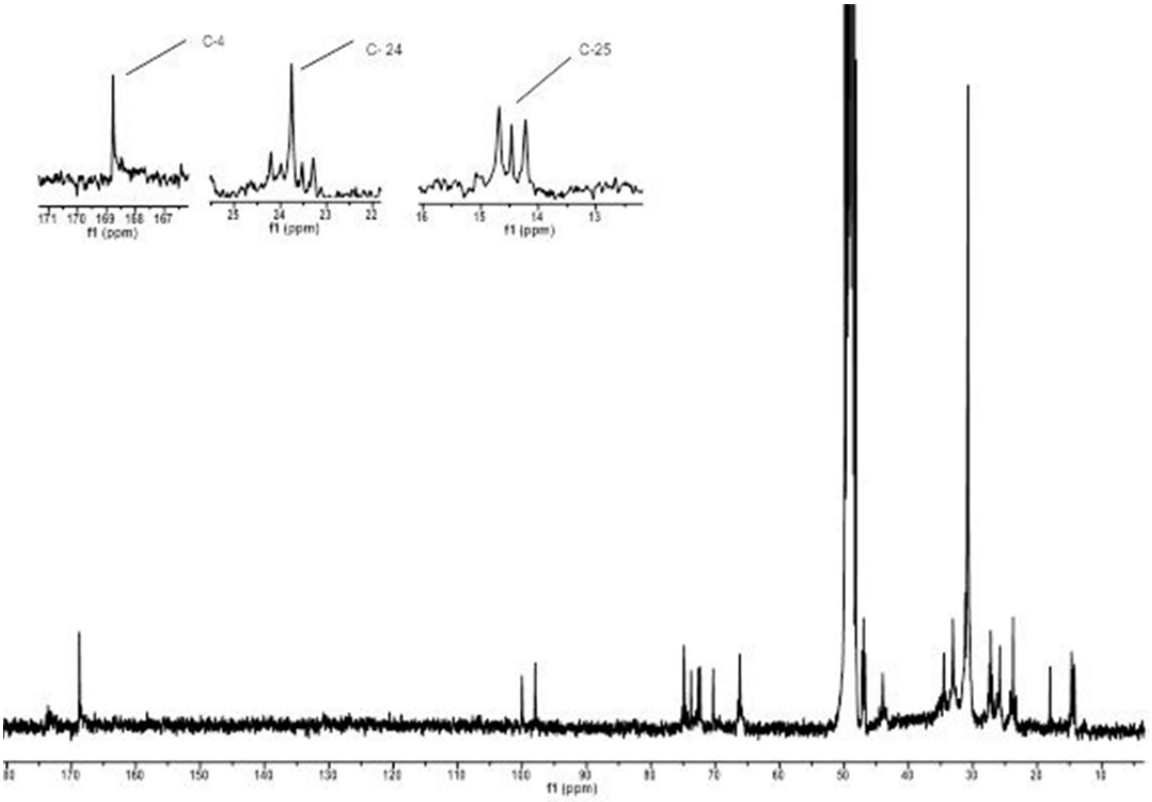

Figure 4.3.20: ^{13}C NMR spectrum of brabantamide A in d_4-methanol after labelling with 1,2-^{13}C - sodium acetate (75 MHz, 66000 scans); the enlarged insets illustrate carbon atoms with satellites in comparison to the obtained singlets

The determination of the C1 of each acetate unit was based on the results from the feeding experiment with single labelled acetate.

Carbon atoms no. 5, 7 and 8 are incorporated by the citrate cycle (see chapters 4.3.5.6 and 4.3.5.7).

4.3.5.5 Results of feeding experiment with 1-^{13}C - L-serine

Serine labelling was performed by addition of 500 mg 1-^{13}C – L-serine (111.1 mg/l), four hours after inoculation, to cultures of *P.* sp. SH-C52 (see chapter 3.1.3). Extraction and workup of the crude extract (183.2 mg) by VLC and HPLC using established procedures (see chapters 3.3.1 – 3.3.3 and 4.3.5.3) yielded 2.8 mg of labelled brabantamide A which could be unambiguously identified by ^1H-NMR (see figure 8.1.15).

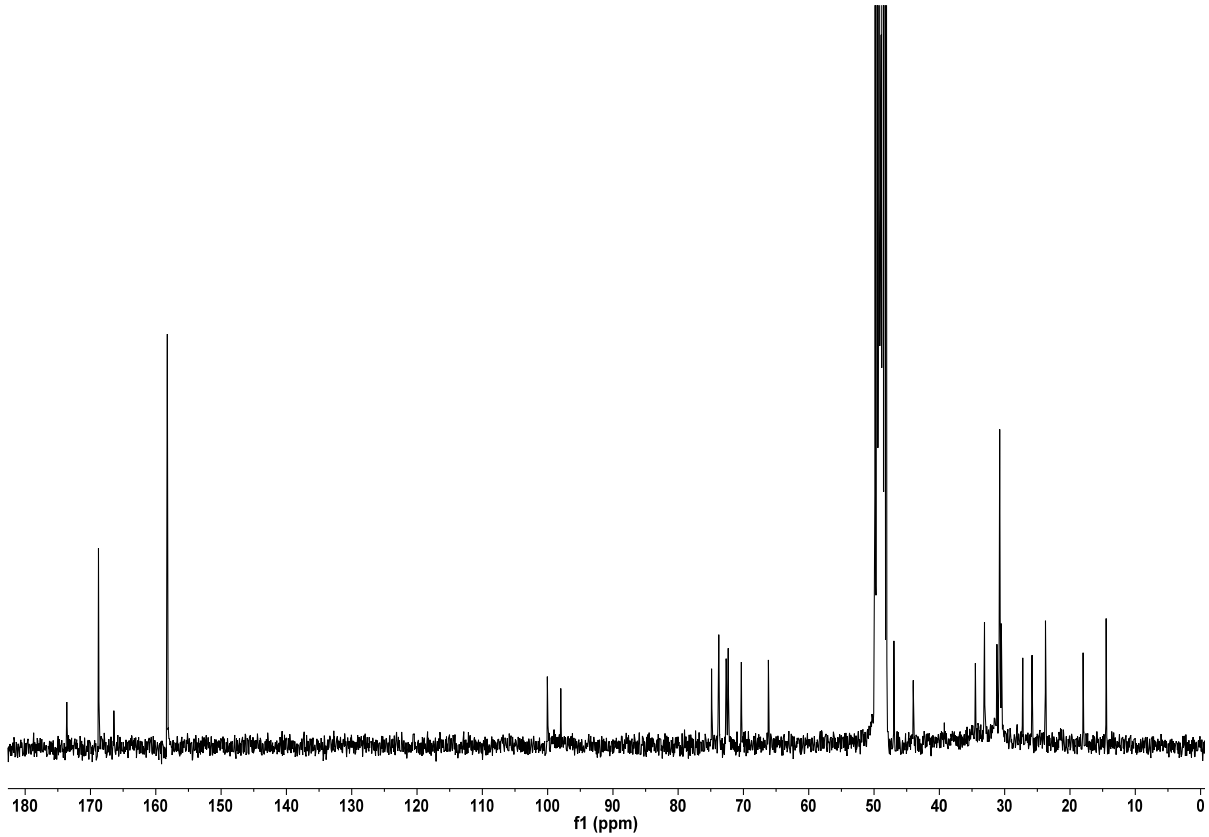

Figure 4.3.21: 1-^{13}C NMR spectrum of brabantamide A after labelling with 1-^{13}C - L-serine in d_4-methanol at 75 MHz (ns = 12260)

In the ^{13}C-NMR spectrum of the purified compound, the resonances for carbon atoms no. 2 and 4 showed significant enhancement (see figure 4.3.21 and 4.3.22 and table 4.3.12). The enrichment of carbon atom no. 4 appears at first unexpected and will be discussed in chapter 4.3.5.6.

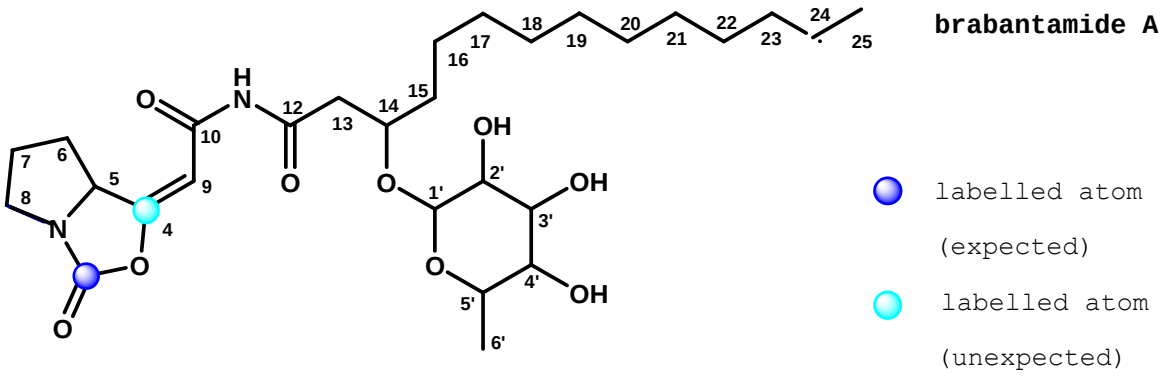

Figure 4.3.22: result of the labelling experiment with 1-^{13}C - L-serine

Table 4.3.12: enrichment of carbon atoms in brabantamide A after labelling with 1-^{13}C – L-serine

carbon no.	A natural	B labelled	C quotient	D enrichment [%]
2	0.383	4.018	10.49	8.4
4	0.644	1.873	2.91	1.5
5	1.057	0.864	0.82	-
6	1.160	1.575	1.36	0.1
7	1.009	0.941	0.93	-
8	0.948	1.033	1.09	-
9	1.054	0.637	0.60	-
10	0.434	0.263	0.61	-
12	0.587	0.471	0.80	-
13	1.032	0.813	0.79	-
14	1.054	0.929	0.88	-
15	1.161	1.168	1.00	-
16	0.845	1.173	1.39	0.2
17-22	6.716	8.997	1.34	0.1
23	1.139	1.278	1.12	-
24	1.115	1.213	0.90	-
25	1.032	1.276	1.24	-
1′	1.070	0.658	0.61	-
2′	1.095	1.294	1.18	-
3′	1.170	1.145	0.99	-
4′	1.073	1.199	1.12	-
5′	1.046	0.963	0.92	-
6′	1.000	1.000	1.00	-

For calculation purposes carbon atom no. 6´ was set to 1.000; **A:** integrals of the non-labelled compound, **B:** integrals of the labelled compound, **C:** quotient of the integrals (enriched/ not enriched), **D:** enrichment of carbon atoms (calculation see chapter 3.3.4)

4.3.5.6 Labelling experiment with U-^{13}C L-serine

In order to investigate the incorporation of serine, universally labelled serine (U-^{13}C L-serine) was added to the culture four hours after inoculation at a concentration of 55.6 mg/ml. Subsequently, the established procedure comprising three days of growth, extraction and purification by VLC was applied (see chapters 3.3.1 and 3.3.2). Further purification was achieved by HPLC employing system 4 and column 1 (see chapter 3.3.3) using a gradient starting with a methanol-water mixture (70:30) increasing to 100 % methanol in 30 minutes, followed by ten min isocratic elution with methanol.

The expected peak-pattern of the HPLC-chromatogram could be observed in fraction C and yielded in 3.2 mg brabantamide A which was confirmed by ^{1}H-NMR spectroscopy (see figure 8.1.16).

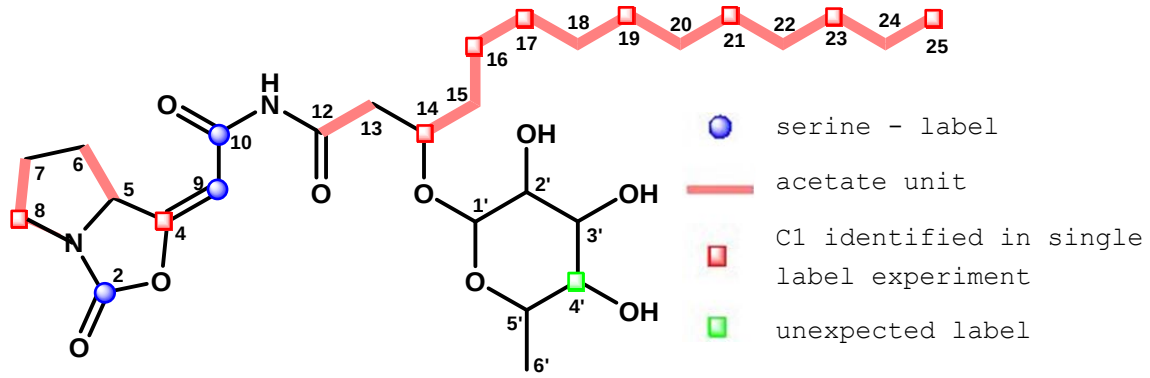

Figure 4.3.23: labelling pattern resulting from the feeding experiment of brabantamide A with U-^{13}C - L-serine

The ^{13}C-spectrum of brabantamide A (see figure 4.3.24) showed enhanced signals of C2, C9 and C10 as expected from the proposed biosynthesis (see chapter 4.3.4). Additionally, the spectrum revealed an incorporation pattern similar to the one observed in the labelling experiment with universally labelled acetate. Thus, all residual carbon atoms except no. 1′, 2′, 3′, 5′ and 6′ belonging to the rhamnopyranose moiety showed enrichments towards the natural abundance of ^{13}C.

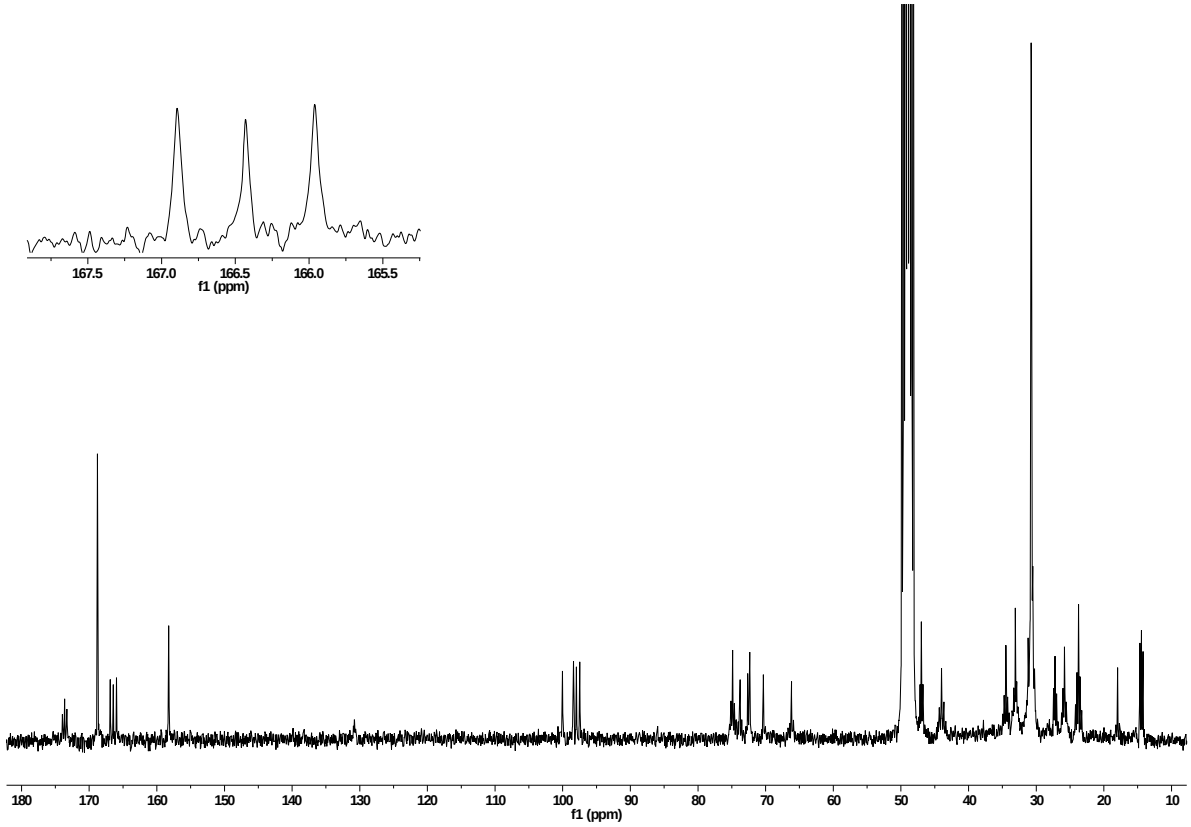

Figure 4.3.24: ^{13}C NMR of brabantamide A after labelling with U-^{13}C - L-serine in d_4-methanol (75 MHz, 21000 scans); the enlarged inset illustrates the usual splitting pattern obtained by incorporation of double labelled precursors

Table 4.3.13: enrichment of carbon atoms in brabantamide A after labelling with U-^{13}C - L-serine

carbon no.	A natural	B labelled	C quotient B/A	D enrichment [%]
2	0.383	2.58	6.74	6.3
4	0.644	3.81	5.92	5.4
5	1.057	0.87	0.82	-
6	1.160	-[a]	-[a]	-[a]
17-22	6.716	30.27	4.51	3.86
1'	1.070	0.92	0.86	-
2'	1.095	1.14	1.04	0.04
3'	1.170	1.36	1.16	0.18
5'	1.046	0.78	0.75	-
6'	1.000	1.00	1.00	-

For calculation purposes carbon atom no. 6´ was set to 1.000; **A:** integrals of the non-labelled compound, **B:** total integrals of the labelled compound, **C:** quotient of the integrals (enriched/ not enriched), **D:** enrichment of carbon atoms (calculation see chapter 3.3.4)

[a] signal could not be integrated due to overlap with resonances of the carbon atoms 17-22

Table 4.3.14: calculation of the incorporated acetate units into brabantamide A after labelling with U-^{13}C - L-serine

carbon no.	A	B	C	D
	J_{cc} [Hz]	total integral of enriched brabantamide A	integration value for uncoupled signal	% relative enrichment from intact incorporation
7	32.0	3.58	1.52	236
8	31.9	3.92	1.78	220
9	70.5	5.69	1.29	441
10	70.4	3.24	0.84	386
12	49.6	2.13	0.76	280
13	50.6	4.41	1.78	248
14	38.9	3.61	1.68	215
15	38.6; 72.9	6.30	2.52	250
16	35.5; 68.5	5.51	1.84	299
23	34.4	5.42	2.46	220
24	34.9; 69.1	5.70	2.02	282
25	34.9	4.66	1.39	335
4'	40.6	3.64	0.84	433

As described in chapter 4.3.5.4, two calculations were applied to enable the incorporation rate of labelled carbon atoms. The

values of the enrichments are listed in tables 4.3.13 and 4.3.14.

The enhancement of the acetate-derived carbon atoms can be attributed to the serine – dehydratase (also called serine – deaminase). This enzyme dehydrates serine in a first step, subsequently followed by deamination under consumption of water, resulting in pyruvate and ammonia (see figure 4.3.25; Kim & Gadd, 2008).

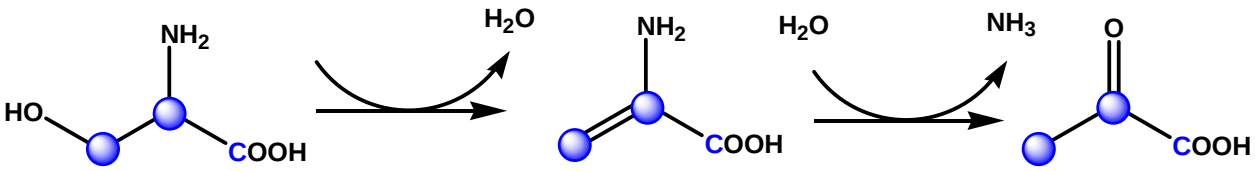

Figure 4.3.25: serine dehydratase (serine deaminase); blue colour indicates labelled carbon atoms

Thus, the received pyruvate can be used for anabolic and catabolic purposes like for example being transformed into acetyl-CoA by a pyruvate-dehydrogenase and recycled into the citrate cycle by citrate-synthase (see figure 4.3.26).

Hence, the labelled precursor can be integrated in brabantamide A as acetate units similar to the labelling experiment with universally labelled acetate. (For detailed description of the citrate cycle see chapter 4.3.5.7)

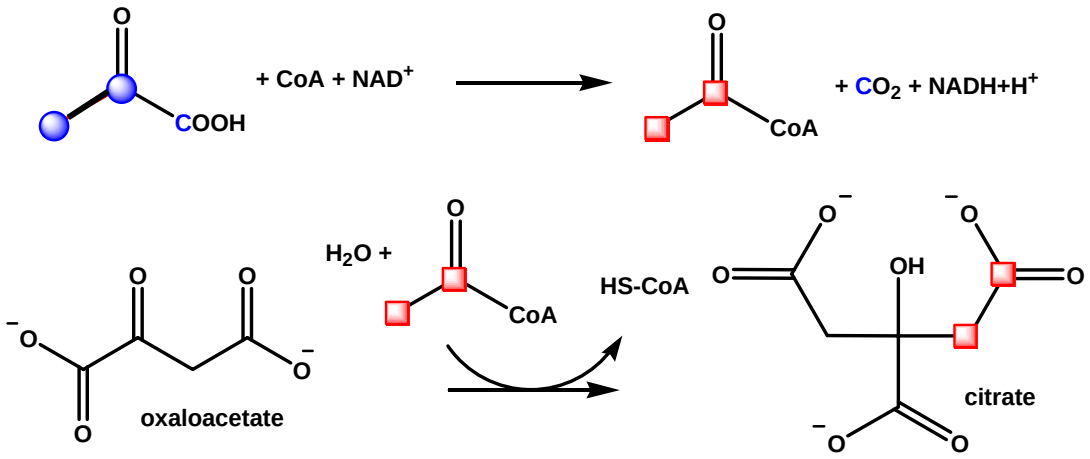

Figure 4.3.26: reactions catalysed by pyruvate dehydratase and by citrate synthase; the applied colour scheme refers to one used in the labelling pattern in figure 4.3.23

The labelling of all acetate-derived carbon atoms was already reported by a research group working with glycine precursors (Cushley *et al.*, 1973). In this work, an additional step, the

glycine-serine interconversion is mentioned, but the following steps leading to the doubly labelled acetate units take place in a similar sequence.

The appearance of the label at C4’ in the rhamnose portion was at first unexpected but can be envisioned by degradation of serine to hydroxyl-pyruvate and channelling into sugar biosynthesis via glycerol-3-phosphate (see appendix, figures 8.1.17 and 8.1.18).

4.3.5.7 Labelling experiment with 1-^{13}C - hydrogen carbonate

The feeding experiment was performed by adding isotopically labelled 1-^{13}C – hydrogen carbonate in a concentration of 222.2 mg/l as described in chapter 3.2. The further processing procedure was adopted from the labelling experiment with 1-^{13}C - L-serine (see chapter 4.3.5.5). Analysis of the resulting fractions by ^{1}H-NMR discovered the labelled metabolite in fraction C.

After purification by HPLC, fraction C-3 could be identified unambiguously as brabantamide A (see figure 8.1.19).

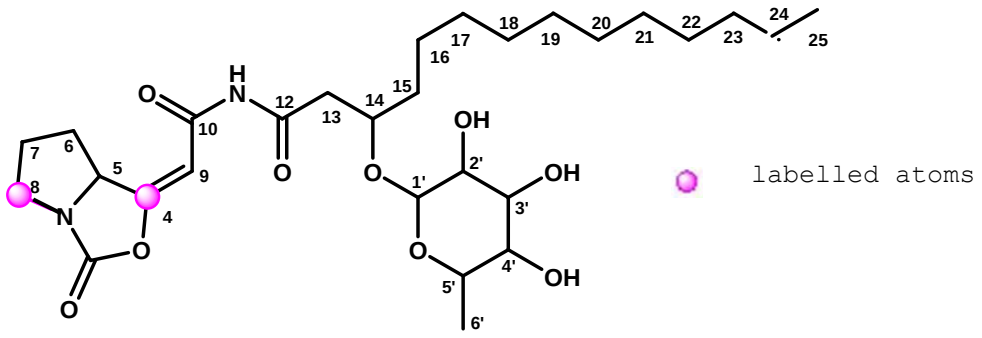

Figure 4.3.27: result of the labelling experiment with 1-^{13}C – hydrogen carbonate

Table 4.3.15: enrichment of carbon atoms in brabantamide A after labelling with 1-^{13}C - hydrogen carbonate

carbon no.	A natural	B labelled	C quotient	D enrichment [%]
2	0.383	0.151	0.39	-
4	0.644	1.565	2.43	1.6
5	1.057	1.026	0.97	-
6	1.160	0.838	0.72	-
7	1.009	0.958	0.95	-
8	0.948	1.520	1.60	0.7
9	1.054	0.858	0.81	-
10	0.434	0.158	0.36	-
12	0.587	0.285	0.49	-
13	1.032	0.644	0.62	-
14	1.054	0.836	0.79	-
15	1.161	0.775	0.67	-
16	0.845	0.823	0.97	-
17-22	6.716	6.157	0.92	-
23	1.139	0.888	0.78	-
24	1.115	0.439	0.39	-
25	1.032	0.670	0.65	-
1′	1.070	0.843	0.79	-
2′	1.095	0.880	0.80	-
3′	1.170	0.919	0.79	-
4′	1.073	0.953	0.89	-
5′	1.046	0.975	0.93	-
6′	1.000	1.000	1.00	-

For calculation purposes carbon atom no. 6´ was set to 1.000, **A:** integrals of the non-labelled compound, **B:** integrals of the labelled compound, **C:** quotient of the integrals (enriched/ not enriched), **D:** enrichment of carbon atoms (calculation see chapter 3.3.4)

The ^{13}C-NMR spectrum of the purified compound obtained enhanced signals of the carbon atoms no. 4 and 8 (see table 4.3.15, figure 4.3.27 and figure 8.1.20, appendix). Therefore, it can be excluded, that the biosynthetic origin of carbon no. 2 is based on the incorporation of hydrogen carbonate.

The incorporation of the labelled hydrogen carbonate into C4 and C8 can be explained by the citric acid cycle (see figure 4.3.28). Hydrogen carbonate can be introduced into the citric acid cycle by the pyruvate carboxylase which catalyses the carboxylation of pyruvate to form oxaloacetate (OAA). Following the citric acid cycle OAA gets transformed to isocitrate which in turn is finally converted step by step into proline. The labelled positions match with the incorporation of proline into brabantamide A according to the hypothesised biosynthesis (see chapter 4.3.4).

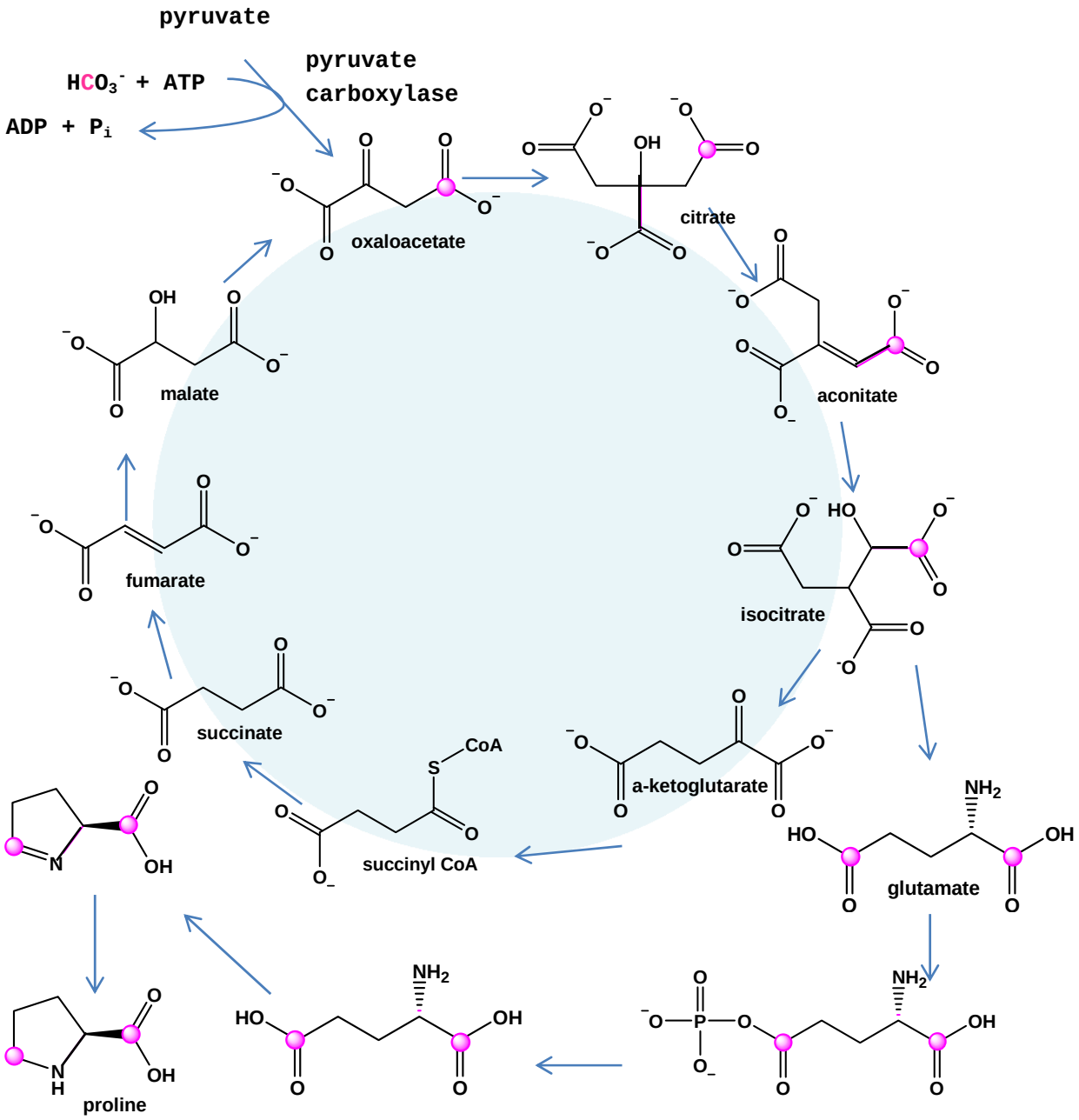

Figure 4.3.28: citric acid cycle; pink spots indicate labelled C-atoms

4.3.5.8 Investigations on proline incorporation

Attempts to prove intact incorporation of 1-^{13}C isotopically labelled proline (55.6 mg/l) failed twice, since brabantamide production was apparently abolished under these conditions.

These results led to the hypotheses that either proline uptake mechanisms in *P.* sp. SH-C52 are malfunctional or that an elevated proline concentration in the medium exert a negative feedback on brabantamide production. However, investigations regarding its proline tolerance on small scale level did not abolish brabantamide production. Neither the addition of D- nor of L-proline at different concentrations (83.3 mg/l or 166.7 mg/l) using the established cultivation methods led to a decrease of production. In contrast, a slight increase in brabantamide production was observed when the culture medium contained L-Pro. Likewise, an enhanced production could be observed when cultures were supplemented with serine (333.3 mg/ml) or the extraction was conducted with Amberlite resin.

Furthermore, the ability of the strain to take up proline was probed with a feeding study using radioactive proline. These experiments were performed by Michaele Josten (IMMIP, Pharmaceutical Microbiology Unit, University of Bonn, Bonn, Germany) according to the method described in chapter 3.1.10. The investigations showed, that *Pseudomonas* sp. SH-C52 is able to assimilate proline (see figure 4.3.29 and the corresponding values in table 8.1.3, appendix).

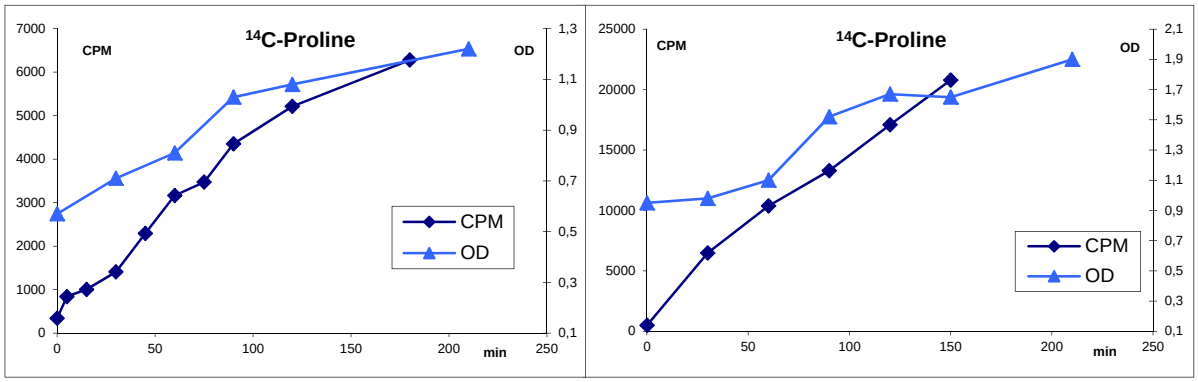

Figure 4.3.29: repeat determination of proline-uptake in *P.* sp. SH-C52; CPM = counts per minute; OD = optical density

A further attempt to verify the proline incorporation was conducted, this time using 1-^{13}C isotopically labelled L-glycine as a precursor of proline in the citric acid cycle (see figure 4.3.28). Hence, 222.2 mg L-glycine were fed analogously to the other labelling experiments. However, no brabantamide production was observed with addition of glycine to the culture media.

4.3.5.9 Further biosynthetic studies using knockout mutants

In order to unravel further steps of the biosynthesis of brabantamide A, further knockout studies were performed, targeting the involved glycosyltransferase and the monooxygenase, respectively. The corresponding knockout mutants C52Δ26 and C52Δ28 were cultivated on a 4.5 l scale analogously to wild-type cultivations (see chapter 3.1.3) and subsequently processed according to the established extraction and separation procedure (see chapters 3.3.1 and 3.3.2). However, neither the expected brabantamide aglycon nor the hypothesised intermediate (see step 4, hypothetical biosynthesis in chapter 4.3.4) could be detected.

Further attempts with optimized ´in-frame´-deletion mutants targeting the glycosyltransferase (strain C52Δ26IF) failed as well as an isotope-guided approach employing 1-^{13}C – L-serine (111.1 mg/l) to track down the expected derivative.

4.3.6 Biological activity of brabantamides

The influence of brabantamides on the growth of a panel of Gram-positive and Gram-negative bacteria and some fungi was determined.
Hereby, brabantamides showed only inhibitory activities against Gram-positive bacteria whereas Gram-negative bacteria and fungi were not affected (see table 4.3.16 and appendix, table 8.1.4; Reder-Christ *et al.*, 2012).

All brabantamides displayed strong inhibitory activity against *A. crystallopoietes*. Furthermore, brabantamides B and C showed good inhibitory effects towards *B. subtilis*, *B. cereus*, *B. megaterium*, *C. xerosis* and *M. luteus* while brabantamide A only showed a small or no bacteria-free areola. In addition, brabantamide A influenced the growth of *S. aureus* and *M. smegmatis* strains, whereas brabantamide B was observed to moderately inhibit the growth of diverse *S. aureus* strains.

Table 4.3.16: antimicrobial disk diffusion inhibitory activities of brabantamides against chosen Gram-positive bacteria (A = brabantamide A; B = brabantamide B; C = brabantamide C)

Organism	**Zone of inhibition [mm]**		
	A	**B**	**C**
Arthrobacter crystallopoietes DSM 20117	13	14	14
Bacillus cereus	n.t.	8[d]	8[b]
Bacillus subtilis 168	4	11[a]	10[a]
Bacillus megaterium	0	11[c]	10[c]
Corynebacterium pseudodiphtheriticum	3	n.t.	n.t.
Corynebacterium diphtheriae	3	n.t.	n.t.
Corynebacterium xerosis Va 167198	3	12[b]	12[b]
Listeria welchimeri DSM 20650	3	0	0
Micrococcus luteus ATCC 4698	n.t.	10[a]	10[a]
Mycobacterium smegmatis ATCC 70084	3	0	0
Staphylococcus aureus SG 511	3	0	0
Staphylococcus aureus 5185 (MS)	3	4[a]	0
Staphylococcus aureus I-11574 (MS)	n.t.	6[a]	0
Staphylococcus aureus LT-1334 (MR)	0	6[a]	0

[a] turbid; [b] very turbid; [c] clear with resistances; [d] bright with turbid court
MS = methicillin-susceptible; MR = methicillin-resistant; n.t. = not tested

The determined MICs (table 4.3.17) of brabantamides matched well to the corresponding inhibition zones. Brabantamides showed significant antibacterial activities against *A. crystallopoietes* DSM 20117, *B. subtilis* 168, *B. megaterium and M. luteus*, while values for *C. xerosis* Va167198, *M. smegmatis* ATCC 70084, *L. welchimeri* DSM 20650 *and S. aureus* SG 511 must be judged as moderate.

It is noteworthy to mention, that brabantamide C shows considerable lower minimal inhibition concentrations towards the tested bacteria than brabantamide A and B. This can be seen as first hint for a structure – activity relationship (see chapter 5.2.3.1).

Since it is known, that the activity of some CLPs is calcium-dependent (Baltz *et al.*, 2005), brabantamide A was re-tested in the presence of Ca^{2+} ions to avoid false-negative results (data not shown). However, no difference in potency was observed which implies that a dependency of calcium is not given. For this reason as well as due to restrictions in available compound material, brabantamides B and C were not re-tested.

Table 4.3.17: minimal inhibition concentrations (MICs) of brabantamides (A = brabantamide A; B = brabantamide B; C = brabantamide C)

Organism	**MIC (µg/ ml)**		
	A	**B**	**C**
Arthrobacter crystallopoietes DSM 20117	12.5	12.5	6.25
Bacillus subtilis 168	12.5	25	6.25
Bacillus megaterium	n.t.	12.5	6.25
Corynebacterium xerosis Va 167198	50	n.t.	n.t.
Listeria welchimeri DSM 20650	25	n.t.	n.t.
Micrococcus luteus	n.t.	12.5	6.25
Mycobacterium smegmatis ATCC 70084	50	n.t.	n.t.
Staphylococcus aureus SG 511	25	n.t.	n.t.

n.t. = not tested

4.3.7 Cytotoxicity of brabantamides

Cytotoxicity tests were performed by the research group of Prof. Dr. H. Brötz-Österhelt (Institute of Pharmaceutical Biology and Biotechnology, University of Düsseldorf, Germany) according to the method described in chapter 3.1.8.

Results of the cytotoxicity are shown in table 4.3.18. The cytotoxicity of brabantamide A against THP1 and BALB cell lines was directly related to the concentration of brabantamide A. First cytotoxic effects could be observed at 32 mg/ml (data not shown). No difference could be monitored between the values for the two different cell lines, even if THP1 represents a more sensitive cell line (see values of cycloheximide).

Table 4.3.18: result of cytotoxicity assay of brabantamide A

Cell line	**IC_{50} [µg/ml]**	
	brabantamide A	**cycloheximide**
THP1 (human acute monocytic leukemia cell line)	47	0.12
BALB/3T3 (mouse embryonic fibroblast cell line)	47	0.5

These findings indicate that brabantamide A shows minimal to no cytotoxicity at concentrations where it is active towards bacteria (12.5 µg/ml). The cytotoxicity occurs at ranges which are around the MIC for *C. xerosis* and *M. smegmatis*, about

twofold the MIC for *S. aureus* and *L. welshimeri* and actually fourfold the MIC for *A. crystallopoietes* and *B. subtilis*, respectively (see table 4.3.17).

Thus, the cytotoxicity of brabantamide A can be classified as uncritical.

4.3.8 Investigations on the mode of action of brabantamides

To gain first insights regarding the target structure of brabantamides, a luciferase reporter gene assay was performed by the working group of Prof. Dr. H. Brötz-Österhelt (Institute of Pharmaceutical Biology and Biotechnology, University of Düsseldorf, Germany).

Five *B. subtilis* reporter strains were used, carrying different antibiotic induced promoters fused to firefly luciferase reporter gene (see chapter 3.1.9). This set of promoter-reporter fusions enables the diagnosis of antibiotic interference in the major biosynthetic pathways of bacteria e.g. in the biosynthesis of DNA (*yorB*-promoter), in protein biosynthesis and by RNA inhibition *(yheI*- and *yvgS*-promoter), and in cell wall biosynthesis and by cell wall stressing agents (*ypuA*-promoter; Urban *et al*., 2007; Hutter *et al*., 2004).

Regarding the latter interferences, a *yvqI*-(=*liaI*) promoter containing reporter strain indicated more specifically inhibition of peptidoglycan biosynthesis (e.g. vancomycin, bacitracin and tunicamycin) and membrane damaging agents (e.g. ethanol; Mascher *et al*., 2003; Petersohn *et al*., 2001). The occurrence of an elevated luminescence signal in one of these reporter strains by a test compound is indicative of promoter induction, thus delivering first starting points for further mode of action studies. In the conducted reporter strain assays brabantamide A was able to induce the *ypuA*- and the *yvqI*-reporter (see figure 4.3.30 and 4.3.31). These results suggest, that brabantamide A causes stress on the cell wall either on the membrane or interferes with peptidoglycan.

The measured effects appeared at a concentration of 8 µg/ml which represents two-thirds of the minimal inhibition

concentration determined for brabantamide A on *B. subtilis*. In higher concentrations no effect on the promoters could be observed what might be caused by a damage of the cells that precludes expression of the reporter gene. The remainder of the reporter-strains did not show an induction in the presence of brabantamide A (for data see appendix figures 8.1.21-8.1.23). The influence of DMSO on the results was excluded by repeating the assay with different DMSO concentrations (data not shown).

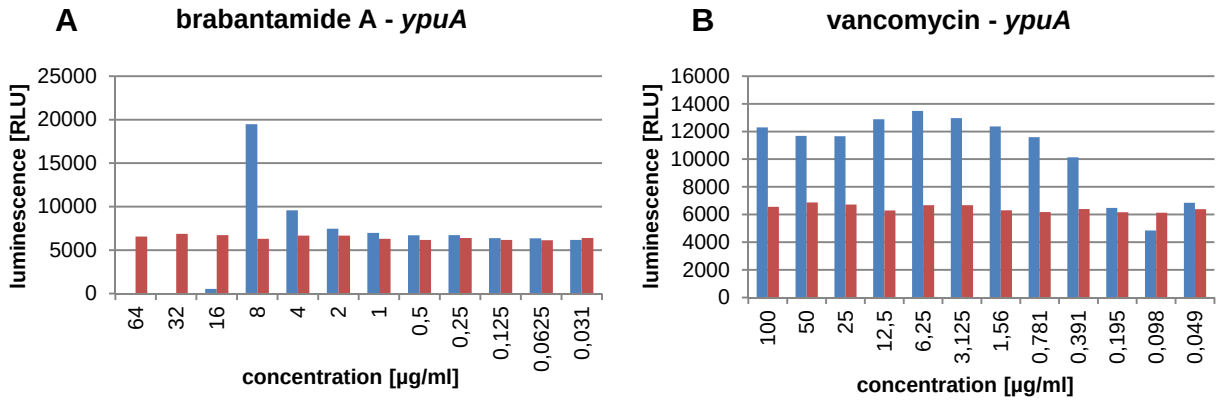

Figure 4.3.30: result of brabantamide A (**A**) on the *ypuA* promoter (indicates cell wall synthesis and cell wall envelope stress) in comparison with the positive control vancomycin (**B**, inhibitor of cell wall synthesis); red and blue bars represent the background control and the tested substance, respectively

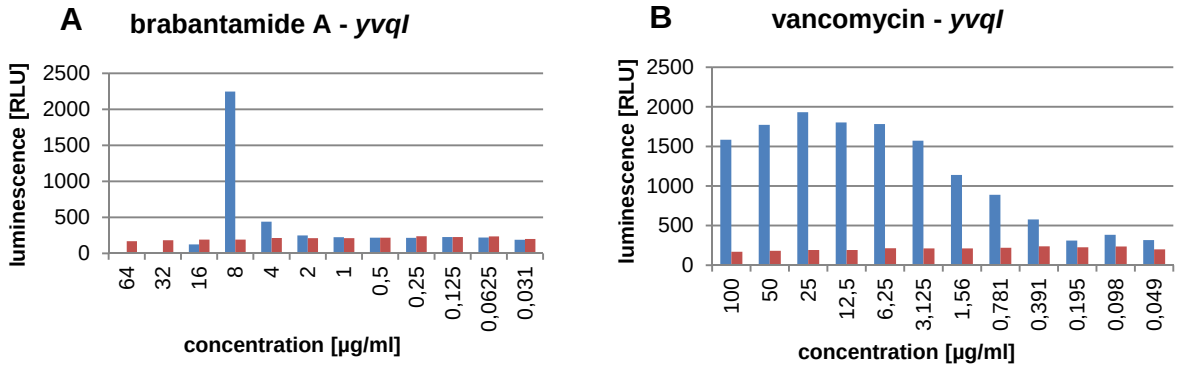

Figure 4.3.31: result of brabantamide A (**A**) on the *yvqI* promoter (indicates cell wall synthesis and cell wall envelope stress) in comparison with the positive control vancomycin (**B**, inhibitor of cell wall synthesis); red and blue bars represent the background control and the tested substance, respectively

4.4 Investigations on Empedopeptin

4.4.1 Isolation of empedopeptin

Empedobacter haloabium nov. spec. (ATCC31962) was cultivated on a 3L scale (3.1.3), extracted (3.3.1) and the resulting crude extract subjected to RP-VLC.

Aberrant from the established standard VLC-scheme (3.3.2) used in this study, a stepwise gradient of water-methanol (70:30-0:100) and methanol-dichloromethane was applied to give 10 fractions. Based on LC-MS profiling, fraction 8 (eluted 100% MeOH) was further purified by RP-HPLC, using system 3 and column 7 (see 3.3.3), employing a linear gradient of 62:38-75:25 MeOH-H_2O (2 mM NH_4OAc) over a period of 30 min with a flow rate of 1.8 ml/min (UV-monitoring at 210 nm).

Purification of the semi pure empedopeptin was continued by a second RP-HPLC on the same system using column 1 (UV-monitoring at 210 nm) using two linear gradients of 60:40 MeOH-H_2O (2 mM NH_4OAc) over a period of 15 min, constantly increasing to 90:10 MeOH-H_2O (2mM NH_4OAc) in a 5 min period, followed by isocratic elution at 90:10 for 10 min. The purification resulted in 6.2 mg of pure empedopeptin. The obtained purity of empedopeptin was monitored by LC-MS analysis (see chapter 3.3.5). During this monitoring, three compounds with similar physicochemical properties could be detected and isolated with very small yields (compound 1: 3.11 mg, compound 2: 1.22 mg and compound 3: 0.58 mg).

4.4.2 Structure elucidation of empedopeptin

The structure elucidation of empedopeptin was mainly based on NMR experiments (see chapter 3.3.4). Based on the limited amount of substance, its poor solubility and the tendency to form micelles, only a ^{1}H-spectrum (see figure 4.4.1), a ^{1}H-^{13}C HSQC

spectrum, a TOCSY- and a NOESY spectrum could be recorded with sufficient quality .

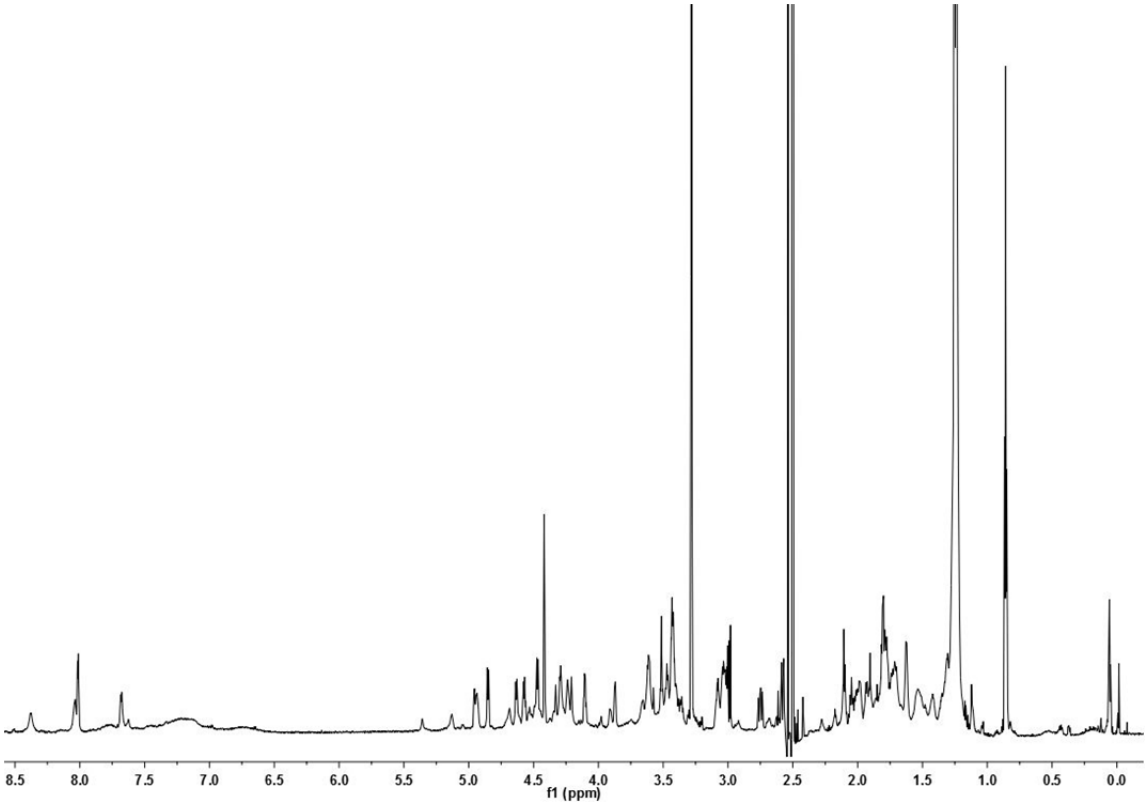

Figure 4.4.1: ^{1}H NMR spectrum of empedopeptin in d_6-DMSO (900 MHz)

The ^{1}H-^{13}C HSQC spectrum correlated all proton resonances to the ^{13}C-NMR resonances of directly bonded carbon atoms (see figure 8.1.24, appendix and table 4.4.1). The analysis of the TOCSY spectrum revealed the presence of characteristic spin systems for two serine moieties, two proline and two 3-hydroxy aspartic acid residues as well as a 3-hydroxy proline, arginine and a 3-hydroxy fatty acid as partial structures (Pretsch *et al.*, 2001).

Interpretation of the proton-proton through-space interactions of empedopeptin, observed in a 2D-NOESY NMR spectrum (see figure 8.1.25, appendix), enabled the assembly of the partial structures to give the suggested peptide sequence of empedopeptin (figure 4.4.2).

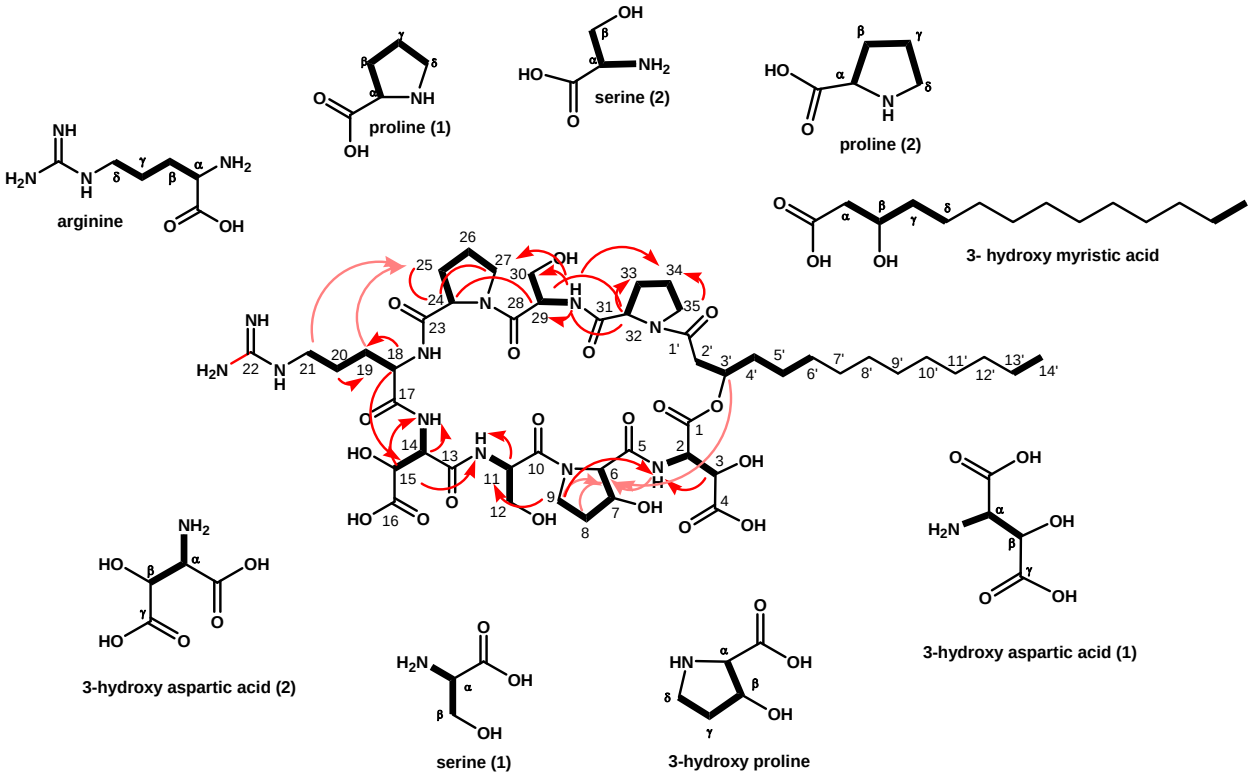

Figure 4.4.2: partial structures deduced from the TOCSY spectrum and complete structure of empedopeptin; black lines indicate TOCSY couplings, red arrows indicate NOESY correlations

For the isolated potential congeners of empedopeptin (compound 1-3) measurements of NMR spectra with sufficient quality were not possible due to the small amount of substances. Nevertheless, a first structure proposal was done by comparison of the determined molecular masses of the structures. Thus, it can be suggested, that compound **1** (empedopeptin B) is the ring-opened congener of empedopeptin (figure 4.4.3 a) showing a molecular mass of 1144.5726 g/mol in the LC-MS spectra (calculated: 1144.2291 g/mol). Compound **2** (empedopeptin C) with a calculated mass of 1158.2127 (measured: ~ 1158) is suggested to be a derivative which consists of three instead of one hydroxylated proline residue (figure 4.4.3 b). Compound **3** (empedopeptin D) could possibly be a variety containing lauric acid instead of myristic acid as fatty acid component (see figure 4.4.3 c) based on the mass difference of 29 to empedopeptin (calc. mass of compound 3: 1097.5241; measured: ~1097).

Table 4.4.1: NMR spectral data for empedopeptin in DMSO

	position	δ_C [ppm]	δ_H [ppm]	NOE	carbon/ nitrogen no.
3-hydroxy	NH	-	7.69	6/7	1^N
aspartic acid	α	54.8	4.63	1^N	2
(1)	β	69.9	4.21		3
3-hydroxy-proline	α	66.6	4.42	8, 1^N	6
	β	69.1	4.42	8, 1^N	7
	γ	32.3	1.78; 1.93	6/7	8
	δ	43.5	3.25; 3.44	6/7, 11, 1^N	9
serine (1)	NH	-	8.34		2^N
	α	51.6 CH	4.57	2^N	11
	β	61.1 CH_2	3.51; 3.62		12
3-hydroxy	NH	-	8.03		3^N
aspartic acid	α	58.3 CH_2	4.29	3^N	14
(2)	β	71.2 CH	3.87	1^N, 2^N	15
arginine	α	52.1 CH	4.24	15, 19	18
	β	28.9 CH_2	1.71	$25^\#$	19
	γ	23.6 CH_2	1.31	19	20
	δ	40.3 CH_2	3.04; 3.08	$25^\#$	21
proline (1)	α	59.8 CH	4.85	25, 27, 29	24
	β	31.4 CH_2	2.05; 2.10	24	25
	γ	22.0 CH_2	1.74		26
	δ	46.2 CH_2	3.31; 3.36	24	27
serine (2)	NH	-	8.00	27, 29, 30, 32, 34	4^N
	α	53.2 CH	4.11	24, 32, 4^N	29
	β	60.4 CH_2	3.43; 3.47		30
proline (2)	α	57.9 CH	4.47	29, 33, 4^N	32
	β	18.6 CH_2	1.98		33
	γ	23.7 CH_2	1.81		34
	δ	46.6 CH_2	3.43; 3.61	34	35
3-hydroxy	α	37.2 CH_2	2.59; 2.75		2′
myristic acid	β	71.6 CH	4.94	$6/7^\#$	3′
	γ	32.8 CH_2	1.62		4′
	δ	31.0; 28.6; 21.8 CH_2	~1.24		5′-13′
	$-CH_3$	13.6 CH_3	0.86		14′

^{N} protons connected to nitrogen atoms
$^\#$ weak signal

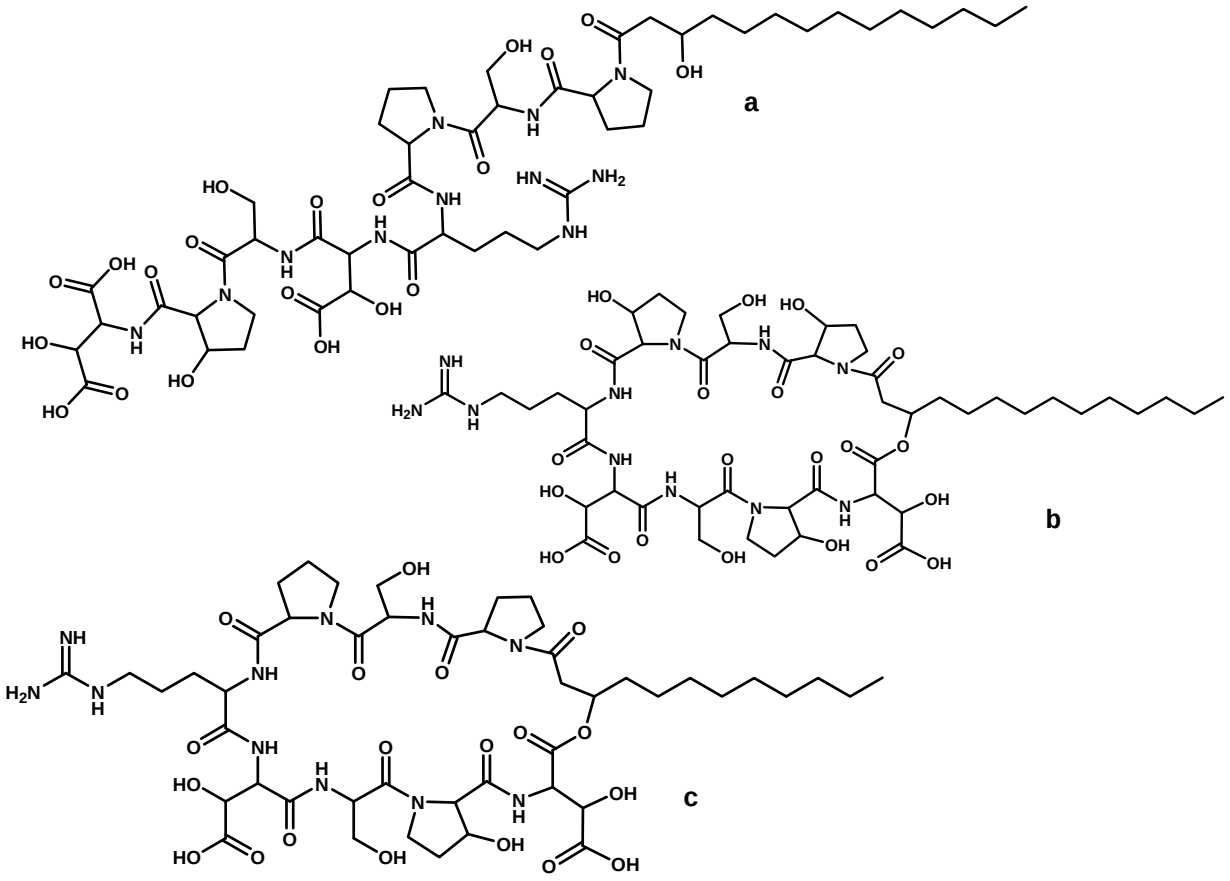

Figure 4.4.3: proposed congeners of empedopeptin: a = empedopeptin B, b = empedopeptin C and c = empedopeptin D

5 Discussion and Outlook

The study was performed within the frame of the DFG research group (FOR 854) "Post-genomic strategies for new antibiotic drugs and targets". In this context, partial project 8 "Genomic mining for antimicrobial lipopeptides" aimed to isolate and test antibacterial cyclic lipopeptides derived from bacteria.

To reach this goal, a genome-driven approach was chosen to identify alleged candidate biosynthetic pathways encoded in genomes of the genus *Pseudomonas* and related genera.

Furthermore, the lipodepsipeptide empedopeptin should be isolated from the strain *Empedobacter haloabium* nov. sp. for the purpose of structural confirmation and collaborative mode of action studies.

In the following, the employed approaches of the study and the achieved objectives will be discussed as well as an insight in potential future perspectives, will be given.

5.1 Applied methods of genome mining

As mentioned above, the concept of genome mining was applied during this study to identify potential strains of the genus *Pseudomonas* or of related genera for the isolation of new antibiotic CLPs. Up to date, genome mining covers four methodologies to discover orphan gene clusters and subsequently isolate and characterise the corresponding product: the ´bioinformatic and screening´ approach, the ´genomisotopic approach´, ´heterologous expression´ and the method of ´knockout and comparative profiling´ (see chapter 1.3; Gross, 2009).

The first method applied in this study was the ´bioinformatic and screening´ approach. Thus, an *in silico* screening employing specific target structures, in this case the sequence of a double terminal TE domain of orfamide, was chosen to identify several *Pseudomonas* strains, which contain similar sequences and

thus were suggested to produce antimicrobial cyclic lipopeptides.

The resulting eight gene clusters were subsequently subjected to a bioinformatical analysis and revealed the potential target structures of the corresponding cyclic lipopeptides (see chapter 4.1). Out of these candidates five were chosen and the corresponding strains i.e. ***Pseudomonas syringae*** pv. syringae B728a and pv. tomato DC3000 as well as ***P.*** sp. SH-C52 were subjected to a broad screening for the predicted lipopeptides (see chapter 4.2).

This first applied approach of genome mining can be assessed as semi-successful. On the one hand, the ´bioinformatic and screening´ approach led to the discovery of the abovementioned eight gene clusters and up to date most of the corresponding cyclic lipopeptides were identified e.g. brabantamides (this study), entolysins (Vallet-Gely ***et al.***, 2010) and syringafactins (Berti ***et al.***, 2007). This can be regarded as very successful, considering that structure elucidation of the remainder of candidate structures is on-going (Watrous ***et al.***, 2012).

On the other hand, this method depends on the expression of the orphan pathway. Therefore, the missing expression of a chosen gene cluster is an obstacle which has to be overcome (Gross, 2009). In this study, these problems occurred in case of ***P. syringae*** pv. syringae B728a and pv. tomato DC3000 as well as ***P.*** sp. SH-C52 regarding the second predicted CLP.

In order to overcome this problem, the OSMAC approach was chosen which did not lead to success either (see chapter 4.2). Contemplating the first two strains and the fact, that some of the desired metabolites were already isolated from them, this might be due to a loss of metabolite production throughout time. In case of ***P.*** sp. SH-C52, the lacking production of the second CLP, termed thanamycin, could be based on production rates which are too low for the applied LC-MS system. This suggestion can be supported by the partial structure elucidation of thanamycin of a collaborative research group employing nanoDESI technology which shows a substantially higher sensitivity (Watrous ***et al.***, 2012).

A second method of the ´genome mining concept´, applied during this study, was the ´genomisotopic approach´. Hereby, the ´in-frame´-deletion mutants targeting the glycosyltransferase (strain C52Δ26IF) of ***P.*** sp SH-C52 was fed with 1-^{13}C-L-serine to track down the expected aglycon-congener. This concept cannot be rated due to the obvious lack of brabantamide production in the knockout strains (see chapter 4.3.5.9).

The method of ´knockout and comparative profiling´ was applied as third genome mining approach in this study. Thereby, both gene clusters of interest in ***P.*** sp. SH-C52 were disrupted in their NRPS moieties to perform knockout studies, followed by comparative profiling (see chapter 4.3.2).

This approach can be regarded as successful in case of the knockout mutant strain C52Δ27. Hereby, comparative metabolite profiling led both to the desired metabolite and provided proof of the cluster (see figure 4.3.5).

In the case of knockout-strain C52Δ33 no differences in the metabolite profile, compared to the one of the wild-type strain could be observed. In order to activate the expression of the ***thaABC*** gene cluster, the strain was included into the abovementioned OSMAC strategy.

In summary, in this study all available genome mining techniques, except the ´heterologous expression´ approach, were employed., The genome mining approach turned out to be a strong concept to identify potential antibiotic producing bacterial strains and provided insights into corresponding candidate structures as well as proof of gene clusters. In combination with ´heterologous expression´ of gene clusters which would overcome the observed lack of expression, genome mining can be regarded as a straightforward strategy in the search for new antibiotic compounds.

A limitation of genome mining represents the restriction that only known biosynthetic machineries can be discovered ***in silico***. Up to date, this criterion is met by four important classes of secondary metabolites: ribosomal and non-ribosomal peptides, polyketides and terpenes (Gross, 2009). Products of specialised pathways will currently not be detected. However, the fact that

peptides, polyketides and terpenoids make up the majority of bioactive compounds relativizes this restriction.

In exchange, genome mining targets candidate structures, which are not captured by traditional bioassay-guided approaches based on the lacking possibility to cultivate many of the producers.

Furthermore, new methods of genome mining like the recently published ´mass spectrometry-guided´ approach (Kersten *et al.*, 2012) indicate that the potential of genome mining is nowhere near exhausted.

5.2 Investigations on brabantamides isolated from *Pseudomonas* sp. SH-C52

In this study, chemical and biosynthetic studies were focussed on the orphan gene clusters of the strain *P.* sp. SH-C52 among other due to an exclusive access given by collaboration with the University of Wageningen which granted investigations without competition.

5.2.1 Investigations on the gene cluster of brabantamides

The gene cluster encoding brabantamides comprises five genes coding for a glycosyltransferase (*braA*), a NRPS (*braB*), a monooxygenase (*braC*), a LuxR-type transcriptional regulator (*braD*) and a RND-type efflux system (*braE*) (Figure 5.2.1).

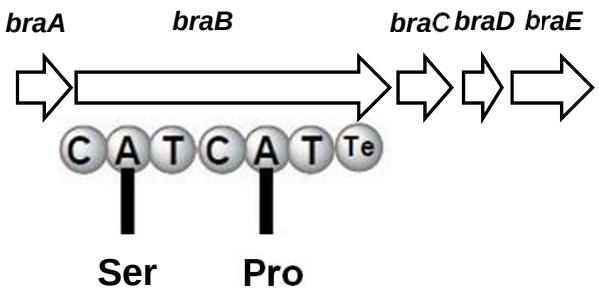

Figure 5.2.1: brabantamide gene cluster comprising *braABCDE*

Since ***braB*** was already discussed in chapter 4.3.1, only the products of the remaining structural and accessory genes will be highlighted in the following.

5.2.1.1 BraA – an inverting rhamnosyltransferase

Glycosyltransferases (GTs) comprise one of the most diverse groups of enzymes. They catalyse the attachment of sugars to an aglycon wherewith they are able to modify every group of biopolymers like proteins and oligosaccharides as well as natural products and are present in nearly all investigated organisms (Hu & Walker, 2002). In contrast to their huge structural and functional variety and the resulting low sequence similarities (Hu & Walker, 2002), the majority of glycosyltransferases can be subdivided into only two structural superfamilies, termed GT-A and GT-B, each consisting of two domains (Erb ***et al.***, 2009). These superfamilies differ in folds, active sites and different mechanisms regarding the glycosyltransfer (Hu & Walker, 2002).

Enzymes belonging to the GT-A class comprise two disparate domains. At the N-terminal domain, several Rossmann folds (ß-sheets flanked by α-helices) recognise the sugar-nucleotide donor, while the C-terminal domain contains the acceptor-binding site and consists of mixed ß-sheets. Glycosyltransferases of the GT-B fold comprise two similar Rosssmann-like folds. Thereby, the acceptor and donor sides are contrary to those of the GT-A fold, i.e. the N-terminal domain provides the acceptor-binding site, while the C-terminal domain binds the donor. In both superfamilies the domains comprise a linker region where the active site is located (Erb ***et al.***, 2009).

A further class of glycosyltransferases, GT-C, was predicted by sequence similarity (Liu & Mushegian, 2003). They consist of a large hydrophobic transmembrane protein having between 8 and 13 transmembrane helices and an active site located on a long-loop region (Strahl-Bohlsinger ***et al.***, 1993; Takahashi ***et al.***, 1996; Maeda ***et al.***, 2001). This classification is problematic because the alignment, which is based on the transmembrane region, does

not include the predicted loop bearing the active site (Lairson ***et al.***, 2008).

Furthermore, glycosyltransferases are classified into clans dependent on the stereochemical outcome of the reaction at the anomeric centre, relative to that of the donor sugar as either retaining or inverting GTs. Thereby, the overall fold of the enzyme does not dictate this outcome as can be seen in examples for both types of reactions found in either GT-A and GT-B (Coutinho ***et al.***, 2003). To date, all enzymes of the predicted GT-C fold are inverting GTs (Lairson ***et al.***, 2008).

Investigations on the glycosyltransferase, encoded by ***braA***, belonging to the gene cluster of brabantamide by homology search (see chapter 4.3.1) revealed the highest sequence similarity to a rhamnosyltransferase deriving from ***Burkholderia thailandensis*** E264 (see table 8.1.1). The relatively low homology of 50% can be explained by the aforementioned huge diversity of GTs. Interestingly, all glycosyltransferases showing noticeable homology to ***braA*** belong to the GT-B superfamily of GTs why it is likely that BraA comprises a GT-B fold as well.

This result could be borne out by comparison of the obtained similar sequences with the Carbohydrate-Active Enzymes database (CAZy, http://www.cazy.org; Cantarel ***et al.***, 2009). The CAZy database proposes the continuously updated classification of GTs into distinct sequence-based families by reference to a classification of Campbell ***et al.*** (Campbell ***et al.***, 1997; Campbell ***et al.***, 1998) and was later complemented by Coutinho ***et al.*** (Coutinho ***et al.***, 2003). At the moment over 100,000 modules of GTs are classified into 94 family numbers. Three of the glycosyltransferases obtained from homology blast performed for BraA - Bcen2424_5095, Bamb4507 and Bcen_3273 - were available at the database, all assigned to the GT1 family.

Since the GT1 family is corresponding to clan II i.e. an inverting enzyme comprising a GT-B fold, it can be assumed that BraA shares these features. The mechanistic strategy of inverting GTs involves a direct displacement S_N2-like reaction (see figure 5.2.2). Thereby, the active-site side chain deprotonates the incoming nucleophile of the acceptor serving as a base catalyst, relieving direct displacement of the activated (substituted) phosphate leaving group (Lairson ***et al.***, 2008).

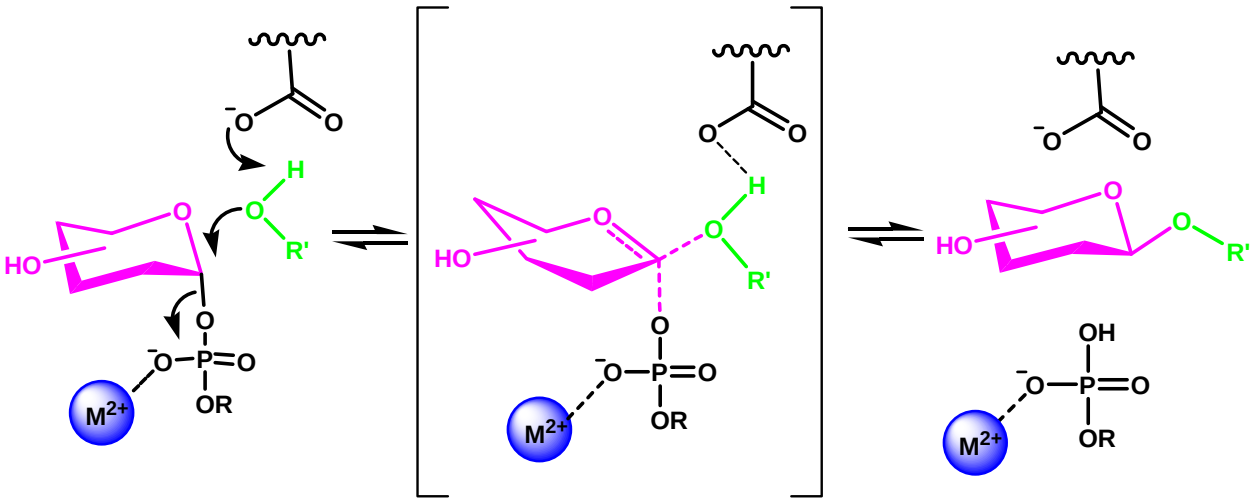

Figure 5.2.2: usual mechanism of inverting GTs with GT-A fold, following an S_N2 mechanism adopted from ***Lairson et al.***, 2008

In difference to the mechanism displayed in figure 5.2.2, GTs of the GT-B fold often use a metal ion-independent mechanism where for example a histidine residue acts as activator (Offen ***et al.***, 2006; Lairson ***et al.***, 2008).

Summarising, the attached L-rhamnose of brabantamide A secures that ***braA*** codes for a rhamnosyltransferase as assumed based on the homology search. Furthermore, it seems likely, that ***braA*** encodes an inverting GT exhibiting GT-B fold that belongs to the GT1 family. The fact that BraA is inverting would lead to the expectation that the attached α-L-rhamnose of brabantamide initially was in ß-form since there is no evidence for a mixture of anomers. Even if inverting GTs are able to invert both anomers, it is known, that they are highly specific and therewith only pick up the needed anomer (Watkins, 1986).

5.2.1.2 BraC – a flavoprotein monooxygenase

Monooxygenases (MOs) belong to the group of oxidoreductases, enzymes which catalyse the electron transfer between molecules, and are responsible for the introduction of one atom of molecular oxygen into an organic substrate. The numerous sundry types of enzymes catalysing monooxygenation reactions include the family of cytochrome P450 MOs as well as non-heme, copper-dependent and flavin-dependent monooxygenases and some MOs which do not depend on any of the abovementioned cofactors (van Berkel ***et al.***, 2006).

Investigations on the monooxygenase belonging to the gene cluster of brabantamide by homology-search (see chapter 4.3.1) revealed the highest sequence similarity for BraC to a putative FAD-dependent monooxygenase from ***Xenorhabdus bovienii*** SS-2004 [YP_003466257.1]. The resulting low homologies, showing a maximum identity of 44% to other described monooxygenases, are not astonishing taking into account that there are multitudes of different MOs (van Berkel ***et al.***, 2006).

Even if the result of the homology blast performed for ***braC*** is vague, all MOs identified thereby belong to the group of flavoprotein monooxygenases (FPMOs; see table 8.1.2). Despite other types of MOs which use e.g. transition metals for the transfer of oxygen into the organic substrate, FPMOs employ a purely organic cofactor, FAD, for the oxygenation which can only react with molecular oxygen in its reduced form. FMPOs can be divided in internal and external monooxygenases. Internal MOs reduce the flavin cofactor by the substrate itself while external MOs reduce the cofactor with the help of electrons provided by consumption of reduced coenzymes like NADH (van Berkel ***et al.***, 2006).

Van Berkel ***et al.*** classified external FPMOs into six subclasses A-F, based on sequence similarity and the presence of specific protein sequence motifs (van Berkel ***et al.***, 2006).

Due to the hypothesised biosynthesis of brabantamide, the monooxygenase encoded by ***braC*** found in the corresponding gene cluster was expected to be a Baeyer-Villiger (BV) monooxygenase. Thus, it was anticipated that BraC belongs to subclass B or C of the FAD-dependent monooxygenases which are known to catalyse BV reactions.

Monooxygenases of the subclasses C-F are encoded by at the minimum two genes, which code for one reductase and at least one monooxygenase (van Berkel ***et al.***, 2006). Due to the absence of a reductase in the brabantamide gene cluster or a further monooxygenase, these subclasses could be excluded for BraC.

The remaining FPMOs of the subclasses A and B are encoded by a single gene and both contain a tightly bound FAD cofactor. Class A and B differentiate in there structural composition of either one or two dinucleotide binding domains, respectively (van Berkel

et al., 2006). These domains (Rossmann folds) bind the ADP moiety of FAD and can be evidenced by the GXGXX(G/A) motif (Wierenga ***et al.***, 1986).

Contrary to the expectation, BraC can be assigned to subclass A showing only one motif for a Rossmann fold in the sequence (see figure 5.2.3). Interestingly, the BVMO-identifying sequence motif (FXGXXXHXXXW(P/D)) or the similar motif for FPMOs (FXGXXXHXXX(Y/F)) elucidated by Fraaije and co-workers is also lacking in the sequence of BraC (Fraaije ***et al.***, 2002).

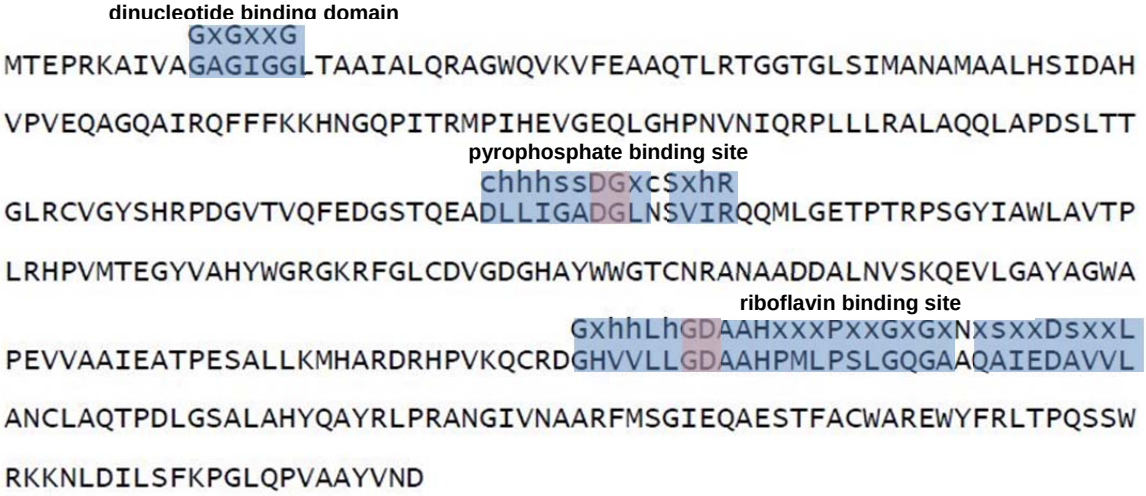

Figure 5.2.3: sequence of BraC with the fingerprint motifs 1-3; the conserved sequence motifs for FPMOs shown above the sequence are adopted from Eppink ***et al.***, 1997; uppercase letters in the profile define amino acid residues, lowercase letters are: x = all residues, c = charged residues, h = hydrophobic residues, s = small residues; violet indicates the highly conserved motifs

Additional structural features found in exponents of subclass A are a second fingerprint motif, GD, whose amino acids are in contact with the riboflavin moiety of FAD (Eggink ***et al.***, 1990) and a third fingerprint sequence (see figure 5.2.3) with the highly conserved DG motif (Eppink ***et al.***, 1997) which is involved in binding the pyrophosphate moieties of both FAD and NADPH (van Berkel ***et al.***, 2006).

Monooxygenases like BraC, belonging to subclass A are dependent of NADPH or NADH. Typical substrates are aromatic compounds that contain an activating hydroxyl or amino group which undergo an electrophilic attack by the C(4a)-hydroxyflavin as oxygenating flavin species.

The 4-hydroxybenzoate 3-monooxygenase from ***Pseudomonas*** qualifies

as prototype enzyme of class A FPMOs which usually catalyse *ortho-* or *para-* hydroxylations of aromatic rings (van Berkel *et al.*, 2006) or modify aromatic polyketides like for example griseorhodin (Li & Piel, 2002). Aside hydroxylation, they are known to catalyse epoxidations as seen in squalene monooxygenase.

Nevertheless, the postulated biosynthesis (see chapter 4.3.4) following a Baeyer-Villiger reaction remains likely, supported by the recently discovered bacterial enzyme MtmOIV, a class A FPMO, which is involved in the biosynthesis of the polyketide mithramycin (Gibson *et al.*, 2005; Prado *et al.*, 1999).
Thus, BraC could be the first flavin-dependent Baeyer-Villiger monooxygenase belonging to class A which is involved in the biosynthesis of a NRPS-derived product.

5.2.1.3 BraD - a LuxR-type transcriptional regulator

Investigations on *braD* by comparative alignments revealed maximum identities of 69 % and 70 % to SalC and SyrF, respectively, both derived from *Pseudomonas syringae* pv. syringae B728a. Both proteins were described to exhibit homology to regulatory proteins of the LuxR family (Lu *et al.*, 2002). The LuxR superfamily consists of transcriptional regulators containing helix-turn-helix DNA-binding motifs at their C-termini which are also present in the sequence of *braD* (data not shown). The majority of these regulators can be classified into two major groups regarding their activation mechanism: (1) regulators that belong to a two-component sensory transduction system and are activated by phosphorylation and (2) regulators activated by binding to an autoinducer like *N*-acylhomoserine lactone (*N*-AHL; de Bruijn & Raaijmakers, 2009). Furthermore, there are numerous LuxR-type regulators which do not belong to these subfamilies e.g. regulators that are activated upon ligand binding like for example MalT of *Escherichia coli*, induced by maltotriose (Schlegel *et al.*, 2002). Further examples of LuxR-type regulators which do not belong either to one of the two subfamilies are SyrG, SalA and SyrF from *P. syringae* pv. syringae the latter representing the second hit regarding the homology blast performed with the sequence of *braD*. *SalA, syrF*,

and *syrG* genes were identified within the *syr-syp* genomic island, encoding the cyclic lipopeptide toxins syringomycin and syringopeptin, whereby the s*yrG* gene is not essential for toxin production but is associated with virulence of *P. syringae* pv. syringae (Lu *et al.*, 2005).

In contrast, *salA* and *syrF* are essential for the production of syringomycin, whereby SalA is required for transcription of *syrF*, and a functional SyrF is essential for transcription of *syrB1* and syringomycin i.e. SalA positively regulates the expression of SyrF (Lu *et al.*, 2002). Furthermore, both genes are involved in the production of syringopeptin production (Wang *et al.*, 2006; Lu *et al.*, 2002).

Based on the high similarity of *braD* to *syrF* it can be assumed, that BraD is a LuxR-type regulator which positively regulates the expression of *braB* and therewith the production of brabantamides.

5.2.1.4 BraE – an outer membrane protein associated with a RND-type efflux system

Investigations on *braE* by comparative alignments revealed maximum identities of 81 % and 80 % to a RND efflux system/NodT [EGH5526.1] and a putative outer membrane protein [AAK83331.1], respectively, both derived from *Pseudomonas syringae*. These genes encode outer membrane proteins associated to efflux transporters, whereby NodT, which also occurred in further homology hits (data not shown), was first described in 1990 contained typical sequences of transit peptides enabling the secretion of proteins through the bacterial inner membrane (Surin *et al.*, 1990).

The described outer membrane proteins belong to the group of the ´outer membrane factor´ (OMF) family which is one of two accessory proteins found in conjunction with ´multidrug resistance transporters´ (MDRs) from Gram-negative bacteria. The second associated protein, the periplasmic protein belongs to the group of ´membrane fusion protein´ (MFP) family (Zgurskaya *et al.*, 2009). The typical MDR efflux pump consists of three genes, and can be classified into families depending on the

number of transmembrane-spanning regions of the transporter protein, the number of components that the pump has (single or multiple), the used energy source and the types of exported substrates (Piddock, 2005).

Regarding the results of the homology blast, it seems likely that ***braE*** belongs to a MDR system of the ´resistance nodulation division´ (RND) superfamily. The putative outer membrane protein termed Orf1 [AAK83331.1] found to be similar to BraE is described as closely related to OprM of ***Pseudomonas aeruginosa*** (Lu ***et al.***, 2002), which is part of a suchlike three-component MDR pump, the MexAB-OprM pump. This pump consists of the subunit protein MexB, an inner membrane-spanning protein, the inner membrane-associated periplasmic MexA and the outer membrane subunit OprM (Nakajima ***et al.***, 2000) and provides a significant contribution to the intrinsic resistance of ***P. aeruginosa*** e.g. towards tetracyclines and chloramphenicol (Poole ***et al.***, 1993). Whether BraE as outer membrane protein and therewith a suggested part of a MDR system possesses a different function if occurring alone or is non-functional in the cluster can currently not be deduced. Further possibilities are that a homolog of ***mexAB*** is localized elsewhere in the genome or that BraE represents a new class of efflux systems with dual functions.

5.2.2 Biosynthetic studies on brabantamides

Brabantamides are NRPS-derived cyclic lipodipeptides. Usually, NRPS either generate a linear peptide by hydrolytic release of the compound from the synthetase or a diketopiperazine is formed after cleavage from the enzyme by the thioesterase module (see chapter 1.1.1). Contrary to the initial bioinformatic predictions, brabantamides revealed an unexpected bicyclic carbamate core connected to a glycosylated fatty acid side chain.

The unique core structure of brabantamide suggested, that there must have taken place a massive rearrangement of carbon atoms during the biosynthesis. The hypothetical biosynthesis generating the bicyclic carbamate was already introduced in

chapter 4.3.4 and had to be verified by means of labelling experiments with stable isotopes (see chapter 4.3.5).

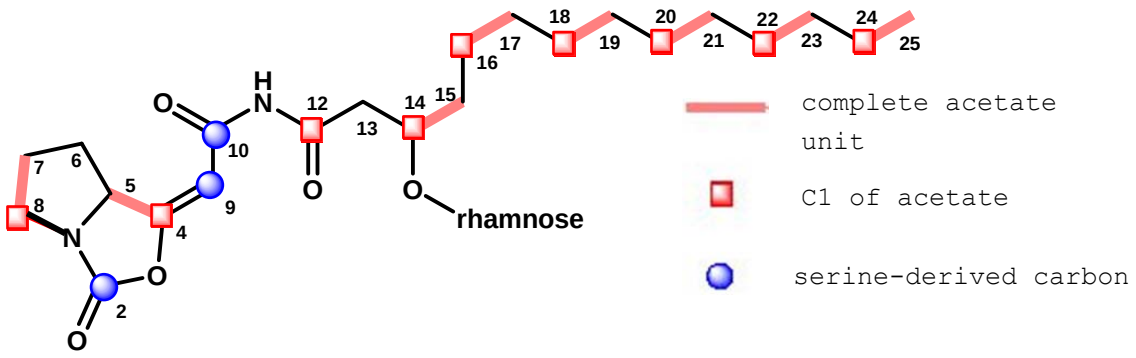

Figure 5.2.4: origin of carbon atoms of brabantamide A which could be verified with labelling experiments

The results obtained from the feeding experiments with 1-^{13}C- and 1,2-^{13}C sodium acetate proofed the biosynthetic origin of the fatty acid side chain, revealing the expected labelling pattern and approved intact incorporation of acetate units, respectively (see figure 5.2.4).

Furthermore, the incorporation of acetate units in carbons number four and five respectively seven and eight can be regarded as an indirect proof for the incorporation of proline, given that proline can be generated by acetate units introduced into the citrate cycle (see figure 4.3.28).

As one of the predicted substrates for the NRPS of brabantamides, the negative results obtained from the incorporation studies with 1-^{13}C L-proline keep unresolved. Maybe, the expected incorporation of L-proline failed due to scale up or the loss of production of the applied cryo-culture. However, the uptake of ^{14}C-labelled proline showed that there is no general problem with the application and up-take of proline in *Pseudomonas* sp. SH-C52, which excludes also the possibility that the applied proline concentrations had a toxic effect on the organism.

Further experiments with single and universally labelled L-serine precursors confirmed the origin of carbon atoms number two, four and nine (see figure 5.2.4). This result is not only indicative for the biosynthetic origin of the carbons but also supports the proposed rearrangement following a Baeyer-Villiger

reaction (see figure 4.3.13) and hence also the investigations regarding the classification of the monooxygenase (see chapter 5.2.1.2).

5.2.3 Brabantamides as bioactive compounds

Brabantamides A, B and C, formerly known as SB-253514, SB-253517 and SB-253518, respectively, were up to date only investigated regarding their function as selective competitive inhibitors of lipoprotein associated phospholipase A_2 ($LpPLA_2$; Thirkettle, 2000a; Thirkettle ***et al.***, 2000; Pinto ***et al.***, 2000). $LpPLA_2$ is a serine dependent lipase which is associated with the presence of low-density lipoprotein (LDL) in plasma and converts oxidised free fatty acids and phosphatidylcholine to lysophosphatidyl-choline, two chemo attractants for circulating monocytes. Thus, inhibition of $LpPLA_2$ activity hinders the build-up of lysophosphatidylcholine and thereby macrophage proliferation and endothelial dysfunction, which provides an attractive strategy in the treatment of atherosclerosis and related disorders (Thirkettle, 2000a). In this context, SB-253514 (brabantamide A) showed ***in vivo*** activity in Watanabe heritable hyperlipidaemic (WHL) rabbits when administered intravenous but not if it was orally applied.

In contrast to this known biological activity, within the frame of this PhD project, brabantamides were encountered as antibiotically active substances (see chapter 4.3.6).

Brabantamides showed significant MICs towards several Gram-positives (see table 4.3.17). Thus, in combination with the low cytotoxicity (see chapter 4.3.7) proved them to be potential antibiotics. Furthermore, a dependency on calcium could be excluded by retesting in the presence of Ca^{2+} ions (see chapter 4.3.6). The lacking activity of brabantamide A towards Gram-negative species is not surprising (see chapter 1.1.4) and is in line with previous observations (Nybroe & Sørensen, 2004; Sinnaeve ***et al.***, 2009a).

Furthermore, during the study first insights into structure-activity relationship (see chapter 5.2.3.1) and the potential target structure as well as the possible mode of action of

brabantamides could be gained (see chapter 5.2.3.2) which will be discussed in the following.

5.2.3.1 Structure – activity relationship

Investigating the MICs of brabantamides (see table 4.3.17) brabantamide C exhibited considerable lower MICs towards the tested strains (***A. crystallopoietes*** DSM 20117, ***B. subtilis*** 168, ***B. megaterium and M. luteus***). Thus, two-fold higher potencies in comparison with brabantamide A and B and regarding the activity towards ***B. subtilis*** 168 a four-fold higher potency in comparison with brabantamide B was observed.

Based on the fact, that the structures only differ in the nature of the lipid portion (see figure 4.3.11), the activity seems to increase with increasing chain length. Furthermore, the saturation of the fatty acid contributes to bioactivity as can be seen in the differing MIC values for brabantamides B and C.

These observations are coincident with diverse studies on the impact of the lipid moiety on the biological properties of cyclic lipopeptides which point out that the antimicrobial behaviour and toxicity are affected massively by the nature of the incorporated fatty acid group (Debono ***et al.***, 1988). This might be due to the general mode of action of cyclic lipopeptides which is commonly ascribed to interactions with membranes and an unspecific detergent-like activity (see chapter 5.2.3.2). Numerous attempts to gain insight into this structure-activity relation underlined this coherence. For example, Youssef ***et al.*** investigated eight lipopeptides comprising the same amino acid but differing in fatty acid composition produced by various ***Bacillus*** species and hypothesized that branched even-numbered fatty acids (in this case, ***iso***-C14 was the only branched even-numbered fatty acid) might give the optimum hydrophilic lipophilic balance required for optimum surface activity (Youssef ***et al.***, 2005). Furthermore, investigations on surfactin and derivatives and their activity towards three enveloped viruses (VSV, SHV-1, SFV) belonging to different virus families (rhabdoviridae, herpesviridae and togaviridae) showed, that with increasing fatty acid hydrophobicity the virus

inactivation capacity of the isoforms increased (Kracht ***et al.***, 1999).

For the above mentioned CLPs only unspecific detergent-like mechanisms are assumed. However, also within the class of specifically acting CLPs, variations of the lipid side chain influence the antibiotic activity. These could be found in investigations on daptomycin and analogues, where an increase up to chain length C-12 to C-13 coincided well with increasing ***in vitro*** and ***in vivo*** activities against ***S. aureus*** and ***Streptococcus pyogenes*** (Debono ***et al.***, 1988) and investigations on polymyxin B and colistin, wherein introduction of fatty acids bearing aliphatic or aromatic ring structures greatly increased their bactericidal activity (Okimura ***et al.***, 2007).

5.2.3.2 Mode of action of brabantamides

The bioactivity of lipopeptides is commonly attributed to membrane interactions and the main destructive action on cell membranes has been referred to their unspecific detergent like activity. This can deduced from their ability to disintegrate lipid bilayers (Coraiola ***et al.***, 2006; Carillo ***et al.***, 2003; Sinnaeve ***et al.***, 2009b). However, based on recent mode of actions studies, a different picture emerged. For an increasing number of CLPs specific mechanisms can be demonstrated, like e.g. for friulimicin B or the below mentioned empedopeptin (Schneider ***et al.***, 2009; Müller ***et al.***, 2012).

Therefore, a first attempt to gain insight into the mode of action of brabantamide A was to investigate molecular interactions between brabantamide A and bacteria-like lipid model membranes (Reder-Christ ***et al.***, 2012). These were analysed in detail via complementary biophysical techniques by the research group of Prof. Dr. G. Bendas (Pharmaceutical Institute, Pharmaceutical Chemistry II, University of Bonn, Germany).

For this purpose, three types of experiments were performed (Reder-Christ ***et al.***, 2012):

1. Investigations on the intensity and kinetic of brabantamide A binding towards lipid biolayers using the quartz crystal microbalance (QCM),
2. detection of changes in membrane permeability e.g. pore formation due to interaction between brabantamide A and the membranes via cyclic voltammetry (CV) and
3. a subphase-assay to investigate surface activity indicating the ability of brabantamide A to insert into a phospholipid monolayer.

Application of the QCM showed, that SB-253514 (brabantamide A) displays a high overall binding affinity to the model membranes which was in the low micromolar range (~ 0.55 µM – 1.28 µM) and is mainly based on their rapid association rates (Reder-Christ ***et al.***, 2012).

The subphase-assay showed a medium incorporation tendency of brabantamide A into monolayers comparable to those of arthrofactin and massetolide A. However, a direct correlation between antibacterial activity and membrane incorporation was not observed but a correlation between structural features of the CLPs and the incorporation tendency (Reder-Christ ***et al.***, 2012).

Furthermore, in CV experiments brabantamide A revealed no membrane permeabilisation effects neither at inhibitory- nor at two-, four- or tenfold MICs. Thus, membrane permeabilisation can be excluded as active principle for the antibacterial activity of brabantamide A.

Therefore, it was concluded, that the bioactivity of brabantamide A is not based on an unspecific detergent-like mechanism but seems to occur via a defined structural target (Reder-Christ ***et al.***, 2012).

Referring to this conclusion, a second attempt to investigate the target structure of brabantamides was intended by luciferase reporter gene assays (see chapter 4.3.8), enabling the diagnosis of antibiotic interference in the major biosynthetic pathways of bacteria. In these assays, brabantamide A was shown to induce only the ***ypuA***- and the ***yvqI***-reporter strains (see figures 4.3.30

and 4.3.31). *YvqI* is strongly induced by cell wall active antibiotics like vancomycin and bacitracin as well as by membrane damaging agents like ethanol (Petersohn *et al.*, 2001). Induction of *ypuA* is generated by cell wall biosynthesis inhibitors and cell envelope stressing agents like vancomycin or the cell membrane perturbing agent polymyxin B (Urban *et al.*, 2007). Thus, the mode of action of brabantamide A points towards an interference with peptidoglycan or triggering of stress either on the cell wall or on the cell membrane.

Even if the effect appeared at a concentration of 8 µg/ml which represents two-thirds of the minimal inhibition concentration determined for brabantamide A on *B. subtilis* and higher concentrations did not reveal any effect what might be due to cell damage, the positive result of the reporter-gene assay provided first insight into the target area.

5.2.4 Future perspectives

The antibiotically active brabantamides are unique regarding their chemical structure and their biosynthesis. Although this study already provided significant insights into their extended activity and biosynthesis, in turn it represents a starting point for further experimental work and scientific questions.

Even if some evidences for the hypothesised biosynthetic assembly of brabantamides could be gained, further insights into the detailed mechanisms of the glycosyltransferase *braA* and the monooxygenase *braC* could be achieved by heterologous expression. This would enable both, the investigation of the precise reaction mechanisms and the investigation of the substrate specifity of both enzymes. Regarding the putative BV-mechanism of BraC, the methodology used for functional studies on MtmOIV from the mithramycin gene cluster could be reproduced. Thereby, the mechanism of this first BV-MO belonging to class A was secured by studies with isolated and overexpressed enzymes complemented by feeding experiments (Gibson *et al.*, 2005).

Furthermore, applied systems for heterologous expression would allow the generation of new congeners by feeding of diverse precursors.

Another possibility to verify the BV mechanism of the MO would be the performance of an additional feeding experiment with stable oxygen isotopes. Thereby, the incorporation of a labelled oxygen precursor via the flavin- associated monooxygenase would provide additional insight (see figure 5.2.5).

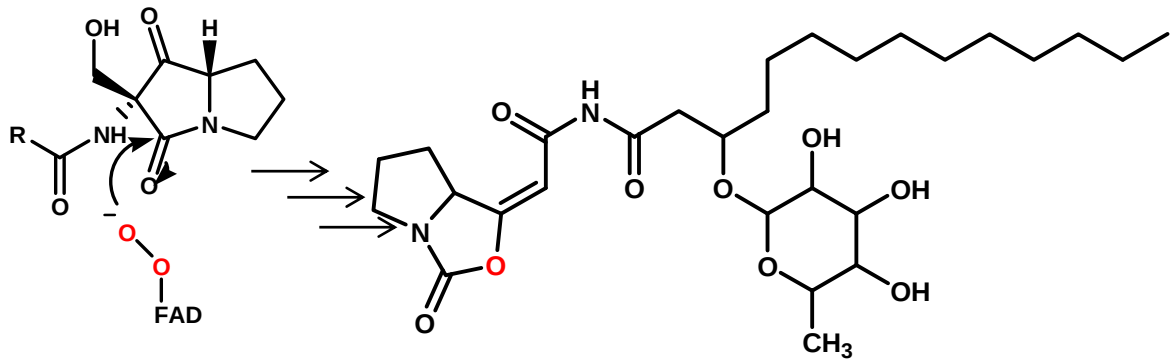

Figure 5.2.5: expected labelling pattern of brabantamide A if fed with $^{17}O_2$ following the hypothetical biosynthesis

Regarding the substrate specifity of the A-domains belonging to ***braB,*** enzyme assays using the exchange of γ-$^{18}O_4$-ATP pyrophosphate could give some indication of the accepted amino acids and might unravel the failed proline incorporation (Phelan ***et al.***, 2009; Felnagle ***et al.***, 2010). In order to gain deeper insight into the C-domain specifity attempts following the example of Mahariel and co-workers are desirable (Kraas ***et al.***, 2010).

The good antimicrobial activities of brabantamides in combination with their low cytotoxicity (see chapter 4.3.7) demonstrate that brabantamides are interesting antibiotic candidates. Especially the potential of brabantamide B which displays a twofold higher potency than brabantamides A and C indicate the need of further investigations regarding the structure-activity relationship.

The chemical structure of brabantamides consist of a 5,5-bicyclic cyclocarbamate structure, which is fused to a glycosylated 3-hydroxy-fatty acid. With these structural motifs brabantamides are unique in two ways: a) the unprecedented 5,5-bicyclic core structure is unparalleled in nature and b) they

represent the only ***Pseudomonas*** CLPs known so far with a glycosylated 3-hydroxy fatty acid side chain. Glycosylated side chains were so far only observed in ***Burkholderia*** CLPs.

Chemical variations can be envisioned to take place at the cyclic peptide core, the fatty acid side chain or the sugar moiety. Typical variations of CLPs include the exchange of incorporated peptide monomers of the cyclic structure or the diversification of the fatty acid moiety. These variations can be seen for example in plusbacins which exchange hydroxy proline against proline, termed plusbacins A and B, respectively and vary in the length of the fatty acid side chain A_1-A_4 and B_1-B_4 (Shoji ***et al.***, 1992a&b). Since the influence of the fatty acid side chain was already discussed in chapter 5.2.3.1, the other possible variations will be highlighted in the following.

The strong influence of the amino acid monomers on the antimicrobial activity of CLPs has been proven in diverse studies. Thus, daptomycin was shown to exhibit lowered in vitro activities by exchanges of the amino acids at positions twelve and thirteen (Strieker & Mahariel, 2009) and for polymyxin B an influence of the composition of monomers or even the side chains of incorporated amino acids could be approved (Kanazawa ***et al.***, 2009).

Furthermore, massetolide A and viscosin exhibited twofold potency against ***M. tuberculosis*** and ***M. avium*** by variations of the side chains of the component amino acids in position four and nine pointing towards a general correlation between greater lipophilicity and increase of potency in antimycobacterial compounds (Gerard et al., 1997).

Beyond that, attempts to predict the bioactivity of nonribosomal peptides by means of their monomeric composition were recently provided by Caboche and co-workers who suggested a direct correlation based on their study of nonribosomal peptides in the Norine database (Caboche ***et al.***, 2010).

Regarding the monomers in brabantamide A, it seems likely that the massive rearrangements during the biosynthesis might hinder a high exchangeability of the two peptides. However, three types of exchanges are conceivable: 1) exchange of proline against hydroxyproline, 2) incorporation of a bioisoster like cysteine

instead of serine and 3) a change in the stereochemistry of serine and/or proline.

The latter mentioned was investigated by ***Pinto et al.*** who reported a twofold higher potency of the ***R***-isomer versus the ***S***-isomer regarding $LpPLA_2$ inhibition (Pinto ***et al.***, 2000).

Concerning other exchanges and variations of the fatty acid side chain (see chapter 5.2.3.1), further insights could be achieved by generation of new related compounds and subsequent analysis of their activity. These efforts could be achieved using either a semi-synthetic approach as seen in investigations regarding polymyxins B (Okimura ***et al.***, 2007) or by combinatorial biosynthesis efforts such as described for mithramycin (Pérez ***et al.***, 2008). Furthermore, the semi-synthesis of several new congeners was described by Pinto and co-workers which were up to date not investigated regarding their antibacterial activity and could be used in this aspect either (Pinto ***et al.***, 2000).

Regarding the fatty acid side chain, a more accessible approach could be the addition of branched-chain amino acids into the growth medium which might alter the fatty acid composition of the produced brabantamides (Youssef ***et al.***, 2005).

It is well established that the attached carbohydrates of many types of bioactive natural products like anthracyclines, macrolide antibiotics or glycopeptides strongly influence their antibiotic activity (Weymouth-Wilson, 1997). Thus, investigations on the deglycosylated compounds would be another helpful approach but the instability of the carbamate structure precludes the application of acidic conditions. Thirkettle and co-workers attained deglycosylation across enzymatic hydrolysis using naringinase (Thirkettle, 2000b). Thereby, comparison of the phospholipid-inhibitory activity of the aglycons and the original compounds could show an increase of potency of the saturated side chain species (brabantamides A and C) but a reduced potency of brabantamide B with the unsaturated side-chain was observed (Thirkettle, 2000b).

Since naringinase was not commercially available, a deletion mutant targeting the glycosyl-transferase encoding gene ***braA*** was generated but abolished production. Therefore, the synthesis of

the deglycosylated compounds seems advisable to investigate the impact of the rhamnose moiety towards antibiotic activity.

5.3 Investigations on empedopeptin

In a side-project of this study, the antimicrobial cyclic lipodepsipeptide empedopeptin should be isolated from the strain ***Empedobacter haloabium*** nov. sp. ATCC31962 with the purpose of structural confirmation and collaborative mode of action studies.

Empedopeptin was first isolated in 1984, where two coherent publications described its isolation, structure elucidation and its antibacterial activity ***in vitro*** and ***in vivo*** (Konishi ***et al.***, 1984; Sugawara ***et al.***, 1984). Thereby, empedopeptin was reported as a potent antibiotic compound, whose antibacterial spectrum resembles that of amphomycin and vancomycin, inhibiting predominantly Gram-positive and anaerobic bacteria, including clinical relevant pathogens such as ***Staphylococcus aureus***, ***Streptococcus pneumoniae***, and ***Clostridium difficile*** (Konishi ***et al.***, 1984).

Even if the potency of empedopeptin as antibiotic was investigated back then, exhibiting MICs in the low micro molar range also against antibiotic-resistant strains accompanied by low acute toxicity and promising therapeutic ***in vivo*** efficacy in lethal bloodstream infections, the mode of action remained unresolved. Furthermore, the structure elucidation was based solely on partial hydrolysis and mass spectral analysis (Sugawara ***et al.***, 1984). No direct evidence was provided in this report about the cyclization scheme which is why it was decided to confirm the structure of empedopeptin by NMR.

During the study a sufficient amount of empedopeptin could be isolated to enable the collaborative group to elucidate the mode of action of empedopeptin. It could be demonstrated that empedopeptin interferes with late stages of cell wall biosynthesis in bacterial cells by inhibition of ***N***-acetyl glucosamine incorporation into the cell wall and thus blocking peptidoglycan biosynthesis (Müller ***et al.***, 2012). Furthermore,

empedopeptin was shown to target primarily lipid II at the outside of the cell wall forming a complex in 1:2 molar stoichiometry and to depend strongly on the presence of Ca^{2+}-ions at concentrations similar of those occurring in human serum presumably due to the induced stronger interaction with its targets and with negatively charged phospholipids in the membrane (Müller ***et al.***, 2012).

Using NMR spectroscopy, the peptide sequence published in 1984 (Sugawara ***et al.***, 1984) could be confirmed. Furthermore, three new congeners (empedopeptin B-D) of empedopeptin were isolated, which are suggested to represent a linear variety, a metabolite with three hydroxylated proline moieties and an alternative with 3-hydroxy lauric acid as fatty acid component, respectively (see figure 4.4.3).

The suggested structure for empedopeptin B deviates from the co-isolated cyclised congeners. The occurrence of the linear form might be due to the separation and purification of the metabolite including numerous solvents at different pH which possibly resulted in the cleavage of the ring system of empdeopeptin A and yielded congener B. Another option could be a hydrolytic cleavage from the NRPS by the thioesterase as described in chapter 1.1.1 without an optional cyclisation like in the proposed biosynthesis of syringafactins (Berti ***et al.***, 2007).

The suggested structure of empedopeptin C seems likely based on the fact, that there is a certain promiscuity of non-ribosomal peptide synthetases, especially regarding their A-domains, which are responsible for the recognition and activation the amino acid precursors. Thus, it is conceivable, that proline might be exchanged by 3-hydroxyproline. Such variations in substrate usage of synthetases were proven for siderophores generated by the same assembly lines which could use similar precursors like 2,3-dihydroxybenzoate (DHB) in place of 2-hydroxybenzoate (salicylate) at one NRPS leading to different products (Wuest ***et al.***, 2009). This promiscuity also appeared in the biosynthesis of anabaenopeptins whose A-domain in the first module activates Arg as well as Tyr (Christiansen ***et al.***, 2011). The authors suggest that this promiscuity has evolved through point mutations. Further examples for the exchange of 3-hydroxy

proline and proline can be found in the plusbacins A_1-A_4 and B_1-B_4 (Shoji ***et al.***, 1992a&b).

The generation of congeners with the same amino acid composition which only differ in the fatty acid side chains as proposed for empedopeptin D is a common variation in the biosynthesis of Pseudomonas CLPs (Gross & Loper, 2009). The variability of the fatty acid moieties can be attributed to their origin in the primary metabolism. This could be shown in a study of Youssef and co-workers who altered the fatty acid composition of the produced bio surfactant by the addition of branched-chain amino acids into the growth medium (Youssef ***et al.***, 2005).

5.3.1 Future perspectives

Within this study, the structure elucidation as well as the illumination of the mode of action represents a significant progress. Nevertheless, a re-isolation of empedopeptin seems indispensable, because so far only the peptide sequence could be confirmed. Still pending is the proof for the cyclisation scheme.

Taking into account, that the majority of cyclic lipopeptides cyclise within the peptide moiety, it seems questionable, that empedopeptin cyclises into the fatty acid side chain. Unfortunately, the recorded spectra could not yet clarify whether the published cyclisation is correct, because no couplings confirming or refuting this theory could be detected in the corresponding HMBC or NOESY spectra.

Upon structure elucidation, the additional obtained material could also serve for the determination of the absolute configuration of the 3-hydroxy group of the lipid side chain.

Another purpose for the re-cultivation is the isolation of the abovementioned novel congeners of empedopeptin which should be investigated in-depth to elucidate their structures and potential bioactivity.

Considering the enormous effort to isolate and purify empedopeptin from ***E. haloabium,*** which is complicated by the handling as a biosafety level 2 strain, the required complex

medium and the low production rate, it would be worth working on systems for heterologous expression of the corresponding gene cluster.

Besides overcoming the above mentioned difficulties, heterologous expression would be an adequate technique to investigate the biosynthesis of empedopeptin and possibly lead to the opportunity to create new congeners with similar or increased bioactivity.

6 Summary

The study was aimed to find new antibacterial cyclic lipopeptides in *Pseudomonas* bacteria using genome mining techniques. Application of this genome-driven approach led to the *in-silico* identification of several orphan biosynthetic gene clusters in plant- and insect-associated *Pseudomonas* strains. The strain *Pseudomonas* sp. SH-C52 was chosen for an in-depth analysis due to the presence of a unique gene cluster coding for an unprecedented lipo-dipeptide, a glycosyltransferase and a novel class of FAD-dependent monooxygenase.

In a first step, using gene knockout experiments and comparative metabolite profiling, it could be demonstrated that the gene cluster is responsible for the production of the known compound SB-253514 (brabantamide A), and its minor congeners SB-253517 (brabantamide B) and SB-253518 (brabantamide C).

The obtained brabantamides were subsequently subjected to a broad antimicrobial screening which revealed significant calcium-independent activities towards selected clinical relevant Gram-positives, e.g. *Bacillus subtilis* 168 and *Arthrobacter crystallopoietes*. The minor metabolites brabantamides B and C exhibited a broader antibiotic spectrum including activity towards *B. megaterium* and *Micrococcus luteus*. Thereby, especially brabantamide B, which contains an unsaturated fatty acid side chain, exhibited a twofold higher antibacterial potency in comparison with brabantamide A. Thus, a correlation between the side chain and the observed activity became apparent and provided first insights into structure-activity relationships.

First preliminary mode of action studies with brabantamide A involving model membrane studies could show that this compound class acts via a defined target and that the antibiotic effects are not mediated by unspecific detergent-like membrane permeabilisation. Complementary luciferase reporter gene assays indicated that brabantamides interfere with peptidoglycan or trigger stress on the cell wall. Furthermore, in cytotoxicity

assays brabantamide A was proven to be not toxic to eukaryotic cell lines at antibiotically active concentrations.

Due to the uniqueness of the 5,5-bicyclic carbamate structure of brabantamides, whose assembly require a massive rearrangement of the carbon skeleton of a linear dilipopeptide precursor, the second part of the study was focussed on their intriguing biosynthesis. Thus, a biosynthesis hypothesis was developed involving a Baeyer-Villiger reaction mechanism, mediated by the novel monooxygenase BraC. In a series of extensive feeding experiments employing ^{13}C-labelled precursors the hypothesis was tested and finally confirmed.

The third part of this study dealt with the potent antimicrobial lipodepsipeptide empedopeptin A. This lipopeptide was isolated along with two new minor congeners, empedopeptin B and C. The peptide sequence of empedopeptin A but not its cyclisation scheme could be confirmed by NMR and MS experiments. In a collaborative effort, also the specific mode of action of empedopeptin A was examined. It could be demonstrated that empedopeptin A inhibits cell wall biosynthesis through Ca^{2+}-dependent complex formation, predominantly with peptidoglycan precursor lipid II, and with lower affinity also with undecaprenyl pyrophosphate and teichoic acid.

7 Literature

Alborn, W., Allen, N., & Preston, D. A.: Daptomycin disrupts membrane potential in growing *Staphylococcus aureus*. *Antimicrob. Agents Chemother.* **1991**, *35* (11), pp. 2282-2287

Aretz, W., Meiwes, J., Seibert, G., Vobis, G., & Wink, J.: Friulimicins: Novel lipopeptide antibiotics with peptidoglycan synthesis inhibiting activity from *Actinoplanes friuliensis* sp. nov.; I. Taxonomic studies of the producing microorganism and fermentation. *J. Antibiot.* **2000**, *53*, pp. 807-815

Bachmann, B. O., & Ravel, J.: *In silico* prediction of microbial secondary metabolic pathways from DNA sequence data. *Meth. in Enzym.* **2009**, *458*, pp. 181-217

Baeyer, A. V., & Villiger, V.: Einwirkung des Caro´schen Reagenz auf Ketone. *Ber. Dtsch. Chem. Ges.* **1899**, *32*, pp. 3625-3633

Balibar, C. J., Vaillancourt, F. H., & Walsh, C. T.: Generation of D amino acid residues in assembly of arhtrofactin by dual condensation/ epimerisation domains. *Chem. Biol.* **2005**, *12*, pp. 1189-1200

Baltz, R. H., Miao, V., & Wrigley, S. K.: Natural products to drugs: daptomycin and related lipopeptide antibiotics. *Nat. Prod. Rep.* **2005**, *22*, pp. 717-741

Bassarello, C.; Lazzaroni, S.; Bifulco, G.; Lo Cantore, P.; Iacobellis, N. S.; Riccio, R.; Gomez-Paloma, L.; Evidente, A.: Tolaasins A-E, five new lipodepsipeptides produced by *Pseudomonas tolaasii*. *J. Nat. Prod.* **2004**, *67*, pp. 811-816

Bemer, P., Juvin, M.-E., Bryskier, A., & Drugeon, H.: In vitro activities of a new lipopeptide, HMR 1043, against susceptible and resistant Gram-positive isolates. *Antimicrob. Agents. Chem.* **2003**, *47* (9), pp. 3025-3029

Bertani G.: Studies on Lysogenesis; I. The mode of phage liberation by lysogenic *Escherichia coli*. *J. Bacteriol.* **1951**, *62* (3), pp. 293-300

Berti, A. D., Greve, N. J., Christensen, Q. H., & Thomas, M. G.: Identification of a biosynthetic gene cluster and six associated lipopeptides involved in swarming motility of *Pseudomonas syringae* pv. tomato DC3000. *J. Bac.* **2007**, *189* (17), pp. 6312-6323

Bode, H. B., Bethe, B., Höfs, R., & Zeek, A.: Big effects from small changes: possible ways to explore nature´s chemical diversity. *ChemBioChem* **2002** *3* (7), pp. 619-627

Bode, H.; Reimer, D.; Fuchs, S. W.; Kirchner, F.; Dauth, C.; Kegler, C.; Lorenzen, W.; Bachmann, A. O.; Grün, P.: Determination of the absolute configuration of peptide natural products by using stable isotope labeling and mass spectrometry. ***Chemistry - A european Journal*** **2012**, *18* (8), pp. 2342-2348

Buber, E., Stindl, A., Acan, N. L., Kocagoz, T., & Zocher, R.: Antimycobacterial activity of lipodepsipeptides produced by ***Pseudomonas syringae*** pv. ***syringae***. ***Nat. Prod. Let.*** **2002**, *16* (6), pp. 419-423

Buell, C. R.; Joardar, V.; Lindeberg, M.; Selengut, J.; Paulsen, I. T.; Gwinn, M. L.; Dodson, R. J.; Deboy, R. T.; Durkin, A. S.; Kolonay, J. F.; Madupu, R.; Daugherty, S.; Brinkac, L.; Beanan, M. J.; Haft, D. H.; Nelson, W. C.; Davidsen, T.; Zafar, N.; Zhou, L.; Liu, Y.; Yuan, Q.; Khouri, H.; Fedorova, N.; Tran, B.; Russell, D.; Berry, K.; Utterback, T.; van Aken, S. E.; Feldblyum, T. V.; D´Ascenzo, M.; Deng, W. L.; Ramos, A. R.; Alfano, J. R.; Cartinhour, S.; Chatterjee, A. K.; Delaney, T. P.; Lazarowitz, S. G.; Martin, G. B.; Schneider, D. J.; Tang, X.; Bender, C. L.; White, O.; Fraser, C. M.; Collmer, A.: The complete genome sequence of the Arabidopsis and tomato pathogen ***Pseudomonas syringae*** pv. tomato DC3000. ***PNAS*** **2003**, *100*, pp. 10181-10186

Bus, J., Sies, I., & Lie Ken Jie, M. S.: ^{13}C- NMR of double and triple bond carbon atoms of unsaturated fatty acid methylesters. ***Chem. and Phys. of Lipids*** **1977**, *18*, pp. 130-144

Busby, D. J.; Copley, R. C. B.; Hueso, J. A.; Readshaw, S. A.; Rivera, A.: SB-253514 and analogues: Novel inhibitors of lipoprotein associated phospholipase A2 produced by ***Pseudomonas fluorescens*** DSM11579; II. Physico-chemical properties and structure elucidation. ***J. Antibiotics*** **2000**, *53* (7), pp. 670-676

Caboche, S., Leclère, V., Pupin, M., Kucherov, G. & Jaques, P.: Diversity of monomers in nonribosomal peptides: towards the prediction of origin and biological activity. J. Bac. **2010**, *192* (19), pp. 5143-5150

Cameotra, S. S., & Makkar, R. S.: Recent applications of biosurfactants as biological and immunological molecules. ***Curr Opin Microbiol*** **2004**, *7*, pp. 262-266

Campbell, J. A., Davies, G. J., Bulone, V. & Henrissat, B.: A classification of nucleotide-diphospho-sugar glycosyltransferases based on amino acid sequence similarities. ***J. Biochem.*** **1997**, *326*, pp. 929-939(article content corrected in ***J. Biochem***. **1998**, *329*, p. 719)

Canepari, P., Boaretti, M., Lleo, M. & Satta, G.: Lipoteichoic acid as a new target for activity of antibiotics: mode of action of daptomycin (LY 146032). ***Antimicrob. Agents Chemother.*** **1990**, *34*, pp. 1220-1226

Cantarel, B. L., Coutinho, P. M., Rancurel, C., Bernard, T., Lombard, V. & Henrissat, B.: The Carbohydrate-Active enZymes database (CAZy): an expert resource for glycogenomics. ***Nucleic Acids Res.*** **2009**, *37*, pp. D233-D238

Carrillo, C., Teruel, J. A., Aranda, F. J. & Ortiz, A.: Molecular mechanism of membrane permeabilization by the peptide antibiotic surfactin. ***Bioch. Biophys. Acta*** **2003**, *1611*, pp. 91-97

Cavalleri, B., Pagani, H., Volpe, G., Selva, E., & Parenti, F.: A-16686, a new antibiotic from Actinoplanes, I. Fermentation, Isolation and preliminary physico-chemical characteristics. ***J. Antibiot.*** **1984**, *37* (4), pp. 309-317

Challis, G. L.: Mining microbial genomes for new natural products and biosynthetic pathways. ***Microbiology*** **2008**, *154*, pp. 1555-1569

Challis, G. L., & Naismith, J. H.: Structural aspects of non-ribosomal peptide biosynthesis. ***Curr. Opin. Struct. Biol.*** **2004**, *14*, pp. 748-756

Challis, G. L., Ravel, J., & Townsend, C. A.: Predictive, structure-based model of amino acid recognition by nonribosomal peptide synthetase adenylation domains. ***Chem. Biol.*** **2000**, *7*, pp. 211-224

Chang, Z.; Sitachitta, N.; Rossi, J. V.; Roberts, M. A.; Flatt, P. M.; Jia, J.; Sherman, D. H.; Gerwick, W. H.: Biosynthetic pathway and gene cluster of curacin A, an antitubulin natural product from the tropical marine cyanobacterium ***Lyngbya majascula***. ***J. Nat. Prod.*** **2004**, *67*, pp. 1356-1367

Christiansen, G., Philmus, B., Hemscheidt, T., & Kurmayer, R.: Genetic variation of adenylation domains of the anabaenopeptin synthesis operon and evolution of substrate promiscuity. ***J. Bac.*** **2011**, *193* (15), pp. 3822-3831

Clugston, S. L., Sieber, S. A., Mahariel, M. A., & Walsh, C. T.: Chirality of peptide bond-formind condensation domains in nonribosomal peptide snythetases: the C5 domain of tyrocidine synthetase is a $^{D}C_{L}$ catalyst. ***Biochemistry*** **2003**, *42*, pp. 12095-12104

Coraiola, M., Lo Cantore, P., Lazzaroni, S., Evidente, A., Iacobellis, N. S. & Dalla Serra, M.: WLIP and tolaasin I, lipodepsipeptides from ***Pseudomonas reactans*** and ***Pseudomonas tolaasii***, permeabilise model membranes. ***Bioch. Bioph. Acta*** **2006**, *1758*, pp. 1713-1722

Corre, C., & Challis, G.: New natural product biosynthetic chemistry discovered by genome mining. ***Nat. Prod. Rep.*** **2009**, *26*, pp. 977 - 986

Coutinho, P. M., Deleury, E., Davies, G. J. & Henrissat, B.: An evolving hierarchical family classification for glycosyltransferases. ***J. Mol. Biol.*** **2003**, *328*, pp. 301-317

Cuppels, D. A.: Generation and characterization of Tn5 insertion mutations in *Pseudomonas syringae* pv. tomato. *Appl. Environm. Microbiol.* **1986**, *51* (2), pp. 323-327

Cushley, R. J., Lipsky, S. R., Wasserman, H. H., Sykes, R. J., Peverada, P. & Shaw, C. K.: Biosynthesis of prodigiosin. ^{13}C labeled alanine, proline, glycine and serine elucidated by Fourier Transform Nuclear Magnetic Resonance. *J. Am. Chem. Soc.* **1973**, *95* (20), pp. 6874-6875

de Bruijn, I. & Raaijmakers, J. M.: Diversity and functional analysis of LuxR-type transcriptional regulators of cyclic lipopeptide biosynthesis in *Pseudomonas fluorescens*. *Appl. Environ. Microbiol.* **2009**, *75*(14), pp. 4753-4761

de Bruijn, I., de Kock, M. J., de Waard, P., van Beek, T. A. & Raaijmakers, J. M.: Massetolide A biosynthesis in *Pseudomonas fluorescens*. J. Bac. **2008**, *190* (8), pp. 2777-2789

de Bruijn, I., de Kock, M. J., Yang, M., de Waard, P., van Beek, T. A. & Raaijmakers, J. M.: Genome-based discovery, structure prediction and fuctional analysis of cyclic lipopeptide antibiotics in *Pseudomonas* species. *Molecular Microbiol.* **2007**, *63* (2), pp. 417-428

de Lucca, A. J., Jacks, T. J., Takemoto, J., Vinyard, B. & Peter, J.: Fungal lethality, binding and cytotoxicity of syringomycin-E. *Antimicr. Agents Chemo.* **1999**, *43* (2), pp. 371-373

Debono, M.; Abbott, B. J.; Molloy, M.; Fukuda, D. S.; Hunt, A. H.; Daupert, V. M.; Counter, F. T.; Ott, J. L.; Carrell, C. B.; Howard, L. C.; Boeck, L. D. & Hamill, R. L.: Enzymatic and chemical modifications of lipopeptide antibiotic A21978C: The synthesis and evaluation of daptomycin (LY146032). *J. Antibiot.* **1988**, *41* (8), pp. 1093-1195

Dewick, P. M. *Medicinal Natural Products - A biosynthetic approach (2nd edition);* John Wiley & Sons: Chichester, 2001

Eggink, G., Engel, H., Vriend, G., Terpstra, P., & Witholt, B.: Rubredoxin reductase from *Pseudomonas aleovorans* - Structural relationship to other flavoprotein oxidoreductases based on one NAD and two FAD fingerprints. *J. Mol. Biol.* **1990**, *212*, pp. 135-142

Emanuele, M. C., Scaloni, A., Lavermicocca, P., Jacobellis, N. S., Camoni, L., Di Giorgio, D., Pucci, P.; Paci, M.; Segre, A.; & Ballio, A.: Corpeptins, new bioactive lipodepsipeptides from cultures of *Pseudomonas corrugata*. *FEBS Letters* **1998**, *433*, pp. 317-320

Eppink, M. H., Schreuder, H. A., & van Berkel, W. J.: Identification of a novel conserved sequence motif in flavoprotein hydroxylases with a putative dual function in FAD/NAD(P)H binding. *Protein Science* **1997**, *6*, pp. 2454-2458

Erb, A., Weiß, H., Härle, J. & Bechthold, A.: A bacterial glycosyltransferase gene toolbox: generation and applications. Phytochem. **2009**, *70*, pp. 1812-1821

Falagas, M. & Kasiakou, S. K.: Colistin: the revival of polymyxins for the management of multidrug-resistant Gram-negative bacterial infections. *Clinical Infectious diseases* **2005**, *40*, pp. 1333-1341

Feil, H.; Feil, W. S.; Chain, P.; Larimer, F.; Di Bartolo, G.; Copeland, A.; Lydikis, A.; Trong, S.; Nolan, M.; Goltsman, E.; Thiel, J.; Malfatti, S.; Loper, J. E.; Lapidus, A.; Detter, J. C.; Land, M.; Richardson, P. M.; Krypides, N. C.; Ivanova, N. & Lindow, S. E.: Comparison of the complete genome sequences of *Pseudomonas syringae* pv. syringae B728a and pv. tomato DC3000. *PNAS* **2005**, *100*, pp. 11064-11069

Felnagle, E. A.; Barkei, J. J.; Park, H.; Podevels, A. M.; Mc Mahon, M. D.; Drott, D. W. & Thomas, M. G.: MbtH-like proteins as integral components of bacterial nonribosomal peptide synthetases. *Biochem.* **2010**, *49* (41), pp. 8815-8817

Fernebro, J.: Fighting bacterial infections- future treatment options. *Drug resistance updates* **2011**, *14*, pp. 125-139

Fischbach, M. A. & Walsh, C. T.: Assembly-line enzymology for polyketide and nonribosomal peptide antibiotics: logic, machinery and mechanisms. *Chem. Rev.* **2006**, *106*, pp. 3468-3496

Fraaije, M. W., Kamerbeek, N. M., van Berkel, W. J. & Janssen, D. B.: Identification of a Baeyer-Villiger monooxygenase sequence motif. FEBS Letters **2002**, *518*, pp. 43-47

Freire-Moran, L.; Aronsson, B.; Manz, C.; Gyssens, I. C.; So, A. D.; Monnet, D. L.; Cars, O.; ECDC-EMA Working Group: Critical shortage of new antibiotics in development against multirdrug-resistant bacteria - time is to react now. *Drug resistance updates* **2011**, *14*, pp. 118-124

Gerard, J., Lloyd, R., Barsby, T., Haden, P., Kelly, M. T. & Andersen, R. J.: Massetolides A-H, antimycobacterial cyclic depsipeptides produced by two Pseudomonads isolated from marine habitats. *J. Nat. Prod.* **1997**, *60*, pp. 223-229

Gibson, M., Nur-el-alam, M., Lipata, F., Oliviera, M. A. & Rohr, J.: Characterization of kinetics and products of the Baeyer-Villiger oxygenase MtmOIV, the key enzyme of the biosynthetic pathway toward the natural product anticancer drug mithramycin from *Streptomyces argillaceus*. JACS **2005**, *127*, pp. 17594-17595

Grgurina, I., Barca, A., Cervigni, S., Gallo, M., Scaloni, A. & Pucci, P.: Relevance of chlorine-substituent for the antifungal activity of syringomycin

and syringotoxin, metabolites of the phytopathogenic bacterium ***Pseudomonas syringae*** pv. ***syringae***. ***Experientia,*** **1994**, ***50*** (2), pp. 130-133

Gross, H.: Strategies to unravel the function of orphan biosynthesis pathways: recent examples and future prospects. ***Appl. Microbiol. Biotechnol.*** **2007**, ***75*** (2), pp. 267 - 277

Gross, H.: Genomic mining - a concept for the discovery of new bioactive natural products. ***Curr. Opin. Drug Discovery Devel.*** **2009**, ***12*** (2), pp. 207 - 219

Gross, H. & Loper, J. E.: Genomics of secondary metabolite production by ***Pseudomonas*** spp. ***Nat. Prod. Rep.*** **2009**, ***26***, pp. 1408-1446

Gross, H., Stockwell, V. O., Henkels, M. D., Nowak-Thompson, B., Loper, J. E. & Gerwick, W. H.: The genomisotopic approach: a systematic method to isolate products of orphan biosynthetic gene clusters. ***Chem. Biol.*** **2007**, ***14***, pp. 53-63

Grundmann, H.; Klugman, K. P.; Walsh, T.; Ramon-Pardo, P.; Siguaque, B.; Khan, W.; Laxminarayan, R.; Heddini, A.; Stelling, J.:(2011). A framework of global surveillance of antibiotic resistance. ***Drug resistance updates*** **2011**, ***14***, pp. 79-87

Guenzi, E., Galli, G., Grgurina, I., Gross, D. C. & Grandi, G.: Characterisation of the syringomycin synthetase gene cluster; A link between prokaryotic and eukaryotic peptide synthetases. ***J. Biol. Chem.*** **1998**, ***49*** (273), pp. 32857-32863

Gunstone, F. D.: The composition of hydrogenated fats by high-resolution ^{13}C nuclear magnetic resonance spectroscopy. ***JAOCS*** **1993**, ***70*** (10), pp. 965-970

Hancock, R. E.: Mechanisms of action of newer antibiotics for Gram-positive pathogens. ***Lancet Infect. Dis.*** **2005**, ***5***, pp. 209-218

Hashizume, H. & Nishimura, Y.: Cyclic lipopeptide antibiotics. ***Studies in Nat. Prod. Chem.*** **2008**, ***35***, pp. 693-751

Hu, Y. & Walker, S.: Remarkable structural similarities review between diverse glycosyltransferases. ***Chem. Biol.*** **2002**, ***9***, pp. 1287-1296

Hutter, B., Fischer, c., Jacobi, A., Schaab, C. & Loferer, H.: Panel of ***Bacillus subtilis*** reporter strains indicative of various modes of action. ***Antimicrob. Agents Chemother.*** **2004**, ***48*** (7), pp. 2588-2594

Ishii, T., Okino, T. and Mino, Y.: A ceramide and cerebroside from the starfish ***Asterias amurensis*** Lütken and their plant-growth promotion activities. ***J. Nat. Prod.*** **2006**, ***69***, pp. 1080-1082

Juguet, M.; Lautru, S.; Francou, F.-X.; Nezbedova, S.; Leblond, P.; Gondry, M. & Permodet, J.-L.: An iterative nonribosomal peptide synthase assembles the pyrrole-amide antibiotic congocidine in ***Streptomyces ambofaciens***. ***Chem. Biol.*** **2009**, *16*, pp. 421-431

Jung, D., Rozek, A., Okon, M. & Hancock, R. W.: Structural transitions as determinants of the action of the calcium-dependent antibiotic daptomycin. ***Chem. Biol.*** **2004**, *11*, pp. 949-957

Kanazawa, K.; Sato, Y.; Ohki, K.; Okimura, K.; Uchida, Y.; Shindo, M. & Sakura, N.: Contribution of each amino acid residue in polymyxin B_3 to antimicrobial and lipopolysaccharide binding activity. Chem. Pharm. Bull. **2009** *57* (3), pp. 240-244

Kersten, R. D.; Yang, Y.-L-; Xu, Y.; Cimermancic, P.; Nam, S.-J.; W., Fenical.; Fischbach, M. A.; Moore, B.S. & Dorrestein, P. C.: A mass spectrometry-guided genome mining approach for natural product peptidogenomics. ***Nat. Chem. Biol.*** **2012**, *7* (11), pp. 794-802

Kim, B. H. & Gadd, G. M. ***Bacterial Physiology and Metabolism.*** Cambridge University Press: Cambridge, **2008**

King, E. O., Ward, M. K. & Raney, D. E.: Two simple media for the demonstration of pyocyanin and fluorescin. ***Journal Lab Clin Med.*** **1954**, *44* (2), pp. 301-307

Konishi, M.; Sugawara, K.; Hanada, M.; Tomita, K.; Tomatsu, K.; Miyak, T.; Kawaguchi, H.: Empedopeptin (BMY-28117), A new depsipeptide antibiotic I. Productoin, Isolation and properties. ***The Journal of Antibiotics*** **1984**, *37* (9), pp. 949-957

Kraas, F. I., Helmetag, V., Wittmann, M., Strieker, M. & Mahariel, M. A.: Functional dissection of surfactin synthetase initiation module reveals insights into the mechanism of lipoinitiation. ***Chem. & Biol.*** **2010**, *17*, pp. 872-880

Kracht, M., Rokos, H., Mushin, O., Kowall, M., Pauli, G. & Vater, J.: Antiviral and hemolytic activities of surfactin isoforms and their methyl ester derivatives. ***J. Antibiotics*** **1999**, *52* (7), pp. 613-619

Kreutzer, M. F.; Kage, H.; Gebhardt, P.; Wackler, B.; Saluz, H. P.; Hoffmeister, D.; Nett, M.: Biosynthesis of a complex yersiniabactin-like natural product via the mic locus in phytopathogen ***Ralstonia solanacearum***. ***Appl. Environ. Microbiol.*** **2011,** *77* (17), pp. 6117-6124

Kuiper, I.; Lagendijk, E. L.; Pickford, R.; Derrick, J. D.; Lamers, G. E. M.; Thomas-Oates, J. E.; Lugtenberg, B. J. J.; Bloemberg, G. V.: Characterisation of two ***Pseudomonas putida*** lipopeptide biosurfactants, putisolvin I and II,

which inhibit biofilm formation and break down existing biofilms. ***Mol. Microbiol.*** **2004**, *51* (1), pp. 97-113

Laganas, V., Adler, J., & Silverman, J.: (2003). In vitro bactericidal activities of daptomycin against ***Staphylococcus aureus*** and ***Enterococcus faecalis*** are not mediated by inhibition of lipoteichoic acid biosynthesis. ***Antimicrob. Agents Chemother.*** **2003**, *47* (8), pp. 2682-2684

Lairson, L. L., Henrissat, B., Davies, G. J., & Winters, S. G.: Glycosyltransferases: Structures, functions and mechanisms. ***Annu. Rev. Biochem.*** **2008**, *77*, pp. 521-555

Lakey, J. H., Lea, E. J., Rudd, B. A., Wright, H. M., & Hopwood, D. A.: CDA is a new chromosomally-determined antibiotic from ***Streptomyces coelicolor*** A3(2). ***J. Gen. Microbiol.*** **1983**, *129*, pp. 3565-3573

Larkin, M. A.; Blackshields, G.; Brown, N. P.; Chenna, R.; Mc Gettigan, P. A.; Mc William, H.; Valentin, F.; Wallace, I. M.; Wilm, A.; Lopez, R.; Thompson, J. D.; Gibson, T. J.; Higgins, D. G.: ClustalW and ClustalX version 2 (2007). ***Bioinformatics*** **2007**, *23* (21), pp. 2947-2948

Lautru, S., Deeth, R. J., Bailey, L. M., & Challis, G. L.: Discovery of a new peptide product by ***Streptomyces coelicolor*** genome mining. ***Nat. Chem. Biol.*** **2005**, *1* (5), S. 265-269

Lavermicocca, P., Iacobellis, N. S., Simmaco, M., & Graniti, A.: Biological properties and spectrum of activity of ***Pseudomonas syringae*** pv. syringae toxins. ***Physiol. Mol. Plant Path.*** **1997**, *50*, pp. 129-140

Lewis, K.: Recover the lost art of drug discovery. ***Nature*** **2012**, *485*, pp. 439-440

Li, A., & Piel, J.: A gene cluster from a marine ***Streptomyces*** encoding the biosynthesis of the aromatic spiroketal polyketide griseorhodin A. ***Chem. Biol.*** **2002**, *9*, pp. 1017-1026

Linne, U., Schwarzer, D., Schroeder, G. N., & Mahariel, M. A.: Mutational analysis of a type II thioesterase associated with nonribosomal peptide synthesis. ***Eur. J. Biochem.*** **2004**, *271*, pp. 1536-1545

Liu, J., & Mushegian, A.: Three monophyletic superfamilies account for the majority of the known glycosyltransferases. ***Prot. Science*** **2003**, *12*, pp. 1418-1431

Loper, J. E., & Lindow, S. E.: Lack of evidence for in situ fluorescent pigment production by ***Pseudomonas syringae*** pv. syringae on bean leaf surfaces. ***Phytopathology*** **1987**, *77* (10), pp. 1449-1454

Lu, S.-E., Scholz-Schroeder, B. K., & Gross, D.: Characterization of the *salA*, *syrF*, and *syrG* regulatory genes located at the right border of the syringomycin gene cluster of *Pseudomonas syringae* pv. syringae. *MPMI* **2002**, *15* (1), pp. 43-53

Lu, S.-E., Wang, N., Wang, J., Chen, Z. J., & Gross, D. C.: Oligonucleotide microarray analysis of the SalA regulon controlling phytotoxin production by *Pseudomonas syringae* pv. syringae. *MPMI* **2005**, *18* (4), pp. 324-333

Madduri, K., Waldron, C., & Merlo, D. J.: Rhamnose biosynthesis pathway supplies precursors for primary and secondary metabolism in *Saccharopolyspora spinosa*. *J. Bac.* **2001**, *183* (19), pp. 5632-5638

Maeda, Y.; Watanabe, R.; Harris, C. L.; Hong, Y.; Ohishi, K.; Kinoshita, K.; Kinoshita, T.: PIG-M transfers the first mannose on the lumenal side of the ER. *EMBO J.* **2001**, *20* (1 & 2), pp. 250-261

Mahariel, M. A., Stachelhaus, T., & Mootz, H. D.: Modular peptide synthases involved in nonribosomal peptide synthesis. *Chem. Rev.* **1997**, *97*, pp. 2651-2673

Mascher, T., Margulis, N. G., Wang, T., Ye, R. W., & Helmann, J. D.: Cell wall stress responses in *Bacillus subtilis*: the regulatory network of the bacitracin stimulon. *Mol. Microbiol.* **2003**, *50* (5), pp. 1591-1604

Mazzola, M., de Bruijn, I., Cohen, M. F., & Raaijmakers, J. M.: Protozoan-induced regulation of cyclic lipopeptide biosynthesis is an effective predation defense mechanism for *Pseudomonas fluorescens*. *Appl. Environ. Microb.* **2009**, *75*, pp. 6804-6811

Medema, M. H., Blin, K., Cimermancic, P., de Jager, V., Zakrzewski, P., Fischbach, M. A., Weber, T., Takano, E. & Breitling, R.: antiSMASH: rapid identification, annotation and analysis of secondary metabolite biosynthesis gene clusters in bacterial and fungal genome sequences. *Nucleic Acids Res.* **2011**, *39*, W339-W346

Miao, V.; Coeffet-LeGal, M.-F.; Brian, P.; Brost, R. Penn, J.; Whiting, A.; Martin, S.; Ford, R.; Parr, I.; Bouchard, M.; Silva, C. J.; Wrigley, S. K.; Baltz, R. H.: Daptomycin biosynthesis in *Streptomyces roseosporus*: cloning and analysis of the gene cluster and revision of peptide stereochemistry. *Microbiology* **2005**, *151*, pp. 1507-1523

Mo, Y.-Y., & Gross, D. C.: Plant signal molecules activate the *syrB* gene, which is required for syringomycin production by *Pseudomonas syringae* pv. syringae. *J. Bac.* **1991**, *173* (18), pp. 5784-5792

Mootz, H. D., Schwarzer, D., & Mahariel, M. A.: Ways of assembling complex natural products on modular nonribosomal peptide synthetases. *ChemBioChem* **2002**, *3*, pp. 490-504

Morikawa, M., Daido, H., Takao, T., Murata, S., Shimonishi, Y., & Imanaka, T.: A new lipopeptide biosurfactant produced by *Arhtrobacter* sp. strain MIS38. *J. Bacteriol.* **1993**, *175* 20, pp. 6459-6466

Müller, A.; Münch, D.; Schmidt, Y.; Reder-Christ, K.; Schiffer, G.; Bendas, G.; Gross, H.; Sahl, H.-G.; Schneider, T.; Brötz-Oesterhelt, H.: Lipodepsipeptide empedopeptin inhibits cell wall biosynthesis through a Ca^{2+}-dependent complex formation with peptidoglycan precursors. *J. Biol. Chem.* **2012**, *287* (24), pp. 20270-20280

Nakajima, A., Sugimoto, Y., Yoneyama, H., & Nakae, T.: Localization of the outer membrane subunit OprM of Resistance-Nodulation-Cell Division family multicomponent efflux pump in *Pseudomonas aeruginosa*. *J. Biol. Chem.* **2000**, *275* (39), pp. 30064-30068

Nutkins, J.; Mortishire-Smith, R. J.; Packman, L. C.; Brodey, C. L.; Rainey, P. B.; Johnstone, K.; Williams, D. H.: Structure determination of tolaasin, an extracellular lipodepsipeptide produced by the mushroom pathogen *Pseudomonas tolaasii* Paine. *JACS* **1991**, *113*, pp. 2621-2627

Nybroe, O. & Sørensen, J.: Production of cyclic lipopeptides by fluorescent pseudomonads. In *Pseudomonas, biosynthesis of macromolecules and molecular metabolism;* Ramos, J.-L., Ed.; Kluwer Academic/Plenum Publishers: New York, 2004, (pp. 147-172).

Offen, W.; Martinez-Fleites, C.; Yang, M.; Kiat-Lim, E.; Davies, B. J.; Tarling, C. A.; Ford, C. M.; Bowles, D. J.; Davies, G. J.: Structure of a flavonoid glucosyltransferase reveals the basis for plant natural product modification. *EMBO J.* **2006**, *25*, pp. 1396-1405

Okimura, K., Ohki, K., Sato, Y., Ohnishi, K., & Sakura, N.: Semi-synthesis of polymyxin B (2-10) and colistin (2-10) analogs employing the trichloroethoxycarbonyl (Troc) group for side chain protection of α,γ-diaminobutyric acid residues. *Chem. Pharm. Bull.* **2007**, *55* (12), pp. 1724-1730

Pérez, M., Baig, I., Brana, F., Salas, J. A., Rohr, J., & Méndez, C.: Generation of new derivatives of the antitumor antibiotic mithramycin by altering the glycosylation pattern through combinatorial biosynthesis. *ChemBioChem* **2008**, *9* (14), pp. 2295-2304

Petersohn, A., Brigulla, M., Haas, S., Hoheisel, J. D., Völker, U., & Hecker, M.: Global analysis of the general stress response of *Bacillus subtilis*. *J. Bac.* **2001**, *183* (19), pp. 5617-5631

Phelan, V. V., Du, Y., Mc Lean, J. A., & Bachmann, B. O.: Adenylation enzyme characterization using γ-18O4-ATP pyrophosphate exchange. *Chem.& Biol.* **2009**, *16*, pp. 473-478

Piddock, L. J.: Multidrug-resistance efflux pumps — not just for resistance. *Nature rev. Microbiol.* **2005**, *4*, pp. 629-626

Pinto, I., Boyd, H., & Hickey, D.: Natural product derived inhibitors of lipoprotein associated phospholipase A_2, synthesis and activity of analogues of SB-253514. *Bioorg. & Med. Chem. Letters* **2000**, *10*, pp. 2015-2017

Pirri, G., Guiliani, A., Nicoletto, S. F., Pizzuto, L., & Rinaldi, A. C.: Lipopeptides as anti-infectives: a practical perspective. *Cent. Eur. J. Biol.* **2009**, *4* (3), pp. 258-273

Poole, K., Krebes, K., Mc Nally, C., & Neshat, S.: Multiple antibiotic resistance in *Pseudomonas aeruginosa*: evidence for involvement of an efflux operon. *J. Bac.* **1993**, *175*, pp. 7363-7372

Prado, L.; Fernández, E.; Weißbach, U.; Blanco, G.; Quirós, L. M.; Brana, A.F.; Méndez, C.; Rohr, J.; Salas, J. A.: Oxidative cleavage of premithramycin B is one of the last steps in the biosynthesis of the antitumor drug mithramycin. *Chem. Biol.* **1999**, *6*(1), pp. 19-30

Pretsch, E., Bühlmann, P., Affolter, C. & Badertscher, M.: *Spektroskopische Daten zur Strukturaufklärung organischer Verbindungen* (4 ed.); Springer Verlag: Berlin, Heidelberg, 2001

Raaijmakers, J. M., Bruijn, I., & Kock, M. D.: Cyclic lipopeptide production by plant-associated *Pseudomonas* spp.: diversity, activity, biosynthesis, and regulation. *MPMI* **2006**, *19* (7), pp. 699-710

Raaijmakers, J. M., de Bruijn, I., Nybroe, O., & Ongena, M.: Natural functions of lipopeptides from *Bacillus* and *Pseudomonas*: more than surfactants and antibiotics. *FEMS Microbiol. Rev.* **2010**, *34*, pp. 1037-1062

Rausch, C., Hoof, I., Weber, T., Wohlleben, W., & Huson, D. H.: Phylogenetic analysis of condensation domains in NRPS sheds light on their functional evolution. *BMC Evolutionary Biol.* **2007**, *7*, 78

Reder-Christ, Katrin; Schmidt, Yvonne; Dörr, Marius; Sahl, H.-G.; Josten, M.; Raaijmakers, J. M.; Gross, H.; Bendas, G.: Model membrane studies for characterization of different antibiotic activities of lipopeptides from *Pseudomonas. Biochimica et Biophysica Acta* **2012**, *1818*, pp. 566-573

Rees, D. O., Bushby, N., Cox, R. J., Harding, J. R., & Simpson, T. J.: Synthesis of [1,2-$^{13}C_2$,^{15}N]-L-homoserine and its incorporation by the PKS-NRPS system of *Fusarium moniliforme* into the mycotoxin fusarin C. *ChemBioChem* **2007**, *8*, pp. 46-50

Roongsawang, N., Hase, K., Haruki, M., Imanaka, T., Morikawa, M. & Kanaya, S.: Cloning and characterisation of the gene cluster encoding arthrofactin synthetase from *Pseudomonas* sp. MIS38. *Chem. Biol.* **2003**, *10*, pp. 869-880

Roongsawang, N., Washio, K. & Morikawa, M.: In vivo characterization of tandem C-terminal thioesterase domains in arthrofactin synthetase. *ChemBioChem* **2007**, *8*, pp. 501-512

Sayed, K. A., Bartyzel, P., Shen, X., Perry, T. L., Zjawiony, J. K. & Hamann, M. T.: Marine natural products as antituberculosis agents. *Tetrahedron* **2000**, *56*, pp. 949-953

Schlegel, A., Bohm, A., Lee, S. J., Peist, R., Decker, K. & Boos, W.: Network regulation of the *Escherichia coli* maltose system. *J. Mol. Microbiol.* **2002**, *4*, pp. 301-307

Schneider, T.; Gries, K.; Josten, M.; Wiedemann, I.; Pelzer, S.; Labischinski, H. & Sahl, H.-G.: The lipopeptide antibiotic friulimicin B inhibits cell wall biosynthesis through complex formation with bactrophenol phosphate. *Antimicrob. Agents Chemo.* **2009**, *53* (4), pp. 1610-1618

Scholz-Schroeder, B. K., Soule, J. D. & Gross, D. C.: The *sypA*, *sypB*, and *sypC* synthetase genes encode twenty-two modules involved in the nonribosomal peptide synthesis of syringopeptin by *Pseudomonas syringae* pv. syringae B301D. *MPMI* **2003**, *16* (4), pp. 271-280

Schwarzer, D., Finking, R. & Mahariel, M. A.: Nonribosomal peptides: from genes to products. Nat. Prod. Rep. **2003**, *20*, pp. 275-287

Schwarzer, D., Mootz, H. D., Linne, U. & Mahariel, M. A.: Regeneration of misprimed nonribosomal peptide synthetases by type II thioesterases. *PNAS* **2002**, *99* (22), pp. 14083-14088

Séquin, U. & Scott, A. E.: Carbon-13 as a label in biosynthetic studies. *Science* **1974**, *186*, pp. 101-107

Shoji, J.; Hinoo, H.; Katayama, T.; Matsumoto, K.; Tanimoto, T.; Hattori, T.; Higashiyama, I.; Miwa, H.; Motokawa, K. & Yoshida, Y.: Isolation and characterisation of new peptide antibiotics, plusbacins A_1-A_4 and B_1-B_4. *J. Antibiotics* **1992a**, *45* (6), pp. 817-823

Shoji, J.; Hinoo, H.; Katayama, T.; Nakagawa, Y.; Ikenishi, Y.; Iwatani, K. & Yoshida, T.: Structures of new peptide antibiotics, plusbacins A_1~A_4 and B_1~B_4. *J. Antibiot.* **1992b**, *45*, pp. 824-831

Sinnaeve, D., Hendrickx, M. S., Van Hemel, J., Peys, E., Kieffer, B. & Martins, J. C.: The solution structure and self-association properties of the cyclic lipodepsipeptide pseudodesmin A support its pore-forming potential. *Chem. Eur. J.* **2009b**, *15*, pp. 12653-12662

Sinnaeve, D.; Michaux, C.; van Hemel, J.; Vandenkerckhove, J.; Peys, E.; Borremans, F. A. M.; Sas, B.; Wouters, J. & Martins, J. C.: Structure and x-

ray conformation of pseudodesmins A and B, two new cyclic lipodepsipeptides from Pseudomonas bacteria. Tetrahedron **2009a**, *65*, pp. 4173-4181

Staunton, J. & Weissman, K. J.: Polyketide synthesis: a millenium review. *Nat. Prod. Rep.* **2001**, *18*, pp. 380-416

Steenbergen, J. N., Alder, J., Thorne, G. M. & Tally, F. P.: Daptomycin: a lipopeptide antibiotic for the treatment of serious Gram-positive infections. *J. Antimicrob. Chemo.* **2005**, *55*, pp. 283-288

Stierle, D. B. & Faulkner, D. J.: Metabolites of the marine sponge *Laxosuberites* sp.. *J. Org. Chem.* 1980, *45*, pp. 4980-4982

Storm, D. R., Rosenthal, K. S. & Swanson, P. E.: Polymyxin and related peptide antibiotics. *Annu. Rev. Biochem.* **1977**, *46*, pp. 723-763

Stover, C. K.; Pham, X. Q.; Erwin, A. L.; Mizoguchi, S. D.; Warrener, P.; Hickey, M. J.; Brinkman, F. S.; Hufnagle, W. O.; Kowalik, D. J.; Lagrou, M.; Garber, R. L.; Goltry, L.; Tolentino, E.; Westbrock-Wadman, S.; Yuan, Y.; Brody, L. L.; Coulter, S. N.; Folger, K. R.; Kas, A.; Larbig, K.; Lim, R.; Smith, K.; Spencer, D.; Wong, G. K.; Wu, Z.; Paulsen, I. T.; Reizer, J.; Saier, M. H.; Hancock, R. E.; Lory, S. & Olson, M. V.: Complete genome sequence of *Pseudomonas aeruginoasa* PAO1, an opportunistic pathogen. Nature **2000**, *406*, pp. 959-964

Strahl-Bolsinger, S., Immervoll, T., Deutzmanni, R. & Tanner, W.: PMTI, the gene for a key enzyme of protein O-glycosylation in *Saccharomyces cerevisiae*. *Proc. Natl. Acad. Sci. USA* **1993**, *90*, pp. 8164-8168

Strieker, M. & Mahariel, M. A.: The structural diversity of acidic lipopeptide antibiotics. *ChemBioChem* **2009**, *10*, pp. 607-616

Stülke, J., Hanschke, R. & Hecker, M.: Temporal activation of ß-glucanase synthesis in *Bacillus subtilis* is mediated by the GTP pool. *J. General Microbiol.* **1993**, *139*, pp. 2031-2045

Sugawara, K., Numata, K.-I., Konishi, M. & Kawaguchi, H.: Empedopeptin (BMY-28117), a new depsipeptide antibiotic; II. Structure elucidation. *J. Antibiotics* **1984**, *37* (9), pp. 958-964

Surin, B. P., Watson, J. M., Hamilton, W. D., Economou, A. & Downie, J. A.: Molecular characterization of the nodulation gene, *nodT*, from two biovars of *Rhizobium leguminosarum*. *Mol. Microbiol.* **1990**, *4* (2), pp. 245-252

Takahashi, M.; Inoue, N.; Ohishi, K.; Maeda, Y.; Nakamura, N.; Endol, Y.; Fujital, T. & Takeda, J.: PIG-B, a membrane protein of the endoplasmatic reticulum with a large lumenal domain, is involved in transferring the third mannose of the GPI anchor. *EMBO J.* **1996**, *14* (16), pp. 4254-4261

Thibodeaux, C. J., Melancon 3rd, C. E. & Liu, H.-W.: Natural product sugar biosynthesis and enzymatic glycodiversification. *Ang. Chem. Int. Ed.* **2008**, *47* (51), pp. 9814-9859

Thirkettle, J.: Novel inhibitors of lipoprotein associated phospholipase A_2 produced by *Pseudomonas fluorescens* DSM 11579. **In** *Biodiversity; New leads for the pharmaceutical and agrochemical industries*; Wrigley, S., Hayes, M., Thomas, R., Chrystal, E. J. T. & Nicholson, N., Eds.; Royal Society of Chemistry: Cambridge, **2000a**, pp. 100-109

Thirkettle, J.: SB-253514 and analogues; novel inhibitors of lipoprotein associated phospholipase A_2 produced by *Pseudomonas fluorescens* DSM 11579; III. Biotransformation using naringinase. J. Antibiotics **2000b**, *53* (7), pp. 733-735

Thirkettle, J.; Alvarez, E.; Boyd, H.; Brown, M.; Diez, E.; Hueso, J.; Elson, S.; Fulston, M.; Gershater, C.; Morata, M. L.; Perez, P.; Ready, S.; Sanchez-Puelles, J. M. & Sheridan, R.: SB-253514 and analogues; novel inhibitors of lipoprotein-associated phospholipase A_2 produced by *Pseudomonas fluorescens* DSM 11579; I. Fermentation of producing strain, isolation and biological activity. *J. Antibiotics* **2000**, *53* (7), pp. 664-669

Urban, A.; Eckermann, S.; Fast, B.; Metzger, S.; Gehling, M.; Ziegelbauer, K.; Rübsamen-Waigman, H. & Freiberg, C.: Novel whole-cell antibiotic biosensors for compound discovery. *Appl. Environm. Microbiol.* **2007**, *73* (20), pp. 6436-6443

Vallet-Gely, I.; Novikov, A.; Augusto, L.; Liehl, P.; Bolbach, G.; Péchy-Tarr, M.; Cosson, P.; Keel, C.; Caroff, M. & Lemaitre, B.: Association of hemolytic activity of *Pseudomonas entomophila*, a versatile soil bacterium, with cyclic lipopeptide production. *Appl. Environm. Microbiol.* **2010**, *76* (3), pp. 910-921

van Berkel, W. J., Kamerbeek, N. M. & Fraaije, M. W.: Flavoprotein monooxygenases, a diverse class of oxidative biocatalysts. *J. Biotechnol.* **2006** *14*, pp. 670-689

Vederas, J. C.: The use of stable isotopes in biosynthetic studies. Nat. Prod. Reports **1987**, *4*, pp. 277-337

Vodovar, N.; Vallenet, D.; Cruveiller, S.; Rouy, Z.; Barbe, V.; Acosta, C.; Cattolica, L.; Jubin, C.; Lajus, A.; Segurens, B.; Vacherie, B.; Wincker, P.; Weissenbach, J.; Lemaitra, B.; Medigue, C. & Boccard, F.: Complete genome sequence of the entomopathogenic and metabolically versatile soil bacterium *Pseudomonas entomophila*. *Nature Biotechnol.* **2006**, *24*, pp. 673-679

Vollenbroich, D., Özel, M., Vater, J., Kamp, R. M. & Pauli, G.: Mechanism of inactivation of enveloped viruses by the biosurfactant surfactin from *Bacillus subtilis*. *Biologicals* **1997**, *25*, pp. 289-297

von Döhren, H., Dieckmann, R., & Vrancic, M.-P.: The nonribosomal code. ***Chem. Biol.*** **1999**, *6* (10), pp. R723-R729

Wang, C. L., Ng, T. B., Yuan, F., Liu, Z. K. & Liu, F.: Induction of apoptosis in human leukemia K562 cells by cyclic lipopeptide from ***Bacillus subtilis*** natto T-2. Peptides **2007**, *28*, pp. 1344-1350

Wang, N., Lu, S.-E., Records, A. R. & Gross, D. C.: Characterization of the transcriptional activators SalA and SyrF, which are required for syringomycin and syringopeptin production by ***Pseudomonas syringae*** pv. syringae. ***J. Bac.*** **2006**, *188* (9), pp. 3290-3298

Watkins, W. M.: Glycosyyltransferases. Early history, development and future prospects. ***Carbohydrate Research*** **1986**, *149*, pp. 1-12

Watrous, J.; Roach, P.; Alexandrov, T.; Heath, B. S.; Yanga, J. Y.; Kersten, R. D.; van der Voort, M.; Pogliano, K.; Gross, H.; Raaijmakers, J. M.; Moore, B. S.; Laskin, J.; Bandeira, N. & Dorrestein, P. C.: Mass spectral molecular networking of living microbial colonies. ***Proc. Natl. Acad. Sci. USA*** **2012**, *109* (26), pp. E1743-E1752

Wenzel, S. C. & Müller, R.: Formation of novel secondary metabolites by bacterial multimodular assembly lines: deviations from textbook biosynthetic logic. Curr. Opin. Chem. Biol. **2005**, *9*, pp. 447-458

Wenzel, S. C.; Kunze, B.; Höfle, G.; Silakowski, B.; Scharfe, M.; Blöcker, H.; Müller, R.: Structure and biosynthesis of myxochromides S1-3 in ***Stigmatella aurantiaca***: evidence for an iterative bacterial type I polyketide synthase for module skipping in nonribosomal peptide biosynthesis. ***ChemBioChem*** **2005**, *6* (2), pp. 375-385

Weymouth-Wilson, A. C.: The role of carbohydrates in biologically active natural products. ***Nat. Prod. Rep.*** **1997**, *14* (2), pp. 99-110

WHO: WHO Global strategy for containment of antimicrobial resistance. www.who.int:http://www.who.int/csr/resources/publications/drugresist/WHO_CDS_CSR_DRS_2001_2_EN/en/, 2001 (retrieved May 28th, 2012)

Wierenga, R. K., Terpstra, P. & Hol, W. G.: Prediction of the occurrence of the ADP-binding ßαß-fold in proteins, using an amino acid sequence fingerprint. ***J. Mol. Biol.*** **1986**, *187*, pp. 101-107

Wuest, W. M., Sattley, E. S. & Walsh, C. T.: Three siderophores from one bacterial enzymatic assembly line. ***JACS*** **2009**, *131* (14), pp. 5056-5057

Yeh, E., Kohli, R. M., Bruner, D. & Walsh, C. T.: Type II thioesterase restores activity of a NRPS module stalled with an aminoacyl-S-enzyme that cannot be elongated. ChemBioChem **2004**, *5*, pp. 1290 –1293

Youssef, N. H., Duncan, K. E. & Mc Inerey, M. J.: Importance of 3-hydroxy fatty acid composition of lipopeptides for biosurfactant activity. ***Appl. Environm. Microbiol.*** **2005**, *71* (12), pp. 7690-7695

Zerikly, M. & Challis, G. L.: Strategies for the discovery of new natural products by genome mining. ***ChemBioChem*** **2009**, *10*, pp. 626- 633

Zgurskaya, H. I., Yamada, Y., Tikhonova, E. B., Ge, Q. & Krishnamoorthy, G.: Structural and functional diversity of bacterial membrane fusion proteins. ***Bioch. Biophys. Acta*** **2009**, *1794*, pp. 794-807

Ziemert, N., Podell, S., Penn, K., Badger, J. H., Allen, E. & Jensen, P. R.: The natural product domain seeker NaPDoS: a phylogeny based bioinformatic tool to classify secondary metabolite gene diversity. ***PLoS One*** **2012**, *7*, e34064

8 Appendix

8.1 Content

Figures:

Tables:

Table 8.1.1: sequences producing significant alignments with the GT from the lipodipeptide cluster of *P.* sp. SH-C52 (see figure 4.2.1).

Description of the sequence (strain), [accession no.]	score	Q. cov.	E-value	Max ident.	Pos.	Gaps
rhamnosyltransferase I, subunit B (*B. thailandensis* E264), [ZP_05590657.1]	395	96 %	8e-131	211/423 50%	270/423 64%	3/423 1%
GT family 28 (*B. ambifaria* IOP40-10), [ZP_02891477.1]	394	94%	1e-130	205/414 50%	259/414 63%	5/414 1%
GT family protein (*B. cenocepacia* MC0-3) [YP_001778806]	391	93%	2e-129	208/411 51%	265/411 64%	5/4111%
GT family 28 (*B. cenocepacia* HI2424), [YP_838721.1]	390	93%	4e-129	209/411 51%	264/411 64%	5/411 1%
GT family 28 (*B. ambifaria* MEX-5), [ZP_02907619.1]	390	94%	5e-129	204/414 49%	259/414 63%	5/414 1%
GT family 28 (*B. cenocepacia* AU 1054), [YP_623141.1]	390	93%	7e-129	209/411 51%	264/411 64%	5/411 1%
GT family protein (*B. ambifaria* AMMD), [YP_776391.1]	387	94%	7e-128	203/414 49%	258/414 62%	5/414 1%
GT family 28 (*B. cenocepacia* PC184), [ZP_04943307.1]	387	93%	8e-128	208/411 51%	263/411 64%	5/411 1%

score: value calculated from the number of gaps and substitutions associated with each aligned sequence (higher scores indicate significant alignments)

Q. coverage = query coverage: percent of match

E-value: describes possibility of false-positive match

Table 8.1.2: sequences producing significant alignments with the MO from the lipodipeptide cluster of *P.* sp. SH-C52 (see figure 4.2.1)

Description of the sequence (strain), [accession no.]	score	Q. cov.	E-value	Max ident.	Pos.	Gaps
putative FAD-dependent MO (*Xenorhabdus bovienii* SS-2004), [YP_003466257.1]	321	96%	3e-103	161/383 42%	226/383 59%	1/383 0%
FAD-binding MO (*Nocardia brasiliensis* ATCC 700358), [ZP_09844437.1]	316	97%	3e-101	171/385 44%	227/385 59%	5/385 1%
putative FAD-dependent MO (S. *bingchenggensis* BCW-1), [YP_004959073.1]	311	95%	2e-99	169/380 44%	231/380 61%	2/380 1%
protein VMA_001458 (*Vibrio mimicus* VM223) [ZP_06032750.1]	306	95%	2e-97	159/380 42%	222/380 58%	1/380 0%
putative FAD-dependent MO (*S. clavuligerus* ATCC 27064), [ZP_06771754.1]	303	96%	3e-96	172/382 45%	228/382 60%	2/381 1%
putative aromatic-ring hydroxylase (*Vibrio mimicus* VM603), [ZP_05721943.1]	295	95%	3e-93	155/380 41%	218/380 57%	1/380 0%
putative FAD- dependent MO (*S. cattleya* NRRL 8057), [YP_004912775.1]	294	97%	1e-92	170/387 44%	225/387 58%	3/387 1%
conserved hypoth. protein (*S. clavuligerus* ATCC 27064), [ZP_05004048.1]	285	93%	4e-89	162/370 44%	217/370 59%	2/370 1%
hypoth. protein (*P. aeruginosa* PACS2), [ZP_01366778.1]	279	91%	8e-87	162/365 44%	214/365 59%	8/365 2%
putative FAD-dependent MO (*P. aeruginosa* 39016), [NP_252018.1]	279	91%	9e-87	162/365 44%	214/365 59%	8/365 2%

score: value calculated from the number of gaps and substitutions associated with each aligned sequence (higher scores indicate significant alignments)

Q. coverage = query coverage: percent of match

E-value: describes possibility of false-positive match

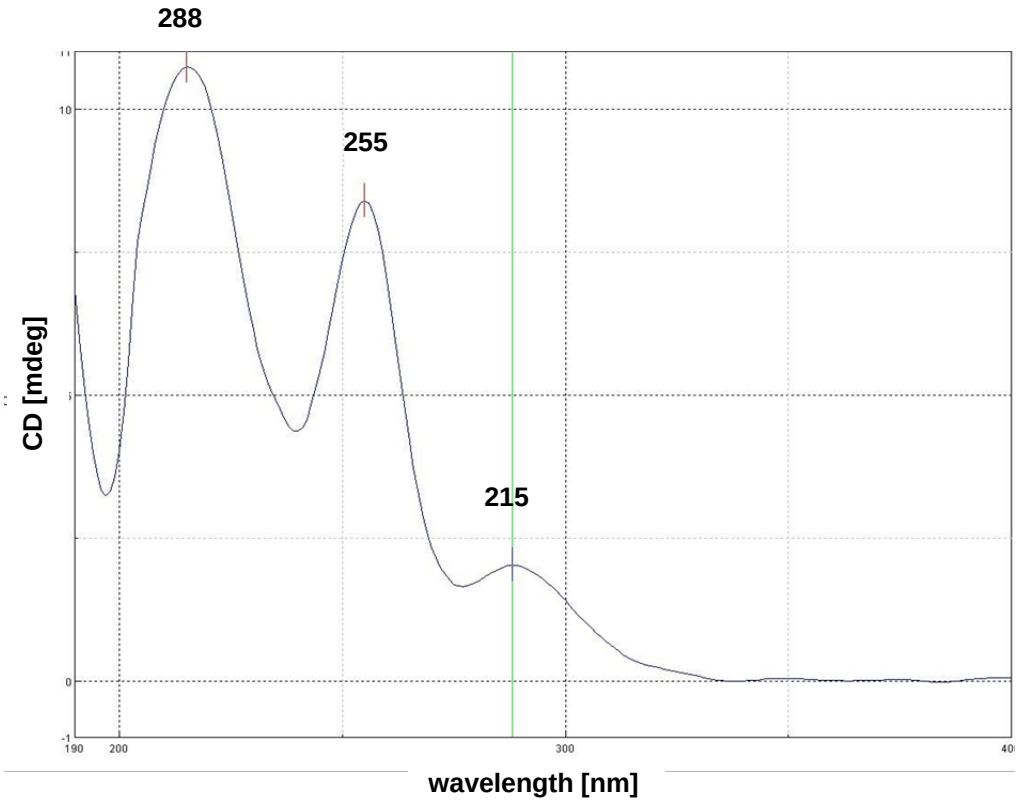

Figure 8.1.1: CD spectrum of brabantamide A measured in methanol

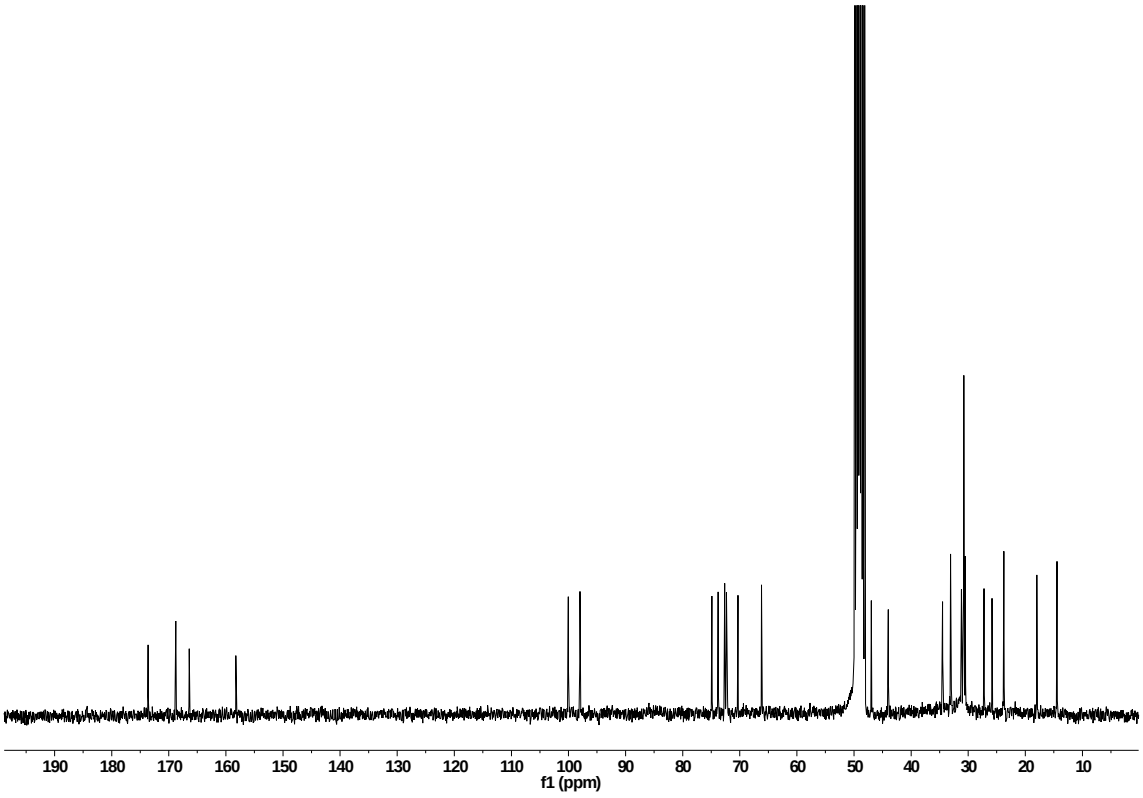

Figure 8.1.2: ^{13}C-NMR spectrum of compound **1** (SB-253514/ brabantamide A) in d_4-methanol (75 MHz)

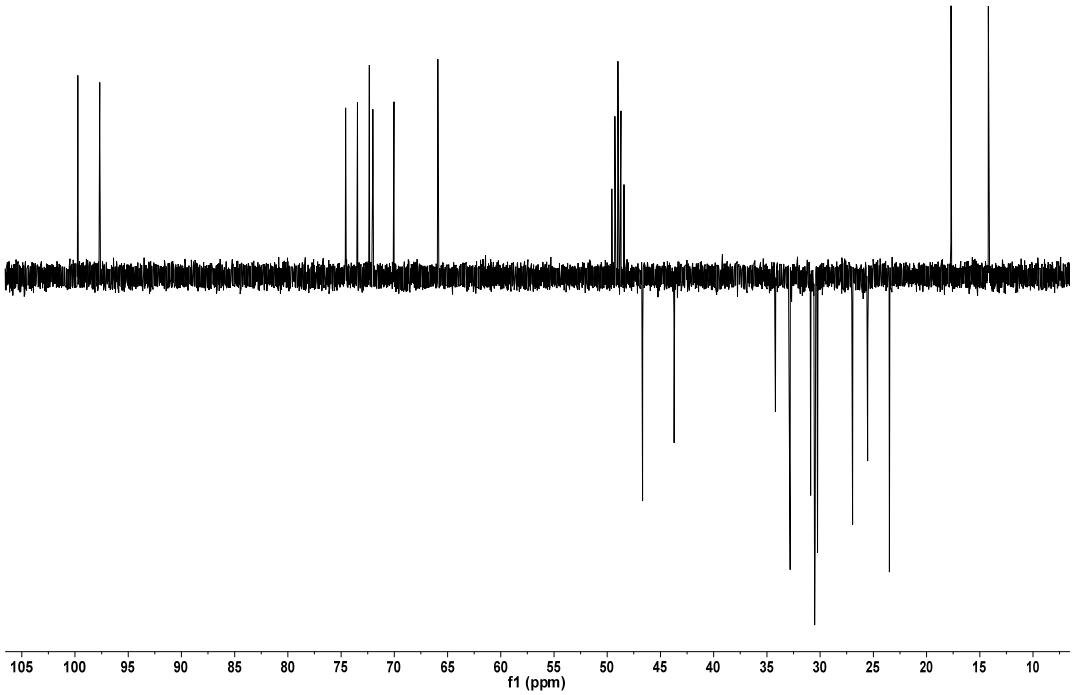

Figure 8.1.3: DEPT135 spectrum of compound **1** (SB-253514/ brabantamide A) in d_4-methanol (300 MHz)

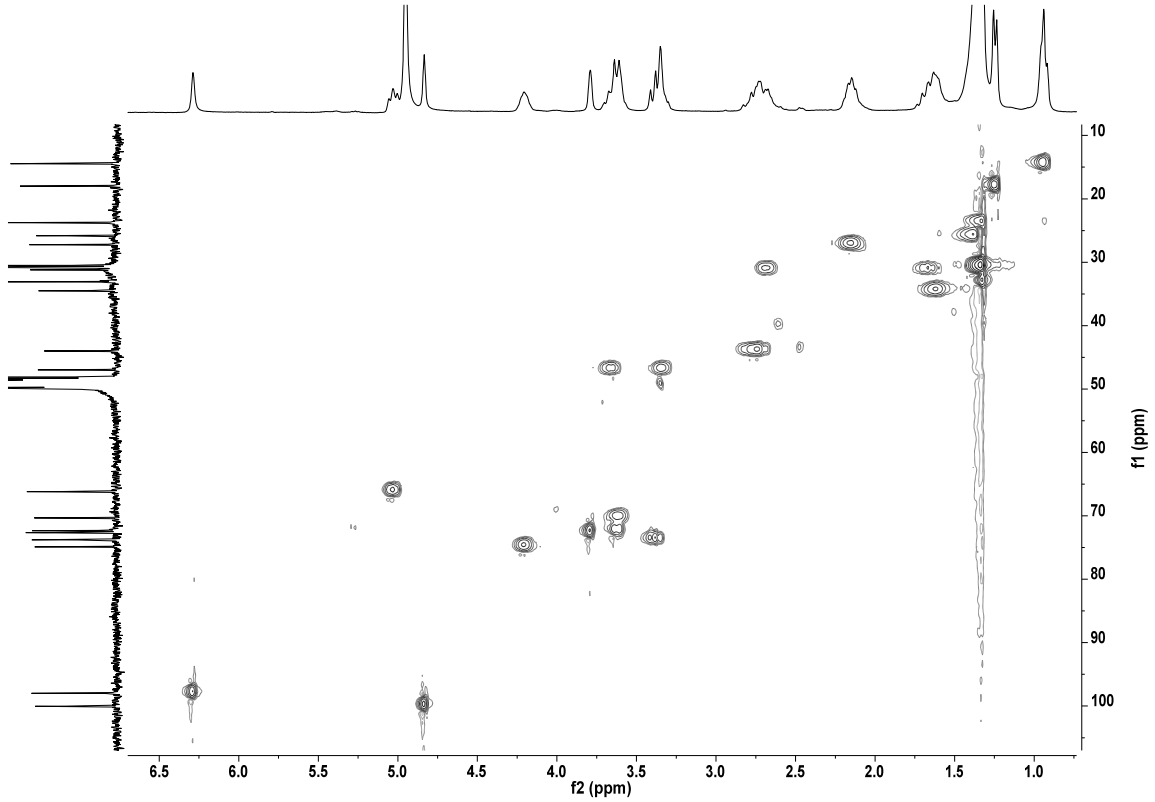

Figure 8.1.4 HSQC spectrum of compound **1** (SB-253514/ brabantamide A) in d_4-methanol (300 MHz)

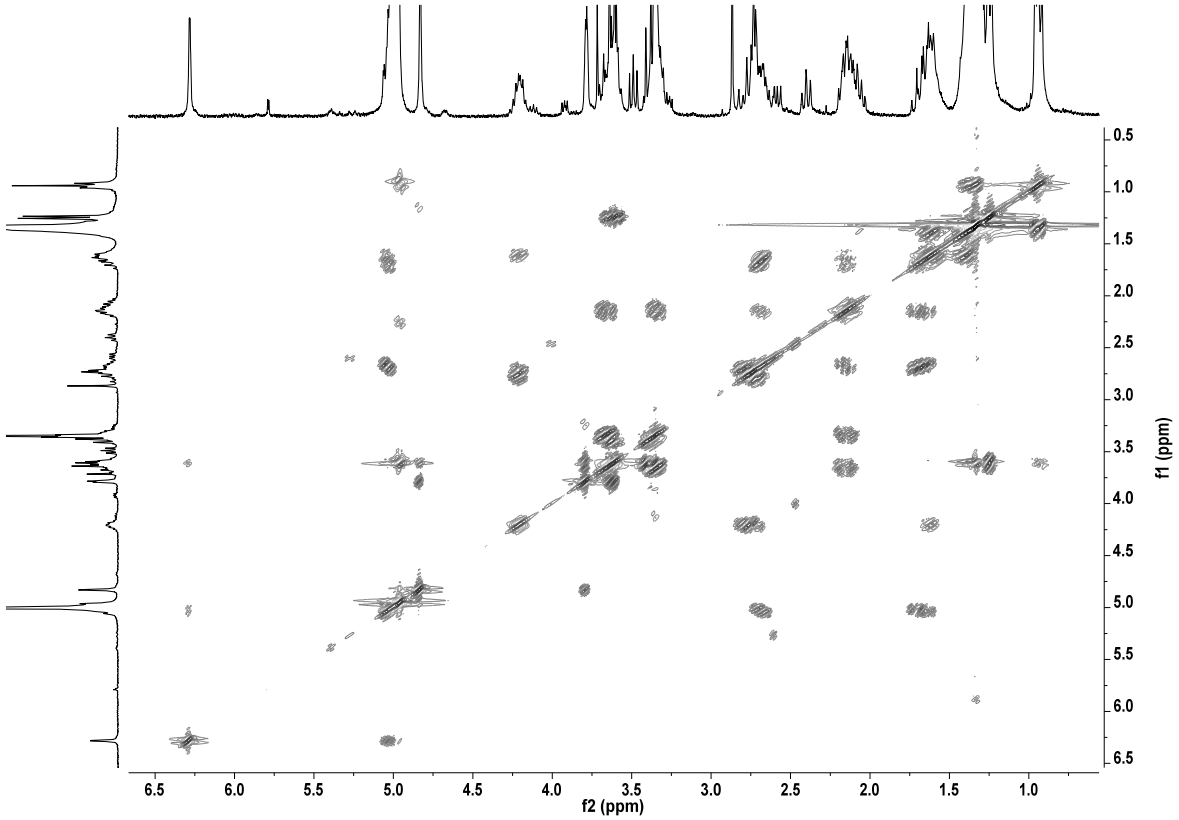

Figure 8.1.5: ^{1}H-^{1}H COSY spectrum of compound **1** (SB-253514/ brabantamide A) in d_4-methanol (300 MHz)

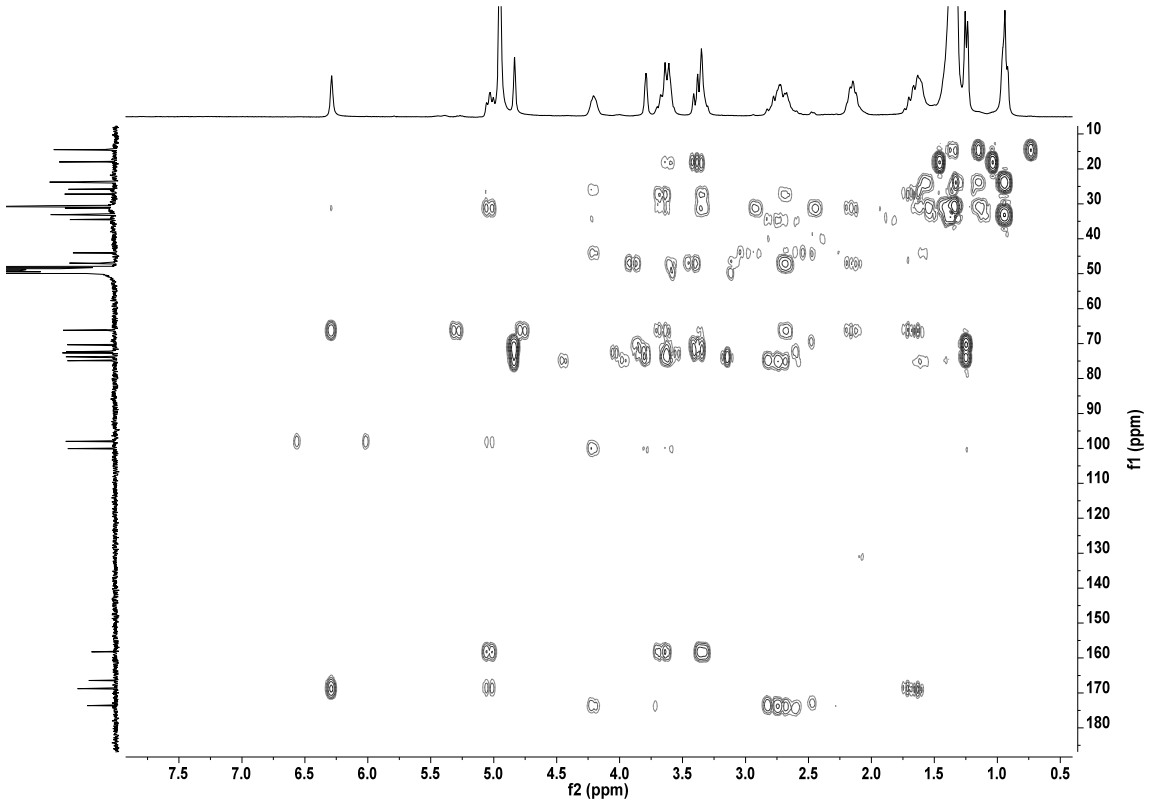

Figure 8.1.6: ^{1}H-^{13}C HMBC spectrum of compound **1** (SB-253514/ brabantamide A) in d_4-methanol at 300 MHz

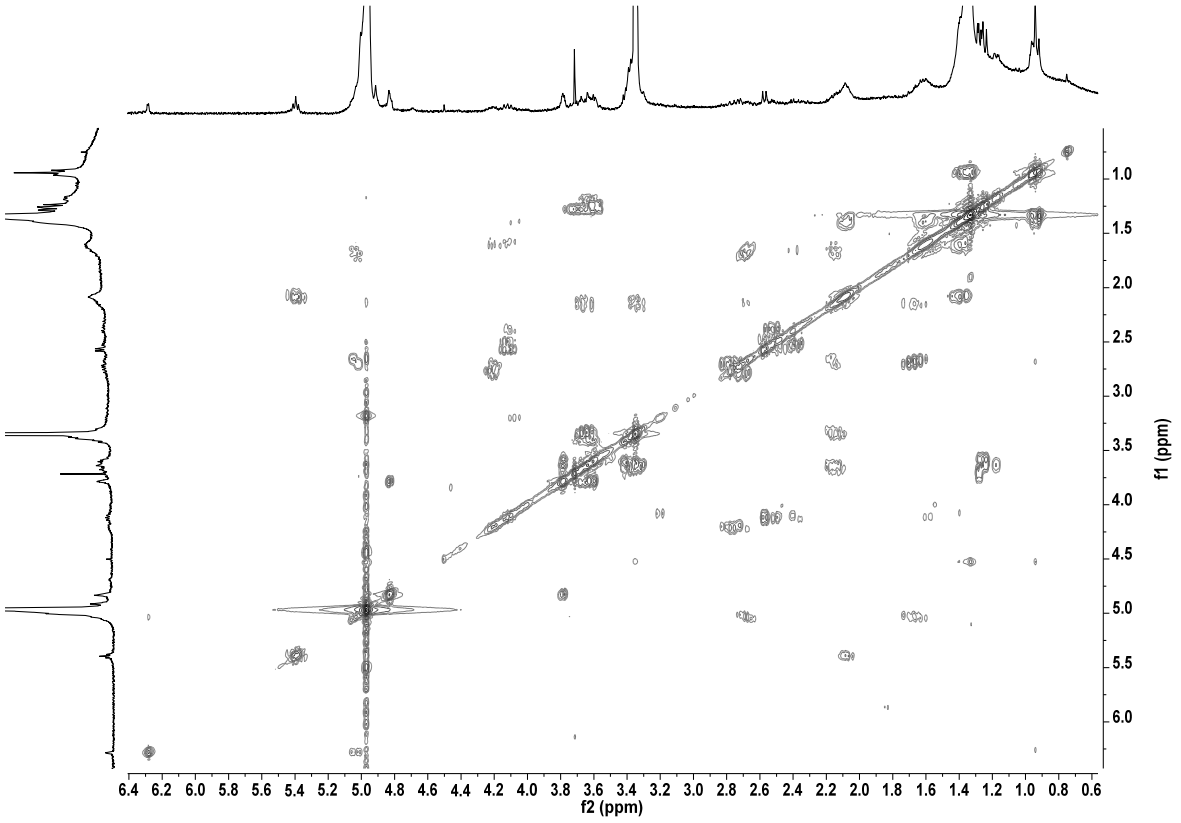

Figure 8.1.7: ^{1}H-^{1}H COSY spectrum of compound **2** (SB-253517/ brabantamide B) in d_4-methanol (300 MHz)

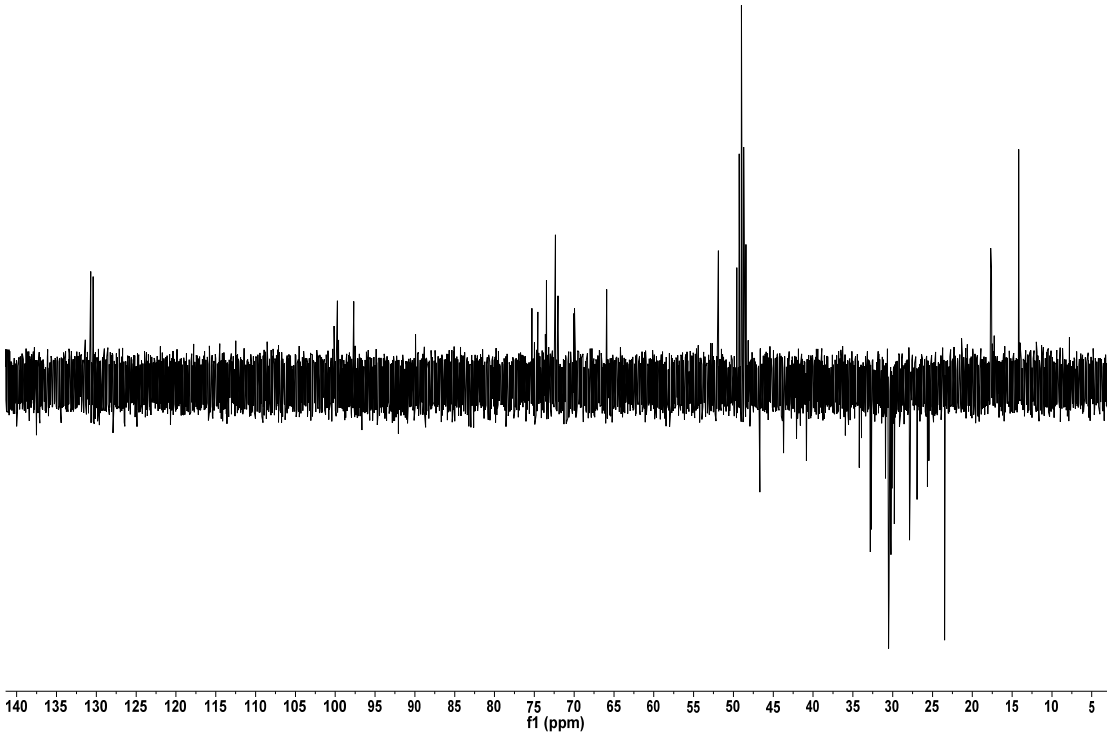

Figure 8.1.8: DEPT135 spectrum of compound **2** (SB-253517/ brabantamide B) in d_4-methanol (300 MHz, 20400 scans)

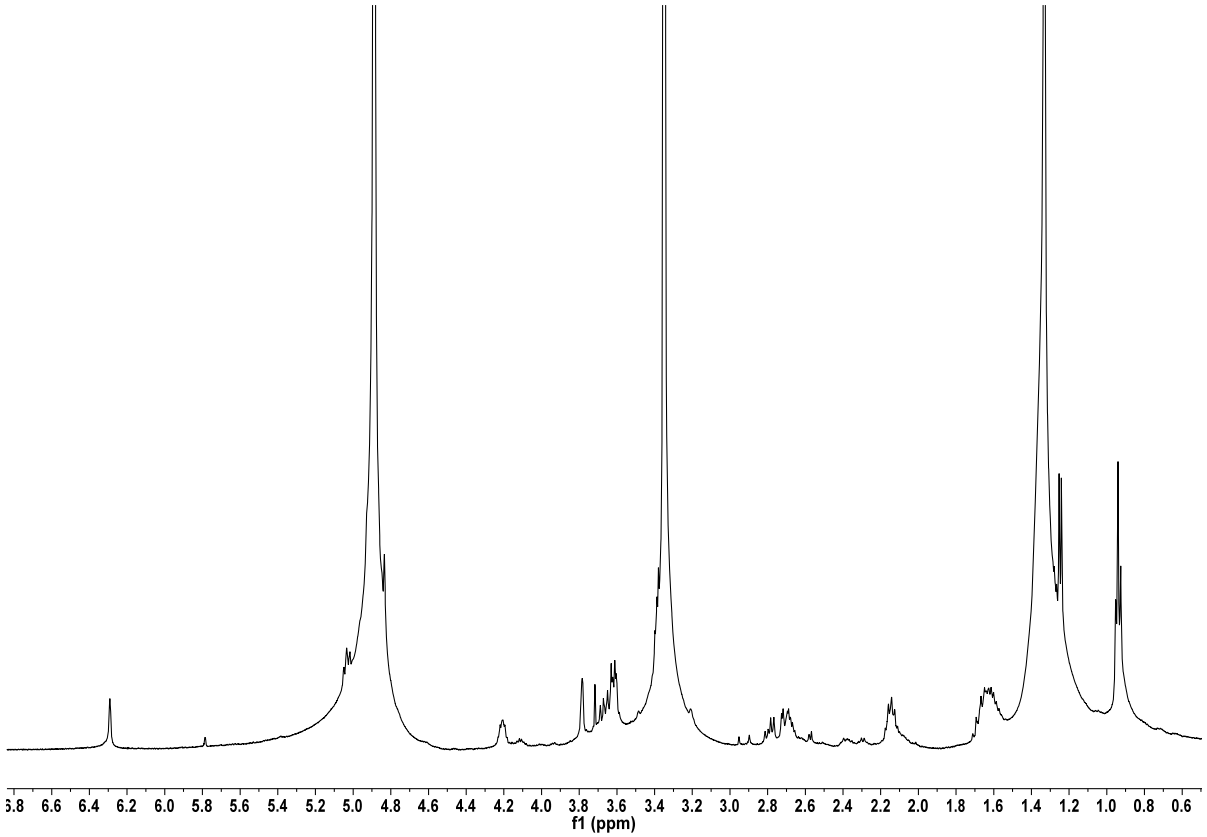

Figure 8.1.9: ^{1}H-NMR spectrum of compound **3** (SB-253518/ brabantamide C) in d_4-methanol (500 MHz)

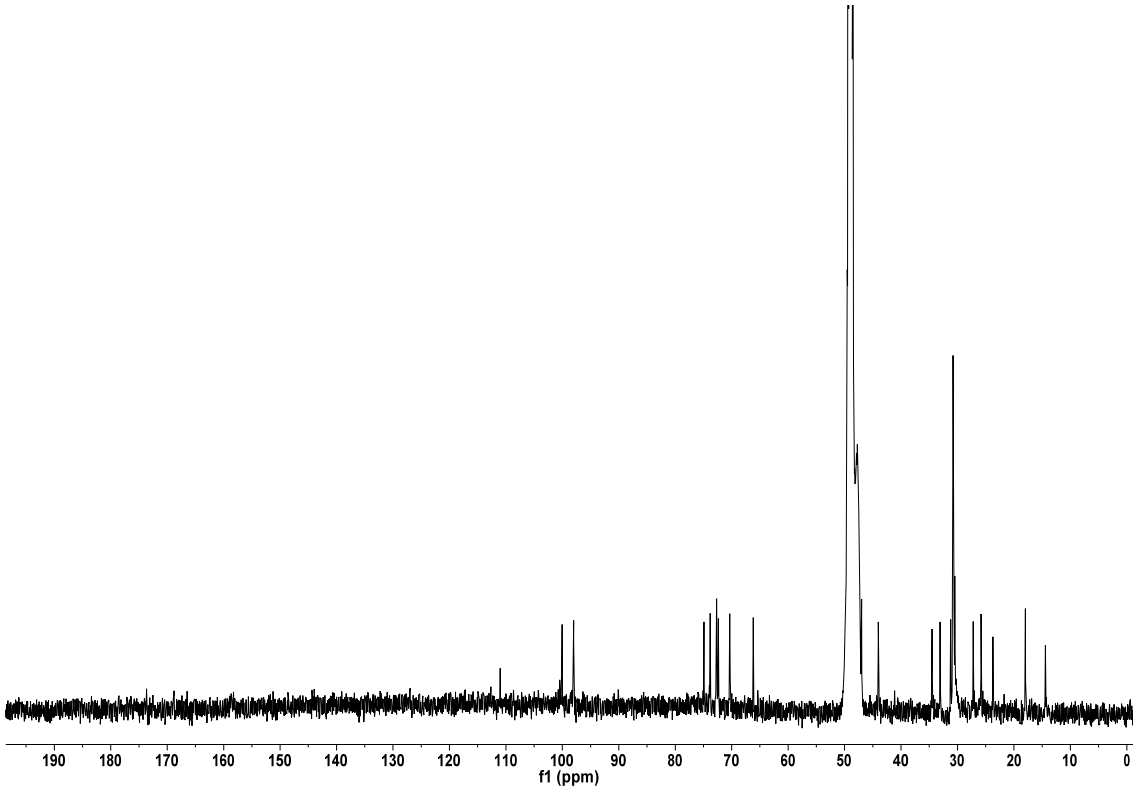

Figure 8.1.10: ^{13}C-NMR of compound **3** (SB-253518/ brabantamide C) in d_4-methanol (125 MHz, 20000 scans)

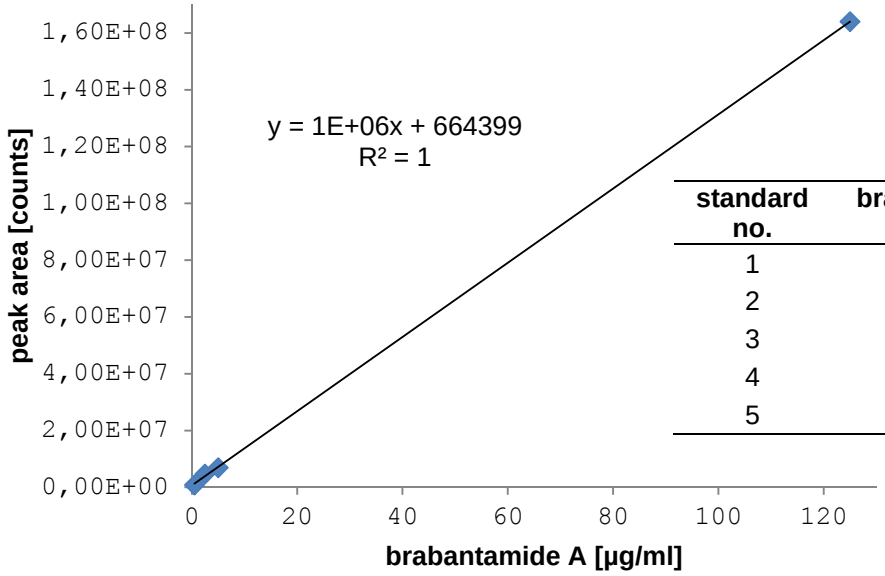

standard no.	brabantamide A [µg/ml]	peak area
1	0.25	-
2	0.5	8,49E+05
3	2.5	4.67E+06
4	5	6.93E+06
5	125	1.64E+08

Figure 8.1.11: calibration line for the determination of production rate of brabantamide A

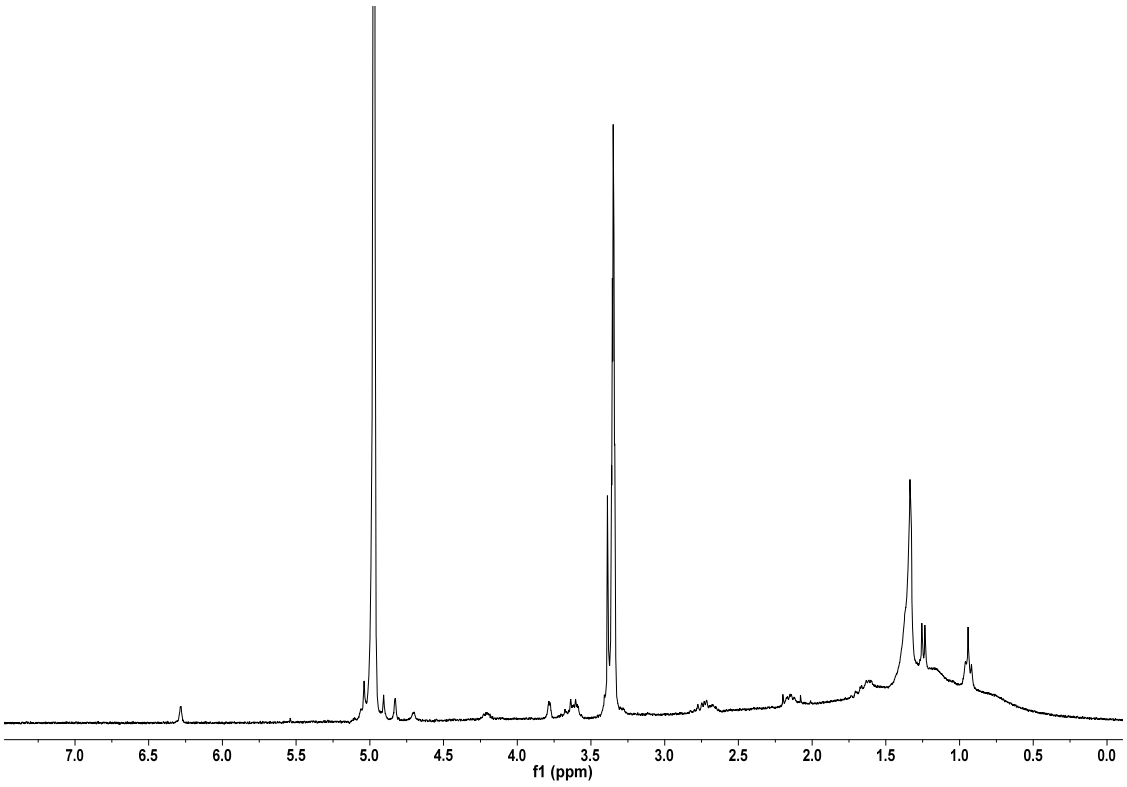

Figure 8.1.12: ^{1}H-NMR of brabantamide A in d_4-methanol after labelling with 1-^{13}C sodium acetate (300 MHz)

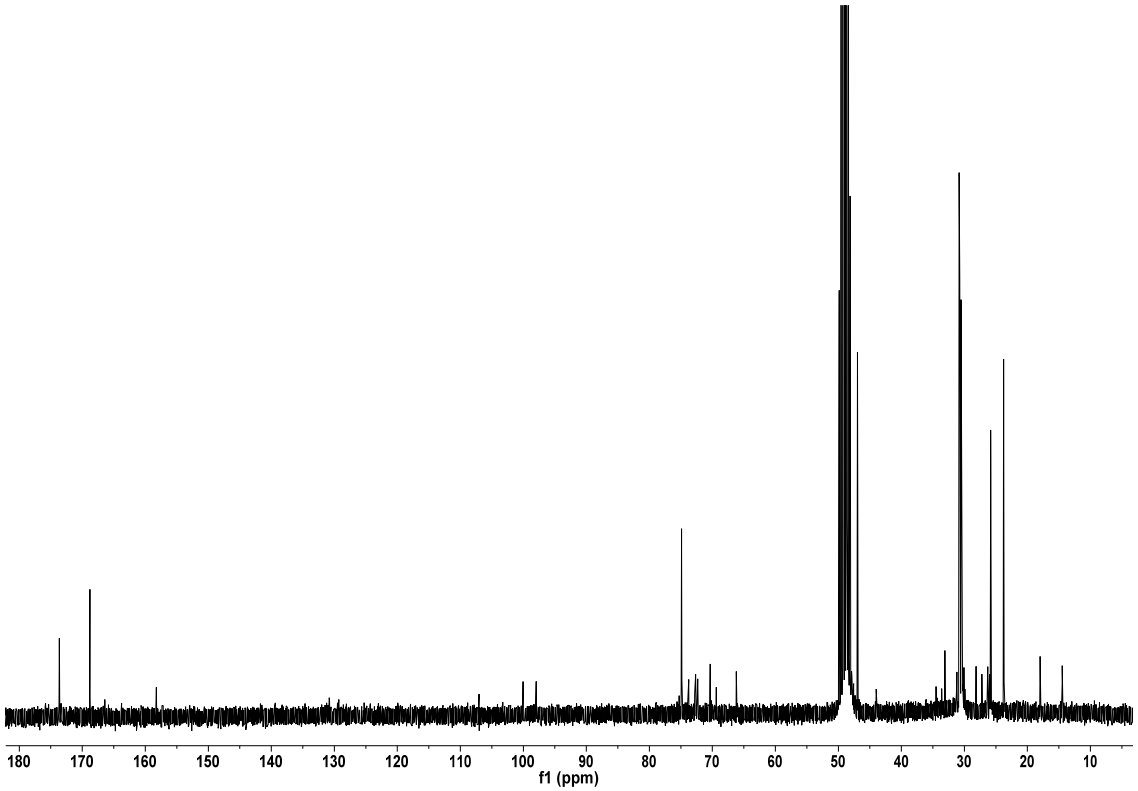

Figure 8.1.13: ^{13}C-NMR of brabantamide A in d_4-methanol after labelling with 1-^{13}C – sodium acetate, 60000 scans (300 MHz)

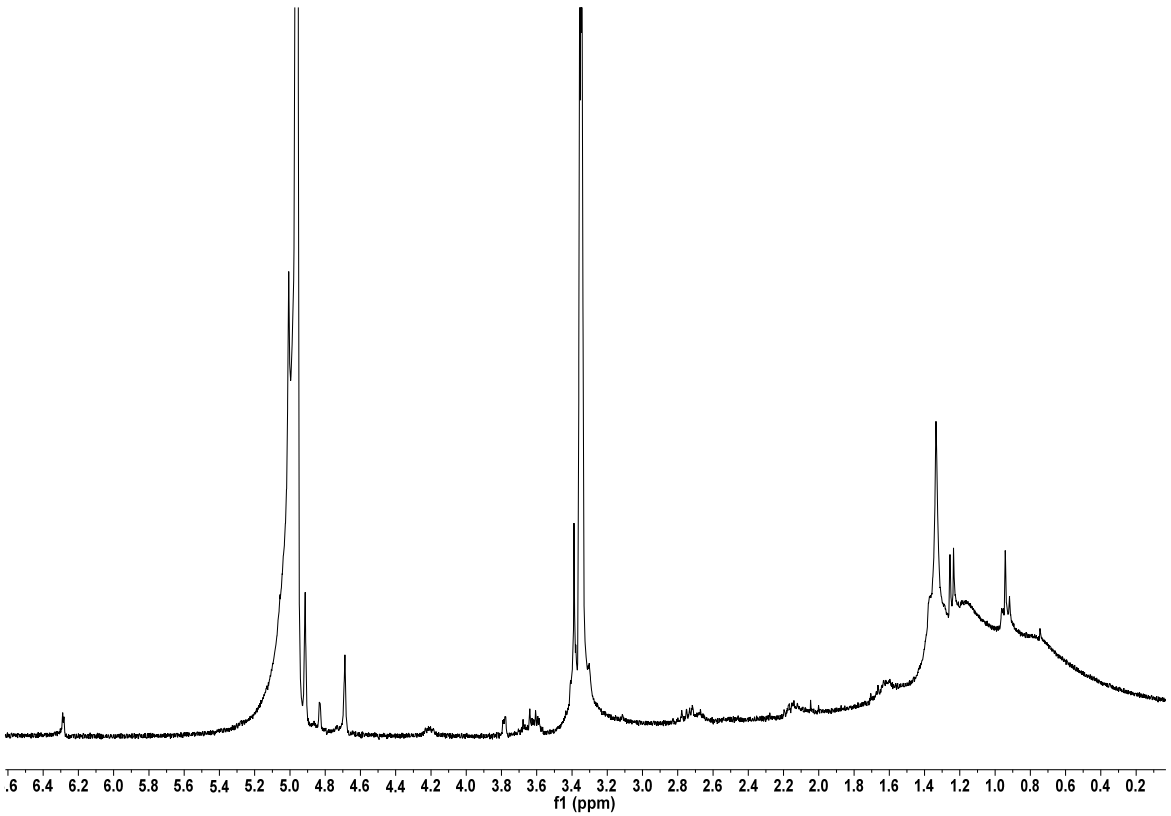

Figure 8.1.14: ^{1}H-NMR of brabantamide A after labelling with U-^{13}C sodium acetate in d_4-methanol (300 MHz)

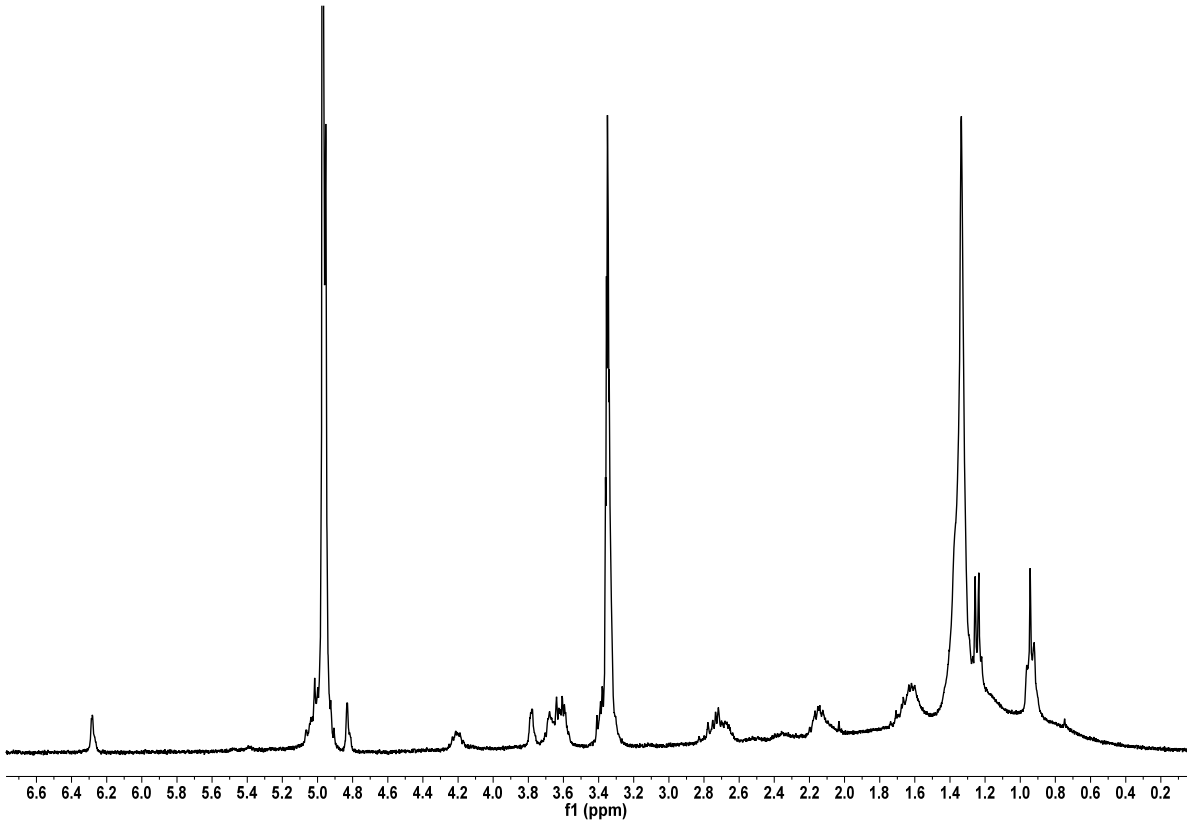

Figure 8.1.15: ^{1}H-NMR of brabantamide A in d_4-methanol after labelling with 1-^{13}C- L-serine (300 MHz)

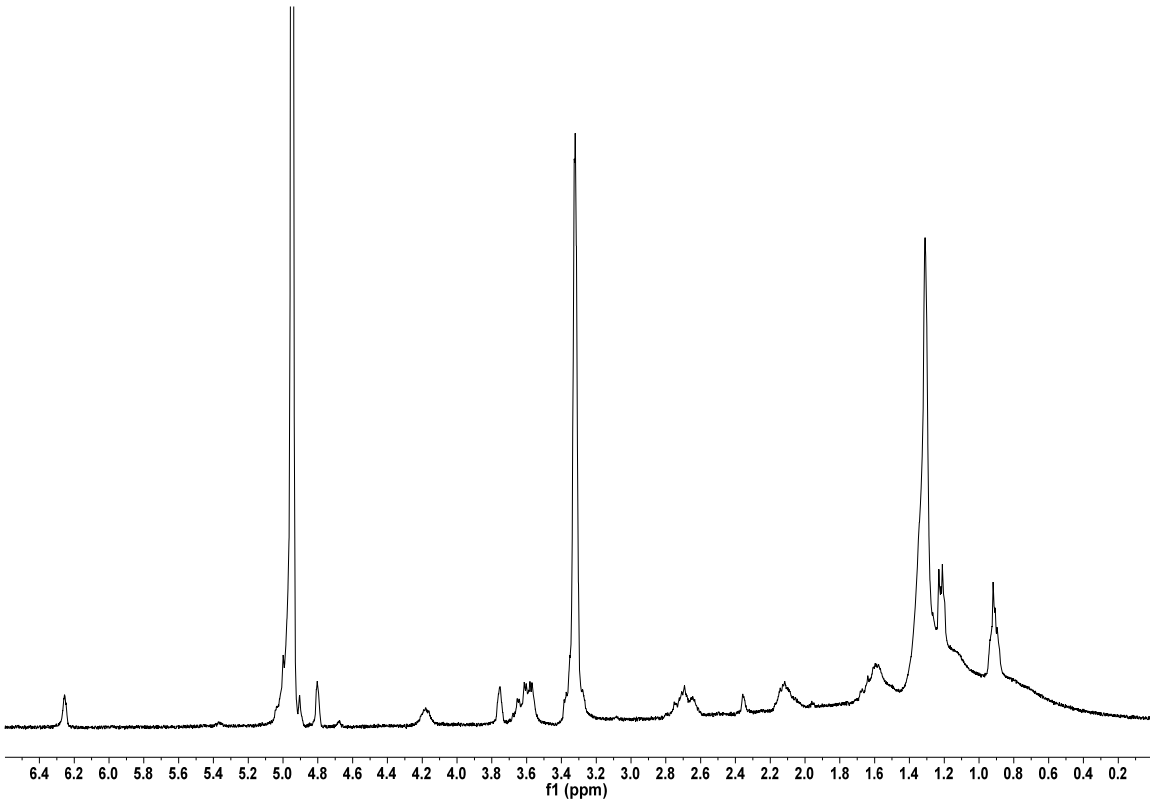

Figure 8.1.16: ^{1}H-NMR spectrum of brabantamide A after labelling with 1,2-^{13}C L-serine in d_4-methanol (300 MHz)

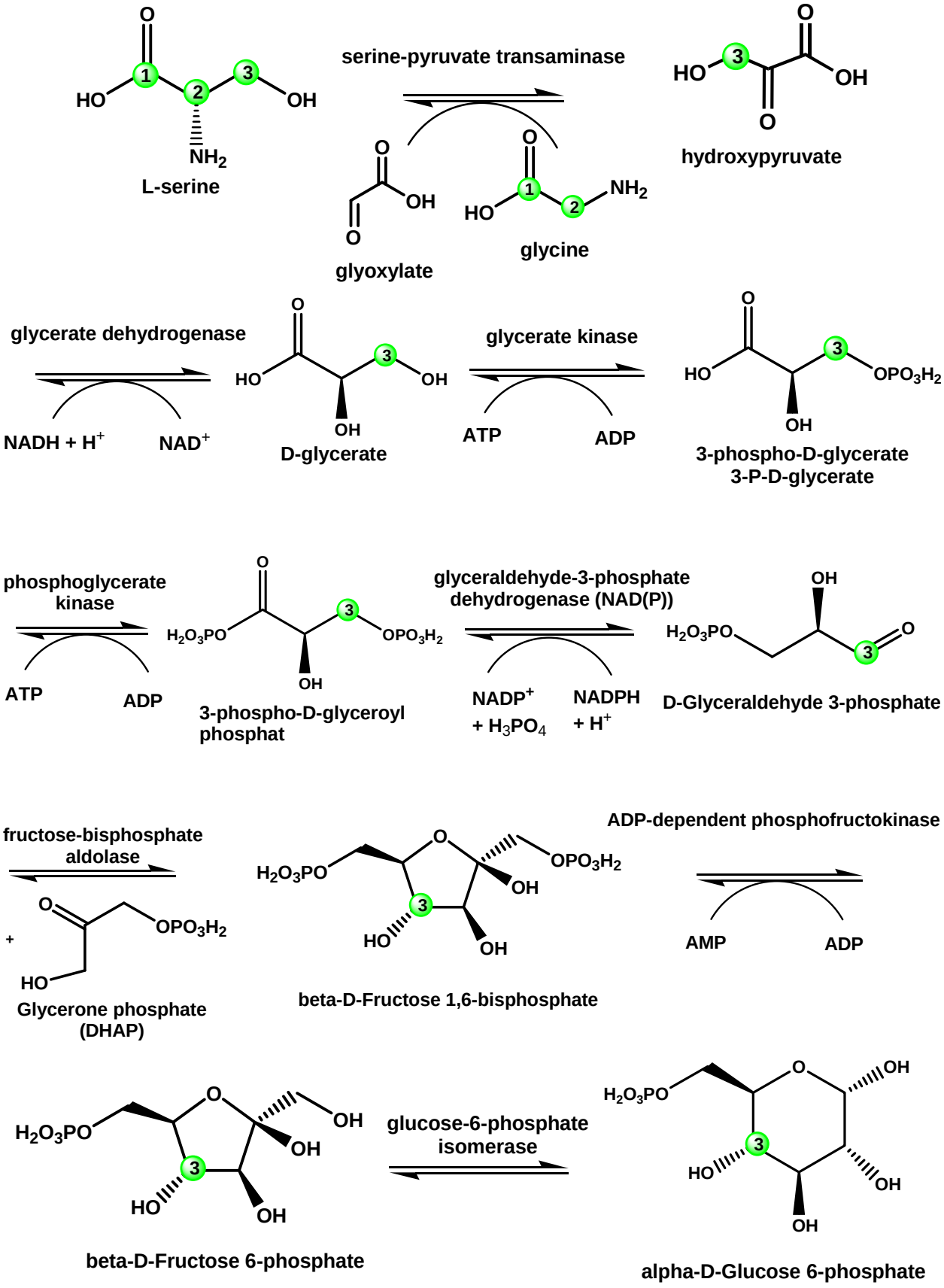

Figure 8.1.17: proposed pathway of the label at C4' in brabantamide A after labelling with 1,2-^{13}C L-serine (pathway is based on KEGG; Madduri *et al.*, 2001; Thibodeaux *et al.*, 2008) – part one

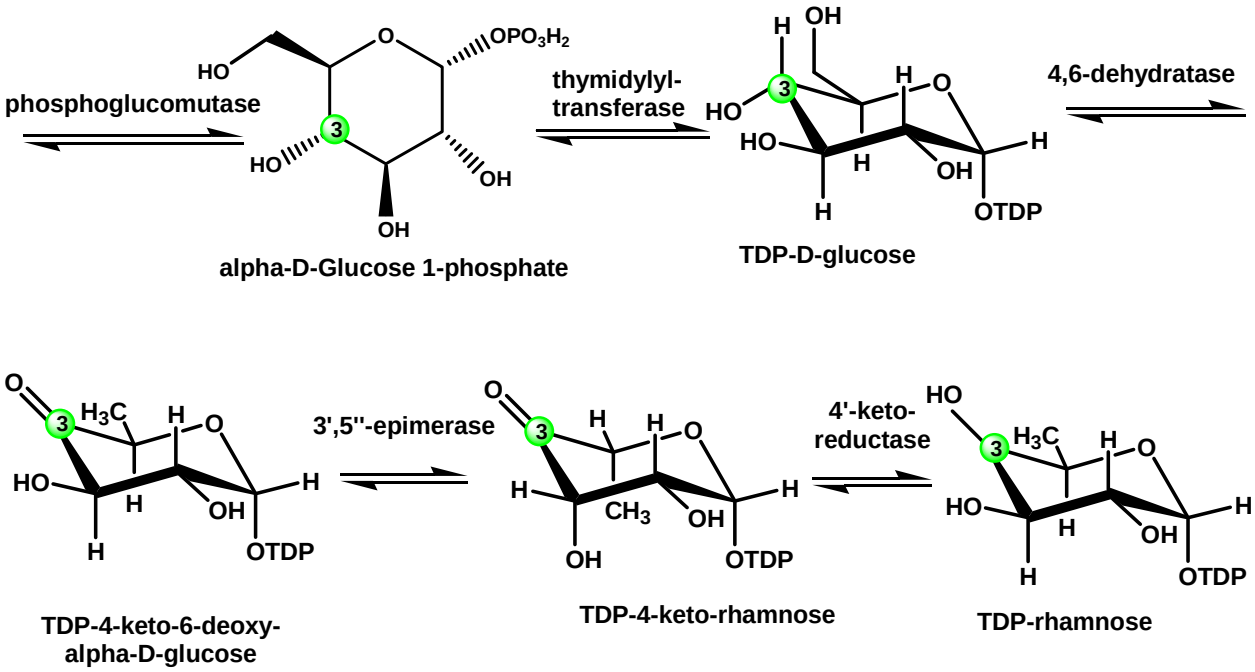

Figure 8.1.18: proposed pathway of the label at C-4' in brabantamide A after labelling with 1,2-^{13}C L-serine (pathway is based on KEGG; Madduri *et al.*, 2001; Thibodeaux *et al.*, 2008) – part two

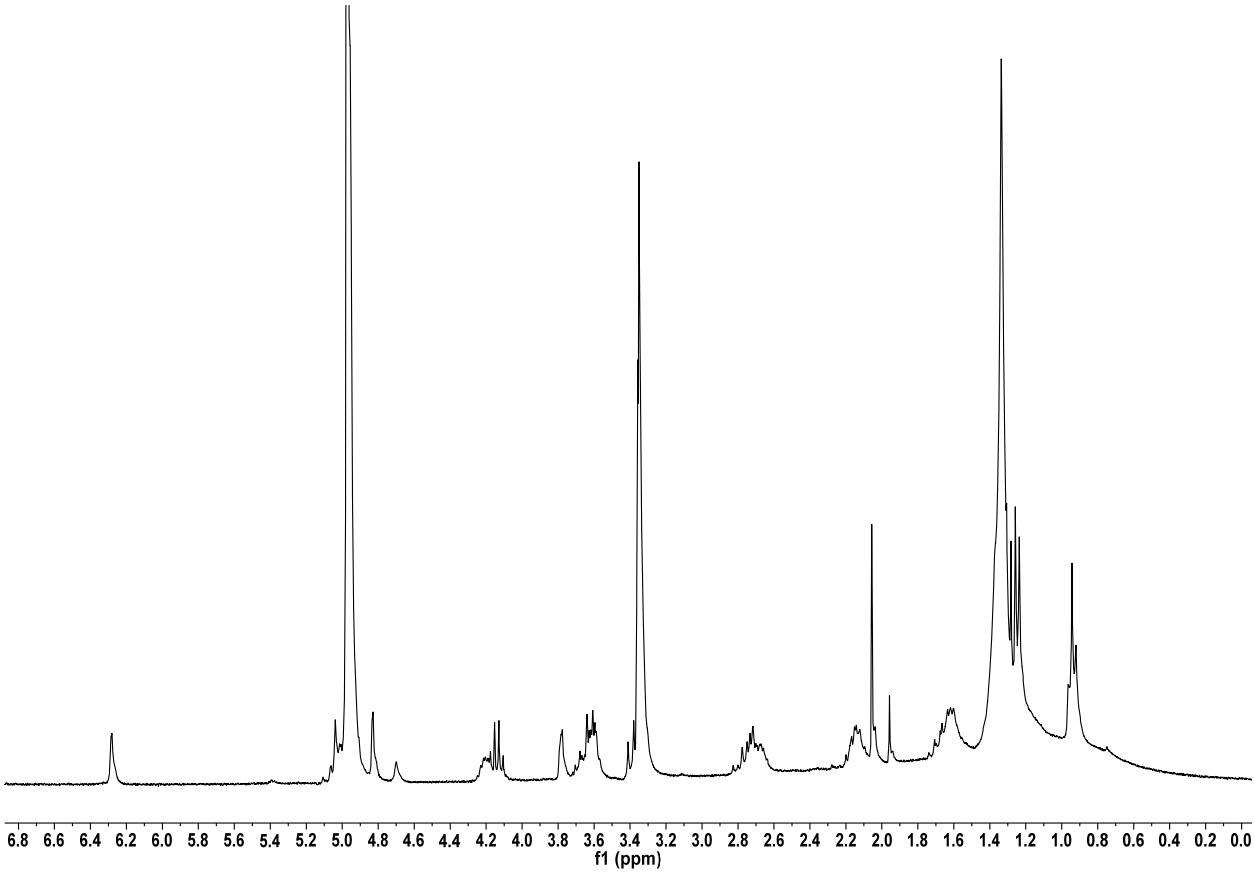

Figure 8.1.19: ^{1}H NMR spectrum of brabantamide A after labelling with 1-^{13}C hydrogen carbonate in d_4-methanol (300 MHz)

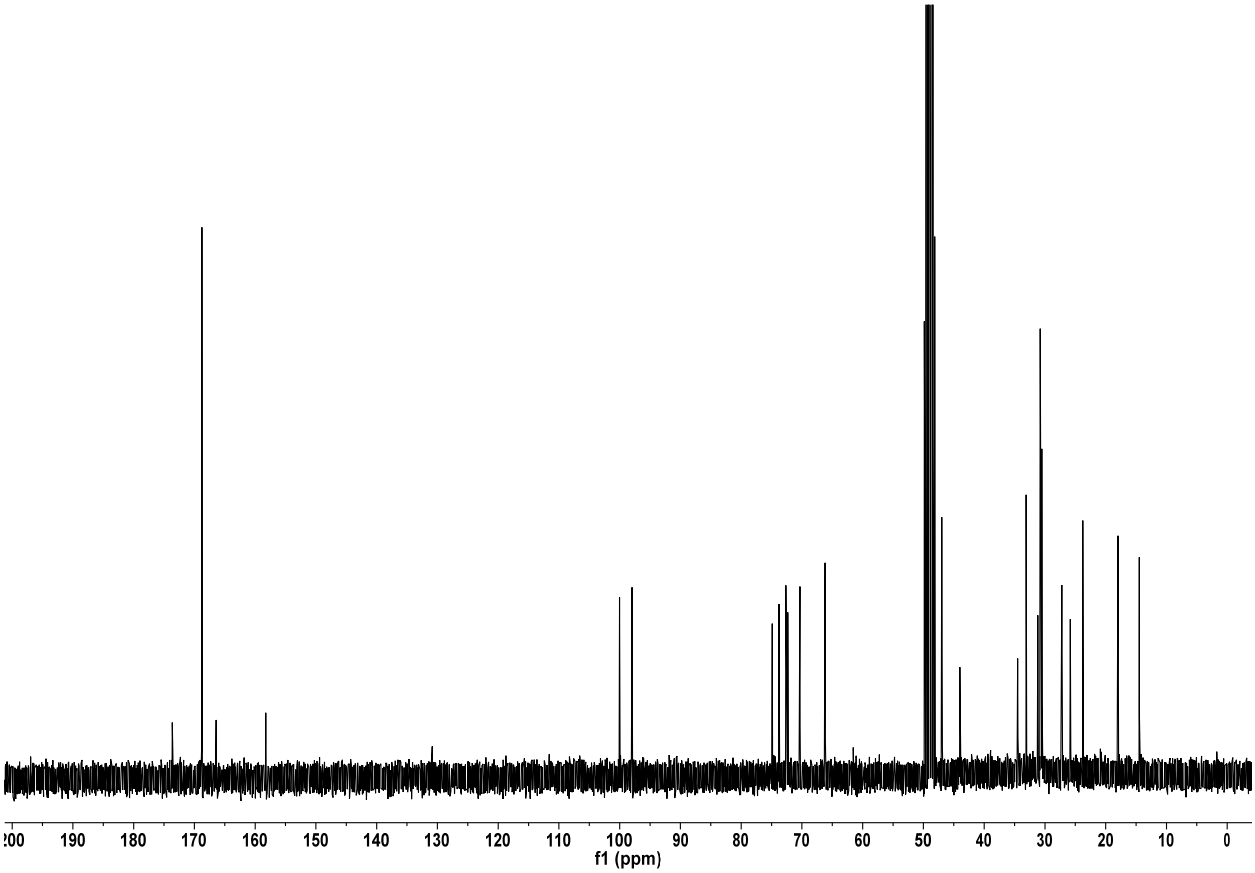

Figure 8.1.20: ^{13}C-NMR of brabantamide A in d_4-methanol after labelling with 1-^{13}C - hydrogen carbonate, 26000 scans (300 MHz)

Table 8.1.3: determination of proline-uptake in *Pseudomonas* sp. SH-C52; CPM = counts per minute; OD = optical density

	1. determination		***2. determination***	
time [min]	**CPM**	**OD**	**CPM**	**OD**
0	342	0.57	489	0.95
5	839			
15	1004			
30	1407	0.71	6484	0.98
45	2290			
60	3164	0.81	10368	1.10
75	3470			
90	4350	1.03	13290	1.52
120	5211	1.08	17085	1.67
150			20787	1.65
180	6277			
210		1.22		1.90
240		1.40		2.16

Table 8.1.4: antimicrobial disk diffusion inhibitory activities of brabantamides (A = brabantamide A; B = brabantamide B; C = brabantamide C)

Organism	**Zone of inhibition [mm]**		
	A	**B**	**C**
Gram-positive bacteria			
Arthrobacter crystallopoietes DSM 20117	13	14	14
Bacillus cereus	n.t.	8[d]	8[b]
Bacillus subtilis 168	4	11[a]	10[a]
Bacillus megaterium	0	11[c]	10[c]
Corynebacterium pseudodiphtheriticum	3	n.t.	n.t.
Corynebacterium diphtheriae	3	n.t.	n.t.
Corynebacterium xerosis Va 167198	3	12[b]	12[b]
Enterococcus faecium I-11305b	0	0	0
Enterococcus faecium I-11054	n.t.	0	0
Listeria welchimeri DSM 20650	3	0	0
Micrococcus luteus ATCC 1856	0	n.t.	n.t.
Micrococcus luteus ATCC 4698	n.t.	10[a]	10[a]
Mycobacterium smegmatis ATCC 70084	3	0	0
Staphylococcus aureus SG 511	3	0	0
Staphylococcus aureus 133	n.t.	0	0
Staphylococcus aureus 5185 (MS)	3	4[a]	0
Staphylococcus aureus I-11574 (MS)	n.t.	6[a]	0
Staphylococcus aureus LT-1334 (MR)	0	6[a]	0
Staphylococcus aureus LT-1338 (MR)	0	0	0
Staphylococcus epidermidis LT-1324 (MR)	0	0	0
Staphylococcus epidermidis ATCC 12228	0	0	0
Staphylococcus epidermidis LT-1324 (MR)	n.t.	0	0
Staphylococcus simulans 22	0	0	0
Gram-negative bacteria			
Citrobacter freundii I-11090	0	0	0
Escherichia coli DH5 alpha	0	n.t.	n.t.
Escherichia coli O-19592	0	0	0
Escherichia coli I-11276b	n.t.	0	0
Klebsiella pneumonia I-10910	0	n.t.	n.t.
K. pneumoniae subsp. *ozeanae*I-10910	n.t.	0	0
Pseudomonas aeruginosa I-10968	0	0	0
Pseudomonas aeruginosa 4991	n.t.	0	0
Serratia marcescens	0	n.t.	n.t.
Stenotrophomonas maltophilia O-16451	n.t.	0	0
Stenotrophomonas maltophilia I-10717	n.t.	0	0
Fungi			
Candida albicans I-11301	n.t.	0	0
Candida albicans I-11301	n.t.	0	0

[a] turbid; [b] very turbid; [c] clear with resistances; [d] bright with turbid court
MS = methicillin-susceptible; MR = methicillin-resistant; n.t. = not tested

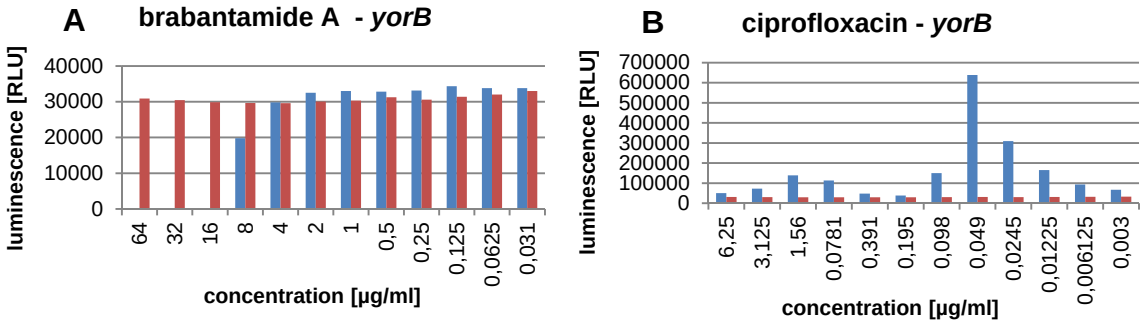

Figure 8.1.21: result of brabantamide A on the *yorB* promoter (indicates inhibition of DNA-synthesis) in comparison with the positive control ciprofloxacin (inhibits gyrase); red and blue bars represent the background control and the tested substance, respectively; A: brabantamide A, B: ciprofloxacin

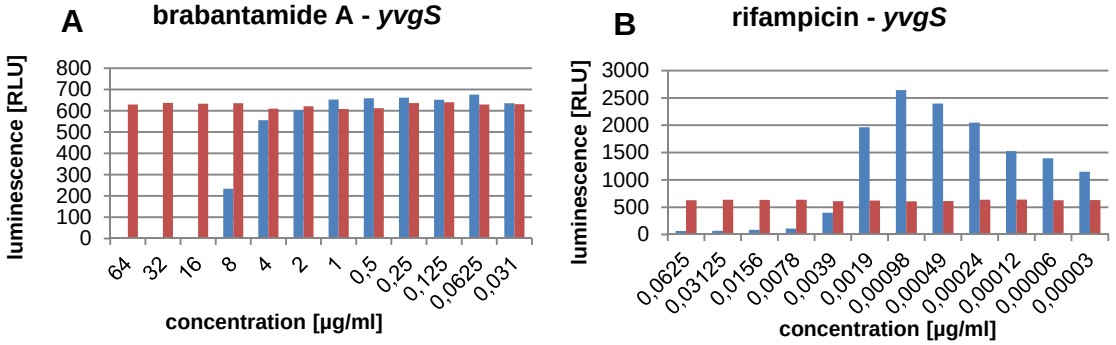

Figure 8.1.22: result of brabantamide A on the *yvgS* promoter (indicates inhibition of RNA biosynthesis) in comparison with the positive control rifampicin (inhibits RNA polymerase); red and blue bars represent the background control and the tested substance, respectively; A: brabantamide A, B: rifampicin

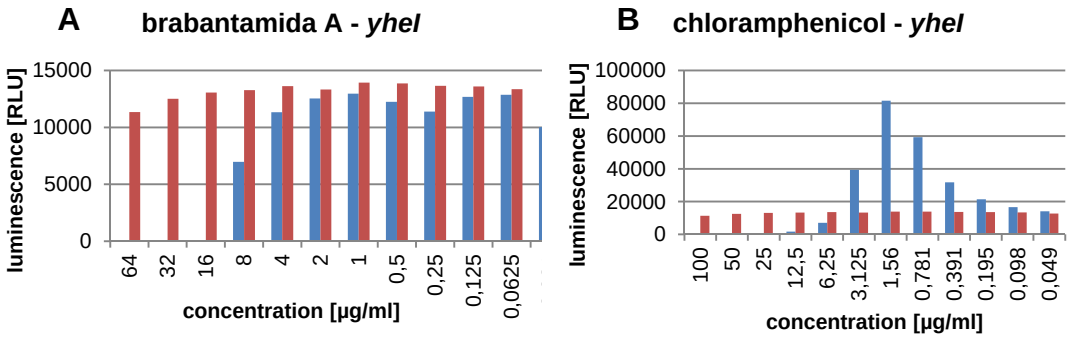

Figure 8.1.23: result of brabantamide A on the *yheI* promoter (indicates inhibition of protein biosynthesis) in comparison with the positive control chloramphenicol (inhibits protein synthesis); red and blue bars represent the background control and the tested substance, respectively; A: brabantamide A, B: chloramphenicol

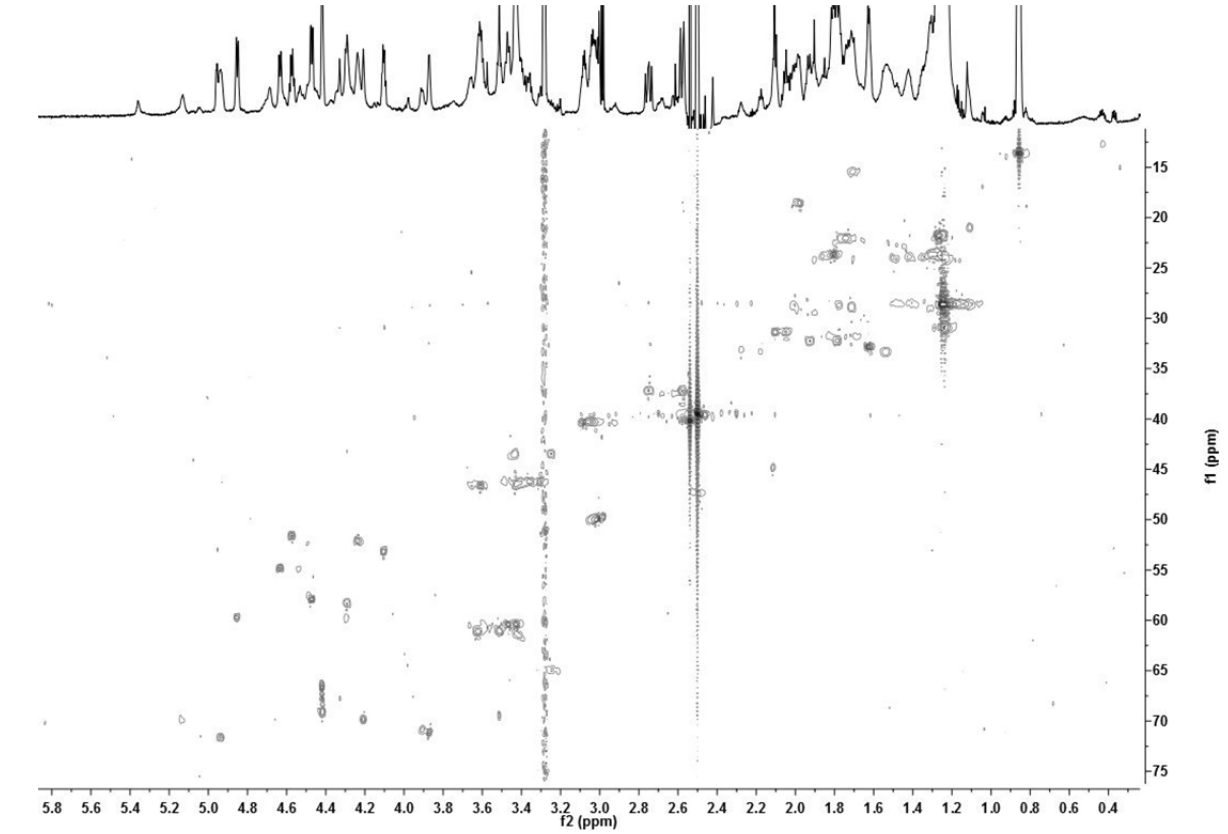

Figure 8.1.24: ^{1}H-^{13}C HSQC spectrum of empedopeptin in d_6-DMSO (900 MHz)

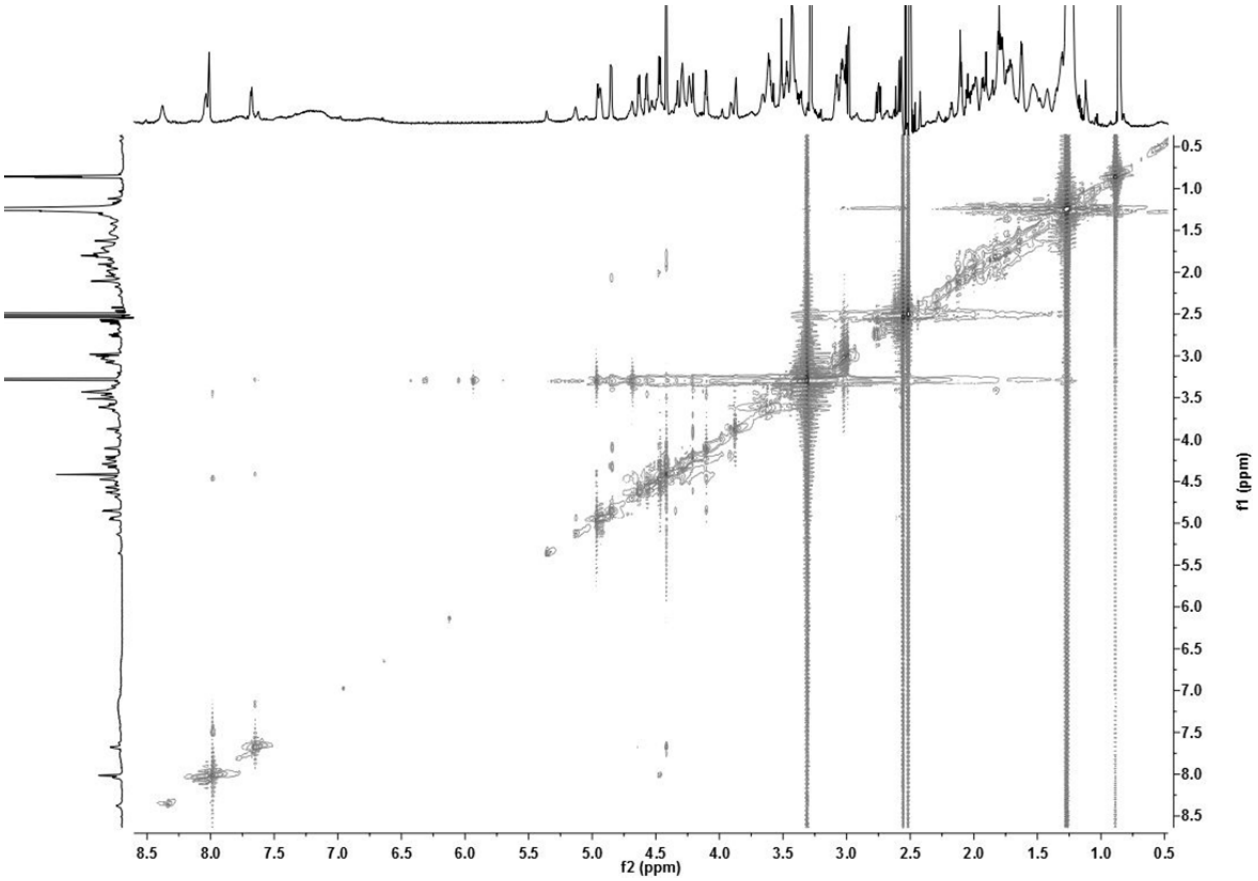

Figure 8.1.25: NOESY spectrum of empedopeptin in d_6-DMSO (900 MHz)